

I give consent to this copy of my thesis, when deposited in the University Library, being available for loan and photocopying.

Date : ..8th May 1982.....Signed :



OPTIMISATION OF ROAD VEHICLE
SUSPENSION SYSTEMS BY APPLICATION
OF DIGITAL AND ANALOGUE COMPUTERS.

Being a thesis ($\frac{1}{3}$ ^{rd.}) submitted for the
Degree of Master of Engineering Science

This thesis embodies the results of supervised
project work making up one-third of the work
for the degree.

By HARRY PUKSAND, B.E.

Date of Submission: September, 1981.

Acknowledgements

I wish to thank the following persons for the assistance rendered to the author during preparation of this thesis:-

DR. A.G. THOMPSON for his active guidance, advice and encouragement.

PROF. R.E. LUXTON for his counsel and assistance.

The Council of S.A. Institute of Technology.

PROF. R.W. SMYTH for his counsel, encouragement and assistance in many ways.

MRS. R. HARRISON for her excellent effort in typing the manuscript.

DECLARATION

I hereby certify that this thesis contains no material which has been accepted for the award of any other Degree or Diploma in any University and that to the best of my knowledge and belief, this thesis contains no material previously published or written by another person except when due reference is made in the text of this thesis.

HARRY PUKSAND

SYNOPSIS

The thesis deals with optimisation of vehicle suspensions based on integral square values of system response as the performance criteria for comparison.

Integral square values are calculated for step input excitation which is shown to be equivalent to random velocity input to road wheels of constant power spectral density, closely approximating the spectra of a typical road surface.

The integral square values are calculated by application of Laplace Transformation and Parseval's Theorem.

The concept of performance index is introduced as a measure of suspension quality, and is defined as the weighted sum of selected integral square values which best characterise the system.

Further it is shown that the integral square values and the performance index due to random road input can also be calculated by application of state variable theory in conjunction with co-variance matrix and solution of the LYAPUNOV Equation. The results are compared, and found to be identical.

Most of the analytical work is based on a simple $\frac{1}{4}$ -car model and closed form solutions are established for integral square values. The analysis is extended to $\frac{1}{2}$ -car model with a time-delay between front and rear inputs, but the analysis for the general case (coupling ratio $\neq 1.0$) breaks down owing to its complexity, and ACSL digital simulation language is used to calculate the integral square response for different values of suspension parameters.

Also the state variable analysis with covariance matrix and LYAPUNOV equation are extended to calculation of integral square values and performance indices of a $\frac{1}{2}$ -car model, using the digital computer to calculate numerical results.

The role of the performance index as the criterion of suspension "quality" is critically examined, with the conclusion that the performance index is a useful concept in a computer minimisation process, but is not an absolute measure of system quality in case of road vehicles, hence direct comparison of suspensions on the basis of the performance index alone is strictly not valid.

The simulation on the analogue computer is also conducted with the view to obtaining a large amount of response data with different values of suspension parameters in a shortest possible time.

The general impression is, however, that the accuracy and repeatability of the analogue machine is not adequate for establishing the points of minima for integral square responses owing to the flatness of the response characteristics. The characteristics are so shallow that statistical processing of analogue computer results is necessary if the uncertainties involved are to be reduced to acceptable level for meaningful results.

Finally different optimisation criteria are compared, with the conclusion that there cannot be an absolute optimum since the final choice and judgement regarding the overall "quality" of a suspension will still remain in the subjective realm of a particular designer, but within relatively narrow limits of parameter values.

NOMENCLATURE

| | |
|----------------|---|
| $A(t)$ | Closed-loop matrix |
| A_1 | System matrix |
| a | Distance of c.g. from front axle |
| B, B_1 | Constant coefficient matrices |
| B_2, B_{2P} | Front and rear damping rates |
| b | Distance of c.g. from rear axle |
| b_1, b_2 | Column vectors, partitioned from B |
| c | Road roughness parameter ($= 2\pi\delta$) |
| D | Time delay ($=L/V$) between the disturbance inputs to front and rear wheels |
| $E\{\cdot\}$ | Expectation or ensemble average |
| F | Feedback matrix |
| g | Gravitational acceleration |
| I | Performance index |
| J | Half the body pitching moment of inertia about the c.g. |
| k_0 | Overall static stiffness of suspension measured at the c.g. |
| k_1, k_{1P} | Front and rear tyre radial rates |
| k_2, k_{2P} | Front and rear suspension spring rates |
| L | Length of wheelbase ($=a+b$) |
| m | Half the total body mass |
| m_1, m_{1P} | Unsprung masses at front and rear |
| m_2, m_{2P} | Equivalent dynamic body masses supported by front and rear suspensions |
| n | exponent |
| $P(t)$ | Symmetric matrix function |
| \bar{P} | Constant matrix |
| Q | Constant weighting matrix |
| q_1 to q_4 | Weighting factors |
| R | Inertia coupling ratio ($=r^2/ab$) |
| $R(t)$ | Symmetric matrix |
| R_1 | Constant weighting matrix |
| r | Body pitch radius of gyration about c.g. |
| s | Laplace transform complex variable |
| S | Power spectral density |
| t | Time, sec. |
| u | Control force vector |
| V | Vehicle speed m/s |
| W | Covariance matrix of disturbance vector w |

NOMENCLATURE

| | |
|------------------|---|
| w | Disturbance input vector |
| w_1, w_3 | Elements of w |
| x_G | Vertical displacement of body c.g. from static equilibrium position |
| x | State vector |
| x_1, x_{1P} | Vertical displacements of front and rear unsprung masses |
| x_2, x_{2P} | Vertical displacements of front and rear sprung masses |
| x_0, x_{0P} | Road input displacements at front and rear contact points |
| y_1 to y_4 | Vertical displacements |
| β | Time scale factor |
| γ | Wave number or spatial frequency cycles/m |
| $\delta(t)$ | DIRAC delta function |
| $v(t)$ | Scalar white noise |
| π | Performance index |
| ρ_1, ρ_2 | Weighting factors |
| τ, τ' | Time delay, also dummy integration variable for time |
| ϕ | State transition matrix |
| ω | Frequency, rad./s. |

CONTENTS

| | <u>Page</u> |
|--|-------------|
| CHAPTER 1. INTRODUCTION | 1 |
| CHAPTER 2. PERFORMANCE CRITERIA | 3 |
| 2.1 Introduction | 3 |
| 2.2 Ride Comfort | 6 |
| 2.3 Road Holding and Ride Safety | 15 |
| 2.4 Wheel Travel | 17 |
| CHAPTER 3. MATHEMATICAL MODELS | 20 |
| 3.1 Introduction | 20 |
| 3.2 Modelling of Tyres | 21 |
| 3.3 Modelling of Road Surface | 25 |
| CHAPTER 4. CALCULATION OF VEHICLE RESPONSE DUE TO ROAD EXCITATION | 33 |
| 4.1 Introduction | 33 |
| 4.2 System Response in Frequency Domain | 35 |
| 4.3 System Response in Time Domain | 38 |
| CHAPTER 5. MODEL RESPONSE BY APPLICATION OF PARSEVAL'S THEOREM | 40 |
| 5.1 Introduction | 40 |
| 5.2 Integral Square Values by Parseval's Theorem | 41 |
| 5.3 Influence of Model Parameters on Integral Square Values | 45 |
| CHAPTER 6. PERFORMANCE INDEX AND WEIGHTING FACTORS | 51 |
| 6.1 Introduction | 51 |
| 6.2 Weighting Factor for Dynamic Tyre Deflection | 51 |
| 6.3 Weighting Factor for Body Force | 52 |
| 6.4 Parameter Values of Mathematical Model | 54 |
| 6.5 Theoretical Optima | 56 |
| 6.6 The Role of Performance Index in Suspension Optimisation Process | 58 |
| 6.7 Optimisation by Computer | 74 |

....cont'd:

CONTENTS

2.

| | <u>Page</u> |
|--|-------------|
| CHAPTER 7. MODEL RESPONSE BY APPLICATION OF STATE VARIABLES AND COVARIANCE MATRIX METHODS | 75 |
| 7.1 Introduction | 75 |
| 7.2 State Variable Analysis Applied to $\frac{1}{4}$ -car model | 75 |
| 7.3 Solution of Lyapunov Equation | 80 |
| CHAPTER 8. ANALYSIS OF $\frac{1}{2}$ -CAR MODEL | 85 |
| 8.1 Introduction | 85 |
| 8.2 Overall Static Stiffness of Suspension | 85 |
| 8.3 Analysis of $\frac{1}{2}$ -car Model | 88 |
| 8.4 Integral Square Response and Performance Index of Uncoupled $\frac{1}{2}$ -car Model (R=1.0) | 92 |
| 8.5 The Influence of Suspension Springs on Integral Square Response | 93 |
| CHAPTER 9. THE INFLUENCE OF COUPLING RATIO ON SUSPENSION RESPONSE | 110 |
| 9.1 Introduction | 110 |
| 9.2 Influence of Speed | 111 |
| 9.3 Damping and Coupling Ratio | 111 |
| 9.4 Suspension Spring Stiffness and Coupling Ratio | 131 |
| 9.5 The Influence of Vehicle Speed on Integral Square Response | 138 |
| CHAPTER 10. STATE VARIABLES AND COVARIANCE MATRIX METHODS APPLIED TO CALCULATION OF INTEGRAL SQUARE VALUES | 161 |
| 10.1 Introduction | 161 |
| 10.2 State Variable Analysis of Half-Car Model | 161 |
| CHAPTER 11. ANALOGUE COMPUTER SIMULATION | 171 |
| 11.1 Introduction | 171 |
| 11.2 Mathematical Model and Parameter Values | 173 |
| 11.3 Scaling, Machine Equations and Patching | 175 |
| 11.4 Results | 179 |
| 11.5 Summary | 192 |

.....cont'd:

CONTENTS

3.

| | <u>Page</u> |
|--|-------------|
| CHAPTER 12. SUMMARY AND CONCLUSIONS | 194 |
| APPENDIX A ANALOGUE COMPUTATION RESULTS | 212 |
| APPENDIX B TABLES OF CALCULATED COEFFICIENTS | 244 |
| APPENDIX C DIGITAL COMPUTER PROGRAMS | 252 |
| BIBLIOGRAPHY | 284 |

OPTIMISATION OF ROAD VEHICLE SUSPENSION SYSTEMS
BY APPLICATION OF DIGITAL AND ANALOGUE COMPUTERS



1. INTRODUCTION

In recent years a large number of papers have been published dealing with the response of road vehicles to road surface inputs, and the associated performance criteria such as the ride comfort, road holding ability, maximum wheel travel relative to vehicle body etc.

A comprehensive list of relevant references has been provided in the appendix which give closer information regarding various aspects of performance criteria.

Much of the theoretical work is associated with the analysis of passive and active suspension systems with a view to optimising dynamic response of the vehicle, the response criteria being based on various practical considerations or on national and international performance standards.

Road surface irregularity is a random process with power spectral density expressed in terms of spatial frequency, consequently dynamic response is usually obtained from the output spectral density using input-output transfer function techniques.

Mean square values of response can be obtained from the output spectral densities by integration which can be carried out analytically for simple transfer functions, or numerically for more complex systems.

The method tends to be cumbersome since it inherently involves a lot of complex algebra and can be quite tedious and prone to accidental errors.

Hence, other methods of analysis have been investigated, and are being used to obtain the same end results, sometimes more elegantly.

The analysis in s-domain using Laplace transformation in conjunction with Parseval's Theorem is very neat, enabling one to calculate the mean square responses for simple systems directly for a random road profile having a particular power spectrum density, but will become

rather forbidding for more complex systems, especially if the time delay is involved in input excitation as it is usually the case for successive sets of road wheels.

In several recent papers (8, 16, 17, 23), a method of analysis based on differential equations involving co-variance matrix in conjunction with state variable theory is proposed for evaluating dynamic responses, but even this latest development has its limitations when applied to passive systems.

The method originates from the studies in the control system theory, and involves the solution of Lyapunov matrix equations which in itself can be a formidable task for large systems. The method can be extended to handle time delayed inputs caused by successive wheels of a road vehicle.

2. PERFORMANCE CRITERIA

2.1 Introduction

A clearly defined performance criterion is always an essential basis and starting point for any optimisation process irrespective of the actual method of optimisation. There cannot be really any optimisation without a well defined performance criteria, i.e. the desired system output to a specified input.

In case of a road vehicle the more significant output parameters are:-

- 1) Ride comfort of the driver and passenger as influenced by translational and rotational acceleration components. A general translational and rotational acceleration vector will be present, but only the components most significant to ride comfort are usually considered.
- 2) Vehicle road holding characteristics which usually are related to the minimum contact force between the tyre and the road surface, i.e. directly related to dynamic tyre deflection.
- 3) Maximum practical wheel travel, i.e. relative displacement of wheel suspension. Several practical considerations set a limit for the maximum wheel travel.

The performance criteria as listed above can be analysed individually, and then the system parameters selected to provide the desired output. Unfortunately, most of the performance criteria are interrelated in such a way that a change in one parameter may result changes in other performance characteristics, often in opposition to the desired effect. On the other hand, a quantity known as the performance index could be formulated for the whole system under investigation. The performance index will involve all the significant features of response, and suspension parameters could be adjusted in order to minimise the performance index so as to ensure the desired overall performance.

A computer optimisation routine can be employed, usually involving two dimensional search, and by adjusting the system parameters a

minimum performance index and corresponding system parameters can be established. The method, in principle, is simple and straightforward, but has some doubtful areas in practice.

The major shortcoming of the method when applied to a road vehicle is that there are no precisely defined performance standards. In case of a road vehicle the performance criteria is the system output which is directly related to system input such as road roughness and vehicle speed. In order to define the standards for the output it also is necessary to define the standards for the input as it cannot be expected that the desirable ride comfort level could be maintained at any arbitrary vehicle speed and road roughness.

In order to appreciate all the implications associated with optimisation, the quantity defined as the performance index for a vehicle will be examined in detail. Refs. 64 and 65 discuss the selection principles of such an index at length.

The performance index is the sum of weighted mean square values of various responses considered important in defining the performance criteria for the system.

For a typical vehicle suspension the performance index is usually defined as:-

$$J = q_1 \bar{\delta}_1^2 + q_2 \bar{\delta}_2^2 + \rho \bar{\delta}_3^2$$

where $\bar{\delta}_1^2$, $\bar{\delta}_2^2$ and $\bar{\delta}_3^2$ are the mean square values of dynamic tyre deflection, relative wheel travel and body acceleration respectively, and q_1 , q_2 and ρ are the corresponding weighting factors.

Without loss of generality one of the weighting factors can be taken as unity, and the other two varied to emphasize one or the other aspect of suspension performance.

The mean square values appearing in the performance index can be obtained by one of the several methods such as Laplace transformation, integration of output spectral density function, application of co-variance matrix analysis, digital computer simulation or

analogue computer simulation.

Constraints can be imposed on the response, and if the constraints are violated, i.e. the limits of set performance criteria exceeded, the respective weighting factors can be increased until the performance criteria are met.

Refs. 64 and 65 list a number of FORTRAN algorithms for constrained and unconstrained optimisation.

In a broad outline, the principal procedure is to select ρ , q_1 and q_2 , and then minimise the performance index by varying the suspension parameters. The response is then calculated with the parameters as obtained in minimisation process, and compared with desired performance. If for example the acceleration criterion is not met, weighting factor ρ is increased and minimisation process repeated until the acceleration meets the set limits. Finally q_1 can be adjusted to satisfy the road holding criteria if q_2 is taken equal to unity. But acceleration limits may be violated in the latter process, hence a continuous verification of vehicle response is essential.

Thus the weighting factors ρ and q_1 can be varied to produce a soft ride with a correspondingly large suspension deflection or a stiff ride with considerably reduced deflections. It is a process of trading off one against the other.

The difficulty with any suspension optimisation problem is that all criteria are relative and the selection of weighting parameters is somewhat arbitrary, depending on individual judgement.

An optimal system is one which minimises the selected performance index. It should be realized, however, that a system would not be optimal under any other performance index, e.g. the vehicle suspension would no longer be optimal if the tyre pressure varies from the selected design value, or the mass distribution of the vehicle varies with the passenger load and luggage. Hence the trends, rather than the points on the plane become significant.

A method of optimisation which would show trends rather than the spot values would be more useful in a situation where several other significant parameters are known to vary as well. It is known that for a given wheel load and tyre pressure the stiffness of a commercial tyre can vary nearly +20% about the nominal value. Also dynamic stiffness of tyres decreases sharply as soon as the tyre is rolling. Attempts have been made to determine the relationship between static and dynamic stiffness of tyres but no general conclusions have been reached.

2.2 Ride Comfort

Probably the most important aspect from the point of view of road vehicle performance is the ride comfort. This aspect has attracted considerable amount of attention in the past, and a large amount of research has been devoted to it over a number of years. There is an extensive amount of literature available dealing with this type of research over the past few decades, but there is no agreement between the various research workers as to what are the limitations and how to really measure and evaluate the ride comfort on a quantitative basis since the whole aspect of ride comfort is too subjective.

It is not the intention here to list all relevant papers dealing with the topic, but to refer the interested reader to ref. (25) which gives an extensive literature survey dealing with human sensitivity to vibration. The results of various experiments suggest that the subjective response of an individual to an imposed vibration depends not only on the mechanical impedance of the human body, but also on a number of psychological and environmental factors.

It has also been established that human sensitivity to vibration is not only a function of velocity and acceleration amplitudes and frequencies but also depends on the character of motion (translation, rotation), direction of motion (horizontal, vertical) and duration of exposure to vibration.

There are currently three basic concepts in use which have been proposed for describing the ride comfort criteria:-

- 1) The concept of a ride index (26, 27)
- 2) The concept of vibratory power absorbed by human body (12, 28, 29)
- 3) Power Spectral Density envelope (30, 31, 32)

Ride indices are numerical evaluations of human response to combinations of acceleration and velocity amplitudes over a range of exciting frequencies.

Fundamental research in this area was conducted mainly by Janeway, and the principles were extended to I.S.O. standards.

The comfort limits as established by Janeway are shown in Fig. 2-1 while the I.S.O graphs defining the limits exposure as function of time are shown in Figs. 2-2, 2-3 and 2-4.

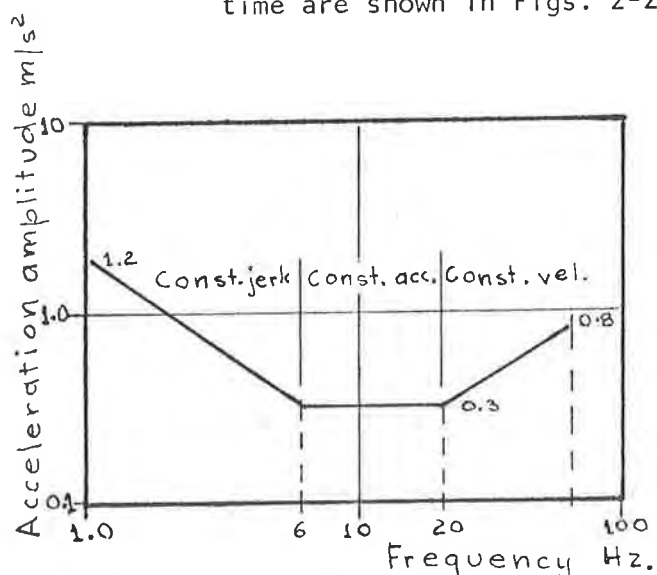


Fig.2.1. Limits of vertical acc.

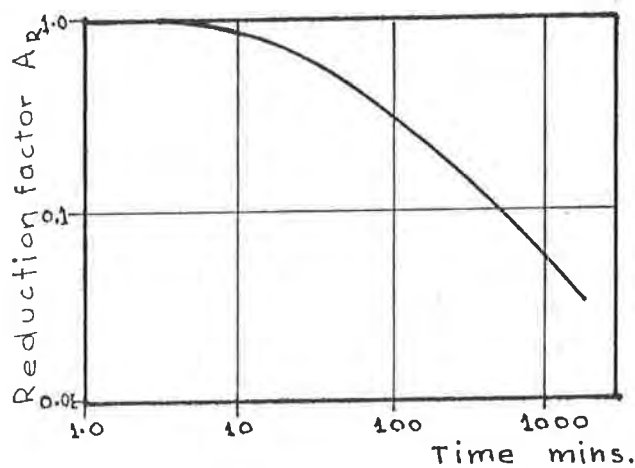


Fig.2.2. Reduction Factor I.S.O.2631

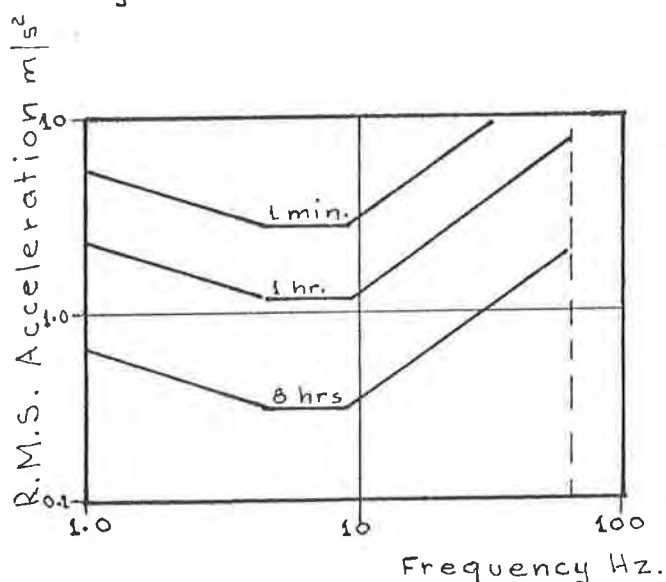


Fig.2.3. Limits of vert. acc. I.S.O.2631

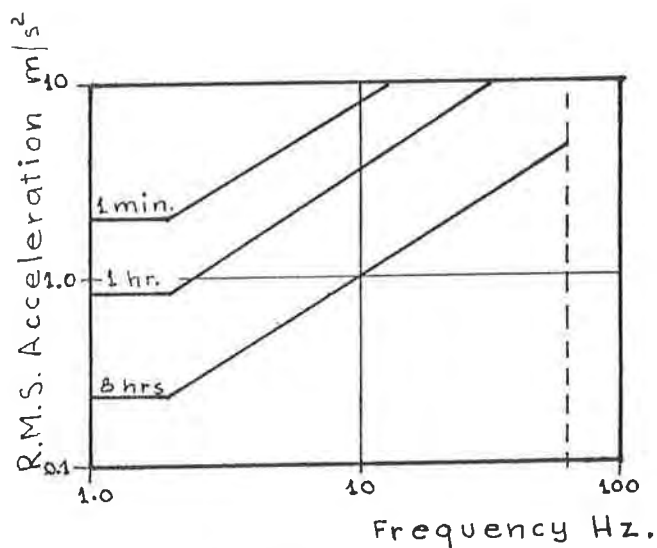


Fig.2.4. Limits of horiz. acc.

The tolerance curves shown were obtained by exposing test subjects to various vibration amplitudes and frequencies and asking them to describe the ride sensation in terms such as uncomfortable, disturbing, objectionable, fatigueing and intolerable. One basic shortcoming of establishing a ride index by these means is the imprecise definition used to describe the acceptable limit of vibration.

This, however, can never be avoided in any subjective assessment of the ride quality of a vehicle.

The second shortcoming is that the research workers have used mainly sinusoidal vibrations in the laboratory to establish the comfort criteria. Since the road surfaces are random profiles, the passengers are subjected to random vibration, but it is difficult to correlate sinusoidal and random vibration criteria for meaningful end results.

To overcome the trend of placing a heavy emphasis on subjective tests for the evaluation of comfort criteria, and avoiding the short-comings mentioned regarding the ride index concept, Pradko and Lee (28) introduced the concept of "absorbed power". They proposed the idea that the rate of flow of energy becomes the parameter that characterises the interaction of vibrating human body and the environment. The energy flow is a function of complex mobility (or mechanical impedance) of human anatomy.

When vibrational forces distort the elastic body, dimensional changes take place, producing reactions that tend to restore the body to the original position, and the work done in the process balances the applied load. Consequently the elasticity of the body produces restoring forces that are related to the displacement. The vibratory motion continues until the energy imparted is dissipated on internal damping.

The energy flow rate is the "absorbed power", defined as

$$AP = \lim_{T \rightarrow \infty} \frac{1}{T} \int_0^T f(t)v(t)dt$$

where $f(t)$ = input force
 $v(t)$ = input velocity.

In tests a limiting value of 290 watts of absorbed power was established as the tolerance limit, and the constant power curve was fitted to sinusoidal as well as random vibration curves. The results indicated that the 'absorbed power' displayed the same characteristics as the subjective judgement criteria.

Since the 'absorbed power' is an energy flow rate determined by the elastic properties of human anatomy, it is possible to measure the variation of this parameter for different people having different seating arrangements.

Usually the average 'absorbed power' is computed as a weighted integral of the acceleration spectral density where the weighting function is the squared magnitude of mechanical impedance of the human body at the boundary between the body and the medium imposing the motion where the acceleration is measured.

In the power spectral density concept of ride comfort, the acceleration spectrum is broken into different frequency bands. A correlation of the square of acceleration in each band with subjective response to vibration will then give a meaningful and useful ride criterion. A good example of this is given in ref. (20) relating to Urban Tracked Air Cushion Vehicle Specification.

The International Standard Organisation's 'Guide for the Evaluation of Human Exposure to Whole-Body Vibration', ISO 2631, has incorporated most of the experimental data regarding human exposure to vibration available from several countries, and has recently gained acceptance for many applications.

I.S.O.2631 defines and gives numerical values for limits of exposure to vibrations transmitted from solid surfaces to the human body in the frequency range of 1 to 80 Hz. These limits cover human sensitivity to vertical, lateral and fore-and-aft vibrations of a periodic, non-periodic or random nature with exposure times ranging from 1 min. to 24 hours. Periodic excitation is evaluated in

terms of r.m.s. acceleration amplitude while broad band excitation is evaluated in terms of r.m.s. acceleration levels measured through a third octave band filter.

According to I.S.O. guide, the humans are more sensitive to vibration frequencies in the range of 4 to 10 Hz for vertical motions, and 1 to 2 Hz range for fore and aft motions, and human tolerance to vibrations is assumed to decrease with increasing exposure time.

The authors in ref.(27) set out to verify the various ride quality criteria in realistic ride environment. The investigation involved two different automobiles, seventy eight test subjects and eighteen different roadway sections. The investigation included the following comfort criteria:-

- (1) Weighting functions derived from I.S.O. 2631, 1974 "Guide for Evaluation of Human Exposure to Whole Body Vibration" (32).
- (2) Urban Tracked Air Cushion Vehicle specification (30).
- (3) "Absorbed power" of Lee and Pradko (28).
- (4) Acceleration limits as function of frequency established by Janeway (26).

In the experiments a 1974 Buick Century Luxus and a 1975 Ford Maverick were driven over a variety of highway test sections, the roughness of which was identified by serviceability index (S.I.) on a six point scale 0 = very rough, 5 = very smooth). The actual sections used varied from S.I. 1.9 to 4.3. Each section was about 380m long without any significant curves or grades throughout the section.

In the tests the vehicle was driven at a constant speed of 80 km/hr over the test sections of varying roughness, from some fairly rough farm roads to very smooth highway sections. Vertical and horizontal accelerations were measured at the floorboard and on a 300 mm

dia plywood disc 6 mm thick placed between the seat of the vehicle and the 70 kg passenger sitting on the disc.

After riding over each test section, the subjects were asked to rate the respective ride from the point of view of ride comfort. Separate runs were made over each test section to record the accelerations and to conduct subjective rating tests. Subjective ratings were based upon a five point scale, ranging from 1 ("the worst ride you can think of") to 5 ("the best ride you can think of").

Examination of all the subjective ratings obtained indicated significant agreement between the individual subjective ratings and the average or mean rating which was called the Mean Personal Rating (MPR) by the authors. In addition, M.P.R's were highly correlated with S.I. ratings originally assigned to each test section by Texas State Department of Highways and Public Transportation, based on the measured roadway profiles.

The final evaluation of the test results showed that a number of different weighted indices, using either the floor-board data, or the seat vibrations, correlated with Mean Personal Ratings. In general, the indices using vertical vibrations correlated better with acceleration measured at the floor-board, while the indices using lateral vibrations correlated better with measurements taken at the seat interface.

Since a number of the proposed ride indices provided equally good correlation, the authors found it difficult to decide which among them is the best criterion, and concluded that most of them may be considered to be equally good.

Since the statistical difference between various ride indices is small, the authors suggest that the choice be based on generality and ease of use. From the standpoint of ease of use, the simple r.m.s acceleration criterion is preferable as no complicated weighting functions or filters are required. In addition, the results indicated that there is very little additional information relating to ride quality above 40 Hz band. Therefore, the r.m.s accelerations within 0 to 40 Hz band were recommended by authors

as the best all-around ride quality indicator, and the "unweighted" r.m.s accelerations were proposed for general use.

Based on the test results, the authors found that the following relationship between the Mean Personal Rating and the r.m.s acceleration gives the best fit:-

$$\text{MPR} = 5.43 - 40.0 \alpha$$

where α is the magnitude r.m.s (g) (the square root of the sum of the squares of vertical and lateral r.m.s accelerations). Acceleration measured at either the floorboard or at the seat. Where acceleration measurements are available only on one axis, the vertical axis is recommended if the measurements are taken at the floorboard, and the best fit equation using the vertical acceleration is

$$\text{MPR} = 5.55 - 49.4 \alpha$$

If seat vibrations are used the lateral r.m.s acceleration is recommended in the relationship:-

$$\text{MPR} = 5.57 - 54.9 \alpha$$

With this ride index $\text{MPR} \geq 4$ ($\alpha < 0.0314$ g or 0.31 m/s²) corresponds to the ride in a good automobile on a very smooth highway at 80 km/hr, $3 < \text{MPR} < 4$ ($0.51 > \alpha > 0.31$ m/s²) to a ride on a typical state highway, and $2 < \text{MPR} < 3$ ($0.64 > \alpha > 0.51$ m/s²) to a ride on a rough secondary road.

Since the study involved the use of different automobiles and variety of road spectra, the authors recommend the results for use with automobiles in general, but caution against directly applying the results of the study to vehicles which may have vibration characteristics significantly different from those of the test vehicles.

Since the work in ref.(27) is of recent origin (1978), the ride comfort ratings as proposed could be used as the basis for sus-

pension optimisation, but again the corresponding road input spectra and the vehicle speed are additional factors which have to be considered.

It thus appears that all a designer can do is to aim for the lowest possible r.m.s acceleration level achievable at the floor level or at the centre of mass of the vehicle, and ensure that for a comfortable ride the r.m.s acceleration should not exceed 0.3 m/s^2 at 80 km/hr vehicle speed on a road profile corresponding to a smooth highway.

Another aspect of ride comfort is the maximum duration of exposure to vibration at certain acceleration level as recommended in I.S.O 2631, 1974.

A number of research workers have been in substantial disagreement with parts of existing guidelines, and doubts have been expressed as to the applicability of the rules in I.S.O 2631 regarding the duration of exposure to vibration.

In order to shed some light to general confusion that seems to prevail, ref.(34) sets out to review in detail the evidence and data which have been used to support the claims in the guidelines that:-

- 1) There is a change of human reaction to vibration as a result of duration of exposure.
- 2) That this change is necessarily such that it results in decrease of comfort and reduces the ability to perform certain tasks (driving the car).
- 3) That the form of the change is adequately represented by the time dependance chart in I.S.O.2631.

The paper then goes on to review the results of some recent studies involving ride comfort of passengers in public transport vehicles, and some recent laboratory results on the performance of simple

tasks, all of which apparently show no evidence of change with time, at least for periods up to four hours.

In summing up all the available evidence, the author concludes that the time dependence curves quoted in I.S.O. 2631 seem to be based on:-

- 1) Subjective tolerance to extreme vibration at levels corresponding to violent aircraft manoeuvres.
- 2) Some unreliable test data obtained from aircraft experience which are limited entirely to frequencies below 1 Hz where motion sickness and other effects are likely to dominate.
- 3) Some curves used in railway vehicle design for which the background research data seems to be unobtainable.

According to the author, the curves relating to duration of exposure were based on results obtained from a laboratory experiment in which the subjects were exposed to vibration for some 5 minutes and then asked to estimate the duration of the exposure which they felt they could accept, in other words, the subjects were asked to extrapolate the exposure curves.

The final conclusion is that there is no evidence to indicate any clear reduction of comfort, or any reduction in performance ability with duration of exposure to vibration which is not already present in the absence of vibration. The author suggests that the effects of duration of exposure on ride comfort which have been quoted by research workers in the past could well have been due to inadequate seating or the effects of tiredness which are present irrespective of vibration.

The author draws a general conclusion that there is no evidence to support I.S.O time dependence effect in so far as it relates to "reduced comfort" or to "fatigue reduced proficiency" at vibration levels typically met in vehicles in service, and for periods up to four hours.

A further claim is made that Lee and Pradko (28) apparently did not measure the absorbed power since there is no evidence of phase angle measurement in their report. It thus appears that they merely provided an acceleration weighting function in the form of human body impedance, i.e.

$$P = \frac{1}{2} FV \cos \phi = \frac{1}{2} |Z| V^2 \cos \phi = \frac{1}{2} |Z| A^2 \cos \phi / \omega^2$$

The average absorbed power is computed as a weighted integral of the acceleration spectral density where the weighting function is the squared magnitude of the mechanical impedance of human body at the boundary between the test subject and the medium imposing the motion where the acceleration is measured.

2.3 Road Holding and Ride Safety

Longitudinal and lateral friction forces developed at the tyre-road interface are necessary for acceleration, braking and steering.

These forces depend on the tyre-road friction characteristics, tyre construction, road surface condition, and the force normal to the tyre/road interface, as well as suspension parameters and dynamic characteristics of the vehicle.

Friction forces are relatively high on a smooth, dry plane pavement, but are reduced due to dynamic wheel force exerted through the wheel of a moving vehicle which is excited by the road surface input.

To maintain adequate directional control of the vehicle, it is necessary to minimise the loss of road-to-wheel contact, i.e. to minimise dynamic tyre force in order to resist lateral skidding and transmit acceleration and braking force from tyres to the road. Hence, the knowledge of dynamic tyre forces is of considerable importance in studies of vehicle safety.

Since most road surface profiles are random functions, the resulting dynamic wheel forces are also random functions, and statistical representation of these forces is required. One statistical method most commonly used to estimate dynamic wheel forces is to determine the road surface power spectral density function, and the vehicle

response characteristics in order to obtain the power spectrum of dynamic wheel force. The power spectrum may be used to compute the r.m.s values of probability of exceeding a particular range of given value of wheel dynamic load. Ref.(39) deals with this aspect quite extensively, and the general conclusion is that dynamic tyre forces should be kept small for ride safety.

It has also been shown (40) that the variations in the normal forces between the tyres and the road influence the steering capability that in turn affect the lateral forces needed to control the vehicle.

The mean square dynamic tyre force is generally used as a measure of control of direction and stability (39, 41).

Optimal road holding is defined as the minimum probability that the randomly varying part of the road-wheel contact force will exceed a given level during a specified time period.

Dahlberg (37, 38) establishes the expected largest value of dynamic force on statistical basis by theoretically evaluating the expected value of the algebraically largest maximum of a stationary random function during the length of sampling period (calculates the mean of the largest value of a stationary Gaussian random process).

The expected value of the algebraically largest maximum of a stationary random function $f(t)$ during the sampling period T is approximately given by (36):-

$$E \left[f(t)_{\max} \right] = \left[\sqrt{2 \ln \nu T} + \gamma / \sqrt{2 \ln \nu T} \right] \sigma_f$$

where γ is the Euler's Constant ($\gamma = 0.572$)

σ_f is the standard deviation of function $f(t)$

and ν is the average frequency of positive mean value crossings.

Using a typical value $\nu T \approx 20$ according to ref. (36), the result is

$$E = f(t)_{\max} = 2.7 \sigma_f$$

Thus one might as well use the expected maximum value as

$$E \left[f(t)_{\max} \right] \approx 3 \times \text{RMS}$$

If the tyre contact is not to be lost for 99.97% of time, it follows that

$$3 \times \text{RMS Dynamic Tyre Force} \leq \text{static gravitational force on the wheel.}$$

This is probably the best assumption the designer can make, but the problem here again is that the value of dynamic tyre force must be associated with a road roughness profile and vehicle speed, i.e. the designer would have to estimate the probable vehicle speed appropriate for traversing a rough road.

This criterion would set an upper limit for dynamic tyre force. The minimum value then follows from trade-off studies in minimisation process.

2.4 Wheel Travel

The primary purpose of a vehicle suspension system is to isolate the passengers and cargo from road roughness and to maintain the desired vehicle body attitude under varying loads and external disturbances such as accelerating and decelerating forces applied to the vehicle through the road wheels.

It is desirable that the dynamic and static characteristics should be invariant under changing vehicle mass and inertia.

For an effective isolation and comfortable ride a soft suspension is required which would have a large deflection. On the other hand, to minimise roll angles and to provide a stable ride, a relatively stiff suspension would be preferable. The implications for passive suspension systems arising from these conflicting requirements are discussed at length in ref.(44).

Evidently the requirements to satisfy different criteria will always conflict to varying degrees, and the limiting wheel travel for passive suspension systems is usually established from pract-

ical considerations.

According to local car industry practice the testing and developing of the suspension system is carried out on the road, starting with a set of springs and shock absorbers which satisfy certain basic criteria, and then modify the component values until the suspension performs satisfactorily according to the subjective judgement of the suspension engineer who tests the vehicle by driving over various road surfaces and spoon drains. A local manufacturer uses a particular spoon drain as the proving ground for the final acceptance testing. If the suspension performs satisfactorily when driven over the drain at certain speed, and provides acceptable ride comfort on various road surfaces, the suspension is considered to be acceptable.

Broad design guidelines relating to locally manufactured passenger vehicles are as under :-

Clearance to bump stops when full laden (including luggage and full tank of fuel) 25 to 30 mm. Total static deflection from unladen to fully laden condition 75 mm max. This figure is mainly stipulated by customer acceptance and vehicle styling. If the deflection is in excess of 75 mm, the vehicle would stand up too high and would not be acceptable to stylists.

Published figures in motor magazines suggest that larger vehicles generally tend to have larger spring deflections, hence provide more comfortable ride. A comprehensive survey of suspension data for different models of passenger vehicles is given in ref.(53) from which it appears that the bump travel (unladen) varies from 70 to 100 mm, with an average value of 80 mm for the front suspension and 85 mm for the rear.

As a starting point for selection of springs a ride frequency of 1 to 1.8 Hz is taken as basis, the aim being that the vehicle should only bounce when hitting a bump and not pitch since pitching motion is considered more objectional from the point of view of ride comfort.

Shock absorbers are selected to give a damping ratio of approximately 0.3 for the sprung mass system.

The smaller the car, the more effect has the load on its suspension characteristics, hence small cars when laden only by the driver feel rough on roads.

The bump clearance is really only a compromise. Suspension engineers would like to have much more clearance, but the stylists would prefer to have much less.

Rebound travel is usually limited to 75 mm, either by straps or providing "stops" in the shock absorbers.

The guidelines as outlined above provide some limiting values for modelling.

3. MATHEMATICAL MODELS

3.1 Introduction

The type of model selected to represent a particular system is closely related to the specified system performance and the required output information.

The motor vehicle is a complex assembly of distributed mass and elasticity, hence a lumped parameter representation will exhibit some inherent shortcomings. In principle, the distributed mass and elasticity of the chassis, drive shaft, transmission, engine etc. could all be incorporated in the model, but then the model itself would become far too complicated, and it is always questionable if excessive complication will actually lead to more accurate analysis.

The simplest model that provides all desired output information to an acceptable degree of accuracy is to be preferred for a number of obvious reasons.

In case of a motor vehicle, the simplest model would be a $\frac{1}{4}$ car model (Fig.3.1) incorporating one wheel, spring damper and the proportion of the sprung mass supported by that spring. Despite the apparent simplicity of the model, much useful information can be derived by its use as shown successfully by several research workers in this field. Ref. (15, 35, 36, 42, 52, 55) outline some of the work.

A $\frac{1}{2}$ car model (Fig.3.2) however, is more realistic since the pitching of the vehicle body is also an important aspect of investigation. In case of a $\frac{1}{2}$ car model it is possible to investigate the coupling between the front and rear motions with time delay that occurs between the inputs to the front and rear wheels. Also the effect of shifting the mass centre of the vehicle by passengers or cargo can be studied in detail.

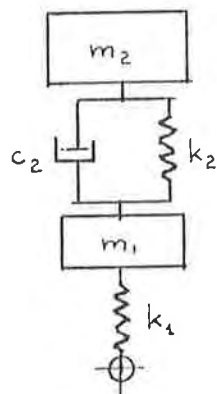


Fig. 3.1

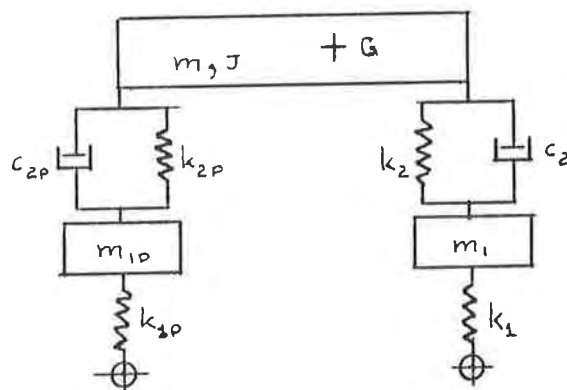
 $\frac{1}{2}$ Car Model

Fig. 3.2

 $\frac{1}{2}$ Car Model

The $\frac{1}{2}$ car model with its four degrees of freedom is quite popular among the research workers, and has been extensively used for suspension analysis and synthesis, but it cannot give any information regarding the body roll. If body roll is considered to be a significant performance criterion, a full car model with 7 degrees of freedom as in Ref. (8) would be the minimum requirement.

3.2 Modelling of Tyres

The basic functions of a pneumatic tyre are to provide support and guidance to the vehicle and filter the vibration transmitted from road surface irregularities. It also will reduce the dynamic forces imparted to the road surface which is quite important from the point of view of damage to road surface.

The cushioning characteristics of a pneumatic tyre can be represented by various mathematical models, and the simplest model consists of a mass element and a linear spring, in parallel with a viscous damper as illustrated in Fig. 3.3. A better approximation to actual tyre behaviour is displayed by the viscoelastic model shown in Fig. 3.4, but this model will add additional complications to analysis. Tyre damping has a relatively little effect on suspension behaviour, hence it is often neglected in the analysis.

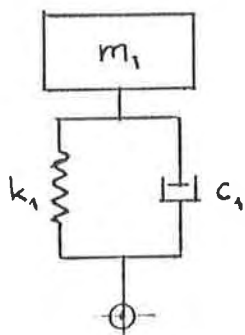


Fig. 3.3

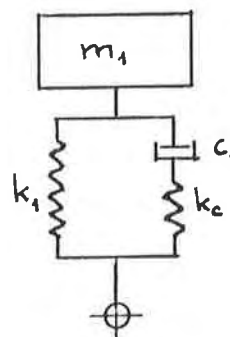


FIG. 3.4

Many different tyre models have been proposed and investigated in detail. Ref.(54) gives a comprehensive overview of various tyre models and discusses their characteristics at length. References (55) and (58) show how surface irregularities are effectively smoothed due to deformation of the tyres and propose suitable mathematical functions to describe the resulting road input.

For good filtering of vibrations, the tyre should have low vertical stiffness, but for good handling a high lateral stiffness would be required. In the present form of construction as an inflated toroidal envelope a low vertical stiffness also results in low lateral stiffness. To improve the lateral stiffness radial ply tyres have been developed by tyre manufacturers, and these tyres have a slightly improved lateral/vertical stiffness ratio but there is a limit that can be achieved in practice.

In general, the tyres have a relatively high vertical stiffness by their function, and there is not very much that can be done in reducing vertical stiffness without significant deterioration in vehicle handling.

As to the actual values of spring and damper elements in the model, there are complications since three distinct types of tyre stiffness may be defined depending on test conditions:- static, non-rolling dynamic and rolling dynamic stiffness.

Static stiffness of a tyre is determined from the slope of static load-deflection curve, it depends on tyre construction and inflation pressure. Since up to 15% of the load may be supported by the tyre carcass which has non-linear characteristics, some nonlinearity in

the deflection curves is to be expected, especially in low load region. Ref.(59) deals quite extensively with this aspect of pneumatic tyres. In the range of practical interest the load-deflection characteristics for both the bias-ply and radial-ply tyres are more-or-less linear, and it can be assumed that tyre stiffness is independent of load.

The graphs of stiffness v.s. inflation pressure of pneumatic tyres are linear for all practical purposes. Typical characteristics are shown in Fig.3.5 plotted with data taken from Ref.(59).

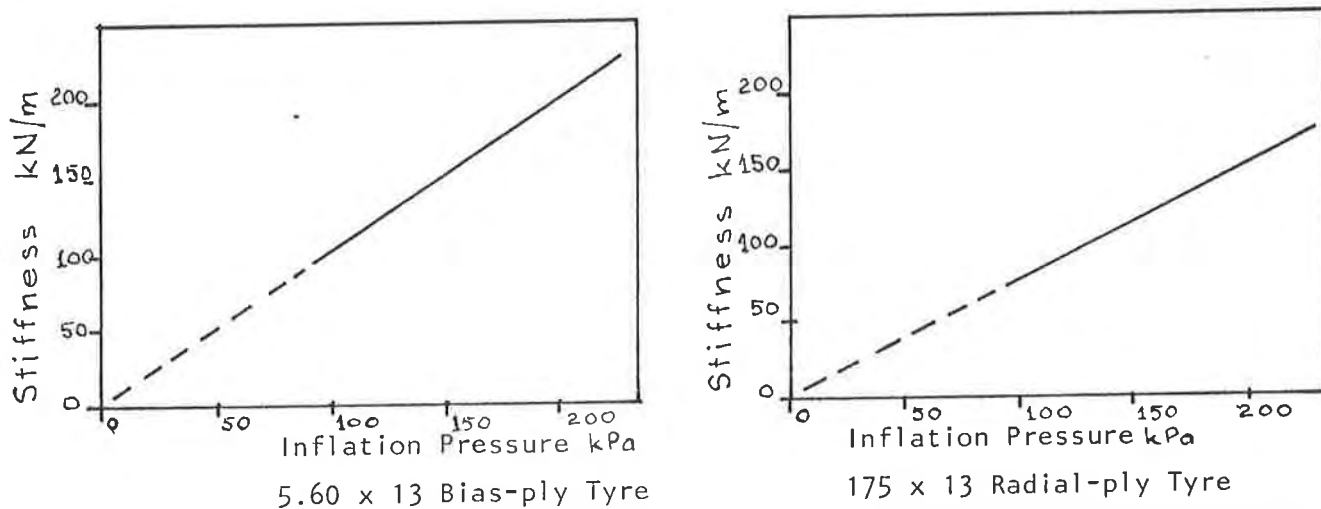
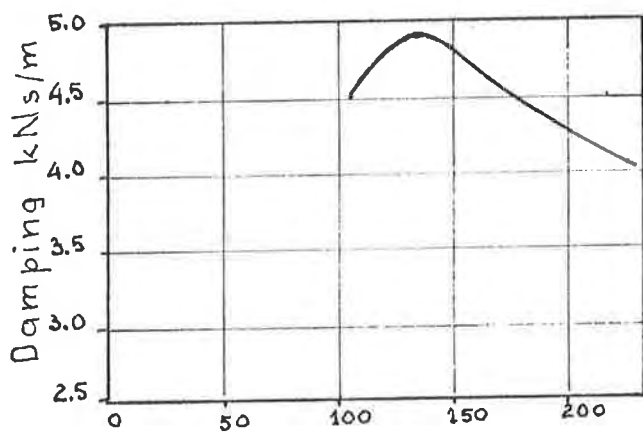


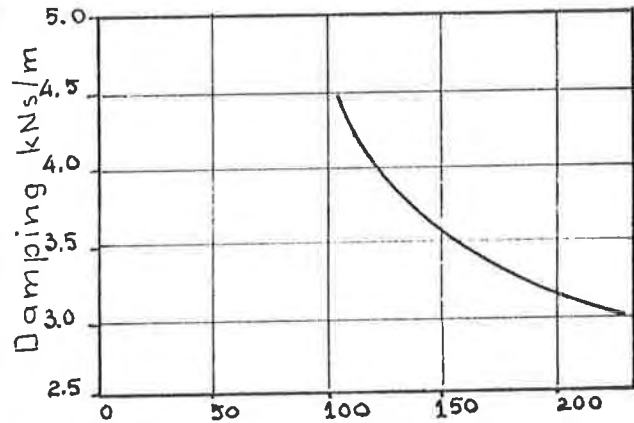
Fig. 3.5: STATIC TYRE STIFFNESS AS FUNCTION OF INFLATION PRESSURE

Non-rolling dynamic stiffness and damping are usually determined in a "drop-test", i.e. the tyre loaded with a certain additional mass is allowed to fall freely from a height at which the tyre is just in contact with the ground. Consequently the tyre remains in contact with the ground during the subsequent vertical oscillations. The vertical acceleration of the tyre can be recorded which on integration give the velocity and displacement records. From the resulting amplitude decay curve tyre stiffness and damping can be calculated if the mass of the wheel assembly is known.

Typical damping characteristics of pneumatic tyres as function of inflation pressure are shown in Fig.3.6. The inflation pressure has relatively small influence on tyre damping since damping is mainly dependent on tyre construction and materials.



Inflation Pressure kPa
5.60 x 13 Bias-ply Tyre



Inflation Pressure kPa
165 x 13 Radial-ply Tyre

Fig. 3.6: DAMPING COEFFICIENT OF TYRES AS FUNCTION OF INFLATION PRESSURE.

The rolling dynamic stiffness of a tyre is obtained by subjecting the tread to a specified rolling harmonic excitation and measuring the response of the tyre. The response is usually measured at the hub while the tyre is excited by rolling it against harmonic profile. The dynamic stiffness and damping are determined from output-input transfer function.

Dynamic stiffness of a pneumatic tyre decreases sharply (by 15%-20%) as soon as the tyre starts rolling but the graph tends to flatten out with increasing speed so that at speeds in excess of 20 km/hr the influence of speed is comparatively insignificant. Since in simulation studies of vehicle ride characteristics the rolling dynamic stiffness is more meaningful, attempts have been made to establish the relationship between the static and dynamic stiffness of pneumatic tyres but the results of these attempts have been inconclusive so far.

It is generally accepted that for car tyres the rolling dynamic stiffness may be 10-15% less than the static stiffness.

The author in Ref.(60) expresses the opinion, however, that the differences between the static and dynamic stiffnesses as reported in the literature may not be due to dynamic effects at all, but the result of applying linear analysis to a non linear system such as the tyre when the parameters are calculated from dynamic test

data.

In addition to operational parameters such as inflation pressure, speed and vertical wheel load, also the design parameters of the tyre such as the crown angle of cords, thread width, number of plies and materials used in tyre manufacture will affect the stiffness.

The damping of a pneumatic tyre is mainly due to hysteresis of tyre materials. It is neither Coulomb friction nor is it the viscous damping but some combination of both, and certainly non-linear. An equivalent damping coefficient is usually arrived at in dynamic tests, and its value depends on design and construction as well as on operating conditions.

There is some evidence that the damping of pneumatic tyres manufactured from synthetic materials is somewhat less than that provided by shock absorbers, and its influence on predicting the dynamic behaviour of the vehicle is relatively small. Hence, in most simulation studies the tyre damping effect is usually neglected, i.e. the parallel damper with the tyre stiffness is omitted from the dynamical model of the tyre.

3.3 Modelling of Road Surface

The road surface over which the vehicle is to travel is always more, or less irregular, random profile, and measurements indicate that it can be described in statistical terms.

The irregularities of many roads can approximately be described in terms of vertical amplitude mean square spectral density $S(\gamma)$ where γ is the wave number (cycles/m) or spatial frequency. It is not possible to establish $S(\gamma)$ for a given road with great precision since the road profiles are not truly realisations of stationary random processes, also the profile records are of finite length of necessity.

Two basic methods are in use for establishing the spectra of a road profile:-

- 1) A road profilometer which follows the road profile is towed behind a test vehicle as in references (8, 56, 57).
- 2) The profile is established by direct vertical measurements from a truly horizontal rail (or beam) which is set up by means of a theodolite. The usual beam length is of the order of 6m, and typical sample length is taken over 3 lengths (Ref.(9)).

Where profile measurements are available, profile spectral density $S(\gamma)$ can be computed directly for a particular section of road. The spectra must cover the range of wave numbers relevant for the required response spectra, i.e. if the response spectra is to be established over the frequency range of $0.5 \text{ Hz} < f < 50 \text{ Hz}$ for the range of vehicle speeds of $5 \text{ m/s} < v < 50 \text{ m/s}$ ($18 \text{ km/hr} < v < 180 \text{ km/hr}$) then the road spectra must cover the wave number range of $0.01 \text{ cycles/m} < \gamma < 10 \text{ cycles/m}$ since $\gamma = f/v$.

Where road profile measurements are not available, and a spectrum representative of a class of roads is required, Robson & Dodd (Ref.(2, 3, 4)) recommend that the following mathematical model for spectral density be used.

$$S(\gamma) = S(\gamma_0) (\gamma_0/\gamma)^{-w} \quad (3.1)$$

where (γ_0) is the vertical amplitude mean square spectral density (m^2/cycle) at the reference spatial frequency which is taken as

$$\gamma_0 = 1/2 \pi \text{ cycles/m}$$

Two values are recommended for the exponent w , as under:-

$$\begin{array}{ll} w = 1.5 & \text{when } \gamma < \gamma_0 \\ w = 2.0 & \text{when } \gamma > \gamma_0 \end{array}$$

These values have also been adopted by I.S.O standards for description of road profile.

Typical parameter values for road spectra as presented by MIRA Report No. 1970/5, are tabulated below.

TABLE 3.1

| Road class | Quality | $S(\gamma_0)$ | w_1 | w_2 |
|-----------------|-----------|---------------|-------|-------|
| Motorways | Very good | 2-8 | 1.945 | 1.360 |
| | Good | 8-32 | | |
| Principal roads | Very good | 2-8 | 2.05 | 1.440 |
| | Good | 8-32 | | |
| | Average | 32-128 | | |
| | Poor | 128-512 | | |
| Minor roads | Average | 32-128 | 2.28 | 1.428 |
| | Poor | 128-512 | | |
| | Very Poor | 512-2028 | | |

$\phi(\gamma)$ measured in units of $10^{-6} \text{ m}^3/\text{cycle}$

Since two different exponent values are used in describing the road spectra, there will be a break in the slope at γ_0 if the data is presented in the form of a log-log plot as it is usually the case. Now the spatial frequency of $1/2\pi$ cycles/m (γ_0) corresponds to a wavelength of 2π m, and the author of Ref.(4) points out that this length (20 ft) also happens to be the standard length in road construction technique in U.S.A. Thus the break in spectral density envelope may be related to a particular method of road construction rather than being a characteristic feature of all road surfaces.

A road with a large value of w implies decreasing road roughness at shorter wave-lengths. As the state of repair of road deteriorates, a decrease in the value of the exponent is to be expected. Also rough country roads suggest a small value of exponent.

Measurements from a large number of roads have been compiled in Ref.(1).

The description of the road surface in the form of a precise mathematical function can only be an approximation to any particular road profile, and in most cases of ride simulation there would be nothing gained by employing a discontinuous road surface function as given by equation 3.1.

Robson in Ref.(6) recommends that for most simulations a simple road surface model of the form

$S(\gamma) = \delta \gamma^{-n}$ would be quite adequate and recommends $n = 2.5$ to be used in conjunction with the range of values for the road roughness coefficient as listed below.

| <u>Type of Road</u> | <u>Range of δ</u> | <u>Mean value of δ</u> |
|---------------------|--|--|
| Major Motorway | $0.03 \times 10^{-6} - 0.5 \times 10^{-6}$ | 0.10×10^{-6} |
| Principal road | $0.03 \times 10^{-6} - 8.0 \times 10^{-6}$ | 0.50×10^{-6} |
| Minor road | $0.50 \times 10^{-6} - 30 \times 10^{-6}$ | 5.0×10^{-6} |

The values listed give $S(\gamma)$ in m^3/cycle where γ is in cycles/m and $n = 2.5$. It is important to realize here that the road roughness coefficient δ is not a dimensionless quantity in this definition but will have the dimensions $(\text{Length})^{3-n}$. This aspect requires careful observance when road surface data in imperial units are converted into metric and vice versa.

In practice, a departure from a straight line log-log plot is also expected at low values of space frequency (large values of wavelength), since the road roughness amplitude cannot increase indefinitely with increasing wavelength.

To overcome this dilemma some research workers(52,70,71) have suggested a modified road surface model in the form

$$S(\gamma) = \frac{A}{\gamma_0^2 + \gamma^2}$$

which represents first order lag, while others (6) recommend the use of a road spectra with limited amplitude at low frequencies and with high frequency cut-off as demonstrated in Fig.3.7.

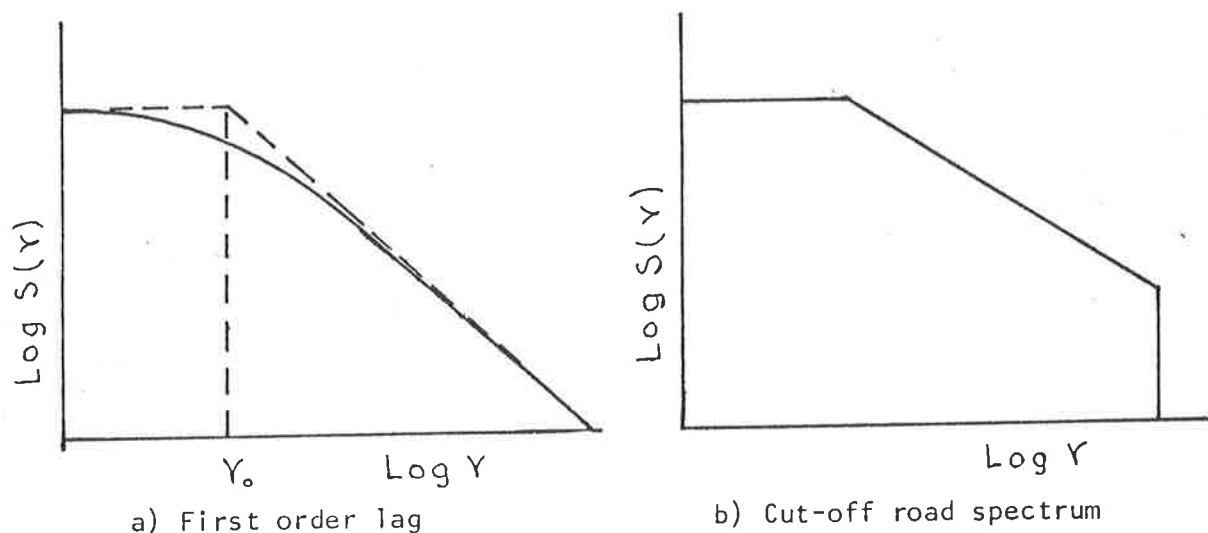


FIG. 3.7: MODIFIED ROAD SPECTRA

Modified road spectra are more realistic since they overcome the problem of the amplitude tending to infinity on low frequencies, but they will create complications in the analysis.

Since a number of workers have used straight-line road profile spectrum quite successfully, it is reasonable to examine the justification for its use.

The input to the model is filtered through the system impedance, and the only frequencies that are effective are those which come within the system pass-band. Very low and very high frequencies are cut off by system filter. Consequently, as long as the mean squares of differences of response are used as the performance criteria and not the absolute displacements, the fact that the road model spectral density tends to very high values at low frequencies should be of little concern.

No spectral description based on road profile measurements can be reliable over more than a few decades of a wave number, hence no analytical representation can be valid outside the region of actual measurement, and a profile spectrum must be obtained over the range of wavenumbers likely to be relevant in prediction of vehicle response over the desired frequency and speed range.

The relationship between the frequency, speed and wave-number

range is shown on the plot in Fig.3.8.

The range of wave numbers for any given range of vehicle speeds and the required frequency range can easily be established from the graph by drawing in the appropriate limits.

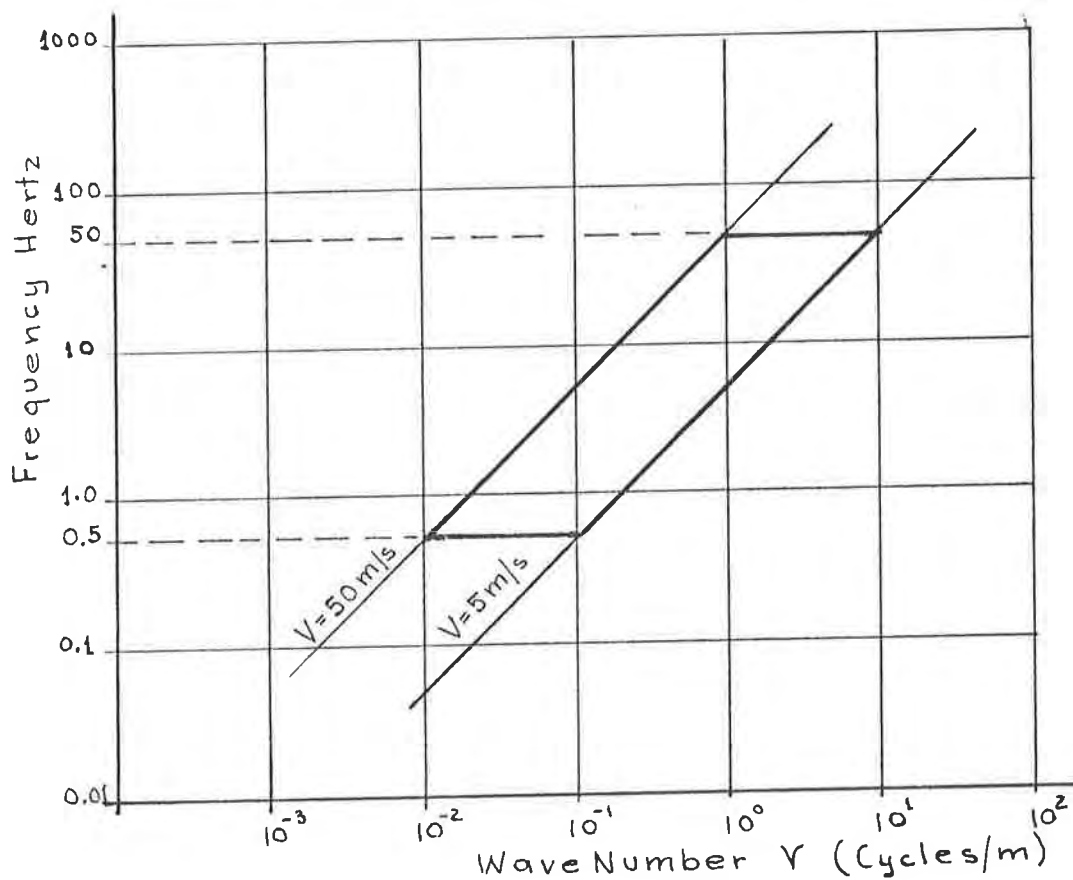


FIG. 3.8: RELATIONSHIP BETWEEN FREQUENCY, SPEED AND WAVE-NUMBER.

The road surface description $S(\gamma)$ as a function of the wave number or spatial frequency is converted into an input time function $S(f)$ or $S(\omega)$ as the vehicle travels over the road surface with speed V .

The input spectral density is now described in terms of frequency f or angular frequency $\omega = 2\pi f$, where $f = V\gamma = V/\lambda$.

It can be shown (Ref.(18,46)), that $S(\gamma)$ and $S(f)$ are related by the following relationship:-

$$S(\gamma) = V S(f) \quad (3.2)$$

$$\text{also } S(f) = 2\pi S(\omega) \quad (3.3)$$

If $S(\gamma)$ is described as $S(\gamma) = \delta\gamma^{-n}$, it then follows that

$$S(f) = V^{-1} \delta\gamma^{-n} \quad (3.4)$$

$$\text{and } S(\omega) = (2\pi V)^{-1} \delta\gamma^{-n} \quad (3.5)$$

but $\gamma = f/V = \omega/2\pi V$, which on substitution into equ. (3.5) gives

$$S(\omega) = (2\pi V)^{-1} \delta\omega^{-n} \quad (3.5)$$

Thus the input spectral density can be expressed in terms of ω and vehicle speed V .

In recent years a large amount of road surface data have been published in technical literature, some data are tabulated below for comparison.

TABLE 3.1 ROAD SURFACE DATA (Metric Units)

| Road Description | δ | n | Source |
|-----------------------|-----------------------|------|----------|
| Typical city road | 1.2×10^{-6} | 2.50 | Ref.(9) |
| Country road | 6.1×10^{-6} | 3.18 | |
| Major motorway | 1.95×10^{-6} | 2.71 | |
| Smooth runway | 4.3×10^{-6} | 3.8 | Ref.(13) |
| Rough runway | 8.1×10^{-6} | 2.1 | |
| Smooth highway | 4.8×10^{-6} | 2.1 | |
| Highway with gravel | 4.4×10^{-6} | 2.1 | |
| Pasture | 3.0×10^{-6} | 1.6 | |
| Ploughed field | 6.5×10^{-6} | 1.6 | |
| Very rough minor road | 2.0×10^{-6} | 2.0 | Ref.(14) |
| Old concrete road | 1.0×10^{-6} | 2.0 | Ref.(15) |

The inspection of tabulated values indicates a wide variation among the roughness parameter δ and the exponent n .

If the model analysis is restricted to a surface corresponding to a typical highway then $\delta = 1.0 \times 10^{-6}$ m with $n = 2.0$ could be used for comparative analysis, and the input spectral density for a vehicle travelling on a typical highway could be described by the expression:

$$S(\omega) = 2\pi V \delta / \omega^2$$

$$\text{or } S(\omega) = (2\pi V) \times 10^{-6} / \omega^2 \quad (3.6)$$

4. CALCULATION OF VEHICLE RESPONSE DUE TO ROAD EXCITATION.

4.1 Introduction

There are several methods which can be applied to obtain the response of a vehicle travelling with a constant speed V on a random road surface described by spectral density function $S(\omega)$.

Some research workers (Ref.(7,8)) argue that mathematical roadway model of the form $S(\gamma) = \delta\gamma^{-n}$ is too inaccurate for road surface description, and have used the actual values obtained by profilometer measurements suitably processed.

The actual method of analysis is often dictated by the required form of the response, e.g., the output spectral density can be obtained from the input spectral density by direct transformation. This, however, is not the only method of obtaining the output spectral density. In Refs.(16,17) the transition matrix solution is used but the output state variables are processed as passenger acceleration spectral density. In Ref.(8) the response is again obtained by transition matrix solution, and the output is transformed into passenger acceleration data in the time domain.

A more widely used technique is to use the transition matrix and covariance analysis to obtain the integral squared values of responses.

4.2 Output Spectral Density by Direct Transformation

If the required response is in the form of specified spectral density envelope such as body acceleration limits of some transport authorities, the spectral density of the response can be obtained by direct transformation

$$S_o(\omega) = H^*(\omega) S_i(\omega) H^T(\omega) \quad (4.1)$$

where S_o is the output spectral density matrix

S_i is the input spectral density matrix
(including cross spectral density terms)

H is the matrix of harmonic transfer functions applicable under discrete frequency excitation, and H^* is the com-

plex conjugate of H . Since harmonic transfer functions depend on system parameters, these can be varied to achieve the desired response.

The road spectral density can be expressed in the form

$$S(\omega) = (2\pi V)^{n-1} \delta \omega^{-n}$$

as previously discussed.

In a $\frac{1}{2}$ car model the front and rear wheels will follow the same track and are subjected to the same excitation, but since multiple excitation is involved, cross-spectral densities are required.

It is shown in Ref.(6) that

$$S_{12}(\omega) = S(\omega) e^{-j\omega\tau}$$

$$\text{and } S_{21}(\omega) = S(\omega) e^{j\omega\tau}$$

where τ is the time delay between the front and rear wheels, i.e.

$$\tau = \text{wheel base length/velocity.}$$

The excitation spectral density of a 2-wheeled $\frac{1}{2}$ car model can then be expressed as

$$S_1(\omega) = (2\pi V)^{n-1} \delta \omega^{-n} \begin{bmatrix} 1 & e^{-j\omega\tau} \\ e^{j\omega\tau} & 1 \end{bmatrix} \quad (4.2)$$

It is evident that the evaluation of the response is considerably simplified if n is an integer.

Very often the performance criteria are specified in terms of mean square values which can be obtained by integration of output spectral density, i.e.

$$\langle y^2 \rangle = \int_0^\infty S_o(\omega) d\omega$$

Closed form solution is possible only for very simple cases, and numerical integration techniques invariably become necessary for

anything beyond a single-degree-of-freedom model.

In general, a variety of methods can be applied for the solution of the problem, either in frequency domain or in time domain.

4.2 System Response in Frequency Domain

The Fourier transform of the autocorrelation function $R_{xx}(\tau)$, and its inverse can be expressed as

$$S_{xx}(\omega) = \int_{-\infty}^{\infty} R_{xx}(\tau) e^{-j\omega\tau} d\tau \quad (4.3)$$

$$\text{and } R_{xx}(\tau) = \frac{1}{2\pi} \int_{-\infty}^{\infty} S_{xx}(\omega) e^{j\omega\tau} d\omega \quad (4.4)$$

The mean square value of a stationary random process can then be expressed as:

$$E [x^2] = R_{xx}(0) = \frac{1}{2\pi} \int_{-\infty}^{\infty} S_{xx}(\omega) d\omega$$

Similarly the bilateral Laplace transformation can be used to define

$$S_{xx}(s) = \int_{-\infty}^{\infty} R_{xx}(\tau) e^{-s\tau} d\tau \quad (4.5)$$

$$\text{and } R_{xx}(\tau) = \frac{1}{2\pi j} \int_{j\infty}^{-j\infty} S_{xx}(s) e^{\tau s} ds \quad (4.6)$$

from Eq. 4.6 it follows directly that

$$E [x^2] = R_{xx}(0) = \frac{1}{2\pi j} \int_{j\infty}^{-j\infty} S_{xx}(s) ds \quad (4.7)$$

The time response $y(t)$ of a passive linear system to an arbitrary input $x(t)$ can be calculated from convolution integral

$$y(t) = \int_{-\infty}^{\infty} x(t - \tau)g(\tau) d\tau \quad (4.8)$$

where $g(t)$ is the unit impulse response function.

By the use of convolution integral and Laplace transformation, it is shown in Ref.(19) that the Laplace transform of the output spec-

tral density can be expressed as

$$S_{yy}(s) = G(-s)G(s)S_{xx}(s) \quad (4.9)$$

$$\text{where } G(s) = \int_{-\infty}^{\infty} g(t)e^{-st} dt$$

$$\text{and } g(t) = \frac{1}{2\pi j} \int_{-j\infty}^{j\infty} G(s) e^{st} ds$$

This is analogous to Fourier transformation where

$$S_{yy}(\omega) = H^*(\omega) H(\omega) S_{xx}(\omega) \quad (4.10)$$

$$\text{where } H(\omega) = \int_{-\infty}^{\infty} g(t) e^{-j\omega t} dt$$

$$\text{and } g(t) = \frac{1}{2\pi} \int_{-\infty}^{\infty} H(\omega) e^{j\omega t} d\omega$$

Now the mean square values of the response can be expressed as

$$E[\bar{y}^2] = \frac{1}{2\pi} \int_{-\infty}^{\infty} |H(\omega)|^2 S_{xx}(\omega) d\omega \quad (4.11)$$

$$\text{or } E[\bar{y}^2] = \frac{1}{2\pi j} \int_{-j\infty}^{j\infty} G(s)G(-s)S_{xx}(s) ds \quad (4.12)$$

The input spectral density due to road profile was discussed at length in chapter 3, and it was shown that the road input spectral density can be approximated by

$$S(\omega) = (2\pi V)^{n-1} \delta \omega^{-n}$$

where very smooth, well maintained roads are characterised by $n \approx 3$ while "average" road surfaces correspond to $n \approx 2$.

With $n = 2$, the equation for the mean square value of the response can be expressed as

$$E[\bar{y}^2] = \frac{1}{2\pi j} \int_{-j\infty}^{j\infty} 2\pi V \delta \left(\frac{G(s)}{S} \right) \left(\frac{G(-s)}{-S} \right) ds \quad (4.13)$$

Equation 4.13 implies that in case of an "average" road profile, the mean square response of a linear model to the random road sur-

face input is of the same form as the response to a step input, since $F(s) = 1/s$ for a unit step, and $Y(s) = G(s) F(s)$.

This aspect will simplify the analytical treatment of the problem to the extent that some closed form solutions are possible. Without this simplification it would be almost impossible to handle the problem analytically.

The use of a step input is also advantageous in the case of an analogue or digital computer simulation since it is much simpler to apply a step function repeatedly and make suitable adjustments to system parameters between trials rather than to apply random input, since the optimisation in statistical sense may require very long integration periods to ensure consistent results. These aspects have been extensively discussed in references (20) and (21).

The mean square value of the response in Eq.4.13 is basically in the form of Parseval's Theorem (19,20,21,22), i.e.

$$\begin{aligned} \text{Integral Square value} &= \int_{-\infty}^{\infty} y(t)^2 dt \\ &= \frac{1}{2\pi j} \int_{-j\infty}^{j\infty} Y(s) Y(-s) ds \end{aligned} \quad (4.14)$$

The integral could be evaluated by one of the following methods:-

- a) Graphical integration
- b) Numerical integration
- c) Contour integration
- d) Tables of integrals, provided that $G(s)/s$ in Eq. 4.13 is a rational function of s and can be expressed in the form $c(s)/d(s)$ where

$$\begin{aligned} c(s) &= c_0 + c_1 s + \dots + c_{n-1} s^{n-1} \\ \text{and } d(s) &= d_0 + d_1 s + \dots + d_n s^n \end{aligned}$$

If the integrals can be expressed in the form

$$E \left[\overline{y(t)^2} \right] = \text{ISV} = \frac{1}{2\pi j} \int_{-j\omega}^{j\omega} \frac{c(s) c(-s)}{d(s) d(-s)} ds$$

then the tables published in references (19) and (22) can be used to evaluate the integrals, provided the power of s does not exceed

4. The formulae for integrals involving powers of s greater than 4 are apparently in error (21).

4.3 System Response in Time Domain

The most direct way of evaluating the response of the mathematical model in time domain is to carry out digital or analogue computer simulation.

A large number of simulation languages are available, some of them quite flexible and powerful. In the framework of this thesis ACSL (Advanced Continuous Simulation Language) has been used quite extensively for performance calculations.

It is a general type simulation language using Runge-Kutta integration routines, very simple to program but has a rather high usage of computer storage. An example of a typical ACSL simulation programme is shown in Appendix C.

Digital simulation has the advantage of very high precision and repeatability, usually not achievable in analogue computation. The main disadvantage of digital simulation is its discrete nature, and occasionally some unexpected phenomena may remain hidden among discrete points while it would be observable in a continuous simulation process.

The analogue computer has the advantage of continuous simulation and extreme flexibility in regard to setting the different parameter values but it is much more suited to qualitative rather than to precise quantitative investigation, especially in a situation where the response changes very slowly for different parameter values, and the minima are very flat.

Direct computer simulation in time domain has the additional advantage that all relevant aspects, such as the peak values and the duration of transients can be investigated in addition to calculated mean square values of the response.

In frequency domain analysis the peak amplitude information remains hidden unless direct Laplace transform inversion techniques are used for evaluating the time response. But this is an almost im-

possible task in the case of a complex multi-degree-of-freedom system, especially if a time-delay between the inputs is involved as is the case for a road vehicle.

An alternative method of evaluating the response in time domain is the analysis based on differential equations for the co-variance matrix of state variables of the model.

It was shown that the road profile power spectrum can be approximated by the expression

$$S(\omega) = 2\pi \delta V / \omega^2$$

This envelope represents the integrated white noise of amplitude $2\pi\delta V$, and the velocity input spectrum at the wheels is approximately white noise of amplitude $2\pi\delta V$ since $s_{\dot{x}} = \omega^2 S_x$.

Since the velocity input to road wheels is approximated by white noise of constant amplitude, covariance equations developed for the analysis of stochastic optimal control systems can be applied for response calculations.

The method can be extended to handle time-delayed inputs such as occur when the successive wheels traverse the road profile.

A number of research workers have successfully applied this method to vehicle suspension analysis and synthesis.

The method is adaptable to digital computer processing without the complex algebra associated with harmonic transfer functions. It also avoids the integration associated with calculation of integral squared values, and the output can be obtained in the form of time functions by the use of transition matrices.

A more common practice, however, is to compute the weighted integral square values directly by matrix operations since this approach is more suited for the optimisation process.

The programming, however, is quite extensive, much more so than for ACSL.

5. MODEL RESPONSE BY APPLICATION OF PARSEVAL'S THEOREM

5.1 Equations of Motion and Laplace Transformation

Consider $\frac{1}{4}$ car model as illustrated in Fig.5.1, where the following parameter definitions apply:-

k_1 = tyre stiffness

m_1 = unsprung mass (wheel, axle, some spring mass)

k_2 = stiffness of suspension spring

B_2 = damping rate of shock absorber

m_2 = sprung mass, i.e. part of body mass effectively supported by the respective suspension.

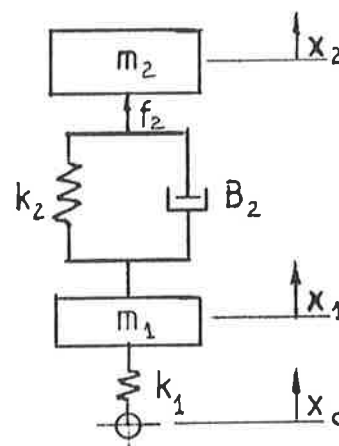


FIG.5.1

Evidently, the model is an oversimplification as it will give no indication of body pitching which is a significant ride comfort criterion.

A suitable performance index could be defined as the weighted sum of integral squared values in the form:-

$$\text{P.I.} = \int_0^{\infty} \rho u^2 + q_1 x_{o1}^2 + q_2 x_{12}^2 dt \quad \text{for a step input,}$$

$$\text{or P.I.} = E \left[\rho u^2 + q_1 x_{o1}^2 + q_2 x_{12}^2 \right] \quad \text{for random road input,}$$

where $u = f_2$ (force applied by suspension at body support point)

$$x_{o1} = x_o - x_1 \quad (\text{tyre deflection})$$

$$x_{12} = x_1 - x_2 \quad (\text{relative wheel travel})$$

and ρ , q_1 and q_2 are the weighting factors.

Equations of motion:-

$$-(x_1 - x_o)k_1 - (x_1 - x_2)k_2 - (\dot{x}_1 - \dot{x}_2)B_2 = m_1 \ddot{x}_1 \quad (5.1)$$

$$-(x_2 - x_1)k_2 - (\dot{x}_2 - \dot{x}_1)B_2 = m_2 \ddot{x}_2 \quad (5.2)$$

Taking Laplace transforms, with all initial conditions equal to zero, the equations can be expressed in matrix form as:-

$$\begin{bmatrix} (s^2 m_1 + s B_2 + k_1 + k_2) & -(s B_2 + k_2) \\ -(s B_2 + k_2) & (s^2 m_2 + s B_2 + k_2) \end{bmatrix} \begin{bmatrix} X_1(s) \\ X_2(s) \end{bmatrix} = \begin{bmatrix} k_1 X_o(s) \\ 0 \end{bmatrix} \quad (5.3)$$

where $X_1(s)$ and $X_2(s)$ are the Laplace transforms of $X_1(t)$ and $X_2(t)$ respectively, and $X_o(s)$ is the Laplace transform of the input $X_o(t)$.

For an input step of magnitude X_o , $X_o(s) = X_o/s$ and the solution of (5.3) is

$$\begin{bmatrix} X_1(s) \\ X_2(s) \end{bmatrix} = \frac{1}{|\text{DET}|} \begin{bmatrix} (s^2 m_2 + s B_2 + k_2) & (s B_2 + k_2) \\ (s B_2 + k_2) & (s^2 m_1 + s B_2 + k_1 + k_2) \end{bmatrix} \begin{bmatrix} k_1 X_o/s \\ 0 \end{bmatrix} \quad \dots (5.4)$$

where

$$\begin{aligned} |\text{DET}| &= (s^2 m_1 + s B_2 + k_1 + k_2)(s^2 m_2 + s B_2 + k_2) - (s B_2 + k_2)^2 \\ &= s^4 m_1 m_2 + s^3 B_2 (m_1 + m_2) + s^2 (m_1 k_2 + m_2 k_2 + m_2 k_1) \\ &\quad + s B_2 K_1 + k_1 k_2 \end{aligned}$$

Hence, the Laplace transforms of the response due to step input are:-

$$\frac{X_1(s)}{X_o} = \frac{(s^2 m_2 + s B_2 + k_2) k_1}{s |\text{DET}|} \quad (5.5)$$

and

$$\frac{X_2(s)}{X_o} = \frac{(s B_2 + k_2) k_1}{s |\text{DET}|} \quad (5.6)$$

5.2 Integral Square Values by Parseval's Theorem.

(a) Dynamic Tyre Deflection.

Laplace transform for dynamic tyre deflection is given by

$$\frac{X_o(s) - X_1(s)}{X_o} = \frac{|\text{DET}| - (s^2 m_2 + s B_2 + k_2) k_1}{s |\text{DET}|} \quad (5.7)$$

$$= \frac{s^3 m_1 m_2 + s^2 B_2 (m_1 + m_2) + s k_2 (m_1 + m_2)}{s^4 m_1 m_2 + s^3 B_2 (m_1 + m_2) + s^2 (m_1 k_2 + m_2 k_2 + m_2 k_1) + s B_2 k_1 + k_1 k_2} \quad (5.8)$$

The function can be expressed in the form

$$\frac{X_o(s) - X_1(s)}{X_o} = \frac{c_3 s^3 + c_2 s^2 + c_1 s + c_o}{d_4 s^4 + d_3 s^3 + d_2 s^2 + d_1 s + d_o} \quad (5.9)$$

where

$$\begin{aligned} c_3 &= m_1 m_2 & d_4 &= m_1 m_2 \\ c_2 &= B_2 (m_1 + m_2) & d_3 &= B_2 (m_1 + m_2) \\ c_1 &= k_2 (m_1 + m_2) & d_2 &= k_1 m_2 + k_2 (m_1 + m_2) \\ c_o &= 0 & d_1 &= B_2 k_1 \\ & & d_o &= k_1 k_2 \end{aligned}$$

According to ref.(19), Appendix D, Table of Integrals, the integral square value of the function is given by the expression

$$I_4 = \frac{c_3^2 (-d_o^2 d_3 + d_o d_1 d_2) + (c_2^2 - 2 c_1 c_3) d_o d_1 d_4 + (c_1^2 - 2 c_o c_2) d_o d_3 d_4 + c_o^2 (-d_1 d_4^2 + d_2 d_3 d_4)}{2 d_o d_4 (-d_o d_3^2 - d_1^2 d_4 + d_1 d_2 d_3)} \quad (5.10)$$

Noting that $c_o = 0$ and $c_3 = d_4 = m_1 m_2$, the expression simplifies to

$$I_4 = \frac{d_4 (-d_o d_3 + d_1 d_2) + (c_2^2 - 2 c_1 c_3) d_1 + c_1^2 d_3}{2 (-d_o d_3^2 - d_1^2 d_4 + d_1 d_2 d_3)} \quad (5.11)$$

After substituting the appropriate values into equation 5.11, the expression for the integral square value of tyre deflection becomes

$$I_4 = \frac{k_1 (m_1 + m_2)^2 B_2^3 + [m_1 m_2^2 k_1^2 - 2 k_1 k_2 m_1 m_2 (m_1 + m_2) + k_2^2 (m_1 + m_2)^3] B_2}{2 k_1^2 m_2^2 B_2^2} \quad (5.12)$$

After cancellation of some common terms, the final form of the equation can be expressed as:-

$$I_4 = \frac{(m_1+m_2)^2}{2m_2^2} B_2 + \left\{ \frac{m_1}{2} - \frac{k_2 m_1 (m_1+m_2)}{k_1 m_2} + \frac{k_2^2 (m_1+m_2)^3}{2(k_1 m_2^2)} \right\} \frac{1}{B_2} \quad (5.13)$$

(b) Relative Wheel Travel

Laplace transform of relative wheel travel is

$$\frac{X_1(s) - X_2(s)}{X_o} = \frac{k_1 m_2 s^2}{s |DET|} \quad (5.14)$$

$$= \frac{k_1 m_2 s}{s^4 m_1 m_2 + s^3 B_2 (m_1+m_2) + s^2 (m_1 k_2 + m_2 k_2 + m_2 k_1) + s B_2 k_1 + k_1 k_2} \quad (5.15)$$

$$= \frac{c(s)}{d(s)}$$

where

$$c_3 = c_2 = c_o = 0$$

$$c_2 = k_1 m_2$$

$$d_4 = m_1 m_2$$

$$d_3 = B_2 (m_1+m_2)$$

$$d_2 = m_1 k_2 + m_2 (k_1+k_2)$$

$$d_1 = B_2 k_1$$

$$d_o = k_1 k_2$$

The integral square value is given by

$$I_4 = \frac{c_1^2 d_3}{2(-d_o d_3^2 - d_1^2 d_4 + d_1 d_2 d_3)} \quad (5.16)$$

On substituting the values, eq. 5.16 becomes

$$I_4 = \frac{(k_1 m_2)^2 B_2 (m_1+m_2)}{2 k_1^2 m_2^2 B_2^2} = \frac{m_1+m_2}{2 B_2} \quad (5.17)$$

(c) Body Force.

$$F_2(s) = [X_1(s) - X_2(s)] (s B_2 + k_2) = m_2 s^2 X_2(s) \quad (5.18)$$

Hence,

$$\frac{F_2(s)}{X_o} = \frac{k_1 m_2 s^2 (s B_2 + k_2)}{s |DET|} \quad (5.19)$$

$$= \frac{s^2 k_1 m_2 B_2 + s k_1 k_2 m_2}{s^4 m_1 m_2 + s^3 (m_1+m_2) + s^2 (m_1 k_2 + m_2 k_2 + m_2 k_1) + s B_2 k_1 + k_1 k_2} \quad (5.20)$$

$$= \frac{c(s)}{d(s)}$$

$$\begin{array}{ll}
 \text{where } c_3 = 0 & \text{and } d_4 = m_1 m_2 \\
 c_2 = k_1 m_2 B_2 & d_3 = B_2 (m_1 + m_2) \\
 c_1 = k_1 k_2 m_2 & d_2 = m_1 k_2 + m_2 (k_1 + k_2) \\
 c_0 = 0 & d_1 = B_2 k_1 \\
 & d_0 = k_1 k_2
 \end{array}$$

This gives:

$$I_4 = \frac{c_2^2 d_1 + c_1^3 d_3}{2(-d_0 d_3^2 - d_1^2 d_4 + d_1 d_2 d_3)} \quad (5.21)$$

on substituting the values into eq.5.21, the result is:-

$$I_4 = \frac{k_1^3 m_2^2 B_2^2 + k_1^2 k_2^2 m_2^2 B_2 (m_1 + m_2)}{2 k_1^2 m_2^2 B_2^2} \quad (5.22)$$

$$= \frac{1}{2} k_1 B_2 + \frac{1}{2} k_2^2 (m_1 + m_2) / B_2 \quad (5.23)$$

The performance index was defined as:

$$I = \int_0^{\infty} [\rho u^2 + q_1 (x_0 - x_1)^2 + q_2 (x_1 - x_2)^2] dt$$

It was shown earlier that in the case of a vehicle travelling over a road profile which has a velocity input spectrum given by white noise of constant amplitude $2\pi\delta V$, the mean square values of response will correspond to those of the step input of the same magnitude.

Hence, the performance index for the model can be expressed as:

$$\begin{aligned}
 I &= \rho c V \left[\frac{k_1}{2} B_2 + \frac{k_2^2 (m_1 + m_2)}{2 B_2} \right] \\
 &+ q_1 c V \left[\frac{(m_1 + m_2)^2}{2 k_1 m_2^2} B_2 + \left\{ \frac{m_1}{2} - \frac{k_2 m_1 (m_1 + m_2)}{k_1 m_2} + \frac{k_2^2 (m_1 + m_2)^3}{2 (k_1 m_2)^2} \right\} \frac{1}{B_2} \right] \\
 &+ q_2 c V \left[\frac{m_1 + m_2}{2 B_2} \right] \quad (5.24)
 \end{aligned}$$

where $c = 2\pi\delta$, and the mean square values as under:

$$\langle u^2 \rangle = c V \left[\frac{k_1 B_2}{2} + \frac{k_2^2 (m_1 + m_2)}{2 B_2} \right] \quad (5.25)$$

$$\langle (x_0 - x_1)^2 \rangle = c V \left[\frac{(m_1 + m_2)^2 B_2}{2 k_1 m_2^2} + \left\{ \frac{m_1}{2} + \frac{k_2 m_1 (m_1 + m_2)}{k_1 m_2} + \frac{k_2^2 (m_1 + m_2)^3}{2 (k_1 m_2)^2} \right\} \frac{1}{B_2} \right] \quad (5.26)$$

$$\langle (x_1 - x_2)^2 \rangle = c V \left[\frac{m_1 + m_2}{2 B_2} \right] \quad (5.27)$$

5.3 Influence of Model Parameters on Integral Square Values

It is now proposed to consider the mean square values of

- (i) Body force
- (ii) Dynamic tyre deflection
- (iii) Relative wheel travel

in turn, and to examine how these are affected by changes to model parameters.

Since the aim of the optimisation process is to minimise each of these quantities, it is instructive to examine their dependence on model parameter values. A designer could draw a number of useful conclusions from such a preliminary study.

(a) Body Force

The integral square value of the body force due to step input is given by

$$\langle u^2 \rangle = \frac{k_1 B_2}{2} + \frac{k_2^2 (m_1 + m_2)}{2 B_2}$$

Effect of Body Mass (m_2)

The expression for the integral square value of body force indicates that the force will increase with the total mass.

The integral square value of body acceleration which is the basic ride comfort criterion is then given by

$$\langle a^2 \rangle = \langle u^2 \rangle / m_2^2 = \frac{k_1 B_2}{2 m_2^2} + \frac{k_2^2 (m_1 + m_2)}{2 B_2 m_2^2} \quad (5.28)$$

which indicates that it will decrease with increasing

body mass. It is a well known fact that partly laden or unladen vehicle provides a rougher ride.

The designer has very little control over the unladen mass of the vehicle, since the basic aim in any vehicle design is to reduce the mass as much as possible to save the material and cost of fuel. There is very little left to skimp since the basic safety aspects must be maintained.

Effect of Radial Stiffness of Tyres (k_1)

For minimum body force the radial stiffness of tyres should be as low as possible. Owing to characteristics of pneumatic tyre construction, the radial stiffness cannot be reduced without reducing the lateral stiffness, but high lateral stiffness is essential for good road holding.

Thus minimum radial stiffness is determined by tyre construction, and the designer cannot influence it to any significant degree, except to select tyres that will give adequate lateral stiffness. This in general, results in far too high vertical stiffness for good ride comfort.

Effect of Spring and Damper Rates (k_2, B_2)

Since the vehicle mass and radial tyre stiffness are really beyond the control of the suspension engineer, the basic influencing parameters left for suspension optimisation are the stiffness of the suspension springs and the damping rate of shock absorbers. Since body force decreases as the square of the stiffness of the suspension spring (Eq.5.25), the vehicle should have as soft springs as possible. But here the limits are set by permissible deflection from unladen to laden condition. Styling requirements dictate the maximum desirable deflection, and usually limit the bump travel to approx. 60 mm. Also, for consistent handling, the height of the mass centre of the vehicle should vary as little as possible with the load.

These limitations dictate a minimum suspension spring stiffness of approximately 15 kN/m for a 4-passenger vehicle, and of approximately 18 kN/m for a 5-passenger vehicle.

With the constraints on suspension parameters as discussed, this only leaves the damping rate of shock absorbers which can be freely adjusted to minimise the body force.

Now,

$$\langle u^2 \rangle = cV \left[\frac{k_1 B_2}{2} + \frac{k_2 (m_1 + m_2)}{2 B_2} \right]$$

on differentiating with respect to B_2 , the result is:-

$$\frac{d \langle u^2 \rangle}{d B_2} = cV \left[\frac{k_1}{2} - \frac{k_2^2 (m_1 + m_2)}{2 B_2^2} \right] \quad (5.29)$$

which gives the value of B_2 for minimum body force as:-

$$B_2 = k_2 \sqrt{(m_1 + m_2) / k_1} \quad (5.30)$$

The minimum value of integral square body force is then given by the expression

$$\langle u^2 \rangle_{\min} = cV k_2 \sqrt{k_1 (m_1 + m_2)} \quad (5.31)$$

i.e. the minimum value of body force is directly proportional to the stiffness of suspension springs.

(b) Dynamic Tyre Deflection

Dynamic tyre deflection relates directly to the contact force between the tyre and the road surface. For good handling, braking, accelerating, etc. this contact force should be as large as possible.

Total contact force = static force + dynamic force, but since dynamic force can have a +ve or a -ve sign, the minimum contact force will be:-

$$F_{cmin} = (m_1+m_2)g - k_1|x_{o1}|_{max}$$

where $|x_{o1}|$ is the absolute value of tyre deflection.

Hence, for good road holding and control of the vehicle, dynamic tyre deflection should be as small as possible.

The integral square value of dynamic tyre deflection is given by eq.5.26 as

$$\langle x_{o1}^2 \rangle = cV \left[\frac{(m_1+m_2)^2 B_2}{2 k_1 m_2^2} + \left\{ \frac{m_1}{2} - \frac{k_2 m_1 (m_1+m_2)}{k_1 m_2} + \frac{k_2^2 (m_1+m_2)^3}{2 k_1^2 m_2^2} \right\} \frac{1}{B_2} \right]$$

The various factors that affect the integral square value of dynamic tyre deflection and road-tyre contact force will be examined in turn.

(i) Radial tyre stiffness - k_1

It is evident from eq. 5.26 that dynamic tyre deflection decreases with increasing radial stiffness of the tyre. But the integral square value of dynamic tyre force is given by

$$\langle f_A^2 \rangle = \langle x_{o1}^2 \rangle k_1^2 \quad (5.32)$$

which indicates that the dynamic tyre force will increase

with increasing radial stiffness of tyres. This implies that in order to maximise the tyre-road contact force, the radial stiffness of tyres should be as low as possible. Low radial stiffness of tyres was found to be desirable from the point of view of ride comfort also. Thus there is no conflict between the different performance criteria, except the manufacturing limitations regarding the radial/lateral stiffness ratio of tyres.

(ii) Unsprung and sprung mass - m_1 and m_2 .

Eq. 5.26 suggests that the integral square value of tyre deflection will increase with increasing values of m_1 and m_2 , but the overall effect will be small since their ratios mainly will be involved.

(iii) Stiffness of suspension springs - k_2 .

The effect is not immediately obvious, but on differentiation with respect of k_2 , and setting the result equal to zero, one obtains the value of k_2 that will minimise the tyre deflection. The value is given by

$$k_{2 \text{ opt}} = k_1 \frac{m_1 m_2}{(m_1 + m_2)^2} = k_1 \left(\frac{m_1}{m_1 + m_2} \right) \left(\frac{m_2}{m_1 + m_2} \right) \quad (5.33)$$

If $m_1 \gg m_2$ as it is usually the case in practice, then for the minimum value of tyre deflection

$$k_{2 \text{ opt}} \approx k_1 m_1 / m_2 \quad (5.34)$$

(iv) Damping rate of shock absorbers - B_2 .

The value of B_2 that minimises the dynamic tyre deflection is again obtained by differentiation, and is given by

$$B_{2 \text{ opt}}^2 = \frac{k_1^2 m_1 m_2^2 - 2 k_1 k_2 m_1 m_2 (m_1 + m_2) + k_2^2 (m_1 + m_2)^3}{k_1 (m_1 + m_2)^2}$$

$$= \frac{k_1 m_1 m_2^2}{(m_1 + m_2)^2} - \frac{2 k_2 m_1 m_2}{m_1 + m_2} + \frac{k_2^2 (m_1 + m_2)}{k_1} \quad (5.35)$$

If now the suspension springs are optimised for minimum tyre deflection according to eq. 5.33, and the value substituted into eq. 5.35, the result is

$$B_{2\text{opt}}^2 = k_1 m_1 \frac{m_2^3}{(m_1 + m_2)^3} \quad (5.36)$$

when these values are substituted into eq. 5.26, the minimum value of integral square tyre deflection is obtained as

$$\langle x_{01}^2 \rangle_{\text{min}} = c V \left[\frac{(m_1 + m_2) m_1}{k_1 m_2} \right]^{\frac{1}{2}} \quad (5.37)$$

(c) Relative Wheel Travel

The integral square value of relative wheel travel was shown to be given by

$$\langle x_{12}^2 \rangle = c V \left[(m_1 + m_2) / 2 B_2 \right]$$

It probably comes as a surprise to notice that the wheel travel is independent of elastic elements of the suspension, and depends only on total mass supported by the wheel, and the damping. For minimum wheel travel the total mass should be as small as possible, and damping should be as large as possible.

The quantity is inversely proportional to damping and there is no turning point.

Note. P.51. Due to bottoming of the suspension on encountering a ramp or large bump there may be substantially more bump travel provided than is required on a stationary random road. Hence eqn (6.5) is not likely to be reliable.

6. PERFORMANCE INDEX AND WEIGHTING FACTORS

6.1 Introduction

In Chapter 5 the performance index for the suspension was defined as

$$I = \int_0^{\infty} (\rho u^2 + q_1 x_{01}^2 + q_2 x_{12}^2) dt$$

with ρ , q_1 and q_2 as the respective weighting factors. Also closed form solutions in terms of suspension parameters were obtained for integral square values for a $\frac{1}{4}$ car model.

The index as formulated above places indirect constraints on the magnitude and duration of vertical acceleration (ride comfort), dynamic tyre deflection (road holding) and relative wheel travel (bottoming of suspension).

It is evident from the general form of the performance index that one of the weighting factors could be assigned quite arbitrarily, and the others adjusted so that the weighted integral square values have approximately the magnitudes of the same order. Otherwise the changes in individual integral square values are not adequately reflected in the changes to performance index.

6.2 Weighting Factor for Dynamic Tyre Deflection

For random road roughness of Gaussian distribution, an approximate ratio for q_1/q_2 can be obtained by comparing the static tyre deflection δ_{st} and the bump travel δ_w of laden vehicle. *
See note

To prevent the loss of tyre contact and bottoming of suspension on rubber stops for 99.87% of time, the necessary conditions are:

$$3 \delta_{x01} k_1 \leq (m_1+m_2)g = \delta_{st} k_1 \quad (6.1)$$

$$\text{and } 3 \delta_{x12} \leq \delta_w \quad (6.2)$$

where δ_{x01} = RMS dynamic tyre deflection
 δ_{x12} = RMS relative wheel travel.

If the weighted quantities are to be of the same order of magnitude, then

$$q_1 \sigma_{x01}^2 \approx q_2 \sigma_{x12}^2 \quad (6.3)$$

Hence

$$q_1 = q_2 \left(\frac{\sigma_{x_{12}}}{\sigma_{x_{01}}} \right)^2 = q_2 \left[\frac{\delta_w k_1}{(m_1 + m_2)g} \right]^2 \quad (6.4)$$

The weighting factors can be normalised without loss of generality by taking one of the weighting factors equal to unity. If q_2 is taken equal to unity, then

$$q_1 = \left[\frac{\delta_w k_1}{(m_1 + m_2)g} \right]^2 \quad (6.5)$$

6.3 Weighting factor for body force

If the limiting R.M.S. value of body force is known, the weighting factor can be approximated from the relationship

$$\rho \sigma_u^2 \approx q_2 \sigma_{x_{12}}^2 \approx q_2 (\delta_w/3)^2 \quad (6.6)$$

from which the weighting factor can be calculated as

$$\rho = q_2 \frac{\delta_w^2}{9 \langle u^2 \rangle} \quad (6.7)$$

The exact value of ρ is immaterial for the purpose of optimisation, only an initial value is required which will be changed during the process of optimisation.

The expression for ρ is quite simple in principle, but the difficulty lies in estimating the R.M.S. value of the body force for the case when the R.M.S. value of wheel travel corresponds to one third of total laden bump travel.

Theoretically it would be possible to specify the R.M.S. acceleration limit σ_a based on ride comfort criteria, then calculate the corresponding value of R.M.S. body force from the relationship

$$\sigma_u = m_2 \sigma_a$$

But the permissible level of RMS body acceleration is a function of exposure time to acceleration (48,49). It would be completely unrealistic to expect 8 hr. exposure at road and speed conditions when the RMS value of wheel travel corresponds to 1/3 total bump

travel. This situation corresponds to a very rough road surface travelled at a moderate vehicle speed.

In view of this dilemma, the following questions arise:-

- (i) For what continuous periods of time is the vehicle expected to travel on rough roads?
- (ii) At what speeds would the vehicle be driven on rough sections of road?
- (iii) What road roughness parameter value would adequately describe the random road profile in question?

If the answers to the questions can be found, it is a simple matter to determine the initial weighting factor for the mean square body force.

One way to overcome the problems associated with road roughness and vehicle speed is to argue as follows:-

The integral square value of wheel travel is given by

$$\langle x_{12}^2 \rangle = c V \left[\frac{m_1 + m_2}{2 B_2} \right] \approx \left(\frac{\delta_w}{3} \right)^2$$

Hence,

$$c V = \left(\frac{\delta_w}{3} \right)^2 \left(\frac{2 B_2}{m_1 + m_2} \right) \quad (6.8)$$

Eq. 6.8 would give the product of road roughness and vehicle speed which corresponds to bottoming of suspension for 0.13% of the time.

The corresponding body force is given by eq. 5.25 as

$$\langle u^2 \rangle = c V \left[\frac{k_1 B_2}{2} + \frac{k_2^2 (m_1 + m_2)}{2 B_2} \right]$$

Combining equations 6.7, 6.8 and 5.25, it follows that (if $q_2=1$)

$$\frac{1}{\rho} \approx \frac{k_1 B_2}{m_1 + m_2} + k_2^2 \quad (6.9)$$

In the previous chapter it was shown that for minimum tyre deflection

$$k_{2opt} = \frac{k_1 m_1 m_2}{(m_1 + m_2)^2}$$

and

$$B_{2opt}^2 = \frac{k_1 m_1 m_2^3}{(m_1+m_2)^3}$$

After substituting the expressions for k_{2opt} and B_{2opt}^2 in eq. 6.9, the result is

$$\frac{1}{\rho} \approx \frac{k_1 m_1 m_2^2}{(m_1+m_2)^3} \quad (6.10)$$

$$\text{or } \rho \approx \frac{(m_1+m_2)^3}{k_1^2 m_1 m_2^2} \quad (6.11)$$

The numerical values in eq. 6.11 are usually known before the suspension optimisation procedure is commenced.

6.4 Parameter Values of Mathematical Model

To demonstrate the various points discussed by way of a numerical example, the equations will be applied to a model of a typical small 4-passenger sedan of British design and manufacture (HILLMAN).

The data for the model as published in references (50) and (51) are reproduced below. (Suffix P refers to rear suspension values)

Front Suspension

| | |
|-------|-------------------------------|
| m_1 | = 28.58 kg |
| m_2 | = 288.94 kg (includes driver) |
| k_1 | = 155860 N/m |
| k_2 | = 19972 N/m |
| B_2 | = 2015 Ns/m |

Rear Suspension

| | |
|----------|----------------------------|
| m_{1P} | = 54.43 kg |
| m_{2P} | = 216.14 kg (incl. driver) |
| k_{1P} | = 155860 N/m |
| k_{2P} | = 22563 N/m |
| B_{2P} | = 1256 N/m |

For $\frac{1}{2}$ car model:

| | |
|--|--------------------------------|
| Total sprung mass | $m = 505.08$ kg |
| Body pitching moment of inertia | $J = 569.63$ kg m ² |
| Length of wheel base | $L = 2.565$ m |
| Distance of front wheels from centre of mass | $a = 1.098$ m |
| Distance of rear wheels from centre of mass | $b = 1.467$ m |
| Bump travel | $\delta_w = 63$ mm. |

The mass distribution of passengers and luggage on loaded axles is typically taken as follows:-

- 50%/50% front/rear for a front seat occupant
- 25%/75% front/rear for a rear seat occupant
- 15%/115% front/rear for luggage.

The usual practice in passenger vehicle industry is to design for a 68 kg adult passenger, and a total of 68 kg of luggage.

The load distribution on the axles of a vehicle occupied by four adults, driver, and full luggage load would then be

| | <u>Front Axle</u> | <u>Rear Axle</u> |
|-----------------------|-------------------|------------------|
| Front seat passengers | 68 kg | 68 kg |
| Rear seat passengers | 34 kg | 102 kg |
| Luggage | -10 kg | 78 kg |
| Total ... | 92 kg | 248 kg |

Hence, the laden sprung masses for the model will be

$$m_2 = 46 + 288.94 \text{ kg} = 334.94 \text{ kg for the front}$$

$$m_{2P} = 124 + 216.14 \text{ kg} = 340.14 \text{ kg for the rear}$$

The data for a typical 5-passenger sedan of local manufacture (CHRYSLER) was also obtained, and is listed below.

| <u>Front Suspension</u> | <u>Unladen</u> | <u>Rear Suspension</u> |
|----------------------------|----------------|-------------------------------|
| $m_1 = 40.82 \text{ kg}$ | | $m_{1P} = 70.31 \text{ kg}$ |
| $m_2 = 381.02 \text{ kg}$ | | $m_{2P} = 322.05 \text{ kg}$ |
| $k_1 = 210000 \text{ N/m}$ | | $k_{1P} = 210000 \text{ N/m}$ |
| $k_2 = 19270 \text{ N/m}$ | | $k_{2P} = 21900 \text{ N/m}$ |
| $B_2 = 1600 \text{ N/m}$ | | $B_{1P} = 1600 \text{ N/m}$ |

For $\frac{1}{2}$ car model:

Total sprung mass $m = m_2 + m_{2R} = 703.07$ kg
 Body pitching moment of inertia $J = 1151.78$ kg m²
 Length of wheelbase $L = 2.820$ m
 Distance of front wheels from C of M $a = 1.292$ m
 Distance of rear wheels from C of M $b = 1.528$ m
 Bump travel 63 mm.

Laden mass distribution.

| | <u>Front Axle</u> | <u>Rear Axle</u> |
|--------------------------|-------------------|------------------|
| 2 front seat passengers | 68 kg | 68 kg |
| 3 rear seat passengers | 51 kg | 153 kg |
| 68 kg of luggage in boot | -10 kg | 78 kg |
| | <hr/> | <hr/> |
| Total ... | 109 kg | 299 kg. |

Laden sprung mass for $\frac{1}{4}$ car model

Front $m_2 = 381.02 + 54.5$ kg = 435.52 kg
 Rear $m_{2P} = 322.05 + 149.5$ kg = 471.55 kg.

6.5 Theoretical Optima

It is now appropriate to calculate the values of optimum suspension parameters for the model, and compare these with actual values.

(a) Suspension springs

It was shown that the stiffness of the suspension spring for minimum integral square value of tyre deflection is given by the expression

$$k_{2OPT} = \frac{k_1 m_1 m_2}{(m_1 + m_2)^2}$$

The values calculated from this equation for the models are listed below for comparison.

| | | <u>Front Suspension</u> | <u>Rear Suspension</u> |
|----------|---------|-------------------------|------------------------|
| | | k_{2OPT} | $k_{2P OPT}$ |
| HILLMAN | Unladen | 12775 N/m | 25047 N/m |
| | Laden | 11296 N/m | 18535 N/m |
| CHRYSLER | Unladen | 18355 N/m | 30888 N/m |
| | Laden | 16454 N/m | 23761 N/m |

In comparing the values, it is interesting to note that the front springs of HILLMAN are considerably stiffer than required from the point of good road holding criterion, while the rear springs are near optimum.

In case of CHRYSLER sedan, the front springs are near optimum while the rear springs are considerably softer than required for optimum road holding.

It appears that optimum road holding of rear wheels has been traded off for some additional passenger comfort.

(b) Shock absorbers

It was shown that the damping rate which corresponds to the minimum integral square value of body force is given by eq. 5.30 as

$$B_{2OPT} = k_2 \left[\frac{m_1 + m_2}{k_1} \right]^{\frac{1}{2}}$$

and the damping corresponding to minimum tyre deflection by eq. 5.35 as

$$B_2^2 = \frac{k_1 m_1 m_2^2}{(m_1 + m_2)^2} - \frac{2 k_2 m_1 m_2}{m_1 + m_2} + \frac{k_2^2 (m_1 + m_2)}{k_1}$$

Again, the optimum values of damping will be tabulated below. Damping rates for minimum RMS acceleration are:-

| | | Front Suspension | Rear Suspension |
|----------|---------|--------------------------|---------------------------|
| | | <u>B_{2 OPT}</u> | <u>B_{2P OPT}</u> |
| HILLMAN | Unladen | 901 Ns/m | 940 Ns/m |
| | Laden | 965 Ns/m | 1135 Ns/m |
| CHRYSLER | Unladen | 884 Ns/m | 934 Ns/m |
| | Laden | 918 Ns/m | 1112 Ns/m |

Damping rates for minimum RMS tyre deflection:-

| | | Front Suspension | Rear Suspension |
|----------|---------|--------------------------|---------------------------|
| | | <u>B_{2 OPT}</u> | <u>B_{2P OPT}</u> |
| HILLMAN | Unladen | 1861 Ns/m | 2082 Ns/m |
| | Laden | 1913 Ns/m | 2340 Ns/m |
| CHRYSLER | Unladen | 2507 Ns/m | 2884 Ns/m |
| | Laden | 2563 Ns/m | 3121 Ns/m |

The examination of tabulated values indicates that the actual damping rates used are generally higher than the optima for ride comfort, but lower than optima for road holding. There seems to be no obvious relationship between the calculated optima and the actual component values, but nevertheless in each case considered the actual component values are somewhere in-between the range of the calculated optima, some closer to one end, the others closer to the other.

This is to be expected since a number of subjective criteria will influence the actual selection and road testing of the suspension during the development stage.

6.6 Role of Performance Index in Suspension Optimisation Process

The concept of a performance index for the mathematical model was discussed at length in Chapter 5, and for the model at hand it was expressed as weighted sum of mean square values of the form:-

$$I = \rho \langle u^2 \rangle + q_1 \langle x_{01}^2 \rangle + q_2 \langle x_{12}^2 \rangle$$

with ρ , q_1 and q_2 as the weighting factors.

Some guide-lines for the selection of the weighting factors were established at the beginning of this chapter where it was shown that if q_2 is taken equal to unity then the remaining weighting factors ρ and q_1 could be estimated from equations 6.5 and 6.11 respectively as

$$q_1 \approx \left[\frac{\delta_w k_1}{(m_1 + m_2) g} \right]^2 \quad \text{and} \quad \rho \approx \frac{(m_1 + m_2)^3}{k_1^2 m_2 m_2^2}$$

The values of weighting factors calculated from equations 6.5 and 6.11 are listed below for comparison.

| | | Values of q_1 | |
|----------|---------|-------------------------|------------------------|
| | | <u>Front Suspension</u> | <u>Rear Suspension</u> |
| HILLMAN | model | 10.0 | 13.7 |
| CHRYSLER | model | 10.2 | 11.8 |
| | | Values of ρ | |
| | | <u>Front Suspension</u> | <u>Rear Suspension</u> |
| HILLMAN | Unladen | 5.5×10^{-10} | 3.2×10^{-10} |
| | Laden | 6.2×10^{-10} | 4.0×10^{-10} |
| CHRYSLER | Unladen | 2.9×10^{-10} | 1.9×10^{-10} |
| | Laden | 3.2×10^{-10} | 2.3×10^{-10} |

It should be noted that the weighting factors are rather strongly dependent on radial tyre stiffness k_1 which in a practical situation can vary over a wide range. The usual variation among identical commercial tyres inflated to the same pressure could be as much as $\pm 15\%$ about the nominal value. In addition, the stiffness is a linear function of inflation pressure which can also vary over a wide range in practice.

Consequently, there is no point in calculating the weighting factors to any great degree of precision, especially in view of the fact that the weighting factors would be modified in subsequent optimisation process.

Once the weighting factors for the model response have been determined, it is now a simple matter to vary the parameters in such a way that the performance index is minimised. This would then correspond to an optimum condition.

The process is quite straight-forward in principle, but there are some inherent uncertainties which will be discussed later.

It was shown that a particular random road input characterised by road roughness parameter δ and vehicle velocity V could be simulated by a step input of magnitude cV where $c = 2\pi\delta$, and the performance index of the model was then defined by eq. 5.24 as

$$\begin{aligned}
I = & \rho cV \left[\frac{k_1 B_2}{2} + \frac{k_2^2 (m_1+m_2)}{2 B_2} \right] \\
& + q_1 cV \left[\frac{(m_1+m_2)^2 B_2}{2 k_1 m_2^2} + \left\{ \frac{m_1}{2} - \frac{k_2 m_1 (m_1+m_2)}{k_1 m_2} + \frac{k_2^2 (m_1+m_2)^3}{2 (k_1 m_2)^2} \right\} \frac{1}{B_2} \right] \\
& + q_2 cV \left[\frac{m_1+m_2}{2 B_2} \right]
\end{aligned}$$

Since cV is the common multiplier for all terms involved, a performance index could be defined as the sum of weighted integral square values of the response to unit step. There would be no loss of information if the common factor is omitted for the sake of simplicity in mathematical manipulations, provided the investigations are confined to constant speed while the model parameters are varied, and the multiplier is inserted later if absolute integral square values are required. Also if q_2 is taken equal to unity, then q_1 can be denoted simply as q .

With these modifications, the performance index can be expressed in the form

$$\begin{aligned}
I = & \left[\rho \frac{k_1}{2} + q \frac{(m_1+m_2)^2}{2 k_1 m_2^2} \right] B_2 \\
& + \left[\rho \frac{k_2^2 (m_1+m_2)}{2} + q \left\{ \frac{m_1}{2} - \frac{k_2 m_1 (m_1+m_2)}{k_1 m_2} + \frac{k_2^2 (m_1+m_2)^3}{2 (k_1 m_2)^2} \right\} + \frac{m_1+m_2}{2} \right] \frac{1}{B_2} \quad (6.12)
\end{aligned}$$

which in turn can be expressed as

$$I = \alpha B_2 + \beta/B_2 \quad (6.13)$$

On differentiating the index with respect to B_2 , and equating the result to zero, the equation can be solved for B_2 OPT which minimises the performance index, i.e.

$$B_2^2 \text{ OPT} = \beta/\alpha \quad (6.14)$$

where

$$\beta = \rho \frac{k_2^2 (m_1+m_2)}{2} + q \left\{ \frac{m_1}{2} - \frac{k_2 m_1 (m_1+m_2)}{k_1 m_2} + \frac{k_2^2 (m_1+m_2)^3}{2 (k_1 m_2)^2} \right\} + \frac{m_1+m_2}{2}$$

and

$$\alpha = \rho \frac{k_1}{2} + q \frac{(m_1+m_2)^2}{2 k_1 m_2^2}$$

Evidently, the value of B_2 that minimises the performance index is not only a function of system parameters but it also involves the weighting factors.

To gain a better insight into the relationships, it is instructive to expand eq. 6.14, which defines the condition for minimum performance index, and express ρ as a function of q with $B_{2\text{OPT}}^2$ as a parameter.

The result of this operation is eq. 6.15 below which expresses the relationship between ρ and q for the condition of minimum performance index as

$$\rho = \frac{q \left\{ \frac{m_1}{2} - \frac{k_2 m_1 (m_1+m_2)}{k_1 m_2} + \frac{k_2^2 (m_1+m_2)^3}{2(k_1 m_2)^2} - \frac{B_2^2 (m_1+m_2)^2}{2 k_1 m_2^2} \right\} + \frac{m_1+m_2}{2}}{\frac{k_1 B_2^2}{2} - \frac{k_2^2 (m_1+m_2)}{2}} \quad (6.15)$$

It is evident from the relationship above that for every value of $B_{2\text{OPT}}$ there corresponds an infinite number of pairs of ρ and q that minimise the performance index, and ρ will plot as a linear function of q with $B_{2\text{OPT}}$ as a parameter for the condition of minimum performance index.

The slope of the straight lines comprising the plot is given by

$$\frac{d\rho}{dq} = \frac{\frac{m_1}{2} - \frac{k_2 m_1 (m_1+m_2)}{k_1 m_2} + \frac{k_2^2 (m_1+m_2)^3}{2 (k_1 m_2)^2} - \frac{B_2^2 (m_1+m_2)^2}{2 k_1 m_2^2}}{\frac{k_1 B_2^2}{2} - \frac{k_2^2 (m_1+m_2)}{2}} \quad (6.16)$$

The slope tends to infinity if $\frac{k_1}{2} B_2^2 - \frac{k_2^2}{2} (m_1+m_2) = 0$

$$\text{or if } B_2^2 = \frac{k_2^2 (m_1+m_2)}{k_1} \quad (6.17)$$

This also corresponds to the condition of minimum body force given by eq. 5.30.

The value of q where the vertical graph intersects the q -axis can be calculated from eq. 6.15, and is given by

$$q_{\text{VERT}} = - \frac{k_1 m_2 (m_1+m_2)}{m_1 \{k_1 m_2 - 2 k_2 (m_1+m_2)\}} \quad (6.18)$$

The abscissa has a negative value unless

$$k_2 > \frac{k_1 m_2}{2(m_1+m_2)}$$

In normal suspensions $k_2 \approx k_1/10$, hence this condition will arise only with a -ve weighting factor which is most unlikely. Since q is here constant for all values of ρ , the minimum performance index is a function of ρ only.

The other aspect of interest is the graph of horizontal slope.

From eq. 6.16 it is seen that the graph has zero slope if

$$-\frac{m}{2} - \frac{k_2 m_1 (m_1+m_2)}{k_1 m_2} + \frac{k_2^2 (m_1+m_2)^3}{2 (k_1 m_2)^2} - \frac{B_2^2 (m_1+m_2)^2}{2 k_1 m_2^2} = 0$$

or if

$$B_2^2 = \frac{k_1 m_2^2 m_1}{(m_1+m_2)^2} - \frac{2 k_2 m_1 m_2}{m_1+m_2} + \frac{k_2^2 (m_1+m_2)}{k_1} \quad (6.19)$$

This value of B_2 corresponds to the condition of minimum integral square tyre deflection given by eq. 5.35.

The point of intersection of the horizontal characteristic with the ρ -axis is obtained from eq. 6.15 as

$$\rho_{\text{HORIZ.}} = \frac{(m_1+m_2)^3}{k_1 m_1 m_2 \{k_1 m_2 - 2 k_2 (m_1+m_2)\}} \quad (6.20)$$

All other characteristics corresponding to different values of B_2 OPT (different slopes) will pass through the point defined by the intersection of the vertical and horizontal slope lines.

The conditions are shown in Fig. 6.1 which has been plotted with data corresponding to unladen HILLMAN front suspension.

Similar plots can be prepared also for other models, laden or unladen.

If the weighting factor ρ is selected to correspond to the value given by eq. 6.20, then the minimisation of the performance index will lead to the value of B_2 which corresponds to minimum tyre

FIG. 6.1.

Relationship between Weighting Factors and Damping Rate for minimum Performance Index

Data: HILLMAN Front suspension.

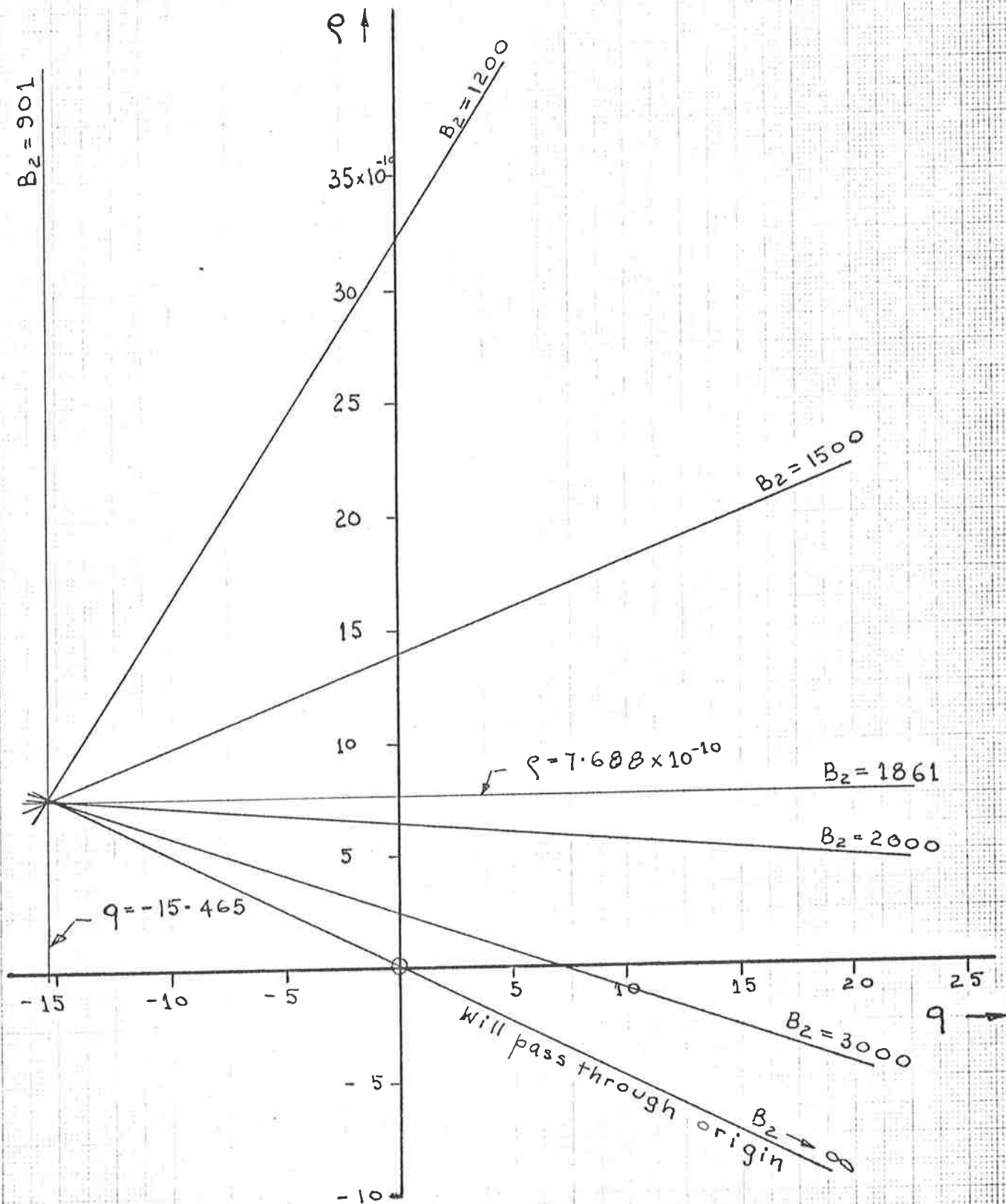
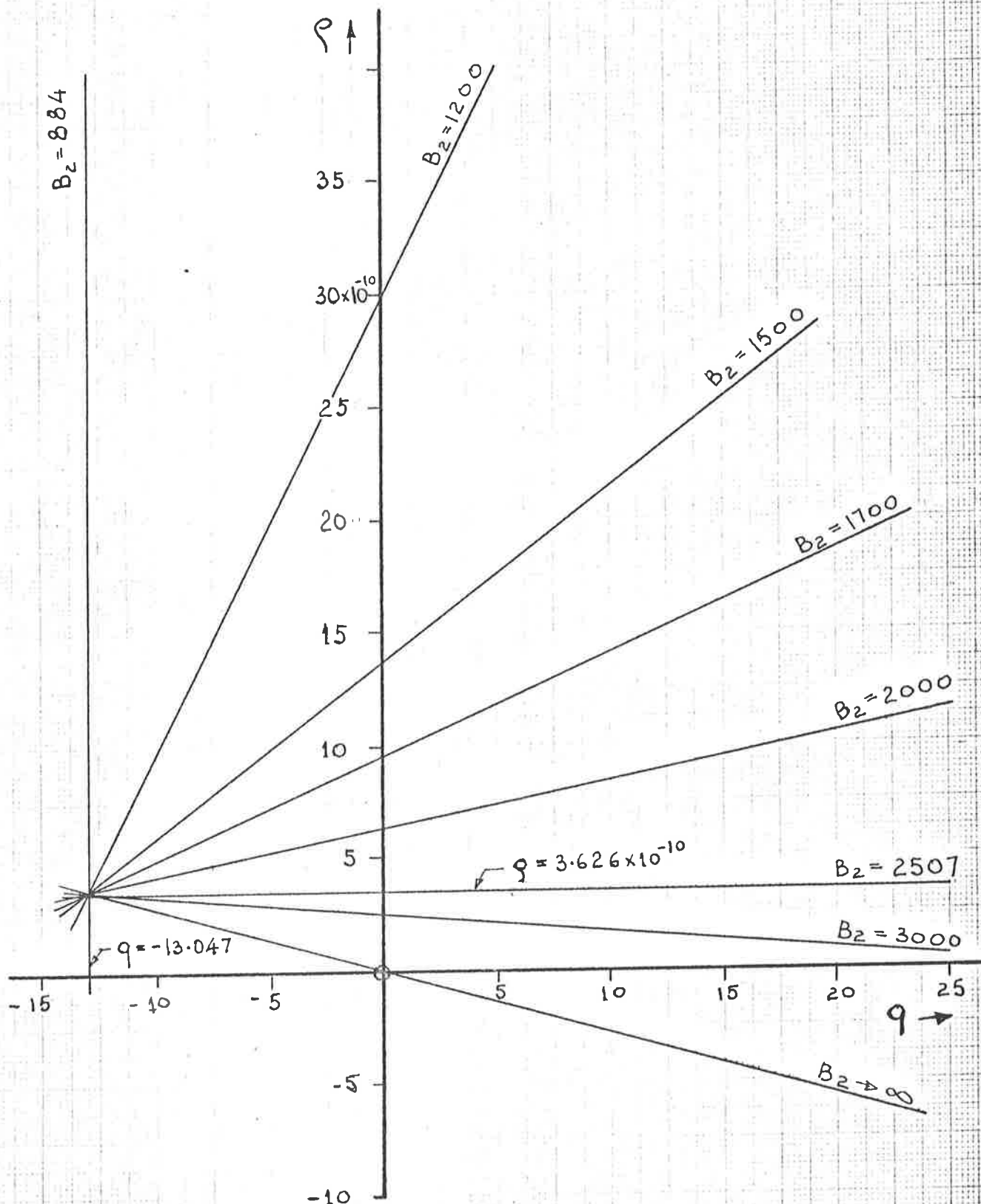


Fig. 6.2.

Relationship between Weighting Factors and Damping Rate for minimum Performance Index

Data: CHRYSLER Front Suspension



deflection, irrespective of the value of q . Hence, the model response will be the same for different values of q , but the value of minimum performance index will vary with q .

Similarly if q is selected to correspond to value given by eq. 6.18 (this is hypothetical since q will be -ve), then the minimisation process will lead to the value of B_2 that corresponds to minimum body force, irrespective of the value of ρ . Again, the model response will be the same for all values of ρ , but the minimum performance index will vary with the value of ρ .

These observations suggest that a closer examination of the performance index concept, and the associated weighting factors is warranted.

It was shown (eq. 6.15) that in case of minimum performance index the following relationship between the weighting factors and damping will hold

$$\rho = \frac{q \left\{ \frac{m_1}{2} - \frac{k_2 m_1 (m_1 + m_2)}{k_1 m_2} + \frac{k_2^2 (m_1 + m_2)^3}{2 (k_1 m_2)^2} - \frac{B_2^2 (m_1 + m_2)^2}{2 k_1 m_2^2} \right\} + \frac{m_1 + m_2}{2}}{\frac{k_1 B_2^2}{2} - \frac{k_2^2 (m_1 + m_2)}{2}}$$

This relationship can be used to eliminate ρ from the expression for the performance index given by eq. 6.12, and the result is

$$I_{\min} = \frac{2 k_1 B_2}{k_1 B_2^2 - k_2^2 (m_1 + m_2)} \left[q \left\{ \frac{m_1}{2} - \frac{k_2 m_1 (m_1 + m_2)}{k_1 m_2} \right\} + \frac{m_1 + m_2}{2} \right] \quad (6.21)$$

Eq. 6.21 gives the minimum value of the performance index for any selected value of B_2 and q , hence enables to plot I_{\min} as a function of B_2 with q as a parameter.

It may be noted that there is an asymptote for the group of characteristics when

$$k_1 B_2^2 - k_2^2 (m_1 + m_2) = 0$$

or when $B_2^2 = k_2^2 (m_1 + m_2) / k_1$

This value of B_2 corresponds to minimum integral square body force,

and the corresponding value of q is given by

$$q = - \frac{\frac{m_1+m_2}{2}}{\frac{m_1}{2} - \frac{k_2 m_1 (m_1+m_2)}{k_1 m_2}} = - \frac{k_1 m_2 (m_1+m_2)}{m_1 \{ k_1 m_2 - 2 k_2 (m_1+m_2) \}} \quad (6.22)$$

Similarly, q can be eliminated from eq. 6.12 by rewriting eq. 6.15 as

$$q = \frac{\rho \left[\frac{k_1}{2} B_2^2 - k_2^2 \left(\frac{m_1+m_2}{2} \right) \right] - \frac{m_1+m_2}{2}}{\frac{m_1}{2} - \frac{k_2 m_1 (m_1+m_2)}{k_1 m_2} + \frac{k_2^2 (m_1+m_2)^3}{2 (k_1 m_2)^2} - \frac{B_2^2 (m_1+m_2)^2}{2 k_1 m_2^2}} \quad (6.23)$$

and on substituting into eq. 6.12, the result of this operation is

$$I_{\min} = \frac{k_1 B_2 \left[\rho \left\{ \frac{m_1}{2} - \frac{k_2 m_1 (m_1+m_2)}{k_1 m_2} \right\} - \frac{(m_1+m_2)^3}{2 (k_1 m_2)^2} \right]}{\frac{m_1}{2} - \frac{k_2 m_1 (m_1+m_2)}{k_1 m_2} + \frac{k_2^2 (m_1+m_2)^3}{2 (k_1 m_2)^2} - \frac{B_2^2 (m_1+m_2)^2}{2 k_1 m_2^2}} \quad (6.24)$$

Now I_{\min} can be plotted against B_2 with ρ as a parameter.

There is an asymptote when the denominator tends to zero. The vertical asymptote is located at B_2 calculated from

$$B_2 = \frac{k_1 m_2^2 m_1}{(m_1+m_2)^2} - \frac{2 k_2 m_1 m_2}{m_1+m_2} + \frac{k_2^2 (m_1+m_2)}{k_1}$$

The expression is familiar from the condition of minimum tyre deflection (eq. 5.35).

The corresponding value of ρ is then given by

$$\rho = \frac{(m_1+m_2)^3}{k_1 m_1 m_2 \{ k_1 m_2 - 2 k_2 (m_1+m_2) \}}$$

This is also familiar, and corresponds to the height of horizontal slope line above the origin on ρ - q graph discussed previously.

If now sets of values of I_{\min} are plotted against B_2 with ρ as a parameter, and on the same graph are superimposed sets of values of I_{\min} with q as a parameter, a field of intersecting characteristics is obtained as shown in Fig. 6.3.

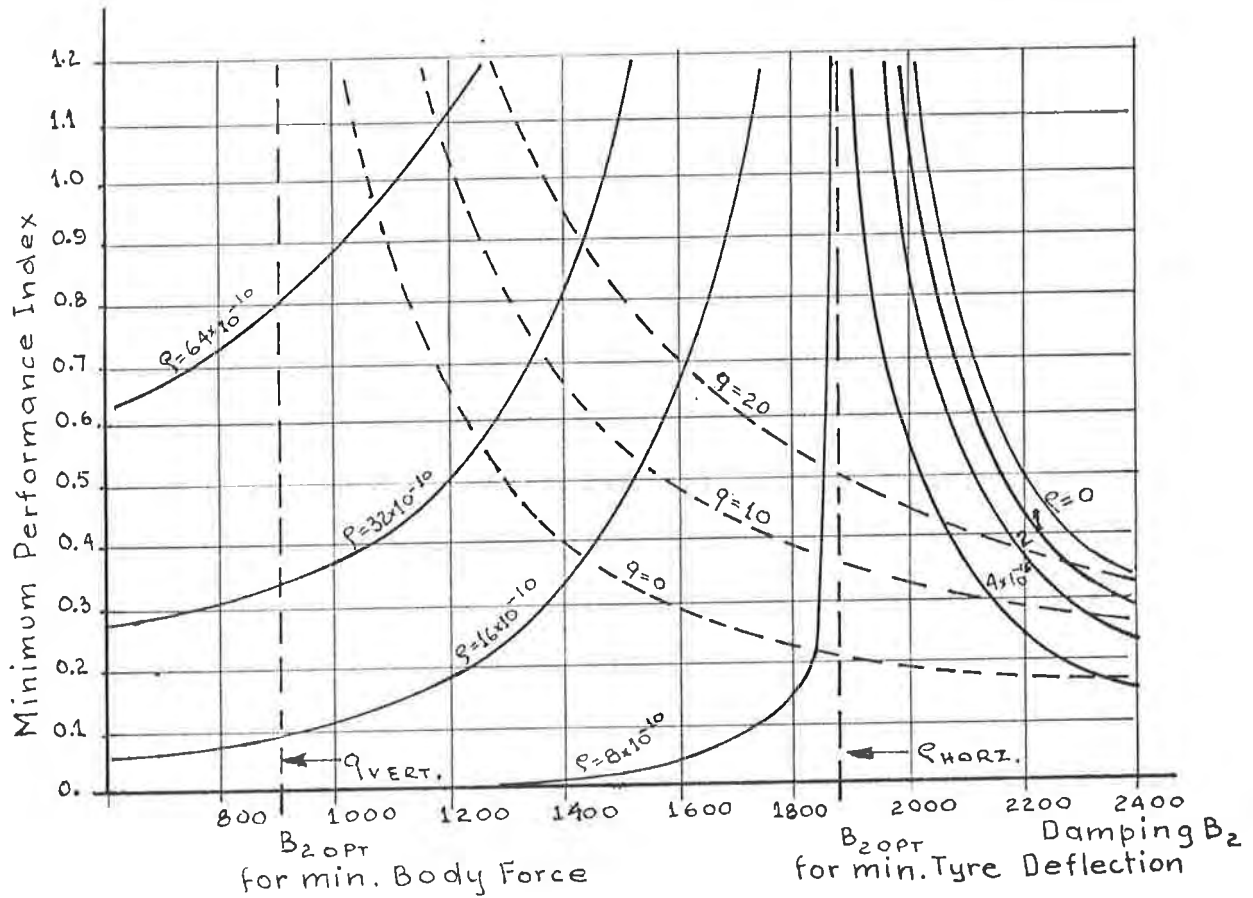


Fig. 6.3 - RELATIONSHIP BETWEEN WEIGHTING FACTORS

The points of intersection of the characteristics define the value of B_2 which will minimise the performance index for the values of q and ρ that correspond to intersecting characteristics.

Fig. 6.3 clearly demonstrates that for any value of I_{min} (any horizontal line), there corresponds an infinite number of pairs of weighting factors, each pair defining a unique value of B_2 which minimises the performance index for the given weighting factors. Since B_2 changes with weighting factors, the model response will also change, but the value of minimum performance index remains constant. Hence, depending on the weighting factors, any response is possible for a given value of minimum performance index. Conversely, if B_2 is kept constant (i.e. the model response remains constant), the value of minimum performance index will vary with the weighting factors as one moves along the vertical line drawn through the points of intersection of the characteristics and the corresponding value of B_2 .

It may now be argued that the performance index has no significance at all in the optimisation process since it is clearly a function of arbitrary and subjective weighting factors, and any value of performance index is possible irrespective of the actual system response. Thus the comparison of different models on the basis of a performance index is quite pointless.

However, the performance index will play an essential and useful role in a computer optimisation process.

Referring to Fig. 6.3, it can be seen that if any value of q is held constant and the value of ρ is increased, the minimisation process will travel along the constant q characteristic towards the value of B_2 that corresponds to the minimum body force, i.e. by increasing the weighting factor on body force and minimising the performance index, one will arrive at the model which has a lower body force than the previous model. When ρ reaches infinity B_2 will correspond to the value that results in the minimum body force, irrespective of the other weighting factors. This also corresponds to the case when the body force is taken as the sole performance criterion.

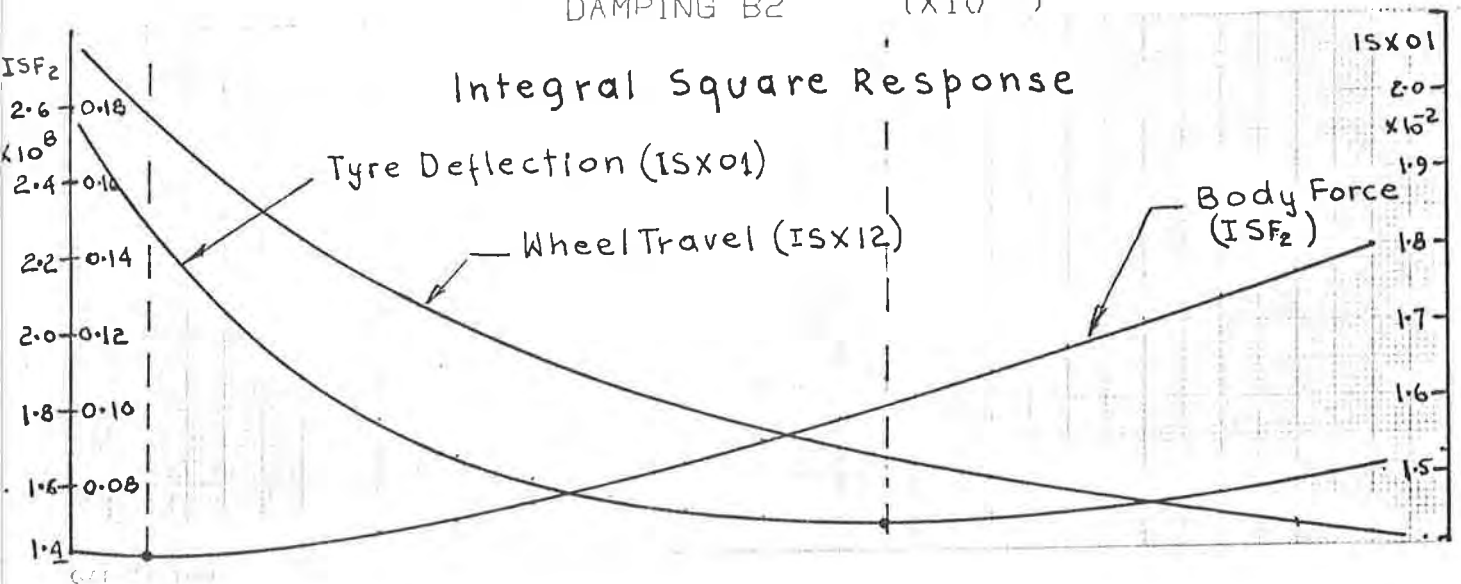
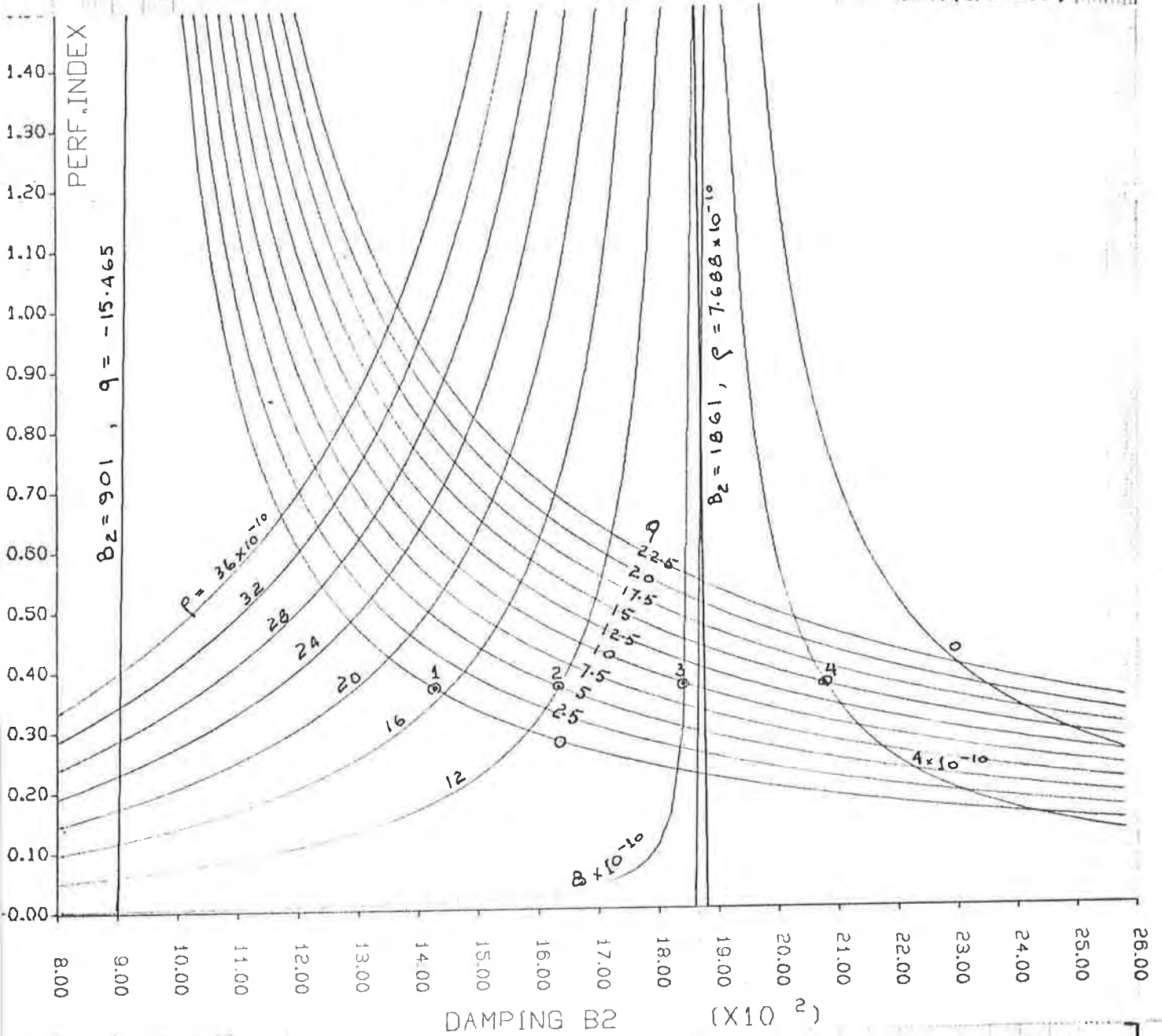
Similarly, as q is increased along a constant ρ characteristic, the minimisation process will lead to the values of B_2 which will result in lower value of tyre deformation. When $q \rightarrow \infty$, B_2 will correspond to the value that gives the minimum value of tyre deformation.

This situation corresponds to the case when the tyre deformation is taken as the sole performance criterion.

Fortran program $B_2 OPT$ shown in Appendix C was developed to calculate the data for plotting the graphs. Some of the plotting was carried out on CALCOMP plotter using program $B_2 PLOT$, also shown in Appendix C.

Figs. 6.4 and 6.5 show graphs plotted for HILLMAN front suspension, unladen and ~~un~~laden respectively, while Figs. 6.6 and 6.7 show the corresponding graphs for CHRYSLER front suspension.

Fig. 6.4. Relationship between min. Performance Index, Damping Rate and Weighting Factors. HILLMAN Front Suspension (Unladen)



To verify the correctness of graphs, a few check points were calculated using HILLMAN front suspension data.

On substituting the numerical data into eq. 6.14, the value of B_2 for minimum performance index is given by

$$B_2^2 \text{ OPT} = \frac{6.3326 \times 10^{10} \rho + 13.414 q + 158.76}{7.793 \times 10^4 \rho + 3.874 \times 10^{-6} q} \quad (6.24)$$

and the value of min. performance index is then calculated from

$$I_{\min} = (7.793 \times 10^4 \rho + 3.874 \times 10^{-6} q) B_2 \text{ OPT} + (6.3326 \times 10^{10} \rho + 13.414 q + 158.76) / B_2 \text{ OPT} \quad (6.25)$$

The results of the check calculation are listed in Table 6.1 below

TABLE 6.1

| Point | ρ | q | $B_2 \text{ OPT}$ | I_{\min} |
|-------|----------------------|-----|-------------------|------------|
| 1 | 17×10^{-10} | 0 | 1418 | 0.3757 |
| 2 | 12×10^{-10} | 5 | 1635 | 0.3692 |
| 3 | 8×10^{-10} | 10 | 1844 | 0.3727 |
| 4 | 4×10^{-10} | 15 | 2077 | 0.3710 |

These points are shown on graph in Fig. 6.4.

It is worth noting that while the performance index is approximately of the same magnitude for the points considered, the response of the model varies from point to point as can be seen from integral square values of model response plotted in the same figure.

Fig. 6.5. Relationship between min. Performance Index, Damping Rate and Weighting Factors.
 HILLMAN Front Suspension (Laden)

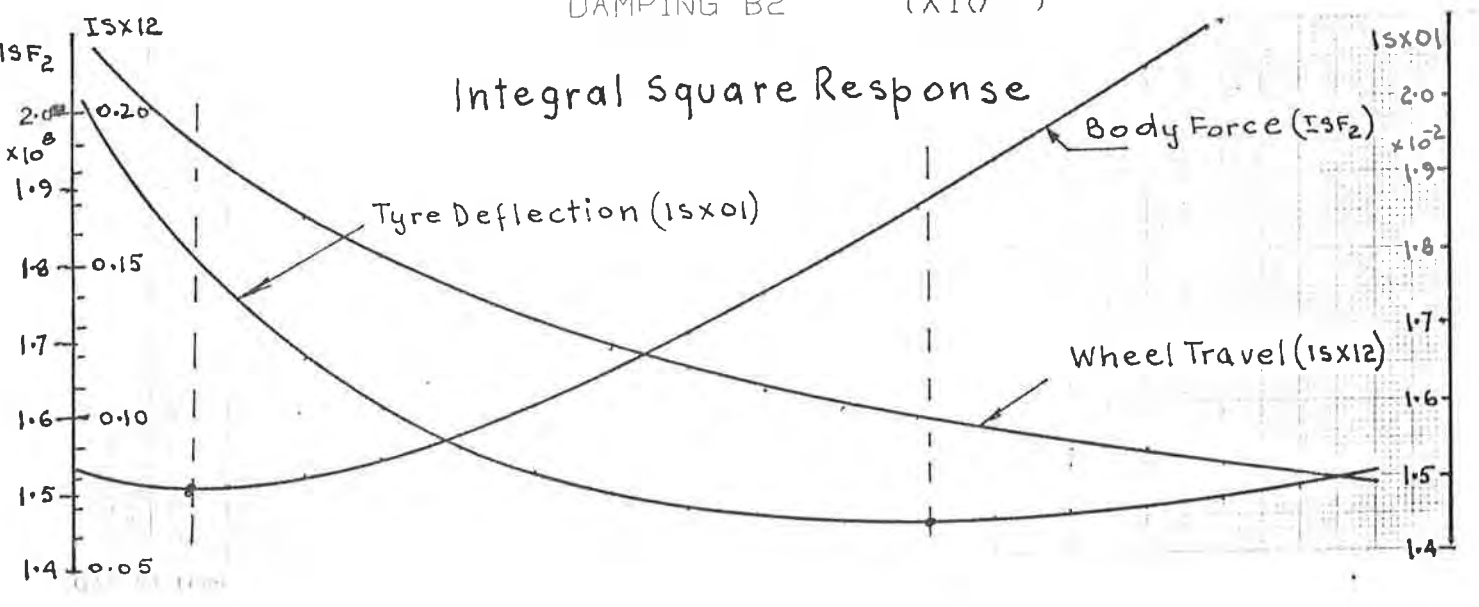
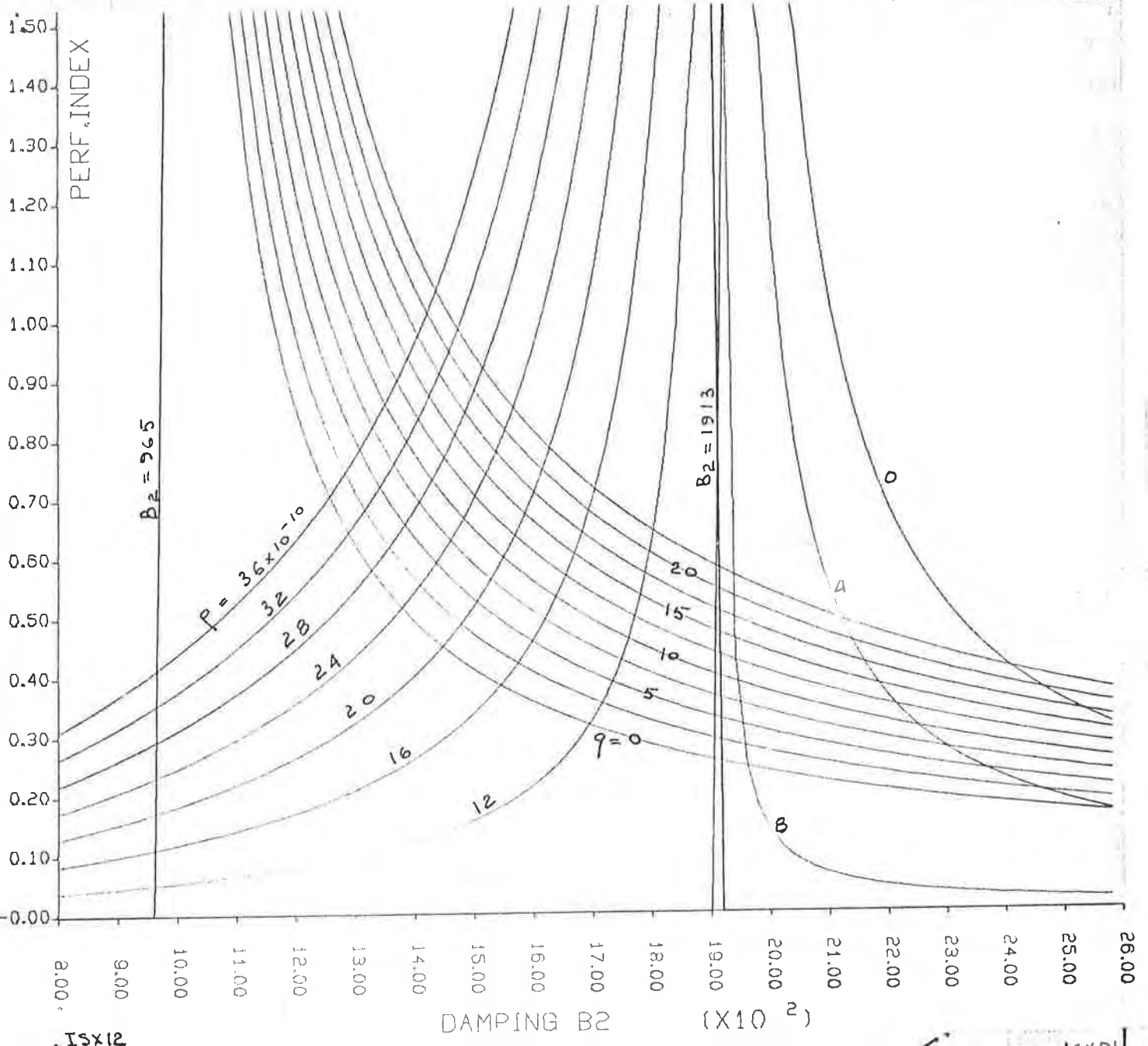


Fig. 6.6. Relationship between min. Performance Index, Damping Rate and Weighting Factors.
 CHRYSLER Front Suspension (Unladen)

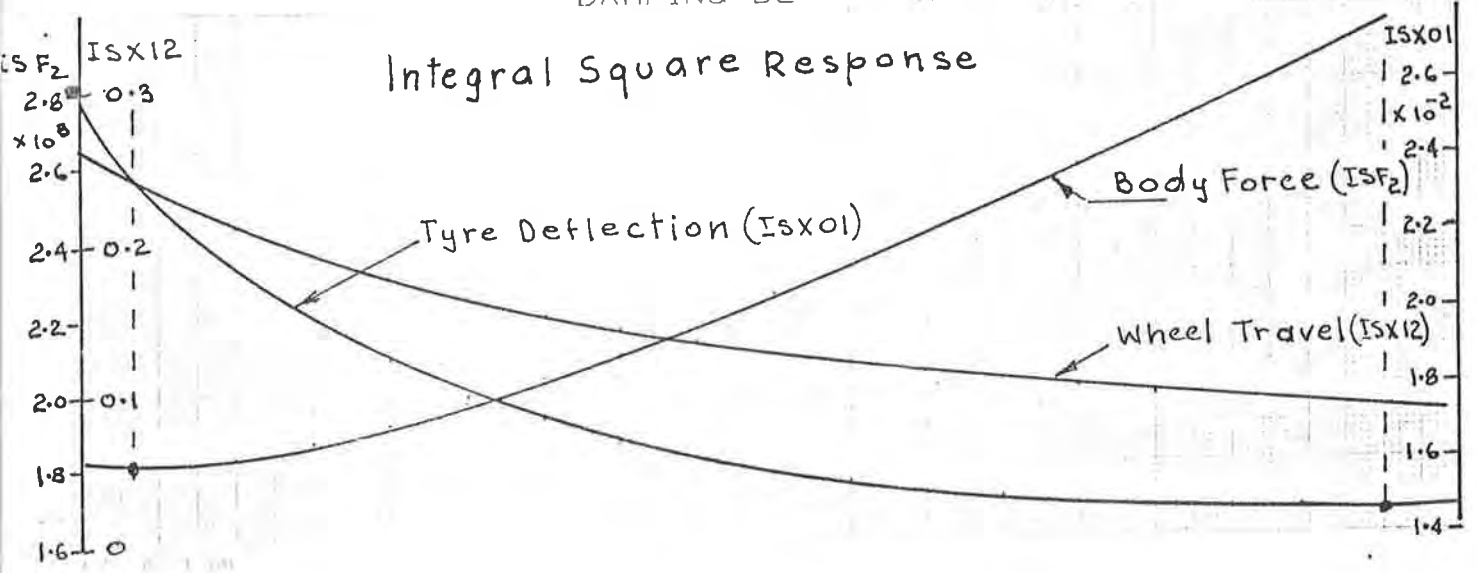
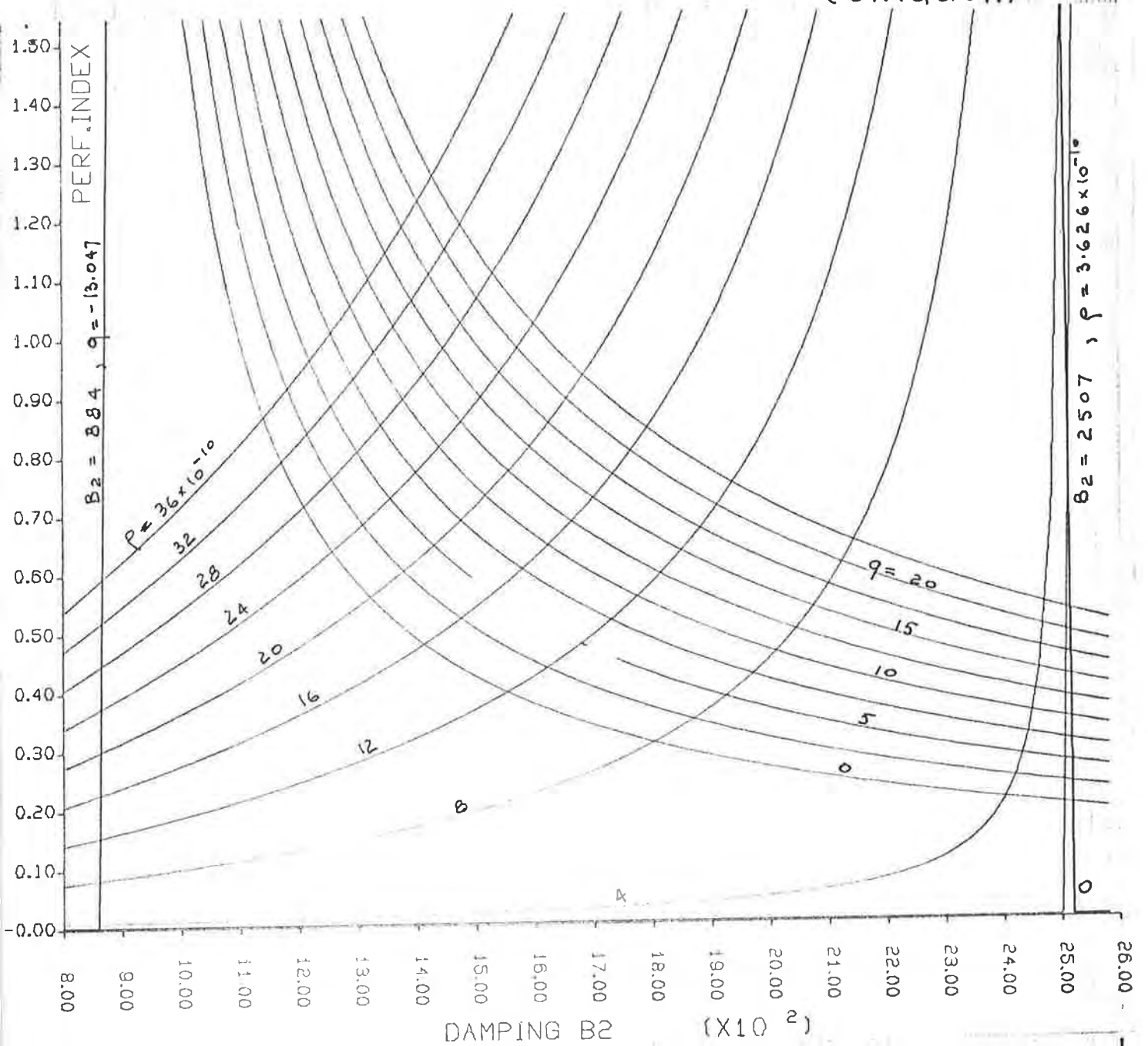
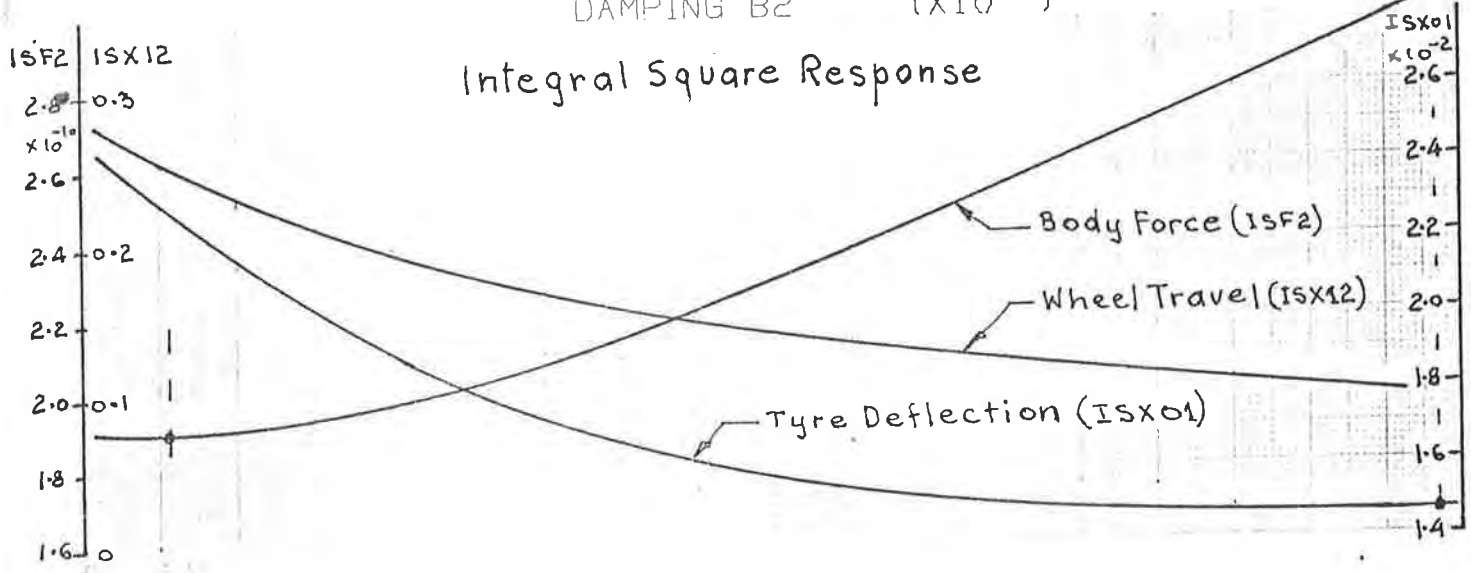
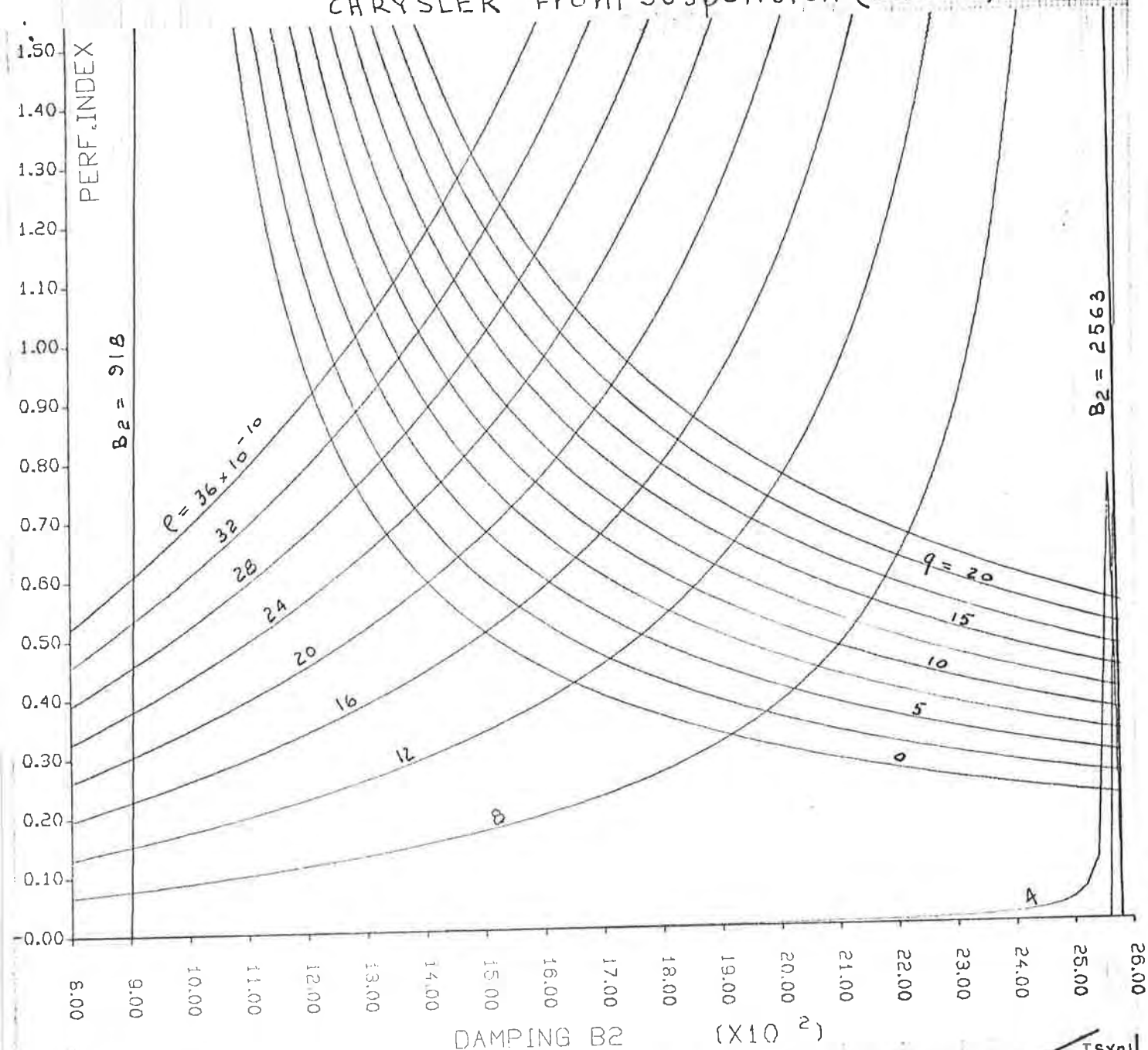


Fig. 6.7. Relationship between min. Performance Index, Damping Rate and Weighting Factors. CHRYSLER Front Suspension (Laden).



6.7 Optimisation by Computer

Computer optimisation process is usually carried out in the following sequence:

- 1) Establish approximate values for weighting factors, such that the weighted integral square values are of the same order of magnitude.
- 2) Minimise the performance index by an appropriate computer routine (usually a two dimensional search), and obtain the value of $B_{2\text{OPT}}$ corresponding to minimum performance index.
- 3) Calculate (or simulate) the response with the value of B_2 as found, and check if the performance is acceptable.
- 4) If body acceleration is excessive, increase the value of ρ , minimise the index again, and calculate performance with the new value of B_2 .
- 5) If tyre deformation is excessive, increase the value of q , minimise the performance index and check if the response is satisfactory with the value of B_2 established in the minimisation process.

Evidently, the optimisation by a computer can be a fairly long process requiring considerable computing time, and the question will then arise if the use of a computer and the associated performance index concept have any advantages at all.

In the case of a simple $\frac{1}{4}$ car linear model considered in the previous section, closed form solutions for integral square values can be obtained without excessive effort, hence the optimisation by computer is completely unnecessary as all the required quantities can be obtained by simple algebraic manipulations.

On the other hand, computer optimisation becomes an absolute necessity for models having non-linear characteristics and many degrees of freedom since closed form solutions are seldom, if ever available or possible.

This is even more so when a large number of performance criteria are to be considered with the associated weighting factors.

7. MODEL RESPONSE BY APPLICATION OF STATE VARIABLES AND COVARIANCE MATRIX METHODS.

7.1 Introduction

State variables and covariance matrix methods have gained popularity for the analysis and synthesis of dynamical systems, mainly due to ready accessibility to powerful, fast digital computers with large memory capacity.

State variables and covariance matrix techniques were first developed for the analysis, synthesis and optimisation of control systems but the techniques have been rapidly extended to all types of dynamical systems, and a large number of technical papers and texts have been published on the subject. (72, 73, 74, 75, 76, 77)

7.2 State variable analysis applied to $\frac{1}{4}$ car model

The model is again represented by a 2-degree-of-freedom lumped parameter model as in section 5.1, shown in Fig. 7.1.

The equations of motion are:-

$$-(y_2 - y_1)k_2 - (\dot{y}_2 - \dot{y}_1)B_2 = m_2 \ddot{y}_2 \quad (7.1)$$

$$-(y_1 - y_0)k_1 - (y_1 - y_2)k_2 - (\dot{y}_1 - \dot{y}_2)B_2 = m_1 \ddot{y}_1 \quad (7.2)$$

The control force u applied to the unsprung mass m_2 is given by

$$u = f_2 = m_2 \ddot{y}_2 = (y_1 - y_2)k_2 + (\dot{y}_1 - \dot{y}_2)B_2 \quad (7.3)$$

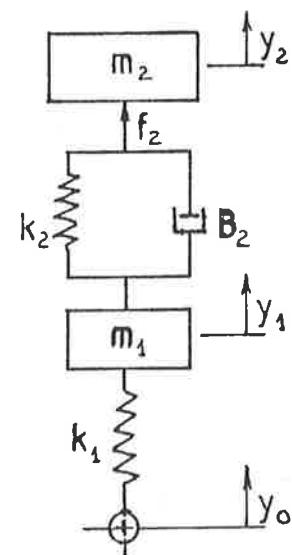


Fig. 7.1

Introducing now state variables

$$x_1 = y_1 - y_0$$

$$x_2 = y_2 - y_1$$

$$x_3 = \dot{y}_1$$

$$x_4 = \dot{y}_2$$

$$\text{then } u = m_2 \dot{x}_4$$

$$\text{and } \dot{x}_4 = \frac{u}{m_2}$$

Now the equations of motion can be expressed in terms of state variables as

$$\begin{bmatrix} \dot{x}_1 \\ \dot{x}_2 \\ \dot{x}_3 \\ \dot{x}_4 \end{bmatrix} = \begin{bmatrix} 0 & 0 & 1 & 0 \\ 0 & 0 & -1 & 1 \\ -k_1/m_1 & k_2/m_1 & -B_2/m_1 & B_2/m_1 \\ 0 & 0 & 0 & 0 \end{bmatrix} \begin{bmatrix} x_1 \\ x_2 \\ x_3 \\ x_4 \end{bmatrix} + \begin{bmatrix} 0 \\ 0 \\ 0 \\ 1/m_2 \end{bmatrix} \{u\} + B\{w\} \quad (7.3)$$

The equation is of the form

$$\{\dot{x}\} + A_1 \{x\} + B_1 \{u\} + B\{w\} \quad (7.4)$$

where $\{w\}$ denotes the external disturbance vector.

The disturbance velocity input $v(t)$ to the road wheels of the model can be approximated by scalar white noise of intensity cV as shown in section 4.3 previously.

Hence, $v(t) = \dot{y}_0(t)$, and $w = v(t)$

$$\text{with } B = \begin{bmatrix} -1 \\ 0 \\ 0 \\ 0 \end{bmatrix}$$

The performance index, denoted by π , is again defined as the weighted sum of mean square values, i.e.

$$\pi = \lim_{t_1 \rightarrow \infty} \frac{1}{t_1} E \left\{ \int_0^{t_1} (\rho u^2 + q_1 x_1^2 + q_2 x_2^2) dt \right\} \quad (7.5)$$

for $0 \leq t \leq t_1$

where ρ , q_1 and q_2 are numerical weighting factors, and $E\{\cdot\}$ denotes the expectation or average.

The performance index can be expressed in matrix form as

$$\pi = \lim_{t_1 \rightarrow \infty} \frac{1}{t_1} E \left\{ \int_0^{t_1} [x^T Q x + u^T \rho u] dt \right\} \quad (7.6)$$

where T denotes the transpose, and Q is the weighting matrix given by

$$Q = \begin{bmatrix} q_1 & 0 & 0 & 0 \\ 0 & q_2 & 0 & 0 \\ 0 & 0 & 0 & 0 \\ 0 & 0 & 0 & 0 \end{bmatrix}$$

The body control force u can also be expressed in terms of state variables as $\{u\} = F\{x\}$

where

$$F = \begin{bmatrix} 0 \\ -k_2 \\ B_2 \\ -B_2 \end{bmatrix}^T$$

The equations of motion can now be expressed in the form

$$\{\dot{x}\} = [A_1 + B_1 F] \{x\} + B\{w\} \quad (7.7)$$

$$\text{or } \{\dot{x}\} = A \{x\} + B\{w\} \quad (7.8)$$

where $A = A_1 + B_1 F$

Also the performance index can be expressed as

$$\pi = \lim_{t_1 \rightarrow \infty} \frac{1}{t_1} E \left\{ \int_0^{t_1} [x^T Q x + x^T F^T \rho F x] dt \right\}$$

$$= \lim_{t_1 \rightarrow \infty} \frac{1}{t_1} E \left\{ \int_0^{t_1} x^T [Q + F^T \rho F] x dt \right\}$$

$$\text{or } \pi = \lim_{t_1 \rightarrow \infty} \frac{1}{t_1} E \left\{ \int_0^{t_1} x^T R x dt \right\} \quad (7.9)$$

where $R = Q + F^T \rho F$

The covariance matrix of the disturbance vector can be expressed as

$$R_w(t, \tau) = E \{w(t) w^T(\tau)\}$$

which can be idealised as

$$R_w(t, \tau) = c V \delta(t - \tau)$$

where δ is the DIRAC delta function (66).

The solution of matrix differential equation of the form

$$\{\dot{x}\} = A\{x\} + B\{w\}$$

is given by the expression

$$x(t) = \Phi(t, t_0) x(t_0) + \int_{t_0}^t \Phi(t, \tau) B(\tau) w(\tau) d\tau \quad (7.10)$$

where $\Phi(t, \tau)$ is the state transition matrix.

For the model being considered $t_0=0$ and $x(t_0)=0$, hence

$$x(t) = \int_0^t \Phi(t, \tau) B(\tau) w(\tau) d\tau \quad (7.11)$$

On substitution the value for $x(t)$ from eq. 7.11 into eq. 7.9, the result is

$$\pi = \lim_{t_1 \rightarrow \infty} \frac{1}{t_1} E\left\{ \int_0^{t_1} \left[\int_0^t w^T(\tau) B^T(\tau) \Phi^T(t, \tau) d\tau R \int_0^t \Phi(t, \tau) B(\tau) w(\tau) dt \right] dt \right\}$$

Taking the expectation, and using the rules of integration of stochastic processes as shown in ref. (66), theorem 1.51, the result is

$$\pi = \lim_{t_1 \rightarrow \infty} \frac{1}{t_1} \text{tr} \left\{ \int_0^{t_1} \int_0^t cV B^T(\tau) \Phi^T(t, \tau) R \Phi(t, \tau) B(\tau) dt \right\} \quad (7.12)$$

If M and N are compatible arbitrary matrices, then $\text{tr}(MN) = \text{tr}(NM)$. Using this rule, and changing the order of integration, the result is

$$\pi = \lim_{t_1 \rightarrow \infty} \frac{1}{t_1} \text{tr} \left\{ \int_0^{t_1} B(\tau) cV B^T(\tau) \left[\int_{\tau}^{t_1} \Phi^T(t, \tau) R \Phi(t, \tau) dt \right] d\tau \right\} \quad (7.13)$$

or

$$\pi = \lim_{t_1 \rightarrow \infty} \frac{1}{t_1} \text{tr} \int_0^{t_1} B(t) cV B^T(t) P(t) dt \quad (7.14)$$

where $P(t)$ is a symmetric non-negative-definite matrix given by

$$P(t) = \int_t^{t_1} \Phi^T(\tau, t) R \Phi(\tau, t) d\tau$$

It can be shown by differentiation (66) that $P(t)$ satisfies the matrix differential equation

$$-\dot{P}(t) = A(t)^T P(t) + P(t) A(t) + R(t) \quad (7.15)$$

For a time-invariant case with constant matrices A, B and R

$$P(t) = \int_t^{t_1} e^{A^T(\tau-t)} R e^{A(\tau-t)} d\tau \quad (7.16)$$

In the limit as $t_1 \rightarrow \infty$, $P(t) \rightarrow \bar{P}$

$$\text{where } \bar{P} = \int_t^\infty e^{A^T(\tau-t)} R e^{A(\tau-t)} d\tau$$

which after the change of variable $\tau - t = \tau'$ becomes

$$\bar{P} = \int_0^\infty e^{A^T \tau'} R e^{A \tau'} d\tau' \quad (7.17)$$

Eq.(7.17) shows that \bar{P} is a constant matrix.

The performance index can now be expressed as

$$\pi = \lim_{t \rightarrow \infty} \frac{1}{t_1} \text{tr} \left\{ \int_0^{t_1} B^T c^T e^{A^T \tau'} \bar{P} e^{A \tau'} dt \right\} = c^T \text{tr} [B B^T \bar{P}] \quad (7.18)$$

Since \bar{P} is a constant matrix, eq. 7.15 becomes

$$0 = A^T \bar{P} + \bar{P} A + R \quad (7.19)$$

from which the value of matrix \bar{P} can be calculated.

Eq. 7.19 is known as the Lyapunov equation, and a number of computer programs have been published in literature for its numerical solution (79,80,81,82,83,84). Closed form solutions in symbols are feasible only for the most elementary systems having one or two degrees of freedom.

A closed form solution will be attempted for the $\frac{1}{4}$ car model in order to compare the results with those obtained in Chapter 5.

7.3 Solution of Lyapunov Equation

$$A^T \bar{P} + \bar{P} A + R = 0$$

where

$$A = A_1 + B_1 F = \begin{bmatrix} 0 & 0 & 0 & 0 \\ 0 & 0 & -1 & 1 \\ -k_1/m_1 & k_2/m_1 & -B_2/m_1 & B_2/m_1 \\ 0 & -k_2/m_2 & B_2/m_2 & -B_2/m_2 \end{bmatrix}$$

$$\bar{P} = \begin{bmatrix} P_{11} & P_{12} & P_{13} & P_{14} \\ P_{12} & P_{22} & P_{23} & P_{24} \\ P_{13} & P_{23} & P_{33} & P_{34} \\ P_{14} & P_{24} & P_{34} & P_{44} \end{bmatrix}$$

The matrix will be symmetrical about the main diagonal.

$$R = Q + F^T \rho F = \begin{bmatrix} q_1 & 0 & 0 & 0 \\ 0 & (q_2 + \rho k_2^2) & -\rho k_2 B_2 & \rho k_2 B_2 \\ 0 & -\rho B_2 k_2 & \rho B_2^2 & -\rho B_2^2 \\ 0 & \rho B_2 k_2 & -\rho B_2^2 & \rho B_2^2 \end{bmatrix}$$

The number of simultaneous equations is expected to be $n(n+1)/2 = 10$ for the case under examination.

The simultaneous equations are arranged in matrix form on next page.

SIMULTANEOUS EQUATIONS FOR SOLUTION OF LYAPUNOV EQUATION

| 11 | 12 | 13 | 14 | 22 | 23 | 24 | 33 | 34 | 44 | | |
|----|----|---------------------|--------------------|----|----------------------|---------------------|--------------------|-------------------------------------|--------------------|----------|--------------------------|
| 0 | 0 | $2 \frac{k_1}{m_1}$ | 0 | 0 | 0 | 0 | 0 | 0 | 0 | p_{11} | q_1 |
| 0 | 0 | $\frac{k_2}{m_2}$ | $-\frac{k_2}{m_2}$ | 0 | $-\frac{k_1}{m_1}$ | 0 | 0 | 0 | 0 | p_{12} | 0 |
| 1 | -1 | $-\frac{B_2}{m_1}$ | $\frac{B_2}{m_2}$ | 0 | 0 | 0 | $-\frac{k_1}{m_1}$ | 0 | 0 | p_{13} | 0 |
| 0 | 1 | $\frac{B_2}{m_1}$ | $-\frac{B_2}{m_2}$ | 0 | 0 | 0 | 0 | $-\frac{k_1}{m_1}$ | 0 | p_{14} | 0 |
| 0 | 0 | 0 | 0 | 0 | $-2 \frac{k_2}{m_1}$ | $2 \frac{k_2}{m_2}$ | 0 | 0 | 0 | p_{22} | $q_2 + k_2^2 \rho$ |
| 0 | 1 | 0 | 0 | -1 | $-\frac{B_2}{m_1}$ | $\frac{B_2}{m_2}$ | $\frac{k_2}{m_1}$ | $-\frac{k_2}{m_2}$ | 0 | p_{23} | $k_2 B_2 \rho$ |
| 0 | 0 | 0 | 0 | 1 | $\frac{B_2}{m_1}$ | $-\frac{B_2}{m_2}$ | 0 | $\frac{k_2}{m_1}$ | $-\frac{k_2}{m_2}$ | p_{24} | $-k_2 B_2 \rho$ |
| 0 | 0 | -1 | 0 | 0 | 1 | 0 | $\frac{B_2}{m_1}$ | $-\frac{B_2}{m_2}$ | 0 | p_{33} | $\frac{1}{2} B_2^2 \rho$ |
| 0 | 0 | 0 | -1 | 0 | -1 | 1 | $-\frac{B_2}{m_1}$ | $\frac{B_2}{m_2} + \frac{B_2}{m_1}$ | $-\frac{B_2}{m_2}$ | p_{34} | $-B_2^2 \rho$ |
| 0 | 0 | 0 | 0 | 0 | 0 | -1 | 0 | $-\frac{B_2}{m_1}$ | $\frac{B_2}{m_2}$ | p_{44} | $\frac{1}{2} B_2^2 \rho$ |

The simultaneous equations in simplified form are listed below:-

$$p_{11} = \frac{k_1}{m_1} (p_{33} + p_{34})$$

$$p_{12} = \frac{k_2}{B_2} (p_{24} + p_{23} - p_{13})$$

$$p_{13} = \frac{1}{2} q_1 \left(\frac{m_1}{k_1} \right)$$

$$p_{14} = -\frac{1}{2} q_1 \left(\frac{m_1}{k_1} \right)$$

$$p_{22} = \left(\frac{k_2}{B_2} + \frac{B_2}{m_2} \right) p_{24} - \frac{B_2}{m_1} p_{23} - \frac{1}{2} k_2 B_2 \rho$$

$$p_{23} = \left(\frac{k_2}{m_2} + \frac{k_2}{m_1} \right) \left(\frac{m_1}{k_1} \right) p_{13}$$

$$p_{24} = \left(\frac{m_2}{k_2} \right) \left[\frac{k_2}{m_1} p_{23} + \frac{1}{2} (q_2 + k_2^2 \rho) \right]$$

$$p_{33} = \left(\frac{m_1}{B_2} \right) \left[\frac{B_2}{m_2} p_{34} - p_{23} + p_{13} + \frac{1}{2} B_2^2 \rho \right]$$

$$p_{34} = \left(\frac{m_1}{k_1} \right) \left[p_{12} + \left(\frac{B_2}{m_2} + \frac{B_2}{m_1} \right) p_{13} \right]$$

$$p_{44} = \left(\frac{m_2}{B_2} \right) \left(\frac{B_2}{m_1} p_{34} + p_{24} + \frac{1}{2} B_2^2 \rho \right)$$

It is now a relatively simple matter to solve for the elements of the \bar{P} - matrix by successive substitution.

The performance index is given by eq. 7.18 as

$$\pi = c V \text{tr} [B B^T \bar{P}] = c V \text{tr} \begin{bmatrix} -1 \\ 0 \\ 0 \\ 0 \end{bmatrix} \begin{bmatrix} -1 & 0 & 0 & 0 \end{bmatrix} [\bar{P}]$$

which becomes

$$\pi = c V \text{tr} \begin{bmatrix} 1 & 0 & 0 & 0 \\ 0 & 0 & 0 & 0 \\ 0 & 0 & 0 & 0 \\ 0 & 0 & 0 & 0 \end{bmatrix} \begin{bmatrix} p_{11} & p_{12} & p_{13} & p_{14} \\ p_{21} & p_{22} & p_{23} & p_{24} \\ p_{31} & p_{32} & p_{33} & p_{34} \\ p_{41} & p_{42} & p_{43} & p_{44} \end{bmatrix} \quad (7.20)$$

$$\text{which gives} \quad \pi = c V p_{11} \quad (7.21)$$

Thus it is not necessary to solve the complete matrix, but nevertheless, the algebraic manipulation will be considerable.

The values of the elements of the \bar{P} -matrix have been calculated, and are listed below.

$$p_{11} = q_1 \left[\frac{(m_1+m_2)^2 B_2}{2 k_1 m_2^2} + \left\{ \frac{m_1}{2} - \frac{m_1 k_2 (m_1+m_2)}{m_2 k_1} + \frac{(m_1+m_2)^3 k_2^2}{2 m_2^2 k_1^2} \right\} \frac{1}{B_2} \right] \\ + q_2 \frac{m_1+m_2}{2 B_2} + \rho \left[\frac{k_1 B_2}{2} + \frac{(m_1+m_2) k_2^2}{2 B_2} \right]$$

$$p_{12} = q_1 \frac{m_1 k_2}{2 k_1 B_2} \left[\frac{k_2 (m_1+m_2)^2}{k_1 m_1 m_2} - 1 \right] + q_2 \frac{m_2}{2 B_2} + \rho \frac{m_2 k_2^2}{2 B_2}$$

$$p_{13} = q_1 \frac{m_1}{2 k_1}$$

$$p_{14} = -q_1 \frac{m_1}{2 k_1}$$

$$p_{22} = q_1 \frac{m_1 k_2^2 (m_1+m_2)}{2 k_1^2 m_1 B_2} + q_2 \left[\frac{B_2}{2 k_2} + \frac{m_2}{2 B_2} \right] + \rho \frac{m_2 k_2^2}{2 B_2}$$

$$p_{23} = q_1 \frac{m_1 k_2 (m_1+m_2)}{2 k_1^2 m_2}$$

$$p_{24} = q_1 \frac{k_2 (m_1+m_2)}{2 k_1^2} + q_2 \frac{m_2}{2 k_2} + \rho \frac{m_2 k_2}{2}$$

$$p_{33} = q_1 \left(\frac{m_1}{k_1} \right) \left[\frac{m_1 (m_1+m_2) B_2}{2 k_1 m_2^2} + \left\{ \frac{m_1 k_2^2 (m_1+m_2)^2}{2 k_1^2 m_2^2} - \frac{m_1 k_2 (2m_1+m_2)}{2 m_2 k_1} + \frac{m_1}{2} \right\} \frac{1}{B_2} \right] \\ + q_2 \frac{m_1^2}{2 B_2 k_1} + \rho \left[\frac{m_1 B_2}{2} + \frac{m_1^2 k_2^2}{2 k_1 B_2} \right]$$

$$p_{34} = q_1 \left(\frac{m_1}{k_1} \right) \left[\frac{(m_1+m_2) B_2}{2 k_1 m_2} + \left\{ \frac{k_2 (m_1+m_2)^2}{2 k_1^2 m_2} - \frac{m_1 k_2}{2 k_1} \right\} \frac{1}{B_2} \right] \\ + q_2 \frac{m_1 m_2}{2 k_1 B_2} + \rho \frac{m_1 m_2 k_2^2}{2 k_1 B_2}$$

$$P_{44} = q_1 \left[\frac{(m_1+m_2) B_2}{2 k_1^2} + \left\{ \frac{k_2^2 (m_1+m_2)^2}{2 k_1^3} + \frac{k_2 m_2^2}{2 k_1^2 m_1} \right\} \frac{1}{B_2} \right]$$

$$+ q_2 \frac{m_2^2 (k_1+k_2)}{2 k_1 k_2 B_2} + \rho \left[\frac{m B_2}{2} + \frac{m_2^2 k_2 (k_1+k_2)}{2 k_1 B_2} \right]$$

Finally, the performance index can be expressed as:-

$$\pi = c V q_1 \left[\frac{(m_1+m_2)^2 B_2}{2 k_1 m_2^2} + \left\{ \frac{m_1}{2} - \frac{m_1 k_2 (m_1+m_2)}{m_2 k_1} + \frac{k_2^2 (m_1+m_2)^3}{2 k_1^2 m_2^2} \right\} \frac{1}{B_2} \right]$$

$$+ c V q_2 \left[\frac{m_1+m_2}{2 B_2} \right]$$

$$+ c V \rho \left[\frac{k_1 B_2}{2} + \frac{k_2^2 (m_1+m_2)}{2 B_2} \right] \quad (7.22)$$

It can be verified that the expression for the performance index as obtained here is identical with eq. 5.24 derived in chapter 5 using Parseval's Theorem, which proves that different methods of analysis will lead to the same result. Matrix methods have the advantage that digital computers can be applied quite readily to handle large matrices associated with systems having a large number of degrees of freedom.

The manual method of evaluating the integral square values by application of Parseval's Theorem is a very tedious process, and prone to manipulative errors. There is also some doubt about the correctness and ready availability of listed integrals for higher order systems.

8. ANALYSIS OF THE $\frac{1}{2}$ CAR MODEL

8.1 Introduction

In case of a $\frac{1}{2}$ car model, the front and rear motions are coupled through the body moment of inertia, hence a simple extension of the various integral square values as derived for a $\frac{1}{4}$ car model is not directly applicable since the model will have four degrees of freedom, and a time delay between the inputs to the front and rear wheels.

Also, since the overall stiffness of the model is to remain constant, representing a fixed permissible amount of deflection due to load, the front and rear spring stiffnesses are no longer independent. If one spring stiffness is changed, the other must also be changed so as to maintain approximately constant overall stiffness of the suspension, i.e. constant deflection of the mass centre of the vehicle under a specified static load.

8.2 Overall static stiffness of suspension

In this section the concept of static stiffness of the model will be developed.

A simplified $\frac{1}{2}$ car model is shown in Fig. 8.1 where k_2 represents the stiffness of the front suspension spring and k_{2P} that of the rear. Let δ_G represent the static deflection of the mass centre of the vehicle due to a vertical force F_G applied at the mass centre G . The equations for force and moment equilibrium are:-

$$(\delta_G + b\theta)k_{2P} + (\delta_G - a\theta)k_2 = F_G \quad (8.1)$$

$$(\delta_G + b\theta)b k_{2P} - (\delta_G - a\theta)a k_2 = 0 \quad (8.2)$$

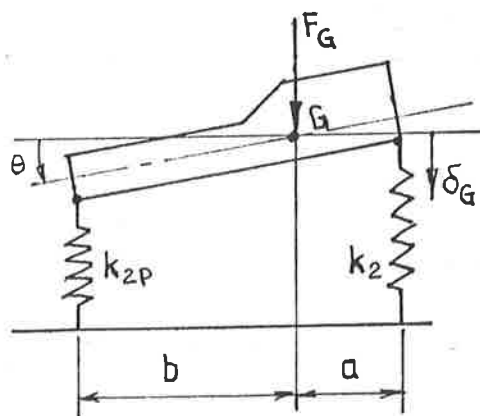


Fig. 8.1

Eliminating θ between eqs. (8.1) and (8.2) by division

$$\frac{F_G - \delta_G (k_2 - k_{2P})}{\delta_G (a k_2 - b k_{2P})} = \frac{\theta (b k_{2P} - a k_2)}{\theta (a^2 k_2 + b^2 k_{2P})}$$

Hence

$$\frac{F_G}{\delta_G} = k_o = (k_2 + k_{2P}) - \frac{(a k_2 - b k_{2P})^2}{a^2 k_2 + b^2 k_{2P}}$$

$$\text{Finally } k_o = \frac{k_2 k_{2P} (a+b)^2}{a^2 k_2 + b^2 k_{2P}} = \frac{k_2 k_{2P} L^2}{a^2 k_2 + b^2 k_{2P}} \quad (8.3)$$

where L is the length of the wheel base.

Only the stiffness of suspension springs is considered since the deflection of the suspension springs under specified payload is the critical factor.

Once the permissible static deflection has been specified, the minimum value of overall static stiffness k_o for the vehicle is more-or-less fixed.

Previous analysis has indicated that for good ride characteristics the suspension springs should be as soft as possible, but here obviously a lower limit is set.

If k_o is to remain constant, then k_2 and k_{2P} are no longer independent. If k_o is to remain constant for any chosen value of front spring stiffness k_2 , the rear spring stiffness k_{2P} must satisfy the relationship

$$k_{2P} = \frac{k_2 k_o a^2}{L^2 k_2 - b^2 k_o} \quad (8.4)$$

Since the overall stiffness k_o is related to the position of the mass centre, the values of k_o for a laden vehicle will differ slightly from those of an unladen vehicle.

The values are listed below for HILLMAN and CHRYSLER models.

HILLMAN model

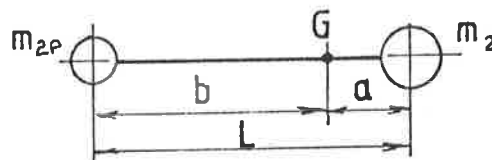
Unladen

$$\begin{aligned} k_2 &= 19972 \text{ N/m} \\ k_{2P} &= 22564 \text{ N/m} \\ m_2 &= 288.94 \text{ kg} \\ m_{2P} &= 216.14 \text{ kg} \\ m &= 505.08 \text{ kg} \\ a &= 1.098 \text{ m} \\ b &= 1.468 \text{ m} \\ L &= 2.566 \text{ m} \end{aligned}$$

$$k_0 = \frac{k_2 k_{2P} L^2}{a^2 k_2 + b^2 k_{2P}} = 40813 \text{ N/m}$$

Laden

$$\begin{aligned} m_2 &= 334.94 \text{ kg} \\ m_{2P} &= 340.14 \text{ kg} \\ m &= 675.08 \text{ kg} \end{aligned}$$



$$\begin{aligned} a &= L \frac{m_{2P}}{m} = 1.293 \text{ m} \\ b &= L \frac{m_2}{m} = 1.273 \text{ m} \\ k_0 &= 42415 \text{ N/m} \end{aligned}$$

CHRYSLER model

Unladen

$$\begin{aligned} k_2 &= 19270 \text{ N/m} \\ k_{2P} &= 21900 \text{ N/m} \\ m_2 &= 381.02 \text{ kg} \\ m_{2P} &= 322.05 \text{ kg} \\ m &= 703.07 \text{ kg} \\ a &= 1.292 \text{ m} \\ b &= 1.528 \text{ m} \\ L &= 2.820 \text{ m} \\ k_0 &= 40289 \text{ N/m} \end{aligned}$$

Laden

$$\begin{aligned} m_2 &= 435.52 \text{ kg} \\ m_{2P} &= 471.55 \text{ kg} \\ m &= 907.07 \text{ kg} \\ a &= 1.466 \text{ m} \\ b &= 1.354 \text{ m} \\ k_0 &= 41146 \text{ N/m} \end{aligned}$$

8.3 Analysis of $\frac{1}{2}$ car model

For the purpose of analysis the car is divided longitudinally by a vertical plane so that m represents half the body mass, and J represents half the mass moment of inertia about the pitching axis through the centre of mass.

The model thus enables to investigate the bounce and pitching but will provide no information regarding yaw and roll.

The front and rear unsprung masses m_1 and m_{1P} each correspond to a single wheel while k_1 and k_{1P} are the radial tyre stiffnesses of the front and rear tyres respectively.

Tyre damping has relatively small effect on overall model behaviour, hence will be disregarded in present analysis.

Only vertical and pitching motions are considered, and body forces u_2 and u_{2P} are assumed to exist between the axles and the body at the front and rear support points respectively. The model has four degrees of freedom and is illustrated in Fig. 8.2. All vertical displacements are measured from the static equilibrium position with the model on a level ground. The suffix P denotes the quantities corresponding to rear suspension.

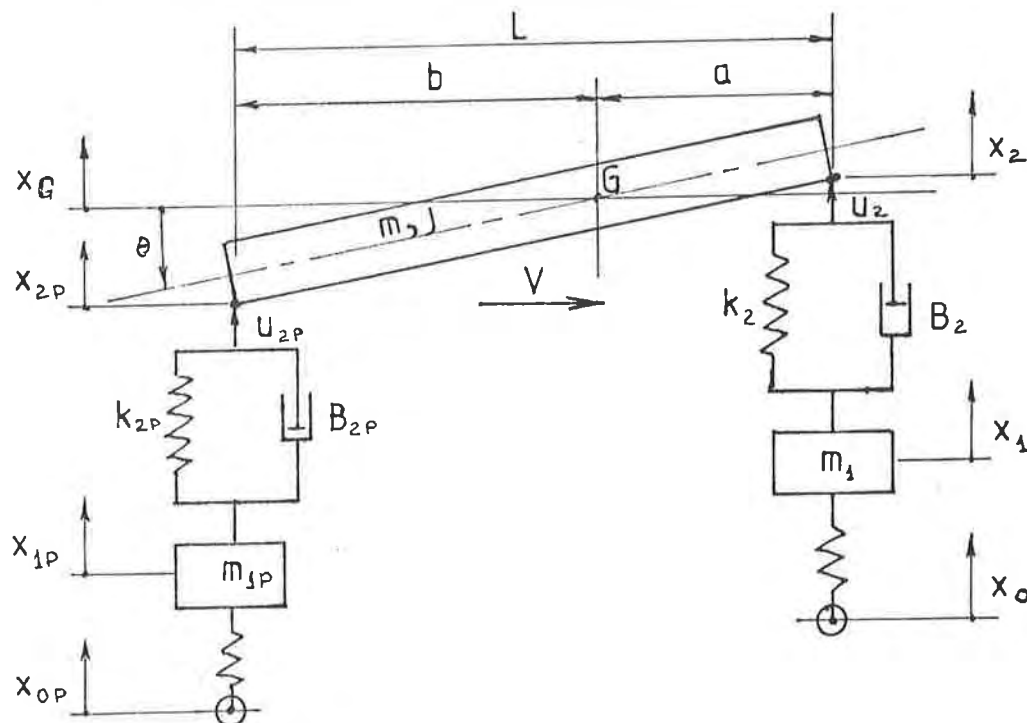


Fig. 8.2 $\frac{1}{2}$ CAR DYNAMICAL MODEL

If the model travels with a constant speed V , then the time delay between the inputs to the front and rear wheels is given by $D = L/V$ where L denotes the length of the wheelbase.

Equations of motion about the static equilibrium position are:-

$$(x_0 - x_1)k_1 - u_2 = m_1 \dot{x}_1 \quad (8.5)$$

$$(x_{0P} - x_{1P})k_{1P} - u_{2P} = m_{1P} \dot{x}_{1P} \quad (8.6)$$

$$a u_2 - b u_{2P} = J \ddot{\theta} \quad (8.7)$$

$$u_2 + u_{2P} = m \dot{x}_G \quad (8.8)$$

$$\text{Now } \theta = (x_2 - x_{2P})/L$$

$$x_2 = x_G + a \theta$$

$$x_{2P} = x_G - b \theta \quad \text{and } x_G = (a x_{2P} + b x_2)/L$$

After eliminating θ and x_G from equations (8.7) and (8.8) the equations become

$$a u_2 - b u_{2P} = J(\dot{x}_2 - \dot{x}_{2P})/L = m r^2(\dot{x}_2 - \dot{x}_{2P})/L \quad (8.9)$$

$$\text{and } u_2 + u_{2P} = m(a \dot{x}_{2P} + b \dot{x}_2)/L \quad (8.10)$$

where r denotes the radius of gyration in the relationship

$$J = m r^2 \quad (8.11)$$

The forces applied to the support points by suspension elements are

$$u_2 = (x_1 - x_2)k_2 + (\dot{x}_1 - \dot{x}_2)B_2 \quad (8.12)$$

$$u_{2P} = (x_{1P} - x_{2P})k_{2P} + (\dot{x}_{1P} - \dot{x}_{2P})B_{2P} \quad (8.13)$$

With these substitutions, the equations of motion become

$$(x_0 - x_1)k_1 - (x_1 - x_2)k_2 - (\dot{x}_1 - \dot{x}_2)B_2 = m_1 \ddot{x}_1 \quad (8.14)$$

$$(x_{0P} - x_{1P})k_{1P} - (x_{1P} - x_{2P})k_{2P} - (\dot{x}_{1P} - \dot{x}_{2P})B_{2P} = m_{1P} \ddot{x}_{1P} \quad (8.15)$$

$$\begin{aligned} -b(x_{1P} - x_{2P})k_{2P} - b(\dot{x}_{1P} - \dot{x}_{2P})B_{2P} + a(x_1 - x_2)k_2 + a(\dot{x}_1 - \dot{x}_2)B_2 = \\ = m r^2(\dot{x}_2 - \dot{x}_{2P})/L \end{aligned} \quad (8.16)$$

$$(x_1 - x_2)k_2 + (\dot{x}_1 - \dot{x}_2)B_2 + (x_{1P} - x_{2P})k_{2P} + (\dot{x}_{1P} - \dot{x}_{2P})B_{2P} = m(a \dot{x}_{2P} + b \dot{x}_2)/L \quad (8.17)$$

For a step input of magnitude x_0 at the front and x_{0P} at the rear, delayed by D sec., Laplace transformation gives

$$(m_1 s^2 + B_2 s + k_2 + k_1)X_1(s) - (B_2 s + k_2)X_2(s) = k_1 X_0/s \quad (8.18)$$

$$(m_{1P} s^2 + B_{2P} s + k_{2P} + k_{1P})X_{1P}(s) - (B_{2P} s + k_{2P})X_2(s) = k_{1P} e^{-Ds} X_{0P}/s \quad (8.19)$$

$$-a(B_2 s + k_2)X_1(s) + (m r^2 s^2/L + a B_2 s + a k_2)X_2(s) + b(B_{2P} s + k_{2P})X_{1P}(s) - (m r^2 s^2/L + b B_{2P} s + b k_{2P})X_{2P}(s) = 0 \quad (8.20)$$

$$-(B_2 s + k_2)X_1(s) + (m b s^2/L + B_2 s + k_2)X_2(s) - (B_{2P} s + k_{2P})X_{1P}(s) + (m a s^2/L + B_{2P} s + k_{2P})X_{2P}(s) = 0 \quad (8.21)$$

The equations could be solved for

$$[X_0(s) - X_1(s)], [X_1(s) - X_2(s)], [X_{0P}(s) - X_{1P}(s)], [X_{1P}(s) - X_{2P}(s)],$$

and then integral square values determined by contour integration on complex plane (52), but the algebra involved would be unmanageable.

Without too much algebraic manipulation $X_2(s)$ and $X_{2P}(s)$ can be eliminated from equations 8.18 and 8.19, leaving two simultaneous equations in terms of $X_1(s)$ and $X_{1P}(s)$ as under

$$\begin{aligned} & \frac{(m_1 s^2 + B_2 s + k_2 + k_1)}{B_2 s + k_2} \frac{m s^2 (r^2 - ab)}{L^2} X_1(s) \\ & - \left\{ \frac{m s^2 (r^2 + a^2)}{L^2} + B_{2P} s + k_{2P} \right\} \frac{(m_{1P} s^2 + B_{2P} s + k_{2P} + k_{1P})}{B_{2P} s + k_{2P}} (B_{2P} s + k_{2P}) X_{1P}(s) \\ & = \frac{k_1 X_0}{s} \frac{m s^2 (r^2 - ab)}{(B_2 s + k_2) L^2} - \frac{k_{1P} e^{-Ds} X_{0P}}{s} \frac{m s^2 (r^2 + a^2)/L^2 + B_{2P} s + k_{2P}}{B_{2P} s + k_{2P}} \quad (8.22) \end{aligned}$$

and

$$\begin{aligned} & \{ [m s^2(r^2+b^2)/L^2 + B_2s + k_2] \left(\frac{m_1 s^2 + B_2s + k_2 + k_1}{B_2s + k_2} \right) - (B_2s + k_2) \} X_1(s) \\ & - \frac{m s^2(r^2-ab)}{L^2} \left(\frac{m_{1P} s^2 + B_{2P} s + k_{2P} + k_{1P}}{B_{2P} s + k_{2P}} \right) \} X_{1P}(s) = \\ & = \left(\frac{k_1 X_0}{s} \right) \left(\frac{m s^2(r^2+b^2)/L^2 + B_2s + k_2}{B_2s + k_2} \right) - \left(\frac{k_{1P} e^{-Ds} X_{0P}}{s} \right) \frac{m s^2(r^2-ab)}{(B_{2P} s + k_{2P}) L^2} \end{aligned} \quad (8.23)$$

It is clear that equations (8.22) and (8.23) become uncoupled if $r^2 = ab$. If the coupling ratio of the model is defined as $R = J/m = r^2/ab$, then the front and rear motions become completely uncoupled when the coupling ratio $R = 1.0$. For an uncoupled system with $R = 1.0$, the equations for the front and rear axle displacements are:-

$$\frac{X_1(s)}{X_0} = \frac{k_1(m_2 s^2 + B_2s + k_2)}{s [(m_2 s^2 + B_2s + k_2)(m_1 s^2 + B_2s + k_2 + k_1) - (B_2s + k_2)^2]} \quad (8.24)$$

and

$$\frac{X_{1P}(s)}{X_{0P}} = \frac{e^{-Ds} k_{1P} (m_{2P} s^2 + B_{2P} s + k_{2P})}{s [(m_{2P} s^2 + B_{2P} s + k_{2P})(m_{1P} s^2 + B_{2P} s + k_{2P} + k_{1P}) - (B_{2P} s + k_{2P})^2]} \quad (8.25)$$

where $m_2 = m(r^2+b^2)/L^2 = mb(a+b)/L^2 = mb/L$ when $r^2 = ab$

and $m_{2P} = m(r^2+a^2)/L^2 = ma(a+b)/L^2 = ma/L$

When the equations (8.24) and (8.25) are compared with the equations derived for $\frac{1}{4}$ car model analysis, it is evident that the expressions are identical. Thus for an uncoupled system all equations derived for the $\frac{1}{4}$ car model are directly applicable, and integral square values for an uncoupled $\frac{1}{2}$ car model (with $R=1.0$) are sums of corresponding integral square values for front and rear suspensions respectively.

Time delay will not affect the integral square values of an uncoupled system since the front axle response is completely independent of the delayed rear axle response and vice versa.

8.4 Integral square response and performance index of uncoupled $\frac{1}{2}$ car model (R=1.0).

The performance index can be expressed as

$$I = \rho [\langle u_2^2 \rangle + \langle u_{2P}^2 \rangle] + q_1 [\langle (x_0 - x_1)^2 \rangle + \langle (x_{0P} - x_{1P})^2 \rangle] \\ + q_2 [\langle (x_1 - x_2)^2 \rangle + \langle (x_{1P} - x_{2P})^2 \rangle] \quad (8.26)$$

For a unit step input the integral square values are:-

I.S.V. Body Force

$$\langle u_2^2 \rangle + \langle u_{2P}^2 \rangle = \left[\frac{k_1 B_2}{2} + \frac{k_2^2 (m_1 + m_2)}{2 B_2} \right] + \left[\frac{k_{1P} B_{2P}}{2} + \frac{k_{2P}^2 (m_{1P} + m_{2P})}{2 B_{2P}} \right] \quad (8.27)$$

I.S.V. Tyre Deflection

$$\langle x_{01}^2 \rangle + \langle x_{01P}^2 \rangle = \frac{(m_1 + m_2)^2 B_2}{2 k_1 m_2^2} + \left\{ \frac{m_1}{2} - \frac{k_2 m_1 (m_1 + m_2)}{k_1 m_2} + \frac{k_2^2 (m_1 + m_2)^3}{2 (k_1 m_2)^2} \right\} \frac{1}{B_2} \\ + \frac{(m_{1P} + m_{2P})^2 B_{2P}}{2 k_{1P} m_{2P}^2} + \left\{ \frac{m_{1P}}{2} - \frac{k_{2P} m_{1P} (m_{1P} + m_{2P})}{k_{1P} m_{2P}} + \frac{k_{2P}^2 (m_{1P} + m_{2P})^3}{2 (k_{1P} m_{2P})^2} \right\} \frac{1}{B_{2P}} \quad (8.28)$$

The integral square values are minimised if the front and rear are independently minimised by selecting the appropriate values of $B_{2 \text{ OPT}}$ and $B_{2P \text{ OPT}}$ as for $\frac{1}{4}$ car models.

I.S.V. Relative Wheel Travel

$$\langle x_{12}^2 \rangle + \langle x_{12P}^2 \rangle = \frac{m_1 + m_2}{2 B_2} + \frac{m_{1P} + m_{2P}}{2 B_{2P}} \quad (8.29)$$

This quantity is independent of spring stiffness, and decreases with increasing damping. There are no turning points.

After having briefly examined the influence of damping on suspension response of an uncoupled system, it is evident that optimum damping values can be selected for front and rear by treating them independently.

8.5 The influence of suspension springs on integral square response

In case of an uncoupled $\frac{1}{2}$ car model ($R=1.0$), only the body force and tyre deflection integral square values are affected by the stiffness of suspension springs while the relative wheel travel is completely unaffected.

I.S.V. Body Force

The value of spring stiffness k_2 that minimises the body force is obtained by differentiation of eq. 8.27 as

$$\frac{k_2 (m_1+m_2)}{B_2} + k_{2P} \left(\frac{d k_{2P}}{d k_2} \right) \frac{m_{1P}+m_{2P}}{B_{2P}} = 0 \quad (8.30)$$

where

$$k_{2P} = \frac{k_2 k_0 a^2}{k_2 L^2 - k_0 b^2}$$

and

$$\frac{d k_{2P}}{d k_2} = - \frac{k_0^2 a^2 b^2}{(k_2 L^2 - k_0 b^2)^2} = - \frac{k_{2P}^2 b^2}{k_2^2 a^2} \quad (8.31)$$

On substitution of the value for $d k_{2P}/d k_2$ into eq. 8.30, the result is

$$\frac{k_2 (m_1+m_2)}{B_2} - \left(\frac{k_2 k_0 a^2}{k_2 L^2 - k_0 b^2} \right) \frac{k_0^2 a^2 b^2}{(k_2 L^2 - k_0 b^2)^2} \frac{(m_{1P}+m_{2P})}{B_{2P}} = 0$$

or

$$k_2 \frac{m_1+m_2}{B_2} \left[1 - \frac{k_0^3 a^4 b^2}{(k_2 L^2 - k_0 b^2)^3} \frac{(m_{1P}+m_{2P})}{m_1+m_2} \frac{B_2}{B_{2P}} \right] = 0 \quad (8.32)$$

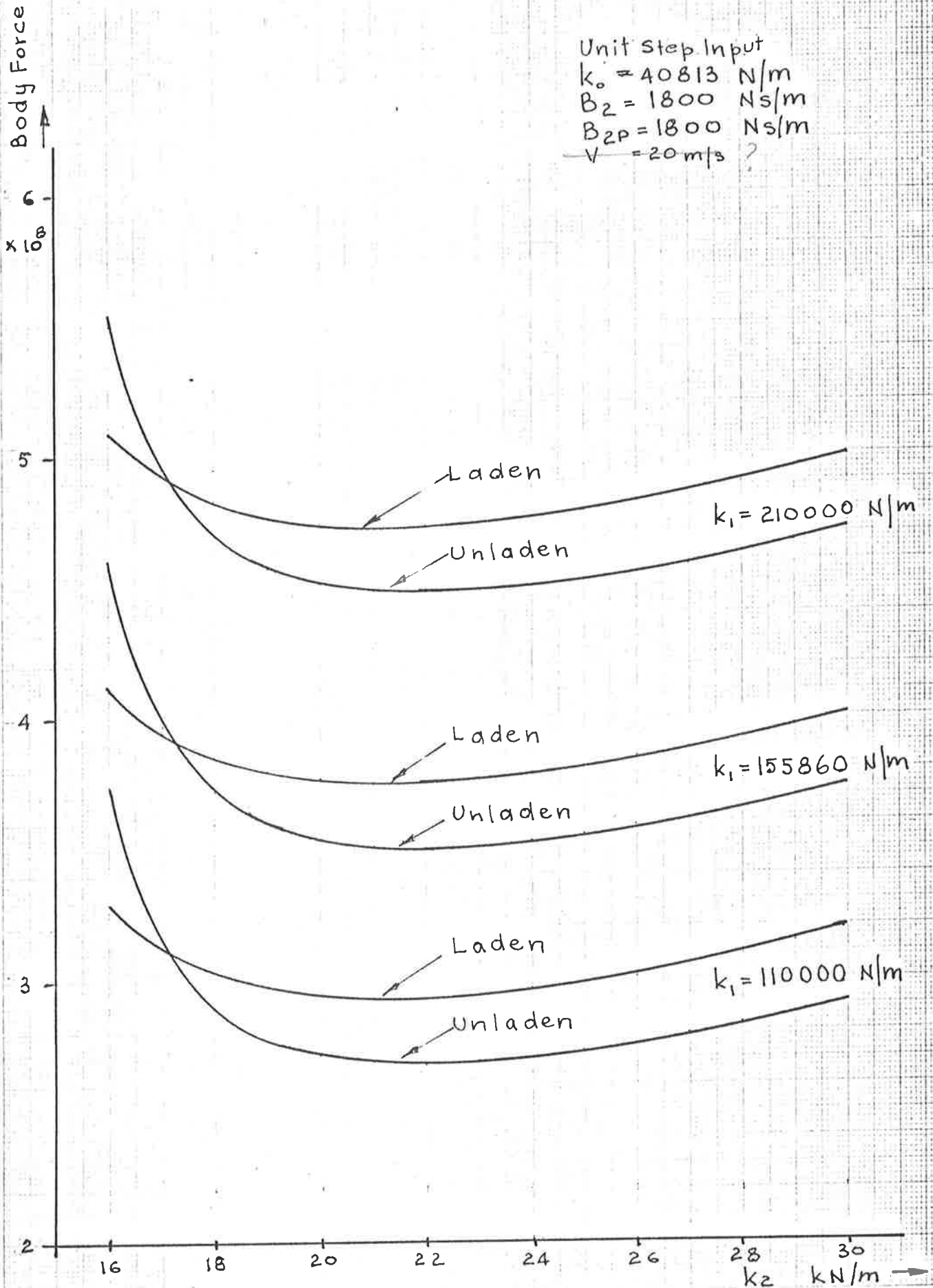
The value of k_2 that minimises the body force can then be calculated from eq. 8.32 as

$$k_2 = k_0 \left\{ \frac{b^2}{L^2} + \left[\frac{a^4 b^2 (m_{1P}+m_{2P}) B_2}{L^6 (m_1+m_2) B_{2P}} \right]^{\frac{1}{3}} \right\} \quad (8.33)$$

Integral square values of body force have been calculated for different values of k_2 , and plotted in Fig. 8.3 for $\frac{1}{2}$ car model using HILLMAN data and $R=1.0$.

Fig. 8.3.

Integral Square Body Force
HILLMAN Half-Car Model ($R=1.0$)



Since the radial stiffness of identical commercial tyres is known to vary over rather wide limits, in addition to variations due to inflation pressure, the graphs have been plotted for different values of tyre radial stiffness.

1.S.V. Tyre Deflection

Differentiating eq. 8.28 with respect to k_2 , and setting the result equal to zero, gives

$$\left\{ -\frac{m_1(m_1+m_2)}{k_1 m_2} + \frac{k_2(m_1+m_2)^3}{(k_1 m_2)^2} \right\} \frac{1}{B_2} + \left\{ \frac{k_0^2 a^2 b^2 m_{1P}(m_{1P}+m_{2P})}{k_2 L^2 - k_0 b^2)^2 k_{1P} m_{2P}} - \frac{k_2 k_0^3 a^4 b^2 (m_{1P}+m_{2P})^3}{(k_2 L^2 - k_0 b^2)^2 (k_{1P} m_{2P})^2} \right\} \frac{1}{B_{2P}} \quad (8.34)$$

Eq. (8.34) can be rearranged as

$$\frac{k_2(m_1+m_2)^3}{(k_1 m_2)^2 B_2} \left[1 - \frac{k_0^3 a^4 b^2 (m_{1P}+m_{2P})^3 (k_1 m_2)^2 B_2}{(k_2 L^2 - k_0 b^2)^3 (m_1+m_2)^3 (k_{1P} m_{2P})^2 B_{2P}} \right] - \frac{m_1(m_1+m_2)}{k_1 m_2} \left[1 - \frac{k_0^2 a^2 b^2 m_{1P}(m_{1P}+m_{2P}) m_2 B_2}{(k_2 L^2 - k_0 b^2)^2 m_1(m_1+m_2) m_{2P} B_{2P}} \right] = 0 \quad (8.35)$$

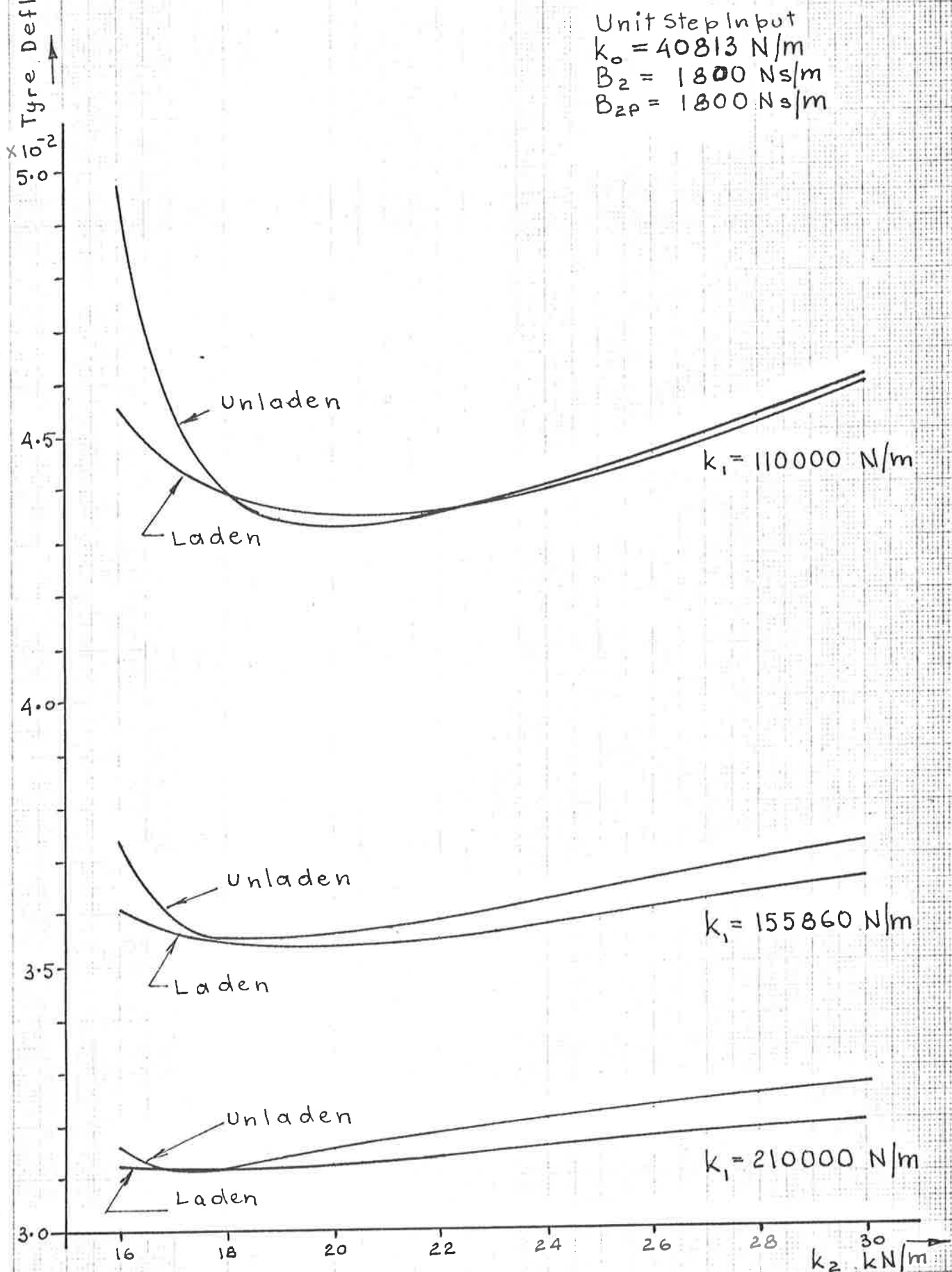
Eq. 8.35 can be solved for the value of k_2 that minimises the integral square value of tyre deflection, but only numerical solution is possible which can be effected on a programmable calculator or on an interactive computer terminal.

Integral square values of tyre deflection are plotted against k_2 in Fig. 8.4.

8.6 Functional relationship between minimum performance index and spring stiffness of an uncoupled $\frac{1}{2}$ car model (R=1.0).

It is of interest to investigate the relationship between the minimum performance index, spring stiffness and weighting factors for an uncoupled model since it is to be expected that some general principles will also apply to coupled models.

Fig. 8.4. Integral Square Tyre Deflection
HILLMAN Half-Car Model



The performance index for the uncoupled $\frac{1}{2}$ car model, excited by unit step input is given by eq. 8.26 as

$$\begin{aligned}
 I = & \rho \left\{ \frac{k_1 B_2}{2} + \frac{k_2^2 (m_1 + m_2)}{2 B_2} + \frac{k_{1P} B_{2P}}{2} + \frac{k_{2P}^2 (m_{1P} + m_{2P})}{2 B_{2P}} \right\} \\
 & + q_1 \left\{ \frac{(m_1 + m_2)^2 B_2}{2 k_1 m_2^2} + \left[\frac{m_1}{2} - \frac{k_2 m_1 (m_1 + m_2)}{k_1 m_2} + \frac{k_2^2 (m_1 + m_2)^3}{2 (k_1 m_2)^2} \right] \frac{1}{B_2} \right\} \\
 & + \frac{(m_{1P} + m_{2P})^2 B_{2P}}{2 k_{1P} m_{2P}^2} + \left[\frac{m_{1P}}{2} - \frac{k_{2P} m_{1P} (m_{1P} + m_{2P})}{k_{1P} m_{2P}} + \frac{k_{2P}^2 (m_{1P} + m_{2P})^3}{2 (k_{1P} m_{2P})^2} \right] \frac{1}{B_{2P}} \left. \right\} \\
 & + q_2 \left\{ \frac{m_1 + m_2}{2 B_2} + \frac{m_{1P} + m_{2P}}{2 B_{2P}} \right\}
 \end{aligned}$$

Differentiation with respect to k_2 gives

$$\begin{aligned}
 \frac{dI}{dk_2} = & \rho \left\{ \frac{k_2 (m_1 + m_2)}{B_2} + k_{2P} \left(\frac{dk_{2P}}{dk_2} \right) \frac{m_{1P} + m_{2P}}{B_{2P}} \right\} \\
 & + q_1 \left\{ \left[- \frac{m_1 (m_1 + m_2)}{k_1 m_2} + \frac{k_2 (m_1 + m_2)^3}{(k_1 m_2)^2} \right] \frac{1}{B_2} \right. \\
 & \left. + \left(\frac{d k_{2P}}{d k_2} \right) \left[- \frac{m_{1P} (m_{1P} + m_{2P})}{k_{1P} m_{2P}} + \frac{k_{2P} (m_{1P} + m_{2P})^3}{2 (k_{1P} m_{2P})^2} \right] \frac{1}{B_{2P}} \right\} \quad (8.36)
 \end{aligned}$$

after substituting for

$$k_{2P} = \frac{k_2 k_0 a^2}{k_2 L^2 - k_0 b^2}$$

$$\text{and } \frac{dk_{2P}}{dk_2} = - \frac{k_{2P}^2 b^2}{k_2^2 a^2}$$

the condition for minimum performance index becomes after rearrangement of eq. 8.36 as

$$\begin{aligned}
& \rho k_2 \left[1 - \frac{k_0^3 a^4 b^2 (m_{1P} + m_{2P}) B_2}{(k_2 L^2 - k_0 b^2)^3 (m_1 + m_2) B_{2P}} \right] \\
& + q_1 \frac{k_2 (m_1 + m_2)^2}{k_1^2 m_2^2} \left[1 - \frac{k_0^3 a^4 b^2 (m_{1P} + m_{2P})^3 m_2^2 B_2}{(k_2 L^2 - k_0 b^2)^3 (m_1 + m_2)^3 m_{2P}^2 B_{2P}} \right] \\
& - q_1 \frac{m_1}{k_1 m_2} \left[1 - \frac{k_0^2 a^2 b^2 m_{1P} m_2 (m_{1P} + m_{2P}) B_2}{(k_2 L^2 - k_0 b^2)^2 m_{2P} m_1 (m_1 + m_2) B_{2P}} \right] = 0 \quad (8.37)
\end{aligned}$$

It is clear that the value of k_2 that minimises the performance index is a function of system parameters, as well as function of weighting factors ρ and q .

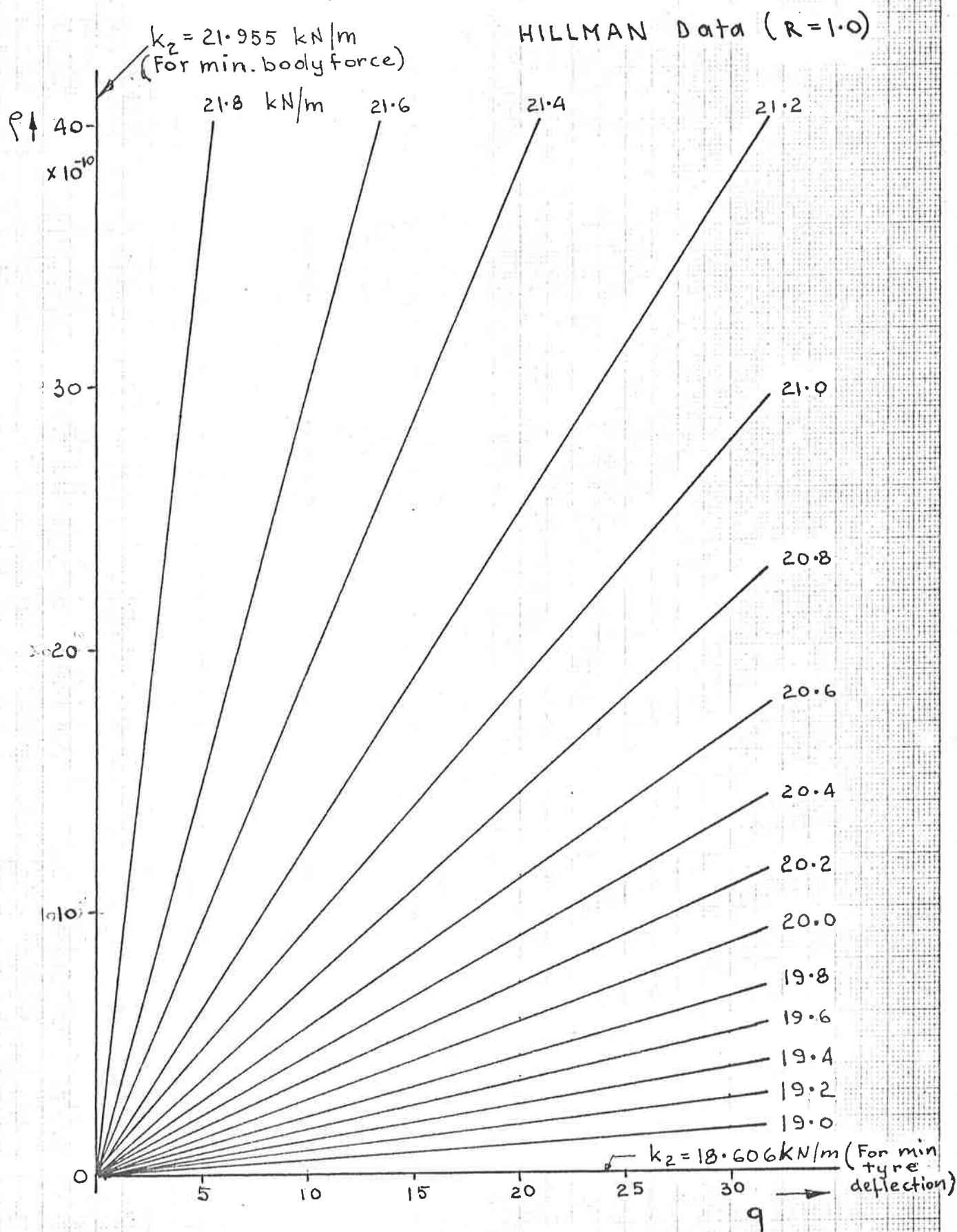
Eq. 8.37 represents a linear relationship between ρ and q with k_2 as a parameter for a given constant B_2/B_{2P} ratio.

The graph of ρ against q will have a horizontal slope when

$$\begin{aligned}
& \frac{k_2 (m_1 + m_2)^2}{k_1 m_1 m_2} \left\{ 1 - \frac{k_0^3 a^4 b^2 (m_{1P} + m_{2P})^3 m_2^2 B_2}{(k_2 L^2 - k_0 b^2) (m_1 + m_2)^3 m_{1P}^2 B_{2P}} \right\} = \\
& = 1 - \frac{k_0^2 a^2 b^2 m_{1P} m_2 (m_{1P} + m_{2P}) B_2}{(k_2 L^2 - k_0 b^2)^2 m_{2P} m_1 (m_1 + m_2) B_{2P}} \quad (8.38)
\end{aligned}$$

The value of k_2 calculated from eq. 8.38 corresponds to the value of k_2 that minimises the integral square of tyre deflection as indicated previously by eq. 8.35.

Fig.8.5. Functional Relationship between Weighting Factors with k_2 as a Parameter



The graph will have a vertical slope when

$$\frac{(k_2 L^2 - k_0 b^2)^3}{k_0^3 a^4 b^2} = \frac{m_{1P} + m_{2P}}{(m_1 + m_2)} \frac{B_2}{B_2}$$

$$\text{or } \frac{k_2}{k_0} = \left[\frac{a^4 b^2 (m_{1P} + m_{2P})}{L^6 (m_1 + m_2)} \right]^{1/3} + \frac{b^2}{L^2} \quad (8.39)$$

The value of k_2 calculated from eq. 8.39 is identical with the value that minimises the integral square of body force.

The linear relationship between ρ and q with k_2 as a parameter is shown in Fig. 8.5 which has been plotted with data corresponding to HILLMAN model for $R=1.0$.

It is evident from the graph that the values of k_2 that minimise the performance index for positive values of weighting factors must lie between the values that minimise the I.S.V. of tyre deflection and the body force respectively.

If I_{\min} is plotted in the form of a carpet plot against k_2 , with ρ and q as parameters, the graph shown in Fig. 8.6 will result.

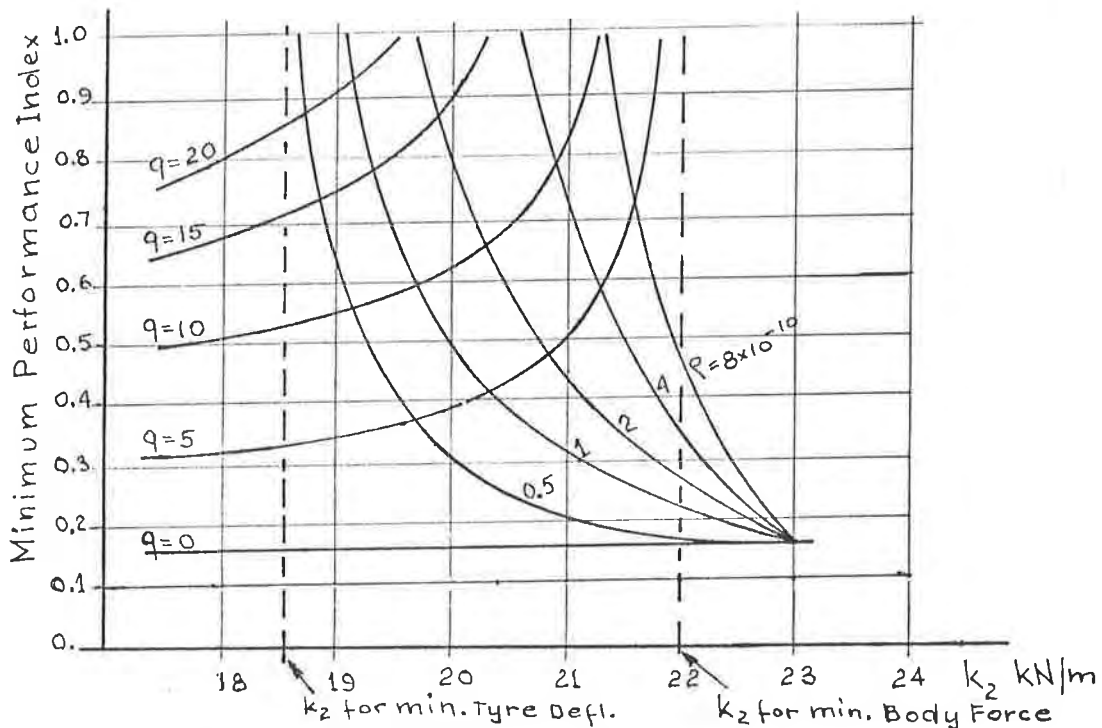


Fig. 8.6 - VARIATION OF I_{\min} WITH k_2



The region corresponding to positive weighting factors is bounded by vertical asymptotes through the values of k_2 that minimise the tyre deflection and the body force respectively.

The general character of the graph is similar to that obtained in case of damping. If one of the weighting factors is held constant, and the other increased, the minimisation process will converge towards the value of k_2 that will reduce the particular response.

It follows that once the weighting factors ρ and q have been selected, the minimum value of the performance index and the corresponding value of k_2 that minimises the performance index are automatically fixed.

If the integral square value of tyre deflection is used as the sole performance criterion, it implies that $q \rightarrow \infty$, and the computer optimisation process will lead to the value of k_2 that will minimise the integral square of dynamic tyre deflection, i.e. to the left-hand asymptote.

Conversely, if body force is the sole performance criterion, the minimisation process will lead to R.H. asymptote.

The relationships are shown in Figs. 8.7, 8.8, 8.9 and 8.10 for HILLMAN and CHRYSLER data with $R=1.0$.

To verify the validity of the graphs, the integral square values of response, and the performance indices for the models were calculated using the program "Performance Index" in ACSL digital simulation language shown in Appendix C. The weighting factors in all calculations were taken as

$$\rho = 8 \times 10^{-10}, \quad q_1 = 10.0, \quad q_2 = 1.0.$$

The performance indices calculated are plotted against k_2 in Fig. 8.11 for the HILLMAN model, and in Fig. 8.12 for the CHRYSLER ($R=1.0$).

The minima are listed in Table 8.1 from which it can be seen that there is complete agreement between direct calculation and digital simulation results.

TABLE 8.1

| Model | l_{\min} | k_2 OPT for l_{\min} |
|------------------|------------|--------------------------|
| HILLMAN (R=1.0) | | |
| UNLADEN | 0.801 | 20.8 kN/m |
| LADEN | 0.865 | 20.9 kN/m |
| CHRYSLER (R=1.0) | | |
| UNLADEN | 1.01 | 20.2 kN/m |
| LADEN | 1.10 | 20.1 kN/m |

Program INDEX 1 in interactive BASIC was also used to check the results.

This program, also shown in Appendix C, calculates the integral square values and the performance index directly from model parameter values (for $R=1.0$), using the integral square expressions derived from Parseval's Theorem.

There is complete agreement between the results obtained by digital simulation and by direct calculation.

The values of k_2 that locate the vertical asymptotes have also been calculated for different values of B_2/B_{2P} ratios, and are listed in Table 8.2 for the HILLMAN model and in Table 8.3 for the CHRYSLER ($R=1.0$).

TABLE 8.2 (HILLMAN MODEL)

| B_2/B_{2P} Ratio | UNLADEN | | LADEN | |
|-----------------------|-------------------------------------|-------------------------------------|-------------------------------------|-------------------------------------|
| | k_2 for min. tyre defl. N/m | k_2 for min. body force N/m | k_2 for min. tyre defl. N/m | k_2 for min. body force N/m |
| 1/3.0 | 18132 | 19319 | 17523 | 17783 |
| 1/2.5 | 18225 | 19692 | 17776 | 18252 |
| 1/2.0 | 18331 | 20181 | 18093 | 19730 |
| 1/1.5 | 18454 | 20868 | 18510 | 18868 |
| 1.0 | 18603 | 21955 | 19111 | 21096 |
| 1.5 | 18721 | 22200 | 19720 | 22659 |
| 2.0 | 18788 | 24190 | 20151 | 23903 |
| 2.5 | 18832 | 25027 | 20482 | 24954 |
| 3.0 | 18862 | 25758 | 20748 | 25872 |

TABLE 8.3 (CHRYSLER MODEL)

| B_2/B_{2P} Ratio | UNLADEN | | LADEN | |
|-----------------------|-------------------------------------|-------------------------------------|-------------------------------------|-------------------------------------|
| | k_2 for min. tyre defl. N/m | k_2 for min. body force N/m | k_2 for min. tyre defl. N/m | k_2 for min. body force N/m |
| 1/3.0 | 16513 | 18230 | 17222 | 17119 |
| 1/2.5 | 16475 | 18631 | 17277 | 17597 |
| 1/2.0 | 16437 | 19157 | 17344 | 18223 |
| 1/1.5 | 16400 | 19894 | 17424 | 19103 |
| 1.0 | 16362 | 21061 | 17527 | 20495 |
| 1.5 | 16338 | 22397 | 17613 | 22088 |
| 2.0 | 16325 | 23461 | 17663 | 23356 |
| 2.5 | 16318 | 24359 | 17606 | 24427 |
| 3.0 | 16313 | 25144 | 17720 | 25363 |

Fig. 8.7. Relationship between min. Performance Index, Spring Stiffness and Weighting Factors.
 HILLMAN Model (Unladen), $R=1.0$

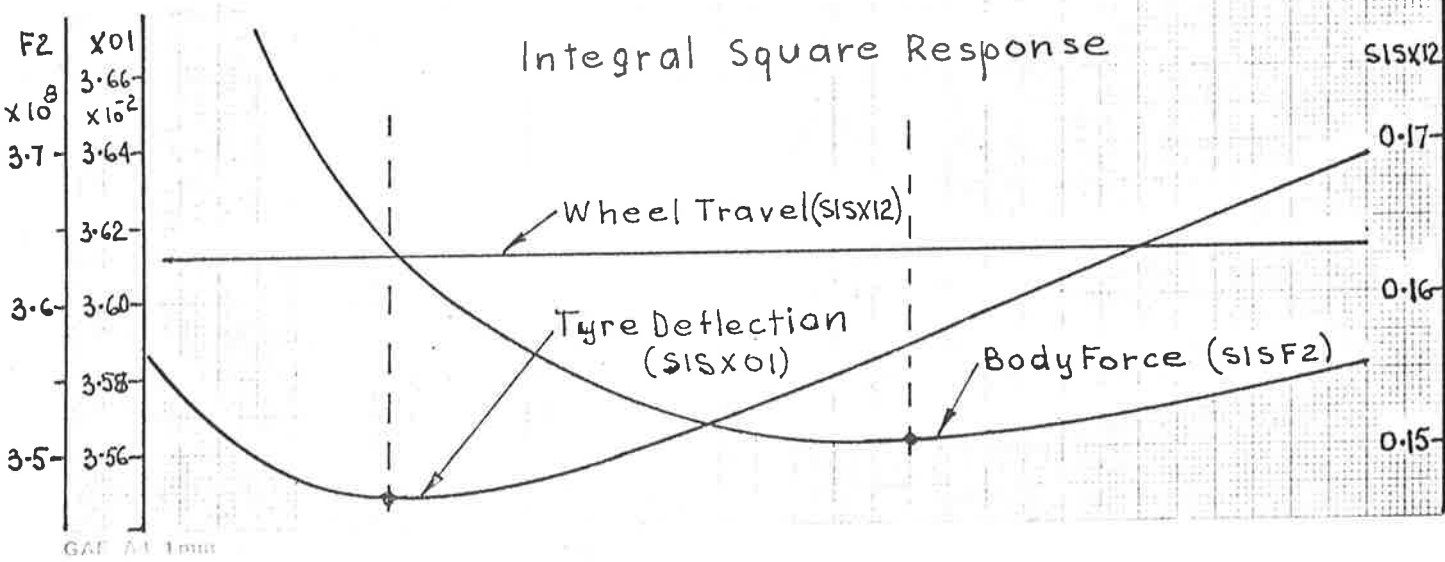
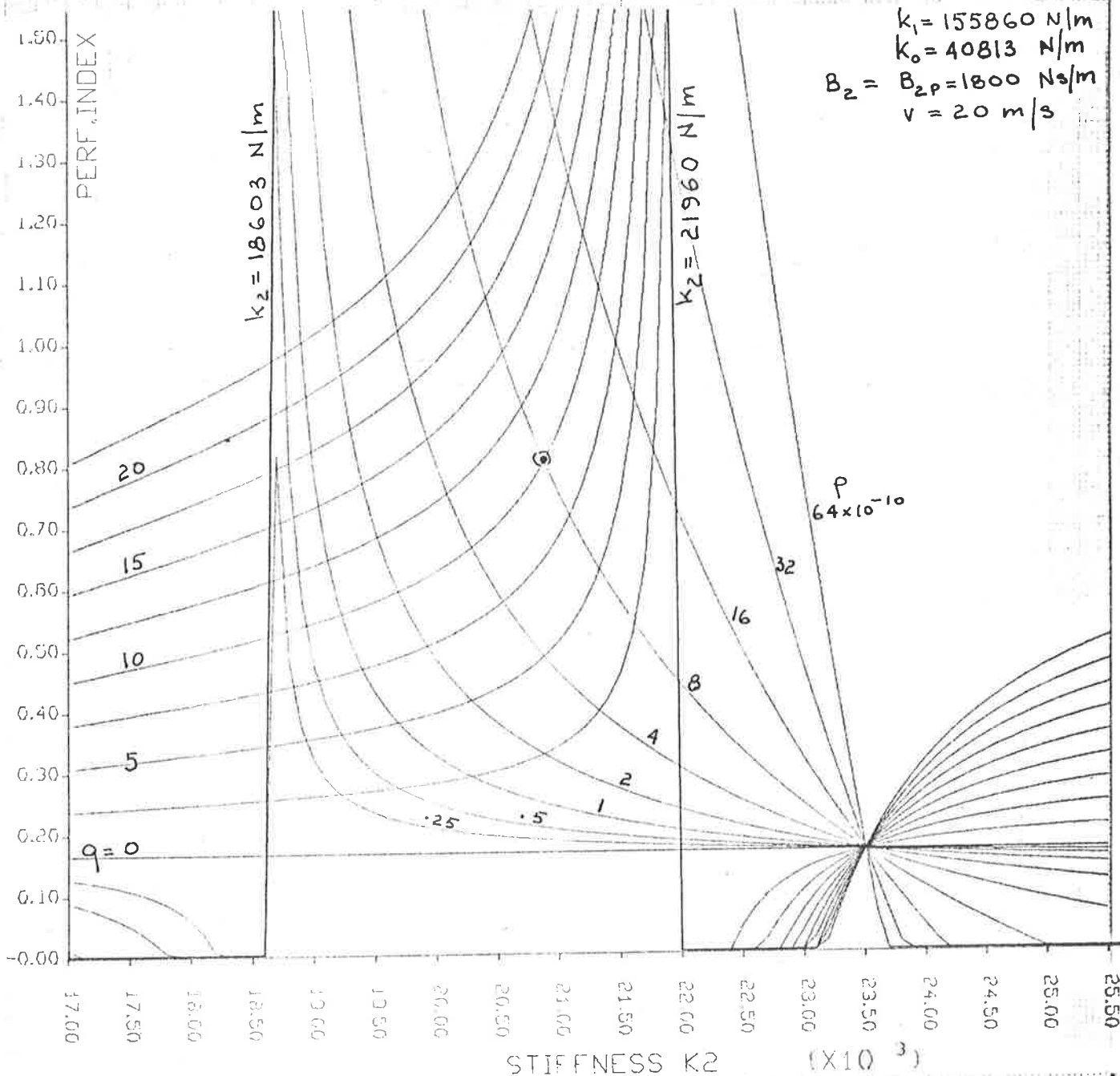


Fig. 8.8. Relationship between min. Performance Index, Spring Stiffness and Weighting Factors. HILLMAN Model (Laden), R=1.0

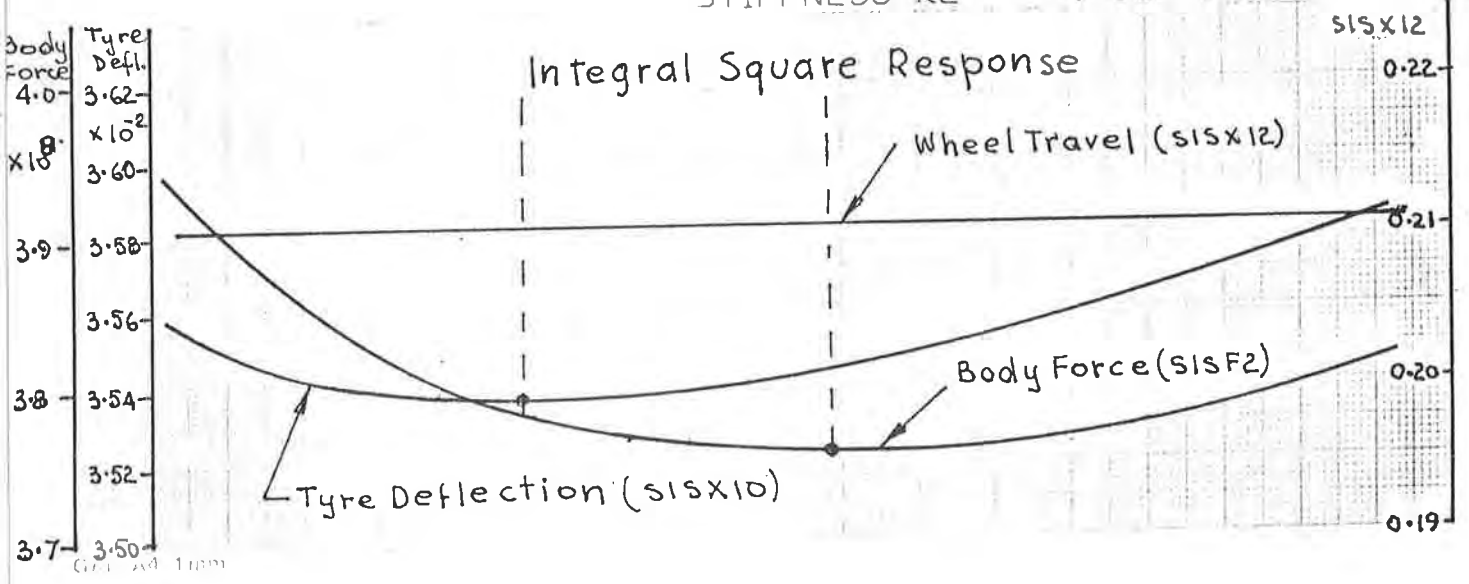
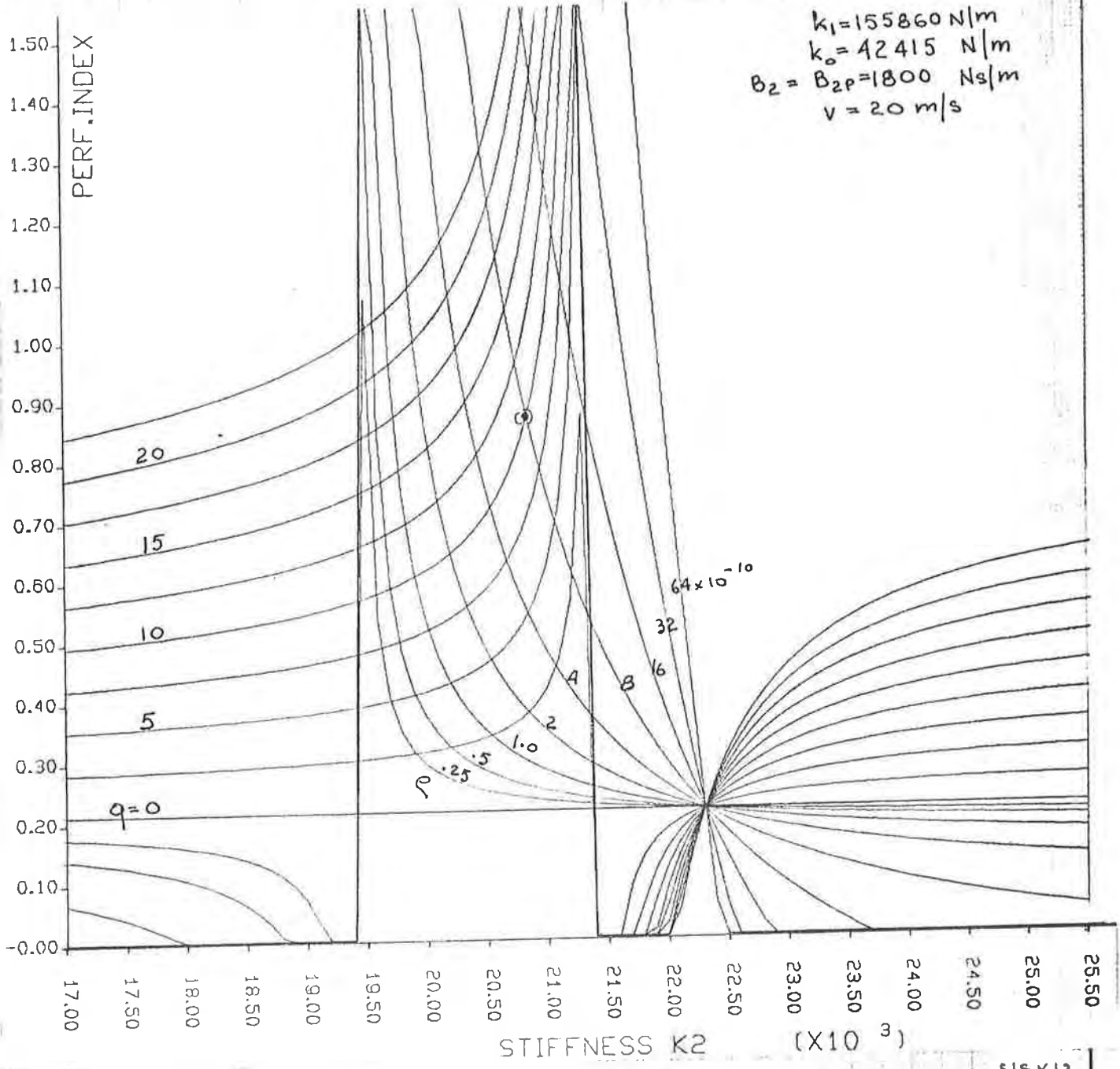


Fig. 8.9. Relationship between min. Performance Index, Spring Stiffness and Weighting Factors. CHRYSLER Model (Unladen), $R=1.0$

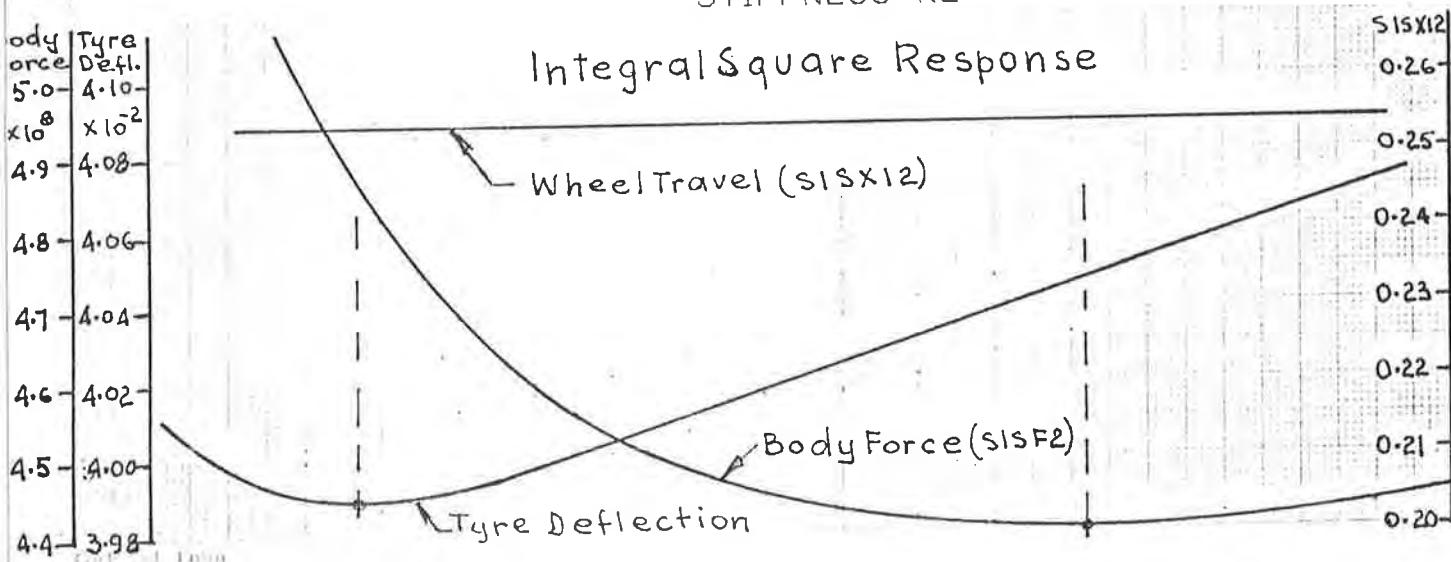
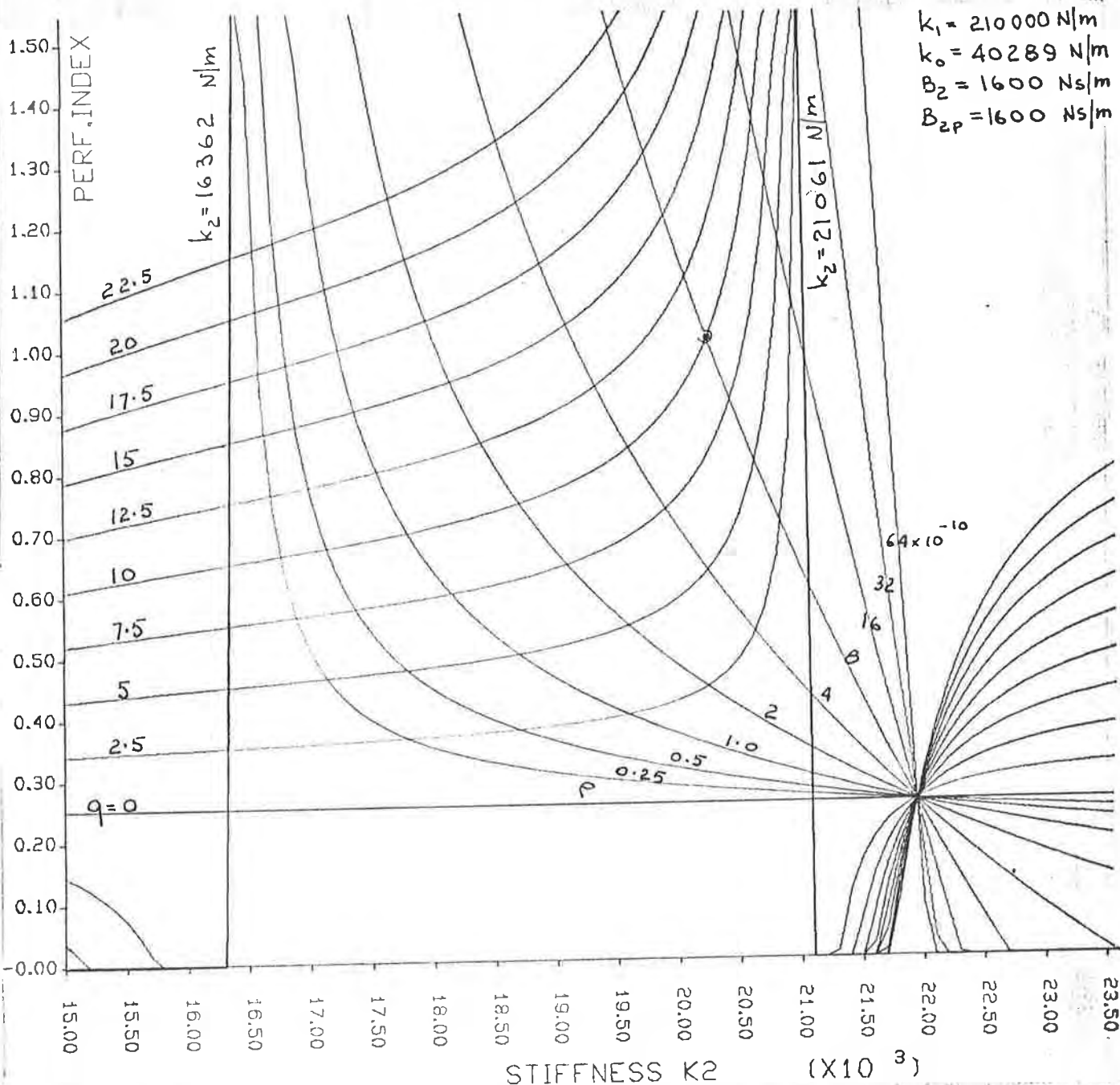


Fig. 8.10. Relationship between min. Performance Index, Spring Stiffness and Weighting Factors. CHRYSLER Model (Laden), $R=1.0$

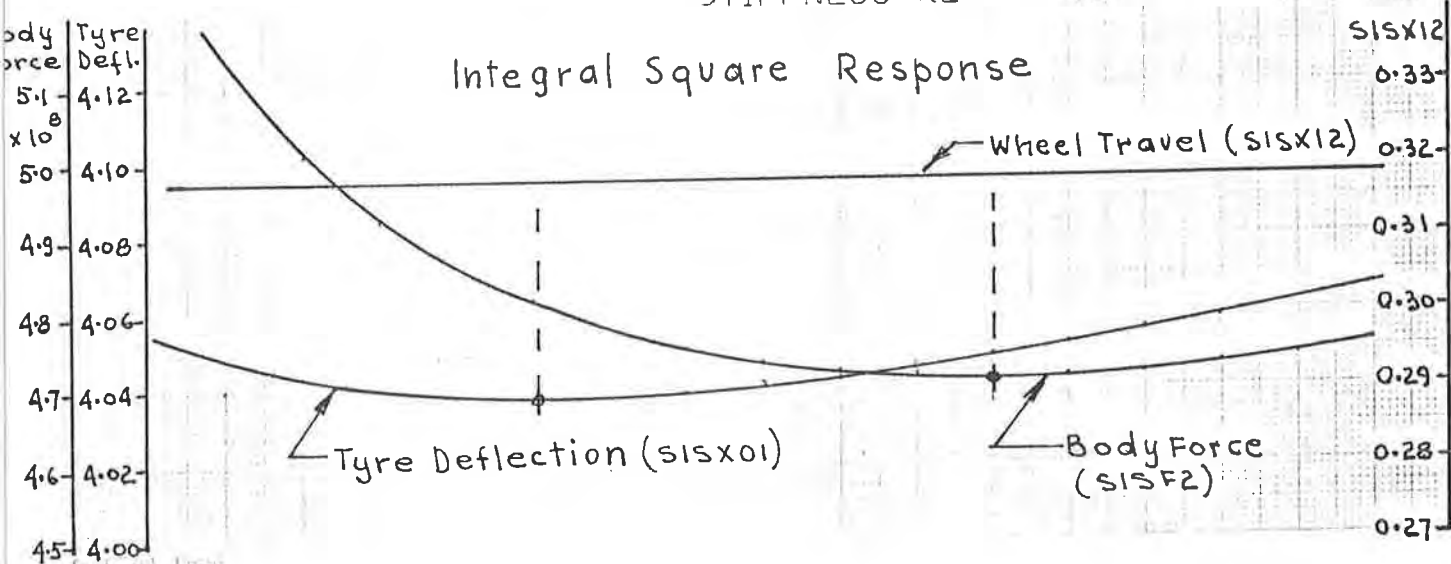
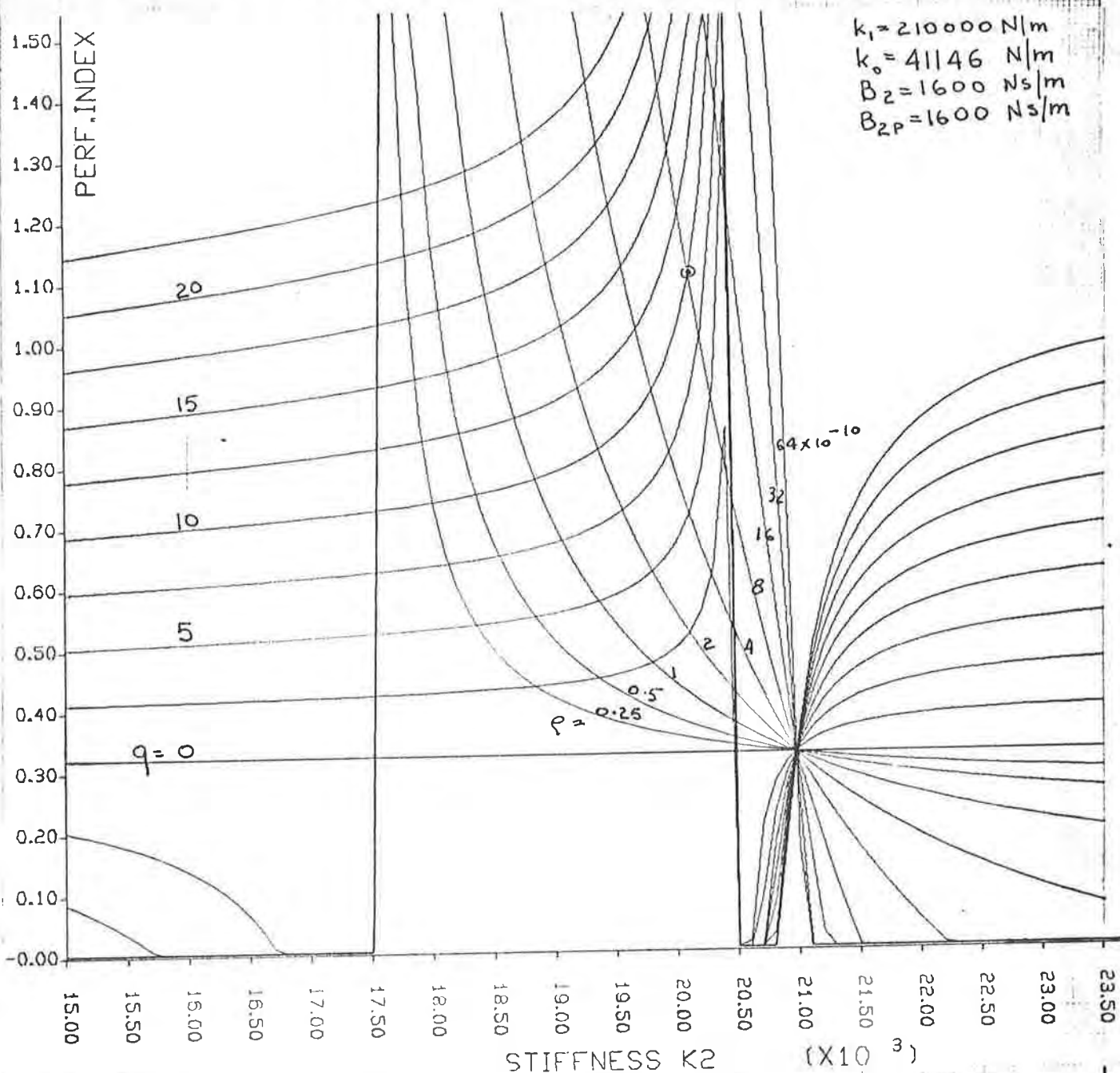


Fig. 8.11. Variation of Perf. Index with Spring Rate.

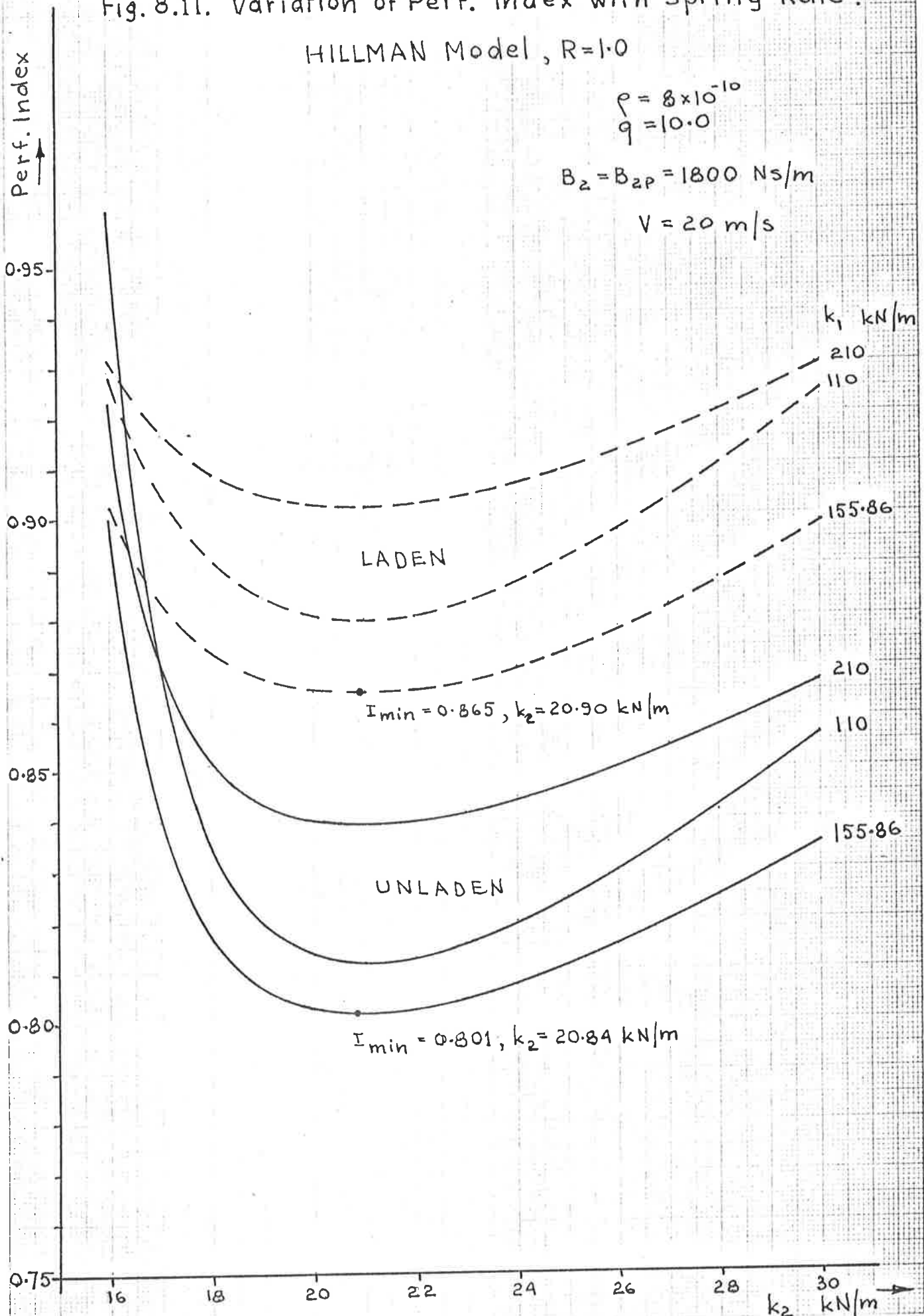
HILLMAN Model, $R=1.0$

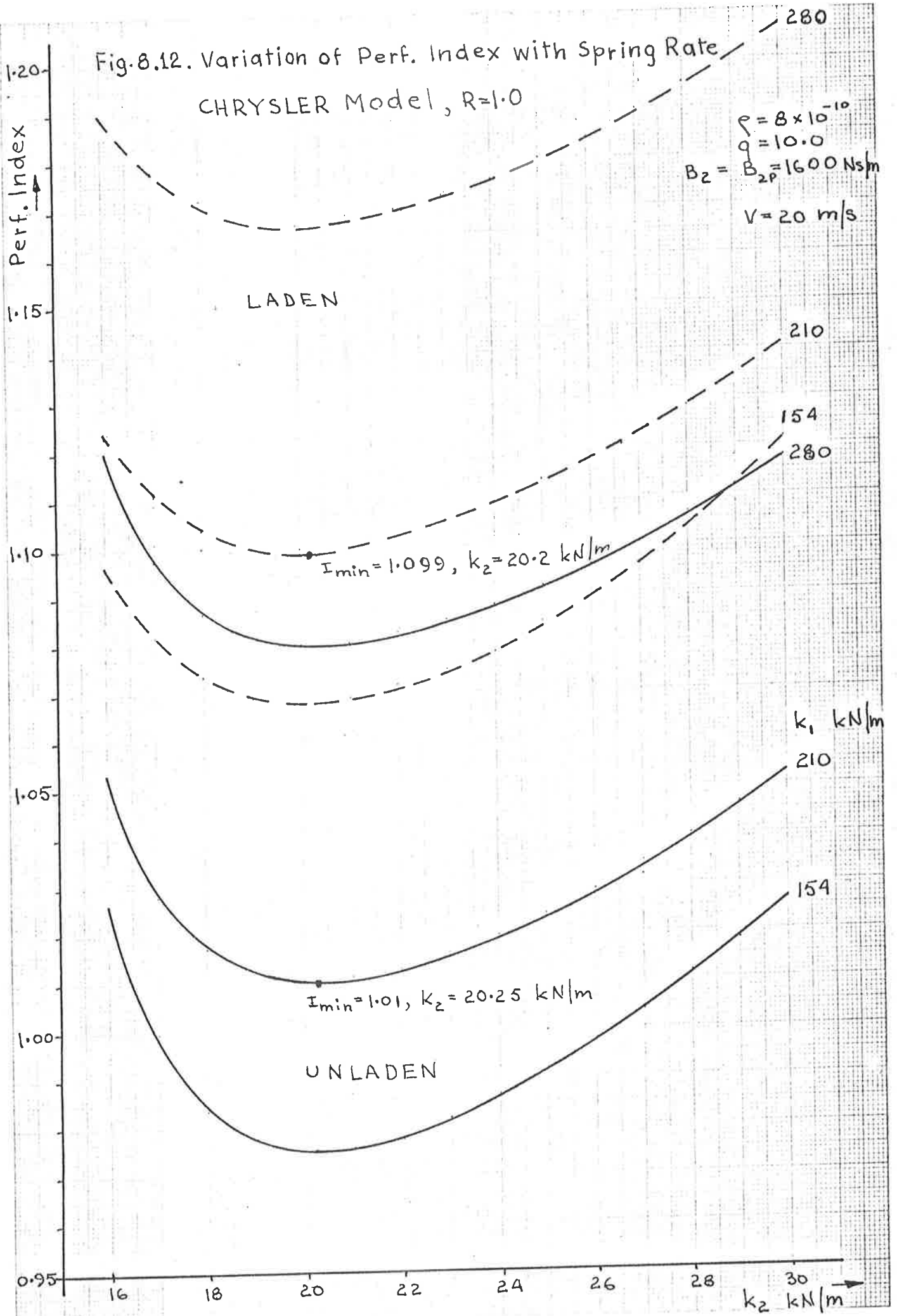
$$\rho = 8 \times 10^{-10}$$

$$q = 10.0$$

$$B_2 = B_{2P} = 1800 \text{ Ns/m}$$

$$V = 20 \text{ m/s}$$





9. THE INFLUENCE OF COUPLING RATIO ON SUSPENSION RESPONSE

9.1 Introduction

The investigations and results so far have been confined to vehicle models having rear and front motions uncoupled, i.e. the models with a coupling ratio $R=1.0$.

The coupling ratio is seldom under the direct control of the suspension engineer since it is determined by the factors such as the location of the engine and transmission, the distribution of the passenger and luggage load, the styling of the bodywork etc.

For an average passenger sedan with front mounted engine and rear wheel drive, the coupling ratio is somewhere between 0.7 and 0.9, larger passenger cars seem to have slightly larger values.

The analytical solution of the model response when $r^2 \neq ab$ is extremely difficult due to cross-coupling and time delay terms.

The equations of motion for the model involve the expressions such as

$$m(r^2-ab)/L^2, \quad m(r^2+b^2)/L^2 \quad \text{and} \quad m(r^2+a^2)/L^2.$$

After substitution of the coupling $R = r^2/ab$, the expressions become:

$$mab(R-1)/L^2, \quad mab(R+b/a)/L^2 \quad \text{and} \quad mab(R+b/a)/L^2.$$

The general solution for integral square values will involve the powers of these terms, in addition to time-delay terms.

For a unity coupling ratio the terms involving $mab(R-1)/L^2$ become zero, and relatively simple solution results. The two other terms involved become m_2 and m_{2P} i.e. that part of sprung mass associated with the front and rear suspensions respectively. In case of a coupled system the response is expected to vary with varying coupling ratio for a constant time delay (constant vehicle speed), and also with a constant coupling ratio for varying speeds (apart from the common amplitude multiplier cV).

9.2 The Influence of Speed

Since the performance index is a good indicator of the overall relative performance of a model, the indices were calculated for different values of coupling ratio and vehicle speed using ACSL digital simulation language. The results of these calculations are shown in Figs. 9.1, 9.1a and 9.1b.

It can be seen that the performance with step input excitation deteriorates rapidly with increasing speed for $R < 1.0$, and improves slightly for $R > 1.0$. When $R = 1.0$ the system is uncoupled, hence the response is independent of vehicle speed (apart from integral square multiplier cV).

9.3 Damping and Coupling Ratio

Integral square values of front and rear responses were computed for different values of front and rear damping at constant vehicle speed and unit step input. The calculations were carried out for the range of coupling ratios varying from 0.6 to 1.3, and the results are shown in Figs. 9.2, 9.3 and 9.4 for integral square values of body force, tyre deflection and wheel travel respectively.

The performance indices for the same conditions are plotted in Fig. 9.5 against damping with the coupling ratio as a parameter.

The examination of computer results indicates that there are practically no cross-coupling effects between the front and rear responses due to damping. The front response is practically unaffected when the rear damping is varied and vice versa, i.e. the front response is determined by the front damper, and the rear response by the rear damper. The maximum error resulting from the neglect of cross-coupling effects due to dampers will not exceed 0.5% for all cases investigated. Thus the front and rear dampers can be optimised independently.

On further analysis of computer results, it becomes evident that the mean square responses can be approximated to a high degree of accuracy by the expressions

$$\text{I.S.V.}_{\text{Body Force}} = C_1 B_2 + C_2/B_2$$

$$\text{I.S.V.}_{\text{Tyre Deflection}} = C_3 B_2 + C_4/B_2$$

$$\text{I.S.V.}_{\text{Wheel travel}} = C_5 B_2 + C_6/B_2$$

for the front and rear.

For an uncoupled system ($R=1.0$), the respective values are

$$C_1 = k_1/2$$

$$C_2 = k_2^2 (m_1+m_2)/2$$

$$C_3 = \frac{(m_1+m_2)^2}{2 k_1 m_2^2}$$

$$C_4 = \frac{m_1}{2} - \frac{k_2 m_1 (m_1+m_2)}{k_1 m_2} + \frac{k_2^2 (m_1+m_2)^3}{2 (k_1 m_2)^2}$$

$$C_5 = 0$$

$$C_6 = \frac{m_1+m_2}{2}$$

For a coupled system the values are complicated by the terms involving the coupling ratio and time delay. C_5 evidently involves the term $(R-1)/L^2$, and m_2 corresponds to $m a b(R+b/a)/L^2$ while m_{2P} corresponds to $m a b(R+a/b)/L^2$.

The coefficients are tabulated in Tables B1 and B2 of Appendix B, and have been plotted against the coupling ratio in Figs. 9.6 and 9.7 for HILLMAN front and rear suspensions respectively, but it is impossible to predict the probable functional relationships from the graphs. Evidently, the relationships are not simple linear functions of the coupling ratio.

It would now be appropriate to investigate the general relationship between the weighting factors and the minimum performance index for different values of damping and coupling ratio.

Since the integral square values of response for a fixed value of coupling ratio can be expressed in the form

$$C_i B_2 + C_{i+1}/B_2 \quad \text{for the front suspension}$$

$$\text{and } C_{iP} B_{2P} + C_{i+1P}/B_2 \quad \text{for the rear suspension}$$

$$\text{where } i = 1, 3, 5$$

the performance index for the model can be written as

$$I = \rho (C_1 B_2 + C_2/B_2) + q(C_3 B_2 + C_4/B_2) + (C_5 B_2 + C_6/B_2) \\ + \rho (C_{1P} B_{2P} + C_{2P}/B_{2P}) + q(C_{3P} B_{2P} + C_{4P}/B_{2P}) + (C_{5P} B_{2P} + C_{6P}/B_{2P}) \quad (9.1)$$

Now the front and rear can be independently optimised since there are practically no cross-coupling effects due to damping.

$$\text{Thus} \quad \frac{\partial I}{\partial B_2} = 0 \quad \text{and} \quad \frac{\partial I}{\partial B_{2P}} = 0 \quad \text{for the minimum}$$

value of performance index.

To minimise the front response, $\frac{\partial I}{\partial B_2} = 0$ must be satisfied, which gives

$$\rho (C_1 - C_2/B_2^2) + q(C_3 - C_4/B_2^2) + (C_5 - C_6/B_2^2) = 0 \quad (9.2)$$

and establishes the functional relationship between the weighting factors for minimum performance index as

$$\rho = - \frac{q(C_3 - C_4/B_2^2) + (C_5 - C_6/B_2^2)}{C_1 - C_2/B_2^2} \quad (9.3)$$

The equation of ρ against q represents a linear graph similar to the graph for an uncoupled system with $R=1.0$.

The slope tends to infinity when $B_2^2 = C_2/C_1$, and this corresponds to the condition of minimum body force, with $ISF2_{\min} = 2\sqrt{C_1 C_2}$. The corresponding value of q where the vertical line intercepts the horizontal axis is given by

$$q_{v.s.} = - \frac{C_2 C_5 - C_1 C_6}{C_2 C_3 - C_1 C_4} \quad (9.4)$$

The slope is zero where $B_2^2 = C_4/C_3$, and this value of B_2 corresponds to the condition of minimum tyre deflection, given by $ISX01_{\min} = 2\sqrt{C_3 C_4}$. The height of the horizontal line above the origin is given by

$$\rho_{H.S.} = - \frac{C_4 C_5 - C_3 C_6}{C_1 C_4 - C_2 C_3} \quad (9.5)$$

The coordinates given by eq. 9.4 and 9.5 define the point through which all characteristics will pass. Fig. 9.8 shows the conditions for HILLMAN front suspension with $R=0.7$.

If the front damper is varied, the condition for minimum performance index is given by

$$\rho (B_2^2 C_1 - C_2) + q(B_2^2 C_3 - C_4) + (B_2^2 C_5 - C_6) = 0 \quad (9.6)$$

It is evident that for any selected pair of weighting factors ρ and q , there corresponds one value of B_2 that will minimise the performance index, i.e. I_{\min} can be plotted against B_2 with ρ and q as parameters. It also means that once the weighting factors have been selected, the value of minimum performance index is fixed for a given model.

The computer program B2MIN shown in Appendix C was used to calculate the values of I_{\min} which have been plotted in Figs. 9.9 and 9.10 for HILLMAN model with $R=0.7$.

The general shape of characteristics is the same for all coupling ratios (including $R=1.0$), only the location of vertical asymptotes corresponding to $q_{V.S.}$ and $\rho_{H.S.}$ will vary as shown in Tables B.3 and B.4 in Appendix B, and plotted in Figs. 9.11 and 9.12.

The graphs in Figs. 9.9 and 9.10 show again that the computer optimisation procedure will lead to the value of damping that minimises the tyre deflection when q is continually increased, and to the value of damping that minimises the body force when ρ is continually increased, all other parameters remaining constant.

Thus the basic computer optimisation routine remains the same, i.e. select the weighting factors, minimise the performance index from which process get the value of damping, then calculate the response and check if the performance is acceptable. For a minimum value of performance index with specified values of weighting factors ρ and q , the corresponding value of damping rate can be calculated from eq. 9.6 as

$$B_2^2 \text{ OPT} = \frac{\rho C_2 + q C_4 + C_6}{\rho C_1 + q C_3 + C_5} \quad (9.7)$$

The damping rates corresponding to minimum performance indices have been calculated for HILLMAN model with weighting factors $\rho = 8 \times 10^{-10}$ and $q = 10.0$, and are listed in Table 9.1 and plotted

in Fig. 9.13 for verification with computer results.

It can be seen that the values as listed do agree with Fig. 9.5 which was plotted with the data from ACSL simulation results.

TABLE 9.1

DAMPING RATES FOR MINIMUM PERFORMANCE INDEX

| COUPLING RATIO | OPTIMUM FRONT DAMPER | | OPTIMUM REAR DAMPER | |
|-------------------|----------------------|--------|---------------------|--------|
| | $B_{2\text{OPT}}$ | Ns/m | $B_{2\text{OPT}}$ | Ns/m |
| 0.6 | | 1726.1 | | 1866.1 |
| 0.7 | | 1755.0 | | 1898.9 |
| 0.8 | | 1784.9 | | 1915.0 |
| 0.9 | | 1814.2 | | 1915.7 |
| 1.0 | | 1843.4 | | 1904.2 |
| 1.1 | | 1869.2 | | 1883.6 |
| 1.2 | | 1890.7 | | 1859.5 |
| 1.3 | | 1904.8 | | 1832.0 |
| 1.4 | | 1917.0 | | 1806.8 |
| 1.5 | | 1924.8 | | 1784.4 |

Fig. 9.1. Variation of Performance Index with Speed and Coupling Ratio.

HILLMAN Model (Unladen)

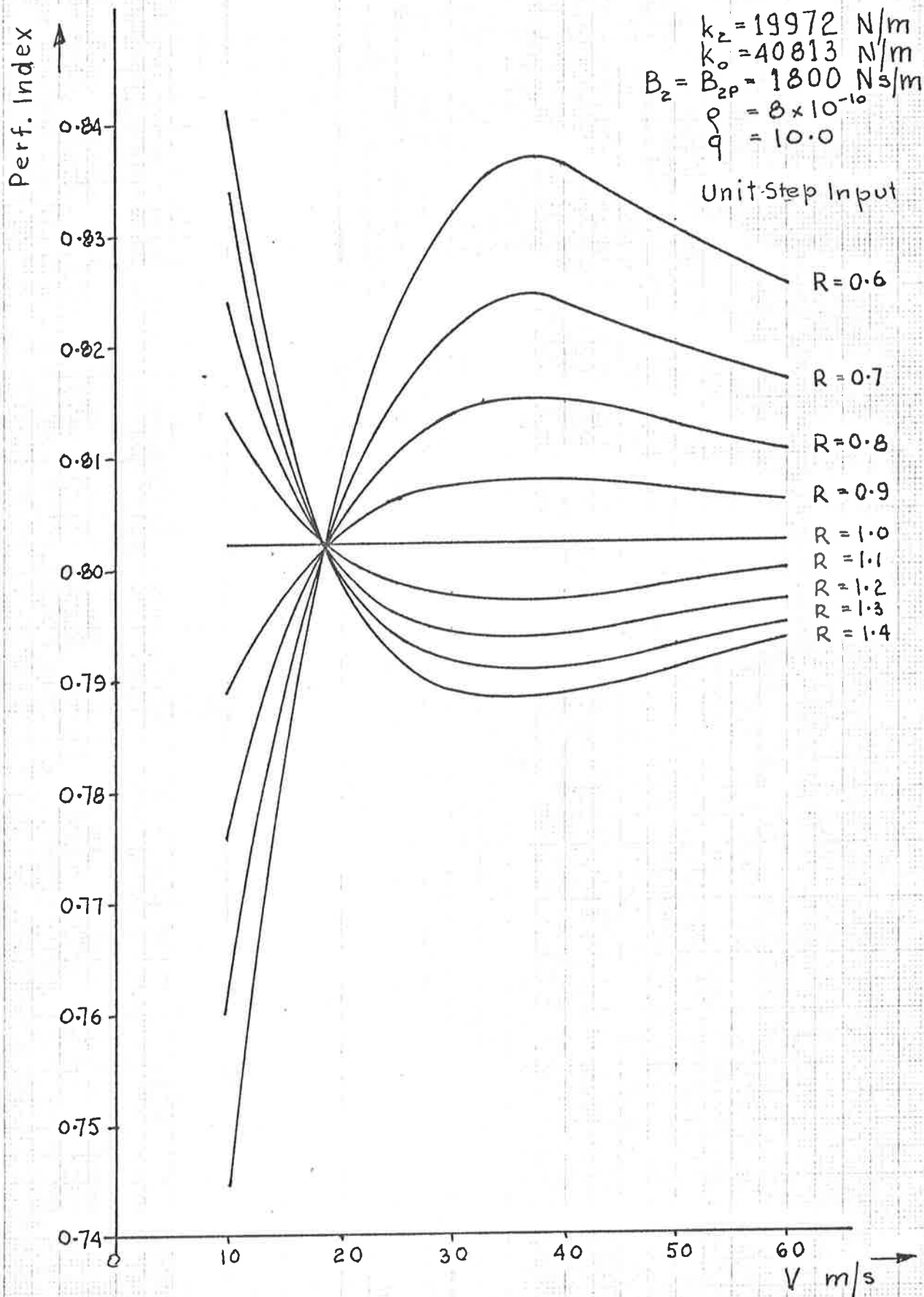


Fig. 9.1a. Variation of Performance Index with Speed and Coupling Ratio

HILLMAN Model (Laden)

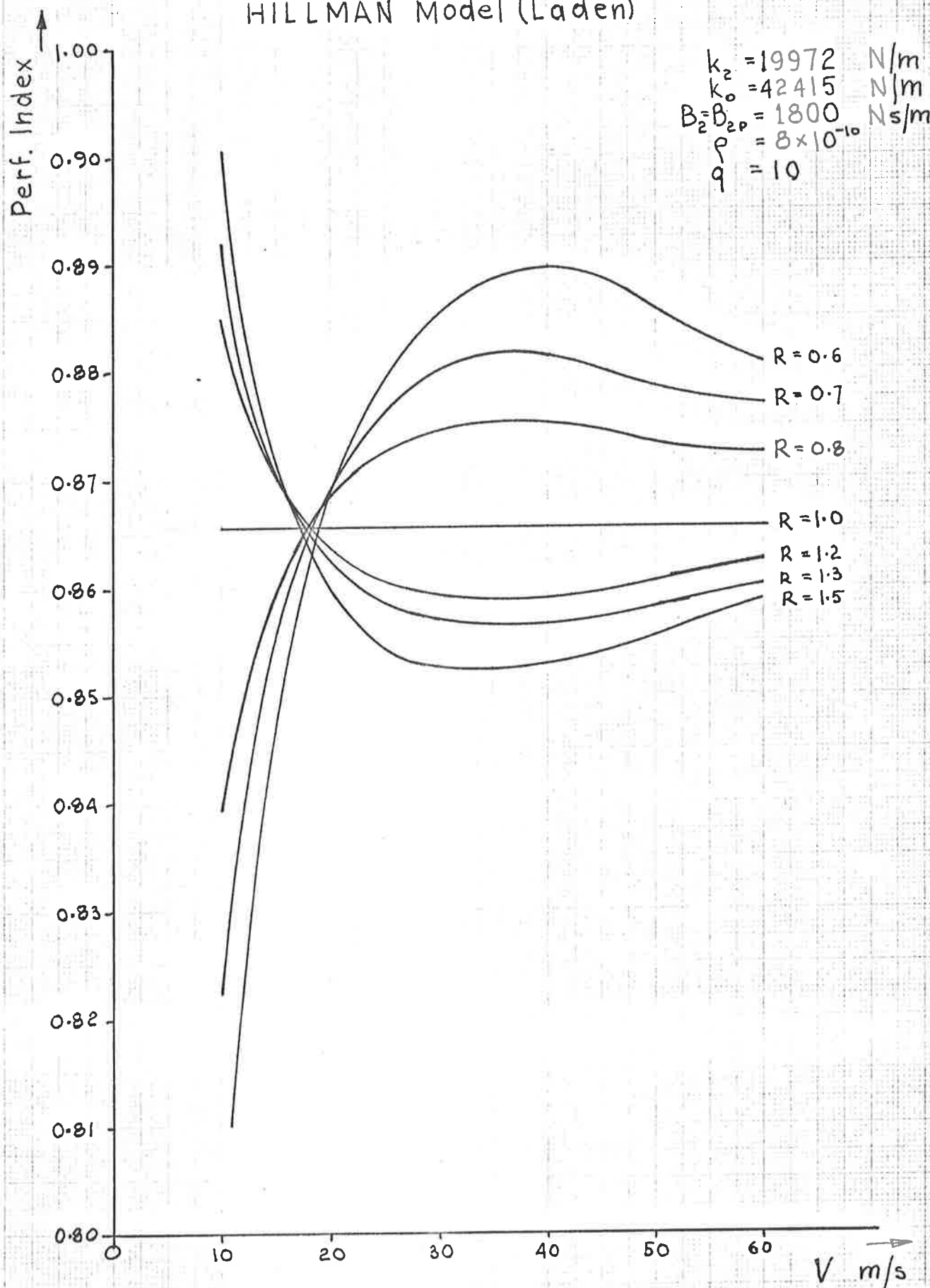


Fig. 9.1b. Variation of Performance Index with Speed and Coupling Ratio.

CHRYSLER Model (Unladen)

$k_2 = 19720 \text{ N/m}$
 $k_s = 40280 \text{ N/m}$
 $B_2 = B_{2p} = 1600 \text{ Ns/m}$
 $\xi = 8 \times 10^{-10}$
 $q = 10$

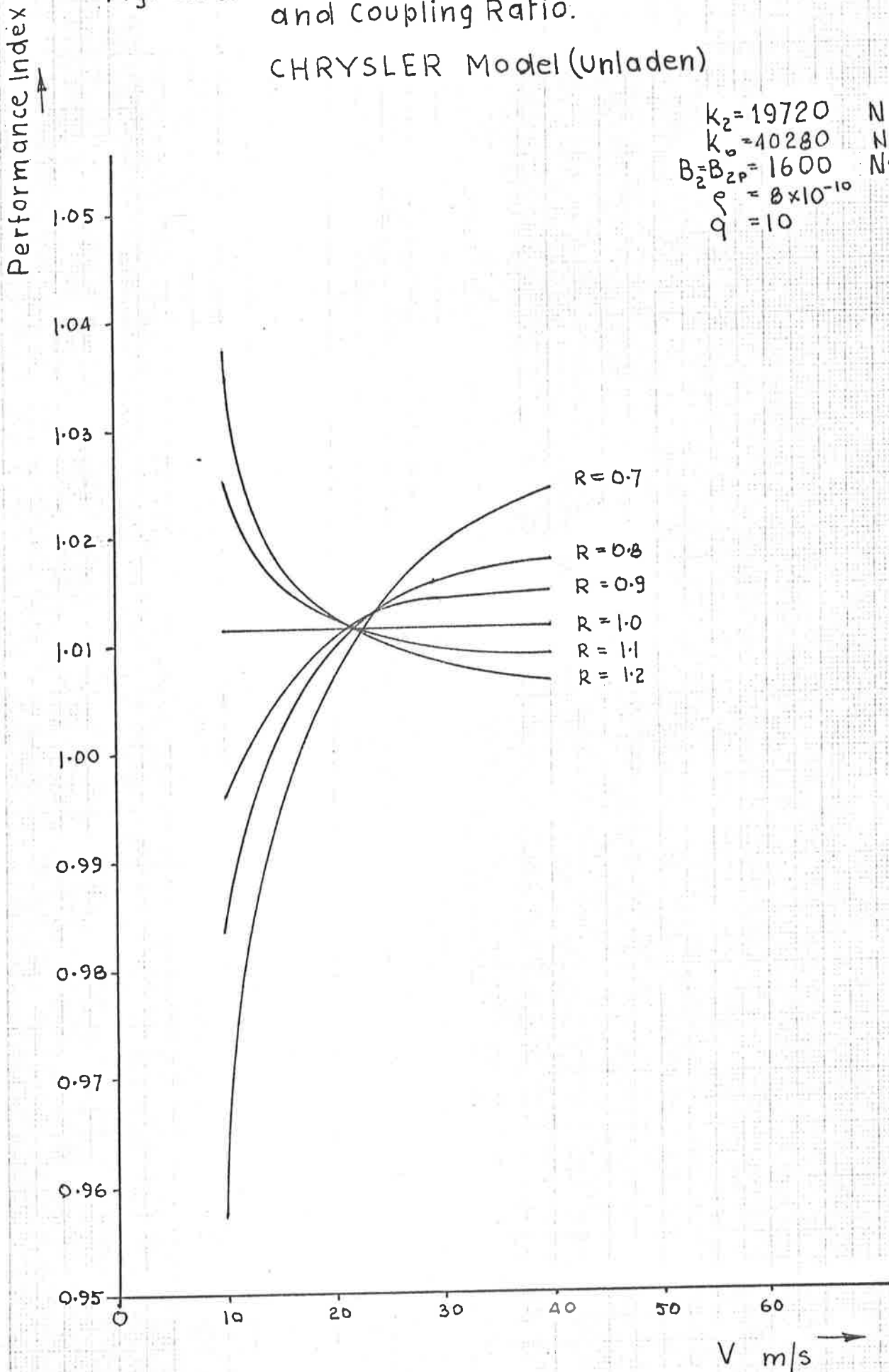


Fig. 9.2. Variation of Integral Square Body Force with Coupling Ratio and Damping Rate.
 HILLMAN Model (Unladen)

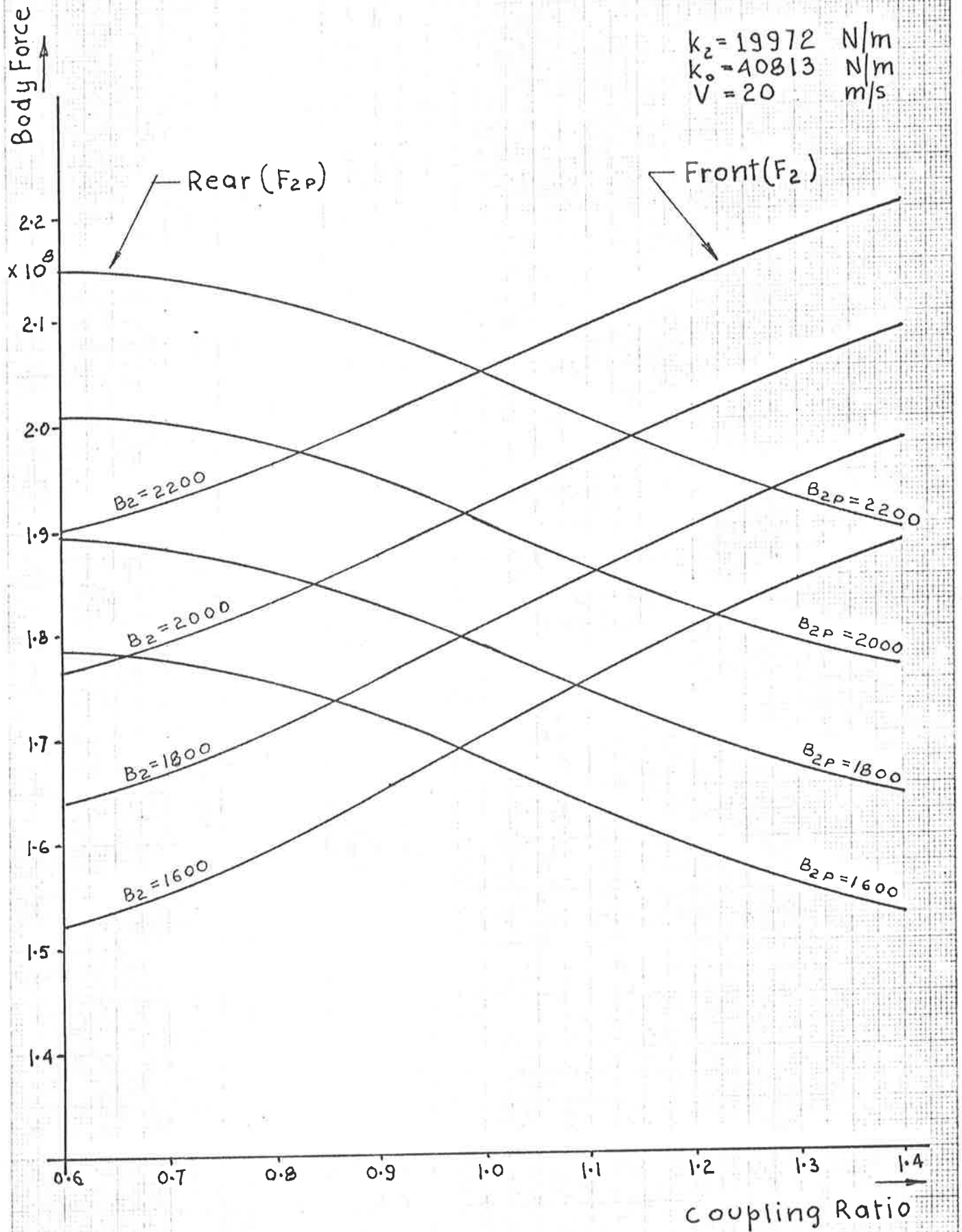


Fig. 9.3. Variation of Integral Square Tyre Deflection with Coupling Ratio and Damping Rate
 HILLMAN Model (Unladen)

$k_z = 19972 \text{ N/m}$
 $k_o = 40813 \text{ N/m}$

$V = 20 \text{ m/s}$

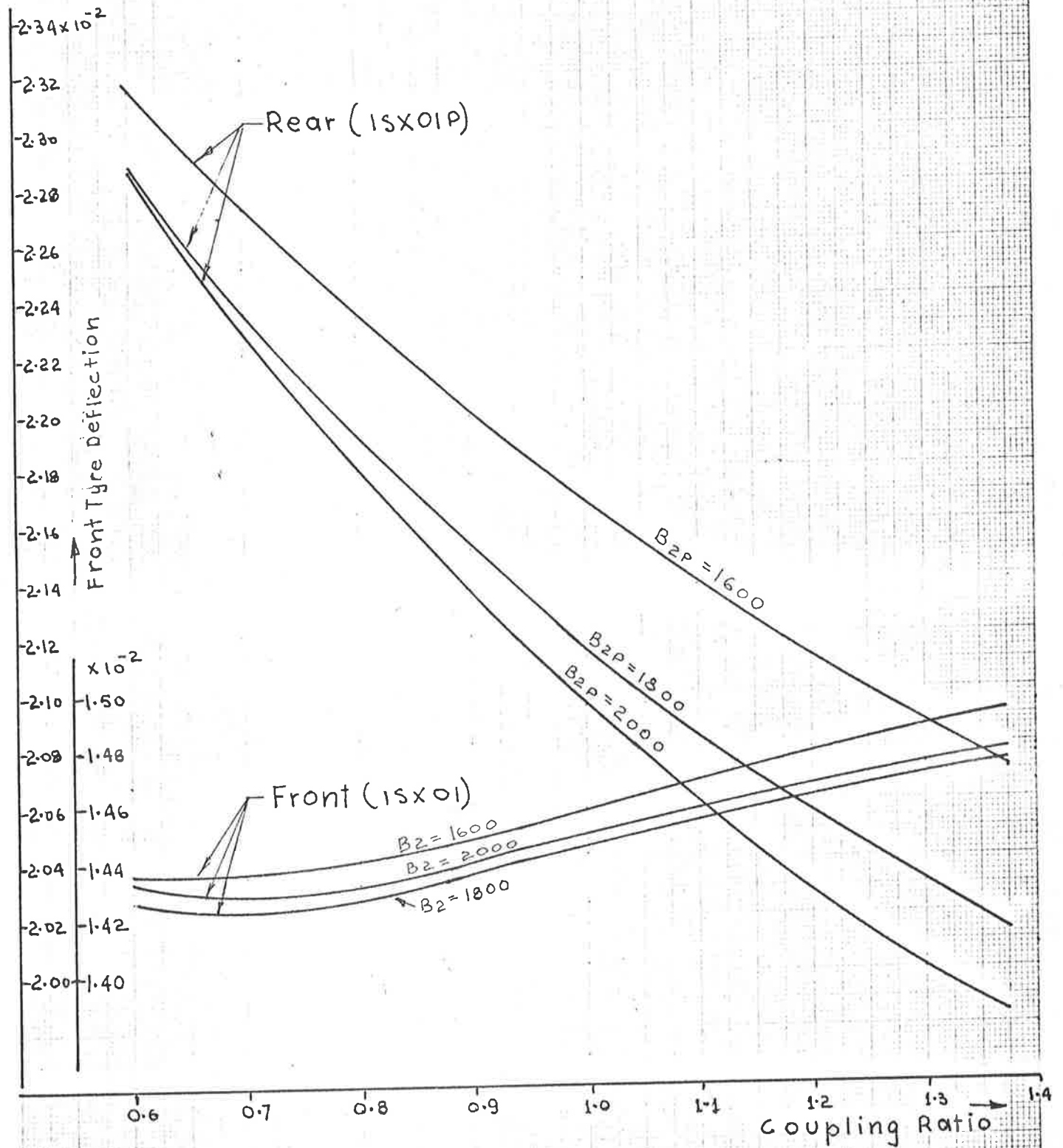


Fig. 9.4. Variation of Integral Square Wheel Travel with coupling Ratio and Damping Rate

HILLMAN Model (unladen)

$k_z = 19972 \text{ N/m}$
 $k_o = 40813 \text{ N/m}$
 $V = 20 \text{ m/s}$

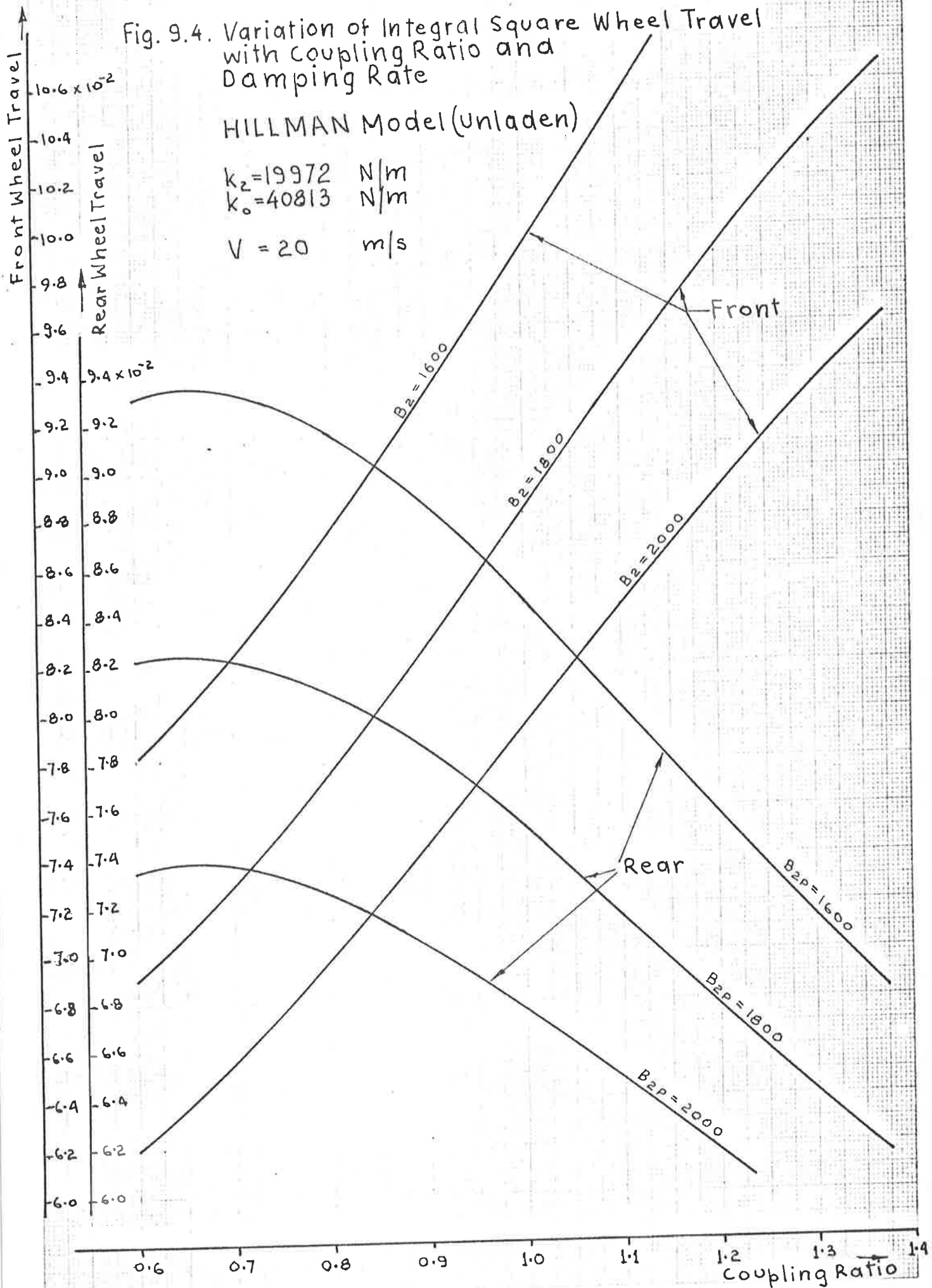


Fig. 9.5. Variation of Performance Index with Damping Rate and Coupling Ratio. HILLMAN Model (Unladen)

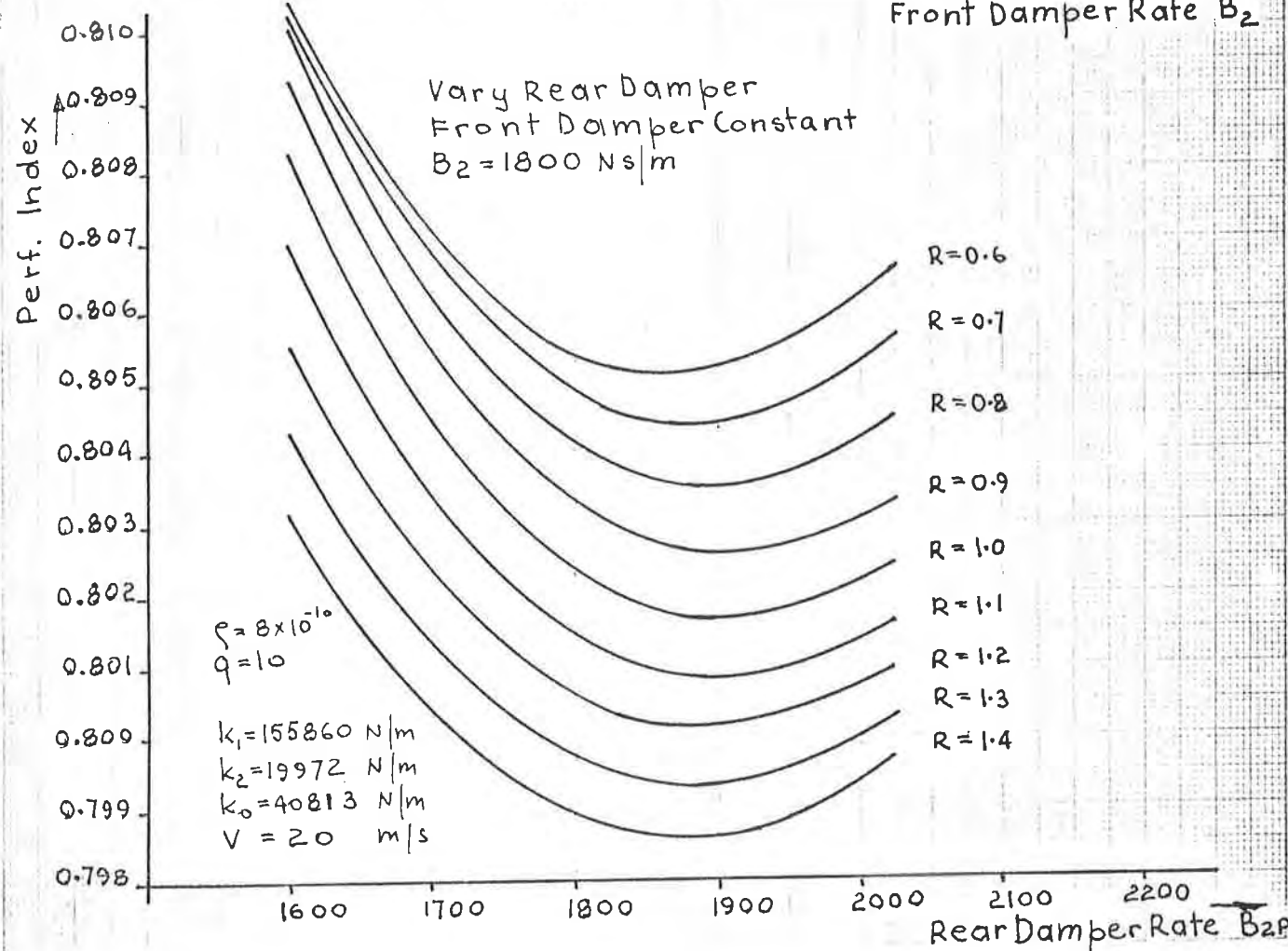
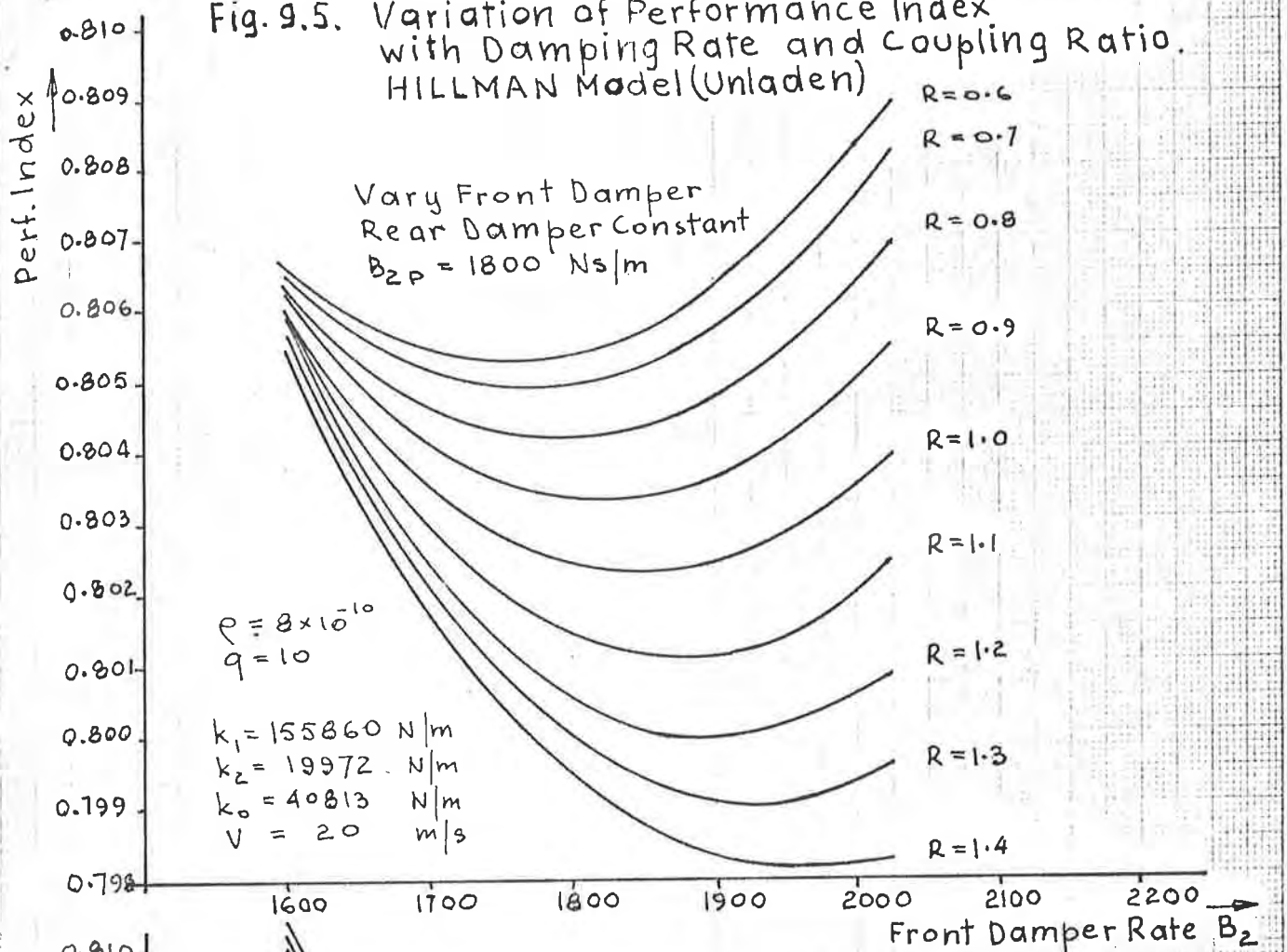


Fig. 9.6. Response Constants for Front Suspension HILLMAN Model (Unladen), $V=20$ m/s.

$k_2 = 19972$ N/m
 $k_b = 40813$ N/m
 $k_1 = 155860$ N/m

$ISF2 = C_1 B_2 + C_2 / B_2$
 $ISX01 = C_3 B_2 + C_4 / B_2$
 $ISX12 = C_5 B_2 + C_6 / B_2$

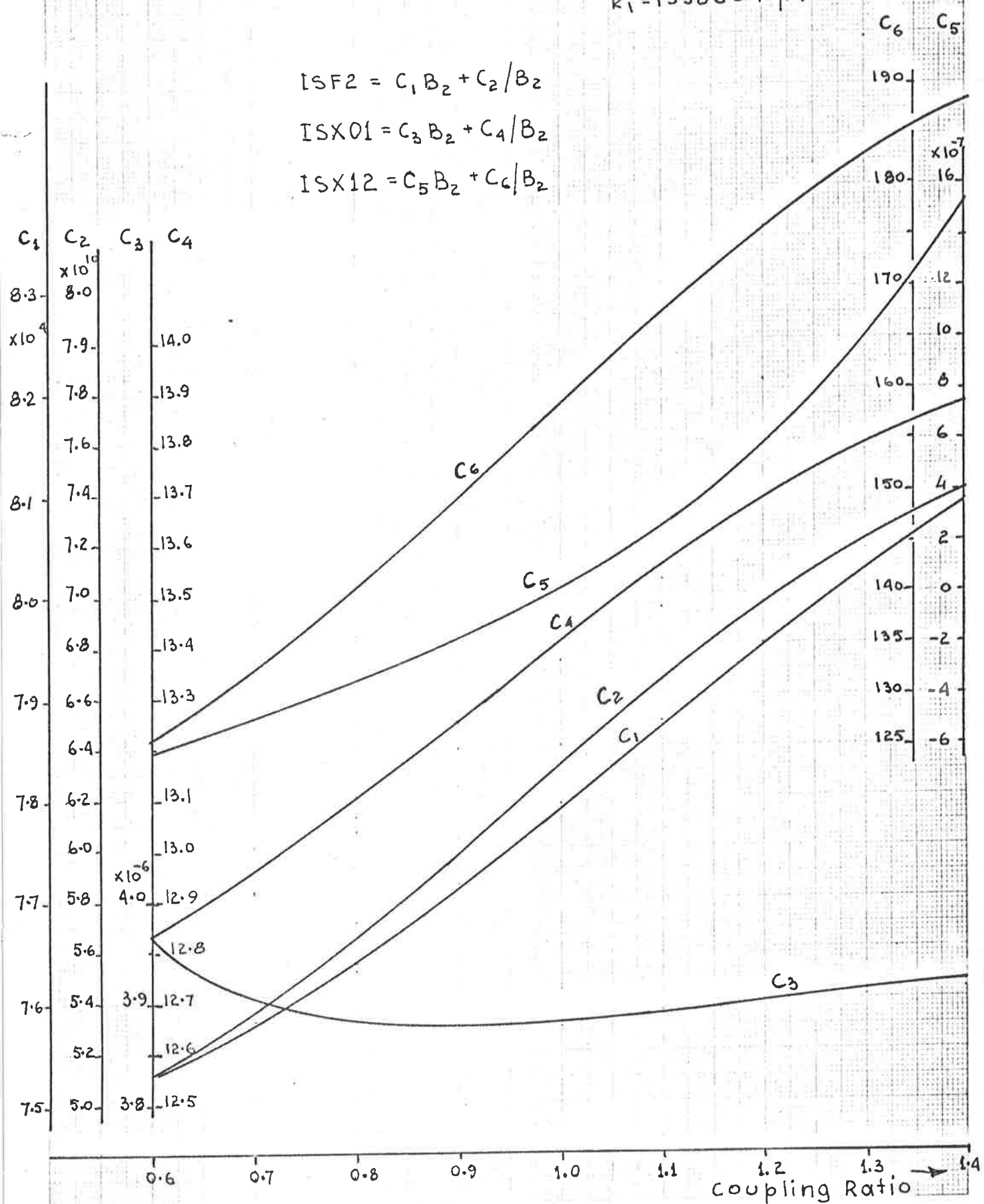


Fig. 9.7. Response Constants for Rear Suspension
HILLMAN Model (Unladen), $V=20$ m/s.

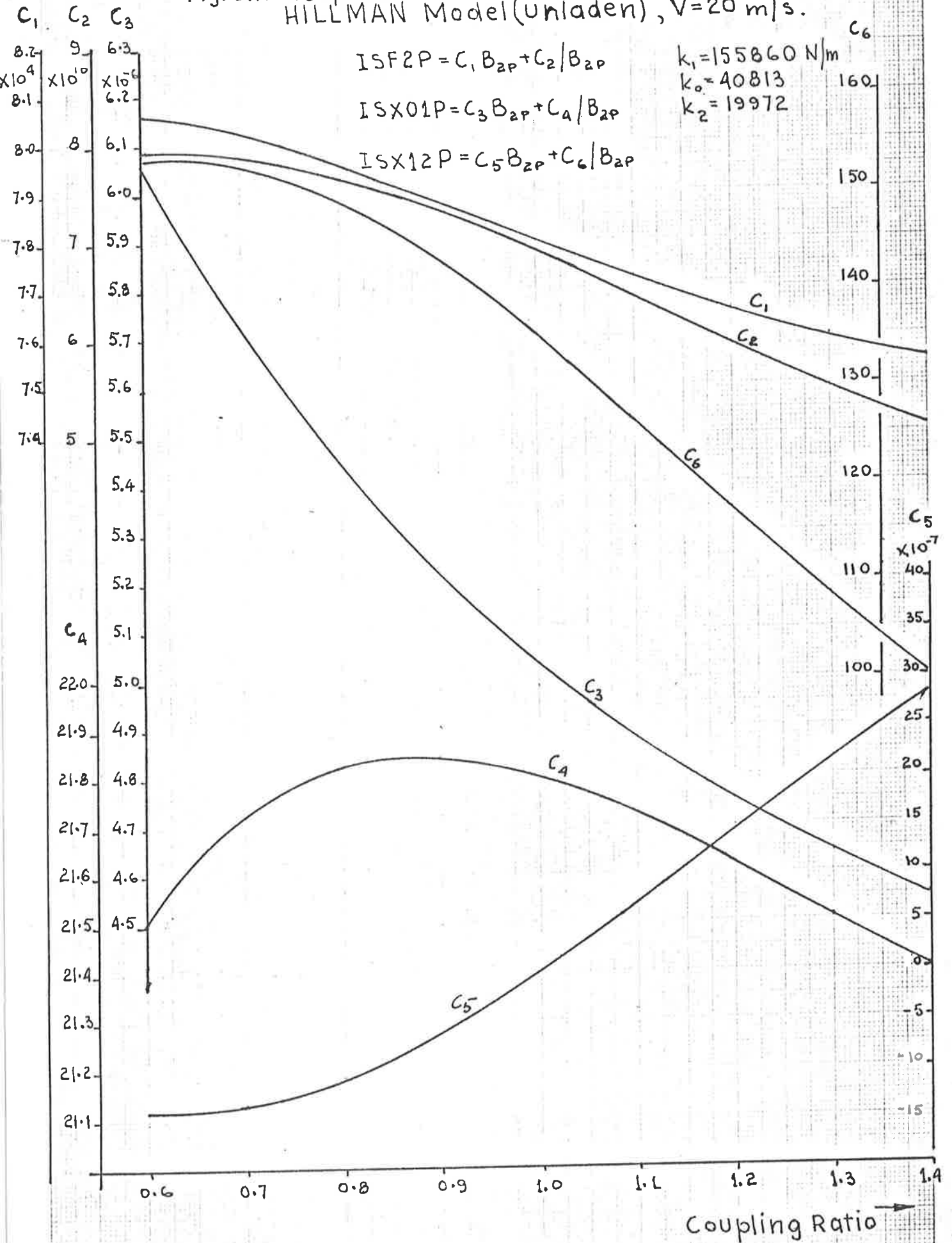


Fig. 9.8. Relationship between Weighting Factors and Damping for min. Performance Index. HILLMAN Front Suspension (Unladen).
 $R=0.7$
 $V=20$ m/s.

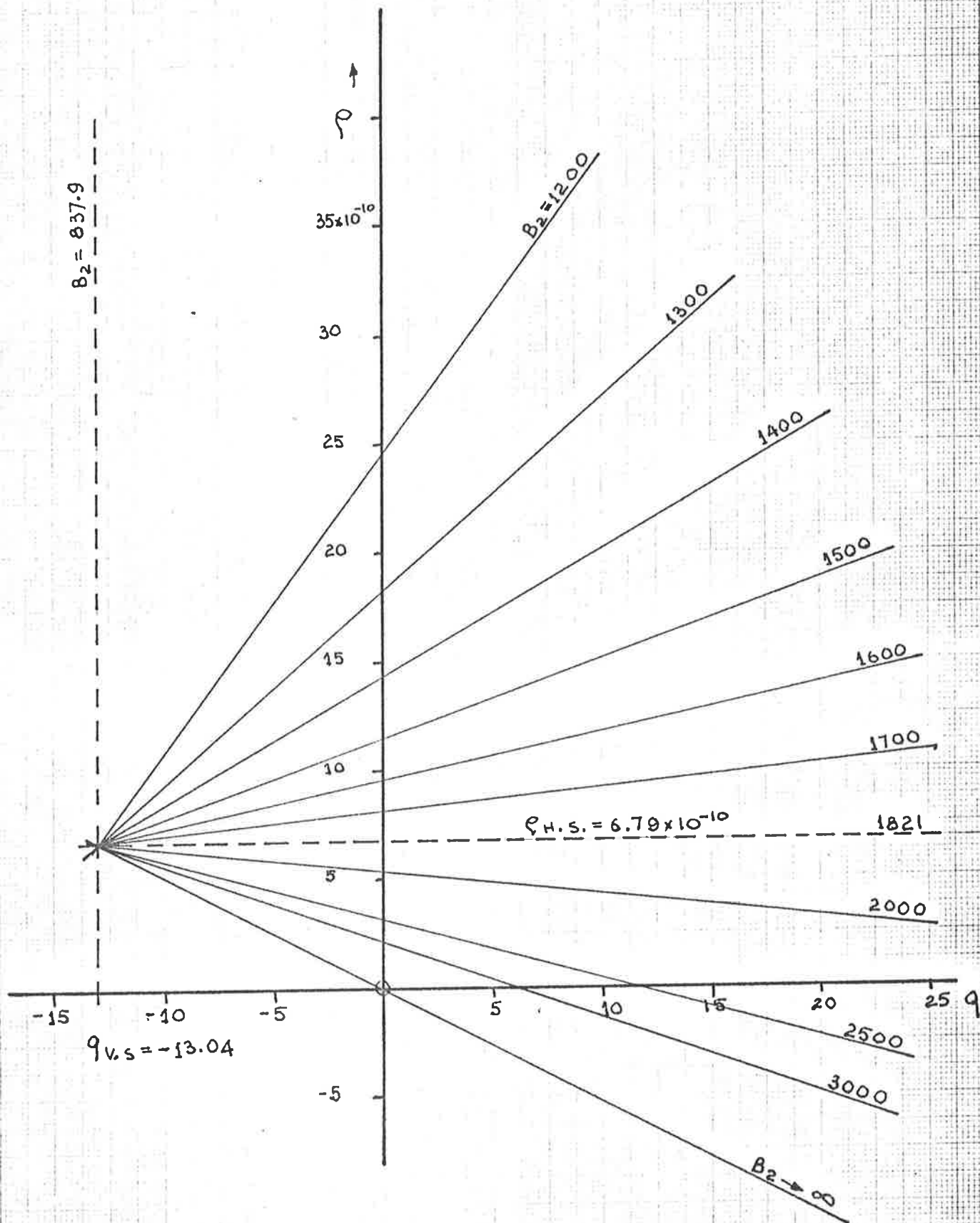
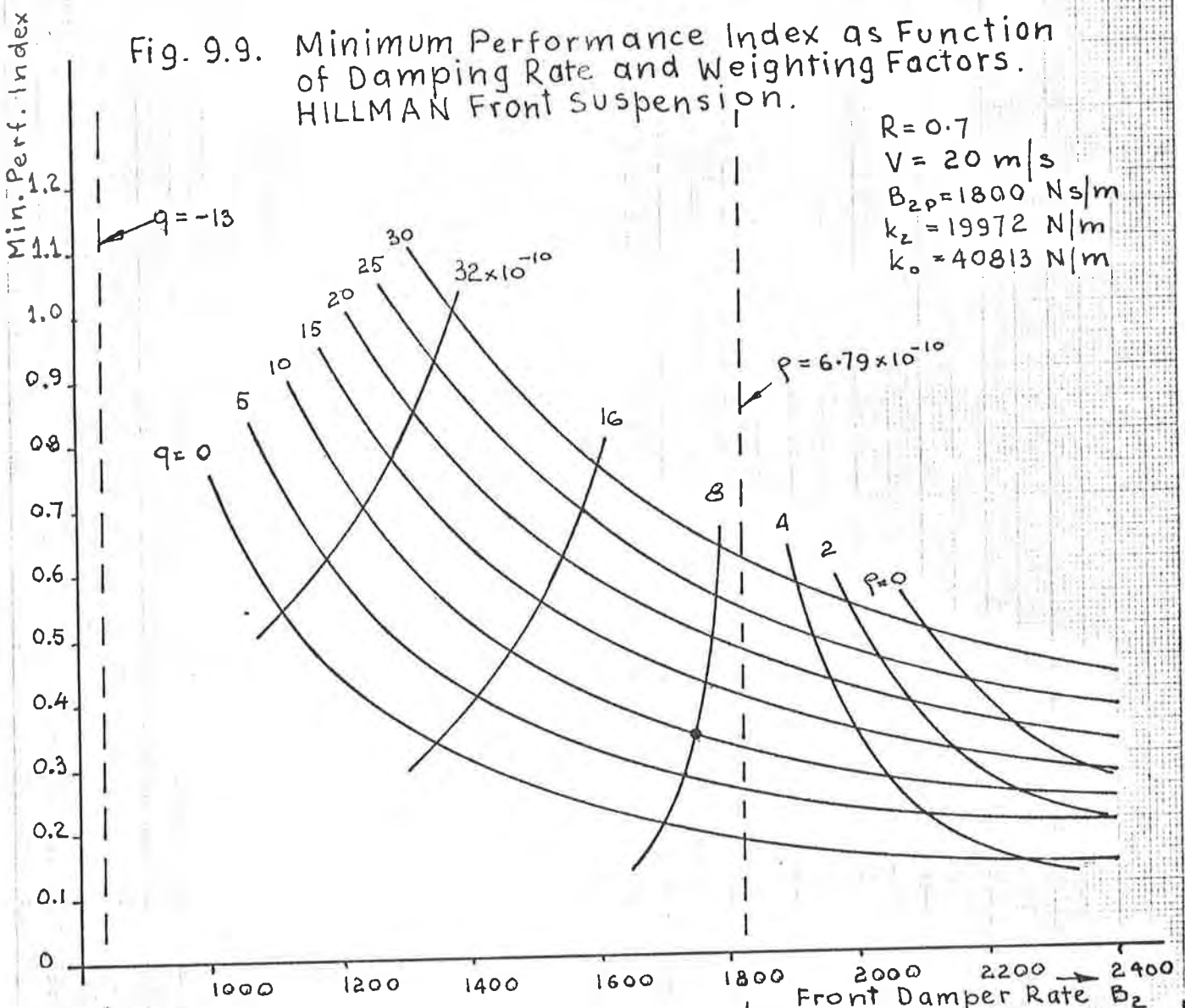


Fig. 9.9. Minimum Performance Index as Function of Damping Rate and Weighting Factors. HILLMAN Front suspension.



Integral Square Response.

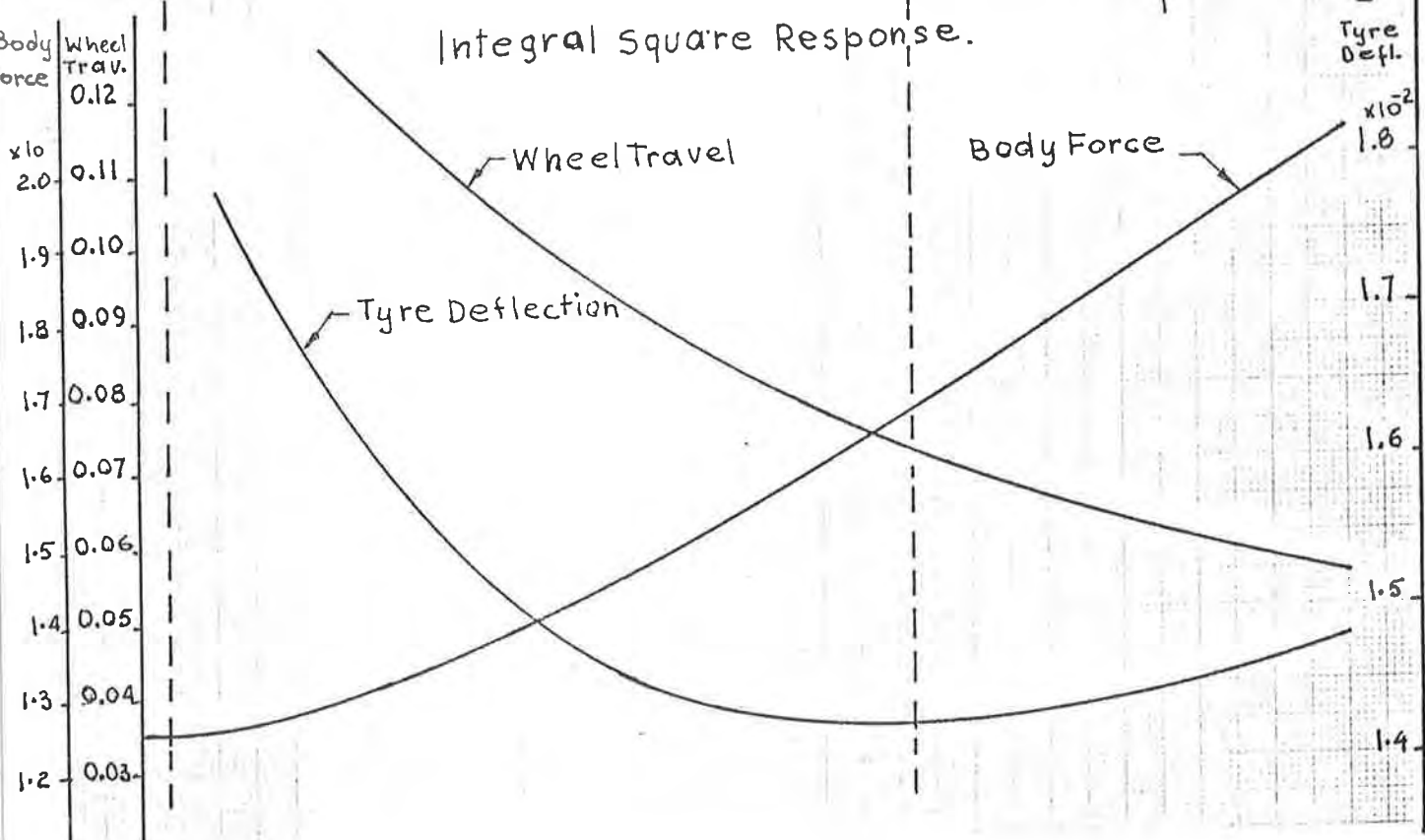


Fig. 9.10.

Minimum Perf. Index
HILLMAN Rear Suspension

$R = 0.7$
 $V = 20 \text{ m/s}$
 $B_2 = 1800 \text{ Ns/m}$
 $k_2 = 19972 \text{ N/m}$
 $k_o = 40813 \text{ N/m}$

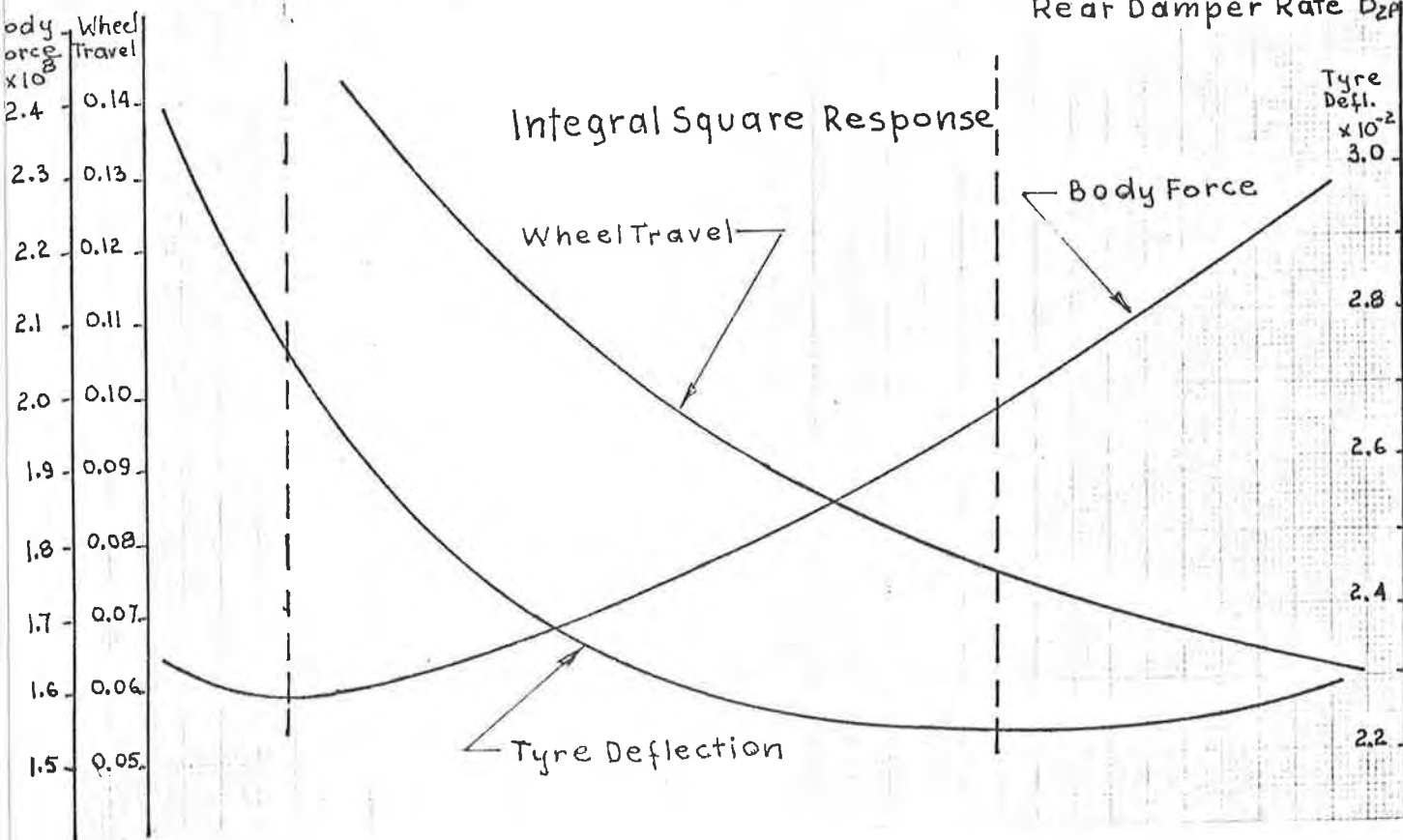
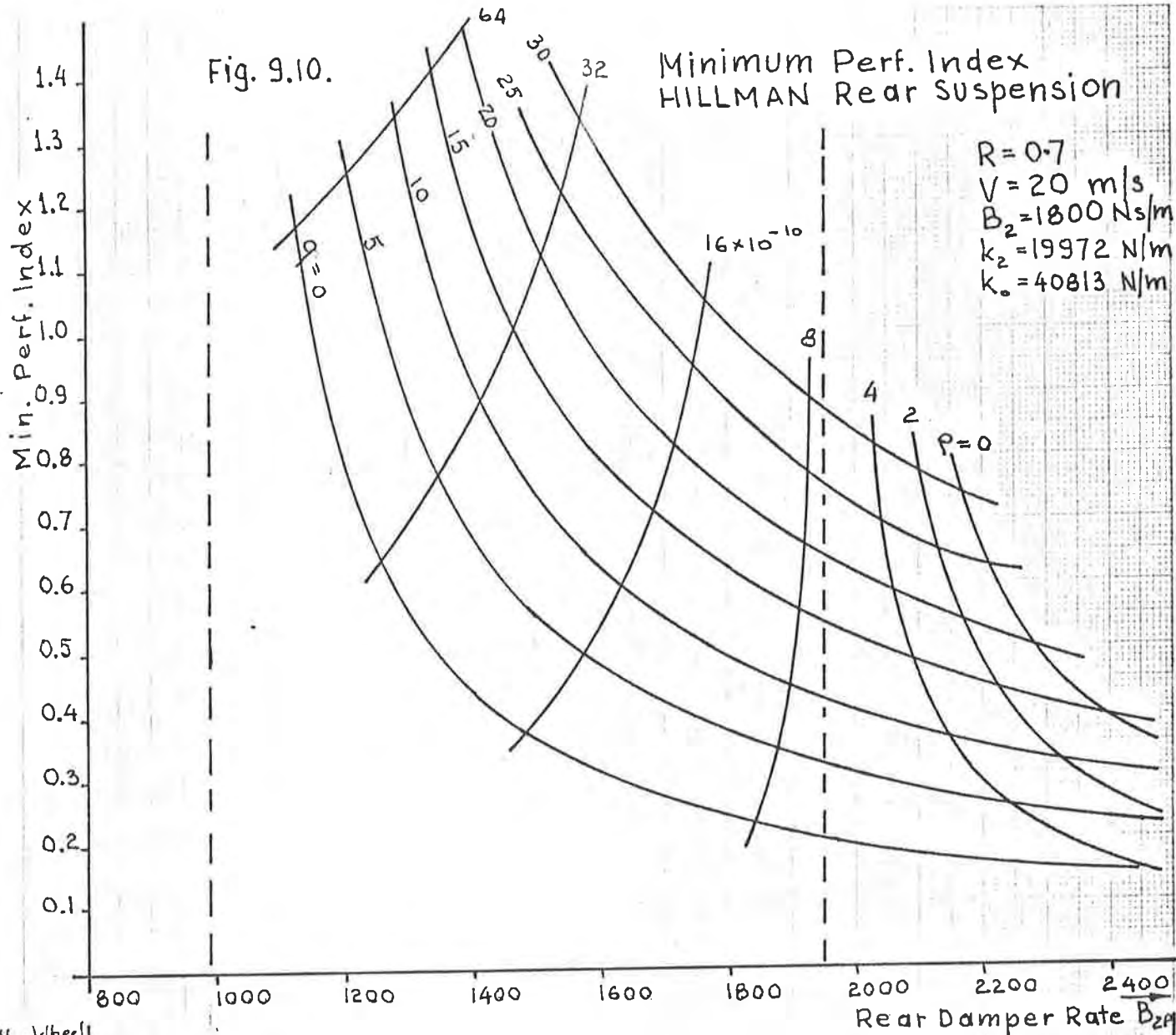


Fig. 9.11. HILLMAN Front Suspension Characteristics.

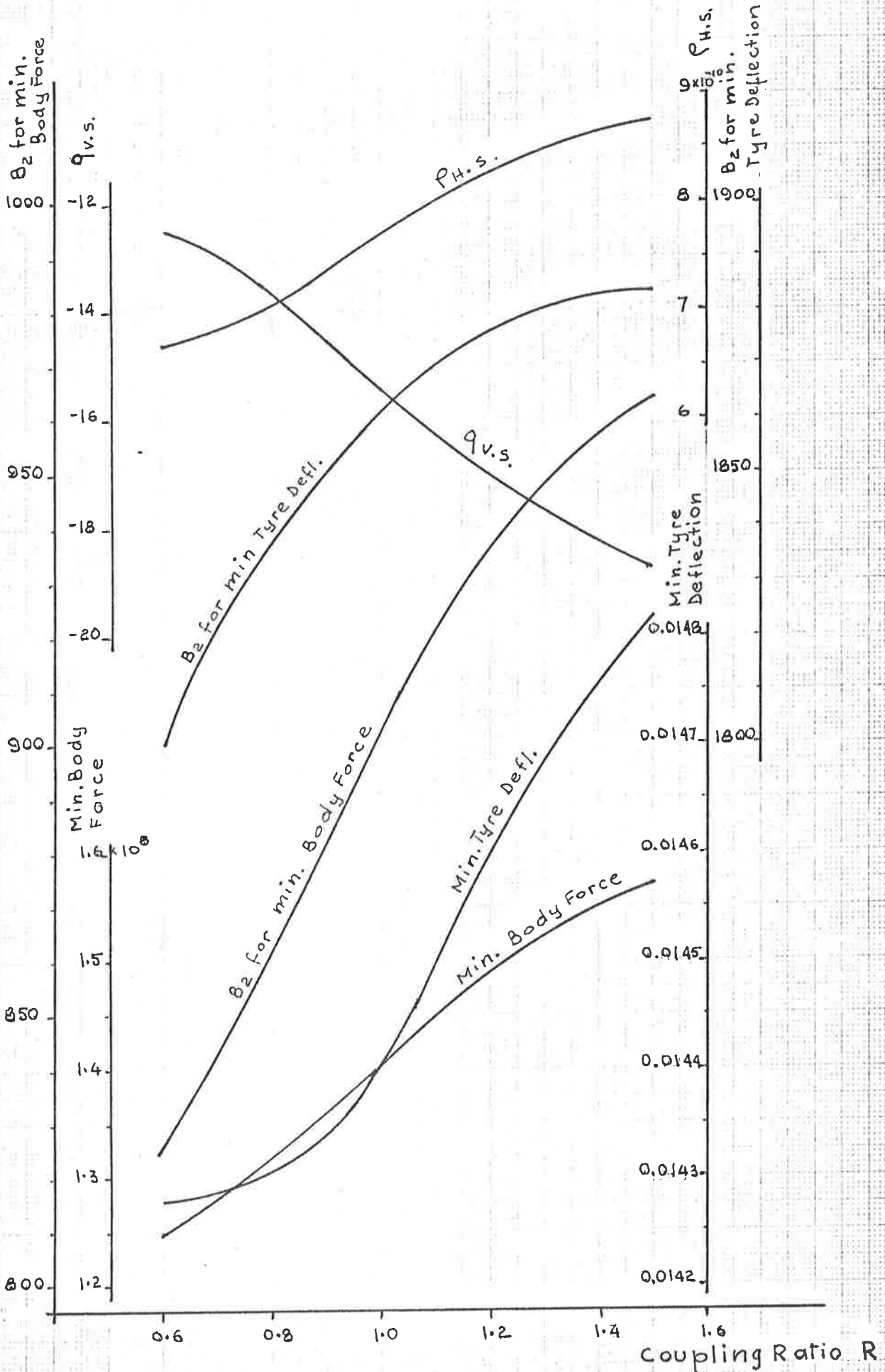


Fig. 9.12. HILLMAN Rear Suspension Characteristics.

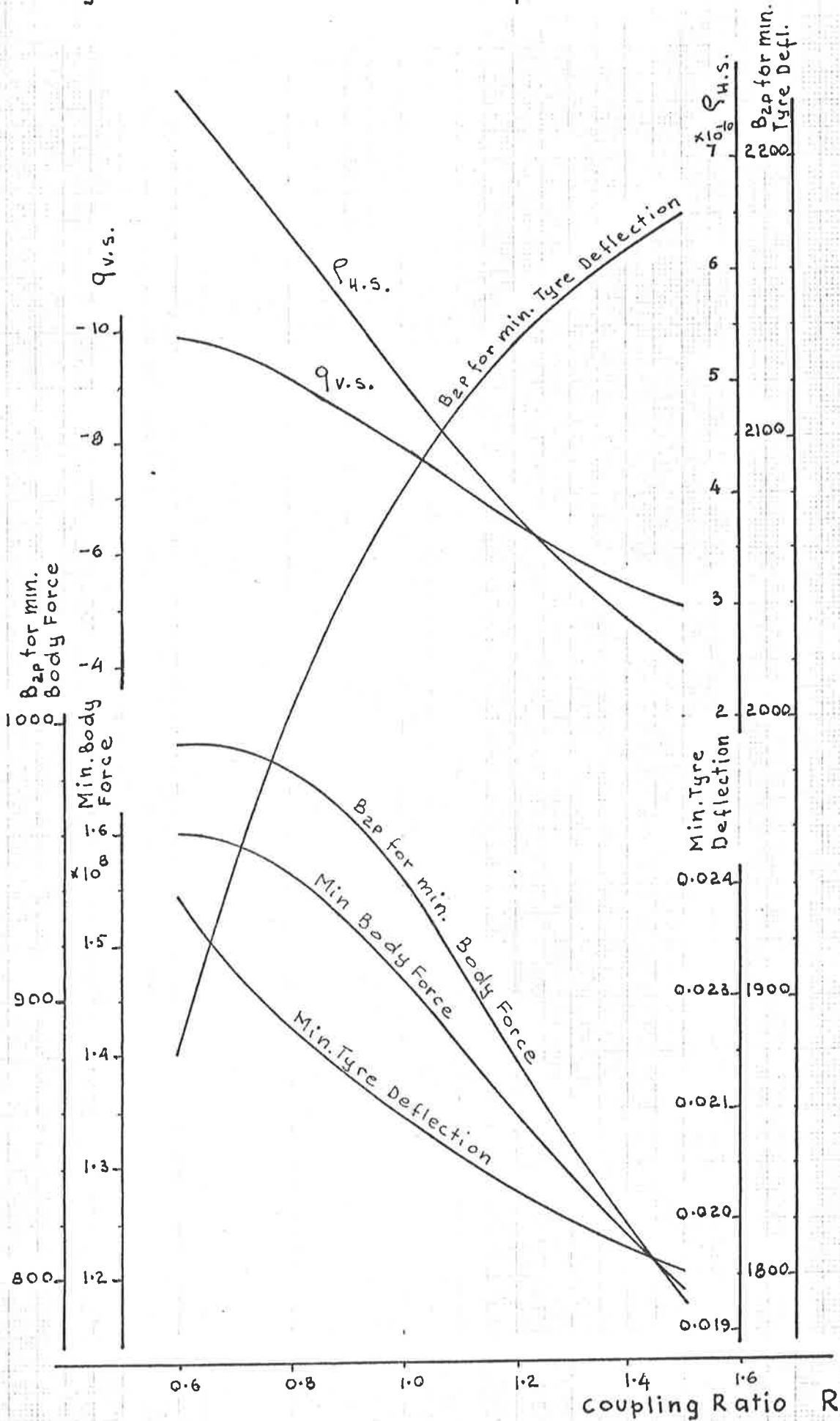
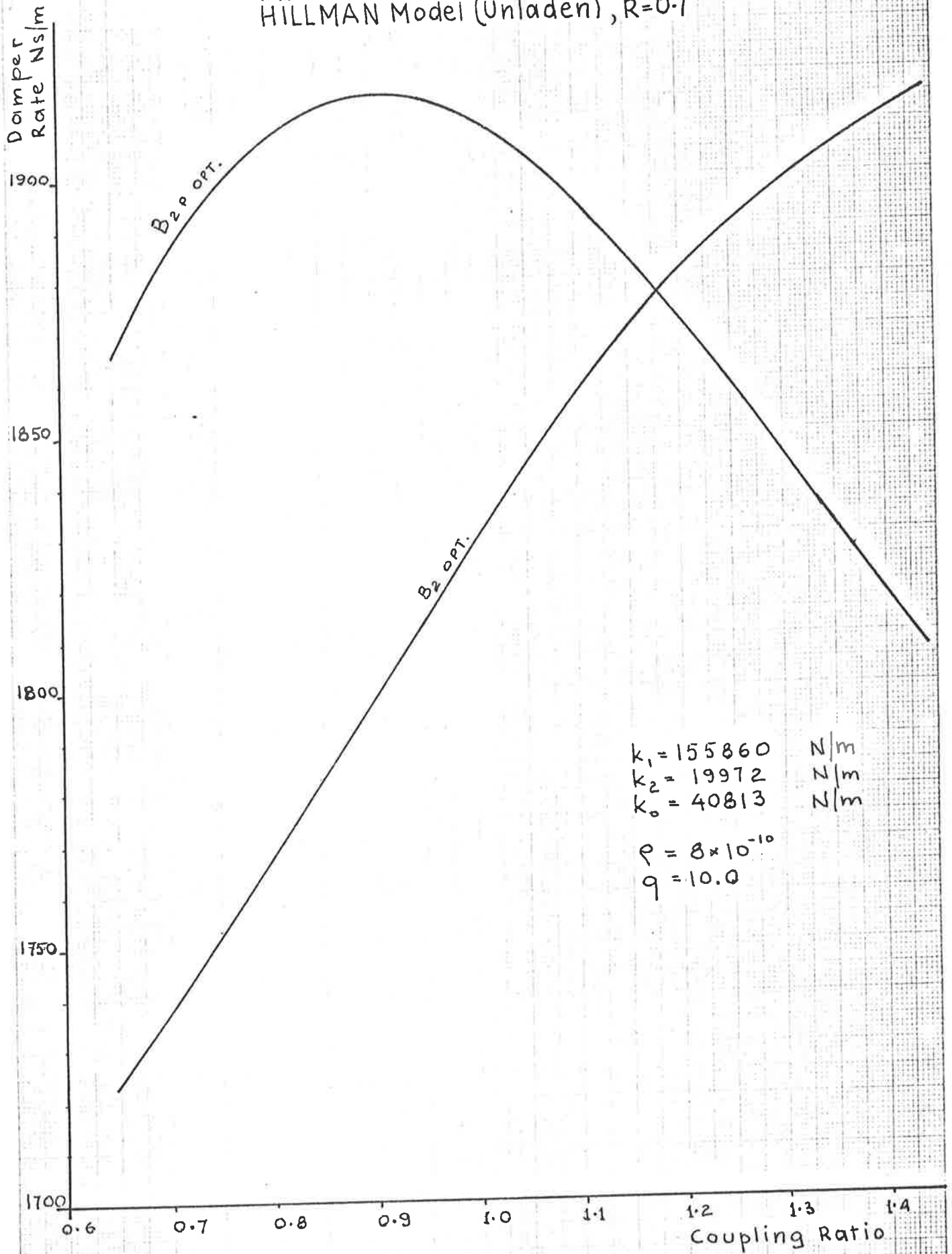


Fig. 9.13. Front and Rear Damping Rate for minimum Performance Index HILLMAN Model (Unladen), $R=0.7$



9.4 Suspension Spring Stiffness and Coupling Ratio

If the overall stiffness k_0 of the model is to remain constant then the rear spring stiffness will be a function of the front spring stiffness and vice versa according to the relationships

$$k_{2P} = \frac{k_0 k_2 a^2}{k_2 L^2 - k_0 b^2} \quad (9.8)$$

and

$$k_2 = \frac{k_0 k_{2P} b^2}{k_{2P} L^2 - k_0 a^2} \quad (9.9)$$

The front and rear springs cannot be optimised independently because of this inter-relationship, in addition, there may be also cross-coupling effects due to springs. These aspects need to be investigated separately.

To get some idea of the system behaviour as the stiffness of the suspension springs is varied, the integral square values of body force, tyre deflection and wheel travel were calculated for HILLMAN model using ASCL simulation language.

The response was calculated for different values of k_2 and k_{2P} , keeping all other parameters constant, including the overall model stiffness k_0 . It really means that the stiffness of rear suspension springs is decreased according to eq. 9.8 as the stiffness of the front springs is increased.

The results of these simulations are shown in Figs. 9.14, 9.15, 9.16 and 9.17.

After examination of the graphs, the following broad observations can be made regarding the response with varying suspension spring stiffness and coupling ratio R :

1.S.V. Body Force (ISF2)

The body force at the front and rear support points generally increases with increasing value of the respective spring stiffness.

But since the overall stiffness is to remain constant, the stiffness

of the rear spring will decrease in accordance of Eq. 9.8 as the stiffness of front springs is increased. Consequently the force at the rear support point will decrease and the force at the front support point will increase with increasing front spring stiffness. Also the force increases at the front with increasing coupling ratio, and decreases at the rear.

Thus the sum of body forces which causes the vertical body acceleration changes relatively little with the spring stiffness and coupling ratio as seen from Fig. 9.14.

I.S.V. Tyre Deflection (ISX01)

Front tyre deflection increases with increasing front spring stiffness and coupling ratio, while the rear tyre deflection decreases with increasing rear spring stiffness to a well defined minimum, and then continually increases.

The sum of front and rear tyre deflections which forms one part of the performance index generally increases with increasing spring stiffness and decreases with an increasing coupling ratio.

The characteristics display well defined minima.

I.S.V. Relative Wheel Travel (ISX12)

Front wheel travel decreases with the increasing value of front spring stiffness and with decreasing coupling ratio while the rear wheel travel displays just the opposite behaviour with the result that the sum of the front and rear integral square values is constant, and entirely independent of spring stiffness. Evidently the wheel travel is mainly determined by the mass distribution in the model.

The preliminary investigation of the model behaviour, having a variable front spring stiffness and constant overall stiffness will not reveal if there is any significant interaction between the front and the rear responses due to suspension springs.

For closer examination of the cross-coupling effects the response

of the model was calculated for different coupling ratios while maintaining a constant rear spring stiffness and varying the front spring stiffness only, and then reversing the process.

This procedure is equivalent to a variable overall stiffness of the model.

The results of these calculations are shown in Figs. 9.18, 9.19, 9.20 for varying front spring stiffness with a constant rear spring stiffness, and Figs. 9.21, 9.22, 9.23 for varying rear spring stiffness with a constant front spring stiffness.

All graphs demonstrate clearly that there are strong interaction effects, except for the case $R=1.0$ which corresponds to an uncoupled system.

The interaction effects increase as the coupling ratio departs more and more from unity. This is to be expected since the cross-coupling terms may involve the powers of the expressions

$$mab(R-1)/L^2, \quad mab(R+a/b)/L^2 \quad \text{and} \quad mab(R+b/a)/L^2$$

as previously discussed.

A number of relationships seem to be linear functions of the spring stiffness which is not obvious when the overall stiffness is maintained constant since the rear spring stiffness is a non-linear function of the front spring stiffness.

Owing to the complexity of the problem, it is not possible to calculate the integral square values by a direct analytical process using the principal parameter values of the model. It is important, however, to gain some insight into the relationship between the weighting factors and the spring stiffness for the case of minimum performance index.

A graphical relationship can be established by carrying out a large number of computer optimisation processes using 2-dimensional search techniques with different values of weighting factors and

plotting the minimum values of performance index against front spring stiffness with the weighting factors ρ and q as the parameters. The graph will then indicate the functional relationships between the quantities involved, and will show the results to be expected when the quantities are varied.

To cover the entire field of interest, a very large number of computer searches would be required for a comprehensive plot which is very expensive and time consuming in terms of available computing resources, unless the simulation is carried out on an analogue computer.

A different approach to the problem would be to establish approximate functional relationships from digital computer simulation results using curve fitting techniques. The results would be sufficiently accurate over a limited range of model parameter values of practical interest, and would show the trends to be expected.

A closer examination of test results calculated with different values of spring stiffness and damping rate, but maintaining a constant overall stiffness, mass distribution and coupling ratio, suggests that the integral square values of response due to step input can be closely approximated over a limited range of parameter variations by the expressions of the form

$$I.S.V._s = A_s B_2 + (X_s + Y_s k_2 + Z_s k_2^2) / B_2 \quad \text{for the front suspension}$$

$$I.S.V._p = A_s B_{2p} + (X_s + Y_s k_{2p} + Z_s k_{2p}^2) / B_{2p} \quad \text{for the rear suspension}$$

The coefficients A_s , X_s , Y_s , Z_s where s denotes an identifying numerical suffix, can be determined from ACSL simulation results using interactive BASIC Program COEF shown in Appendix C. The expressions will incorporate the interaction effects between the front and the rear, and k_{2p} is calculated from the relationship

$$k_{2p} = \frac{k_2 (a/L)^2}{(k_2/k_0) - (b/L)^2}$$

The coefficients for the HILLMAN model are tabulated in Table B.5 for unladen conditions and in Table B.6 for laden conditions

(Appendix B) with the following suffices relating to the integral square values:-

- 1 & 2 Front and rear tyre deflection respectively
- 3 & 4 Front and rear relative wheel travel
- 5 & 6 Front and rear body force.

BASIC Program PERF1, also shown in Appendix C was used to verify the integral square responses for different values of spring stiffness and damping. The agreement was found to be quite good, and adequate to show up any trends.

Since the effect of damping can be investigated independently as discussed in Section 9.3, the damping rates will be held constant at 1800 Ns/m during the investigation of the effect of varying spring stiffness.

With constant damping for front and rear, the sums of integral square values for tyre deflection, relative wheel travel, and body force respectively can be expressed as:

$$SISX01 = ISX01 + ISX01P = (A_0 + B_0 k_2 + C_0 k_2^2) + (D_0 + E_0 k_{2P} + F_0 k_{2P}^2) \quad (9.10)$$

$$SISX12 = ISX12 + ISX12P = (A_1 + B_1 k_2 + C_1 k_2^2) + (D_1 + E_1 k_{2P} + F_1 k_{2P}^2) \quad (9.11)$$

$$SISXF2 = ISF2 + ISF2P = (A_2 + B_2 k_2 + C_2 k_2^2) + (D_2 + E_2 k_{2P} + F_2 k_{2P}^2) \quad (9.12)$$

The coefficients A, B, C, D, E and F for a specified coupling ratio are calculated from values listed in Tables B.5 and B.6 of Appendix B.

The performance index can be written in the form

$$I = \rho(SISXF_2) + q(SISX01) + (SISX12) \quad (9.13)$$

and for a minimum value of performance index

$$dI/dk_2 = 0, \text{ hence}$$

$$\begin{aligned} & \rho [B_2 + 2k_2 C_2 + E_2(dk_{2P}/dk_2) + 2F_2 k_{2P} (dk_{2P}/dk_2)] \\ & + q [B_0 + 2k_2 C_0 + E_0 (dk_{2P}/dk_2) + 2F_0 k_{2P} (dk_{2P}/dk_2)] \\ & + [B_1 + 2k_2 C_1 + E_1 (dk_{2P}/dk_2) + 2F_1 k_{2P} (dk_{2P}/dk_2)] = 0 \end{aligned} \quad (9.14)$$

$$\text{where } dk_{2P}/dk_2 = -(k_{2P} b)/(k_2 a)^2 \quad (9.15)$$

It is evident that for the condition of minimum performance index there will be a linear relationship between the weighting factor ρ and q irrespective of the complexity of the functional relationship of k_2 which determines the slope of the straight line characteristics.

If ρ is plotted against q for a specified value of coupling ratio, then the graph will have an infinite slope when

$$B_2 + 2k_2 C_2 + E_2(dk_{2P}/dk_2) + 2F_2 k_{2P} (dk_{2P}/dk_2) = 0 \quad (9.16)$$

and the value of k_2 calculated from eq. 9.16 will minimise the integral square value of body force.

The graph will have a zero slope when

$$B_0 + 2k_2 C_0 + E_0 (dk_{2P}/dk_2) + 2F_0 k_{2P} (dk_{2P}/dk_2) = 0 \quad (9.17)$$

and the value of k_2 determined from eq. 9.17 will minimise the integral square value of tyre deflection.

One would intuitively think that the optimum value of the spring stiffness will be somewhere between the values that minimise the tyre deflection and body force respectively.

The values of spring stiffness calculated from eqns. 9.16 and 9.17 for different values of coupling ratio are listed in Table 9.2 for the HILLMAN model, for unladen and laden conditions respectively, and show the probable range of optimum stiffness.

TABLE 9.2

SUSPENSION SPRING STIFFNESS FOR MINIMUM TYRE DEFLECTION AND BODY FORCE. HILLMAN DATA.

| R | UNLADEN | | LADEN | |
|-----|---------------------------|---------------------------|---------------------------|----------------------------|
| | k_2 for min. Tyre Defl. | k_2 for min. Body Force | k_2 for min. Tyre Defl. | k_2 for min. Body Force. |
| 0.6 | 18842 | 23902 | 22898 | 24195 |
| 0.7 | 18927 | 23354 | 21806 | 23779 |
| 0.8 | 18882 | 22837 | 20864 | 22863 |
| 0.9 | 18761 | 22370 | 20068 | 22067 |
| 1.0 | 18603 | 21955 | 19437 | 21395 |
| 1.1 | 18431 | 21597 | 18942 | 20838 |
| 1.2 | 18260 | 21300 | 18530 | 20387 |
| 1.3 | 18099 | 21011 | 18254 | 20022 |
| 1.4 | 17936 | 20660 | 18008 | 19725 |
| 1.5 | 17772 | 20520 | 17803 | 19479 |

Interactive BASIC Program MIN shown in Appendix C was developed to calculate the value of k_2 from eq. 9.14, for specified weighting factors and coupling ratio, using a modified Newton-Rhapson routine.

FORTTRAN Programs MINIFZ and MINIPLT were developed later to calculate and plot I_{min} as a function of k_2 with weighting factors ρ and q as parameters.

The graphs in Figs. 9.24 and 9.25 show the relationship between the minimum performance index and suspension spring stiffness for $R=0.7$, with weighting factors as parameters, and in Figs. 9.26 & 9.27 for $R=1.3$.

The graphs display characteristics similar to an uncoupled system ($R=1.0$) where increasing value of q will lead to spring stiffness that minimises the tyre deflection, and increasing value of ρ will

lead to spring that minimises the body force, thus justifying the principles of computer search.

But again, once the weighting factors have been selected, the minimum value of the performance index and the spring stiffness that minimises the performance index are all fixed.

9.5 The influence of Vehicle Speed on Integral Square Response

The vehicle speed has a two-fold effect:

- (1) The integral square values of response due to random road input are cV times that due to unit step input, where c involves the road roughness parameter, and V is the vehicle speed.
- (2) The cross-coupling effects of front and rear responses which depend on the time-delay between the front and rear excitations for a given coupling ratio R .

The time delay affects the phase relationship between the superimposed cross responses. Since the frequency of free oscillations is determined by suspension parameters such as the effective mass and stiffness, the phase between the front and rear responses will affect the amplitude of the combined response.

Integral square values of response for the HILLMAN model with constant suspension parameters are shown in Figs. 9.28 to 9.34 as a function of vehicle speed and coupling ratio R .

The response of an uncoupled system ($R=1.0$) is independent of vehicle speed as expected, and the cross-transfer effects decrease with increasing vehicle speed as indicated by decreasing values of integral square response.

The maximum values of integral square response for the rear wheel correspond to a vehicle speed of approximately 35 m/s, or a time delay of 0.073 sec. between the front and rear wheel excitations. This amount of delay is of the same order of magnitude as the period of the hop frequency of the front wheel (0.085 sec.), which

suggests that the wheel hop frequencies may be mainly responsible for the cross-transfer effects.

This view is further reinforced by the fact that the maxima for laden and unladen conditions occur at the same speed, demonstrated clearly by graphs in Figs. 9.31 and 9.32.

Fig. 9.14.

Integral Square Body Force as Function of Spring Rate and Coupling Ratio.
 HILLMAN Model (Unladen), $V = 20$ m/s.

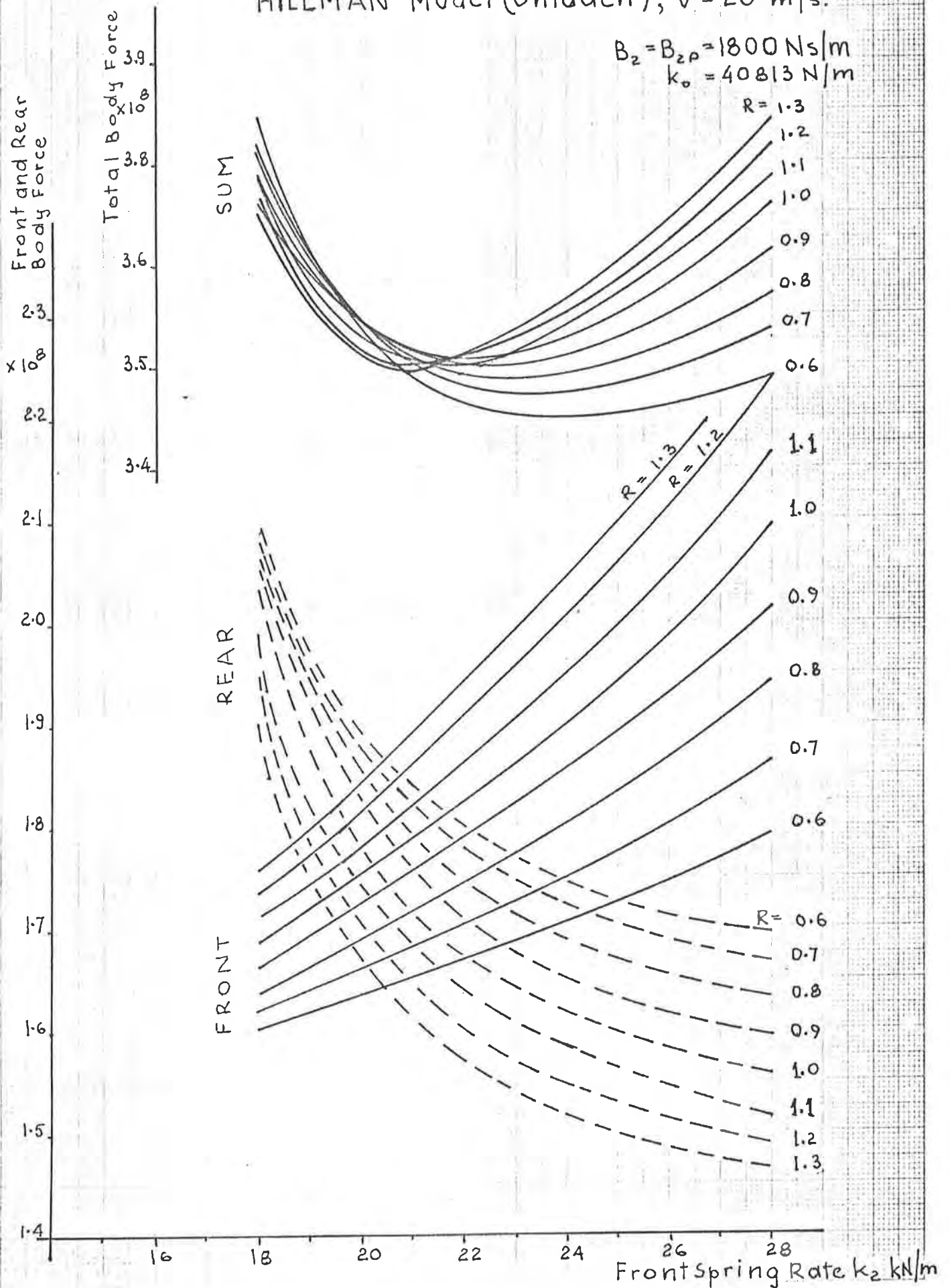


Fig. 9.15. Integral Square Tyre Deflection as Function of Spring Rate and Coupling. HILLMAN Model (Unladen), $V=20$ m/s.

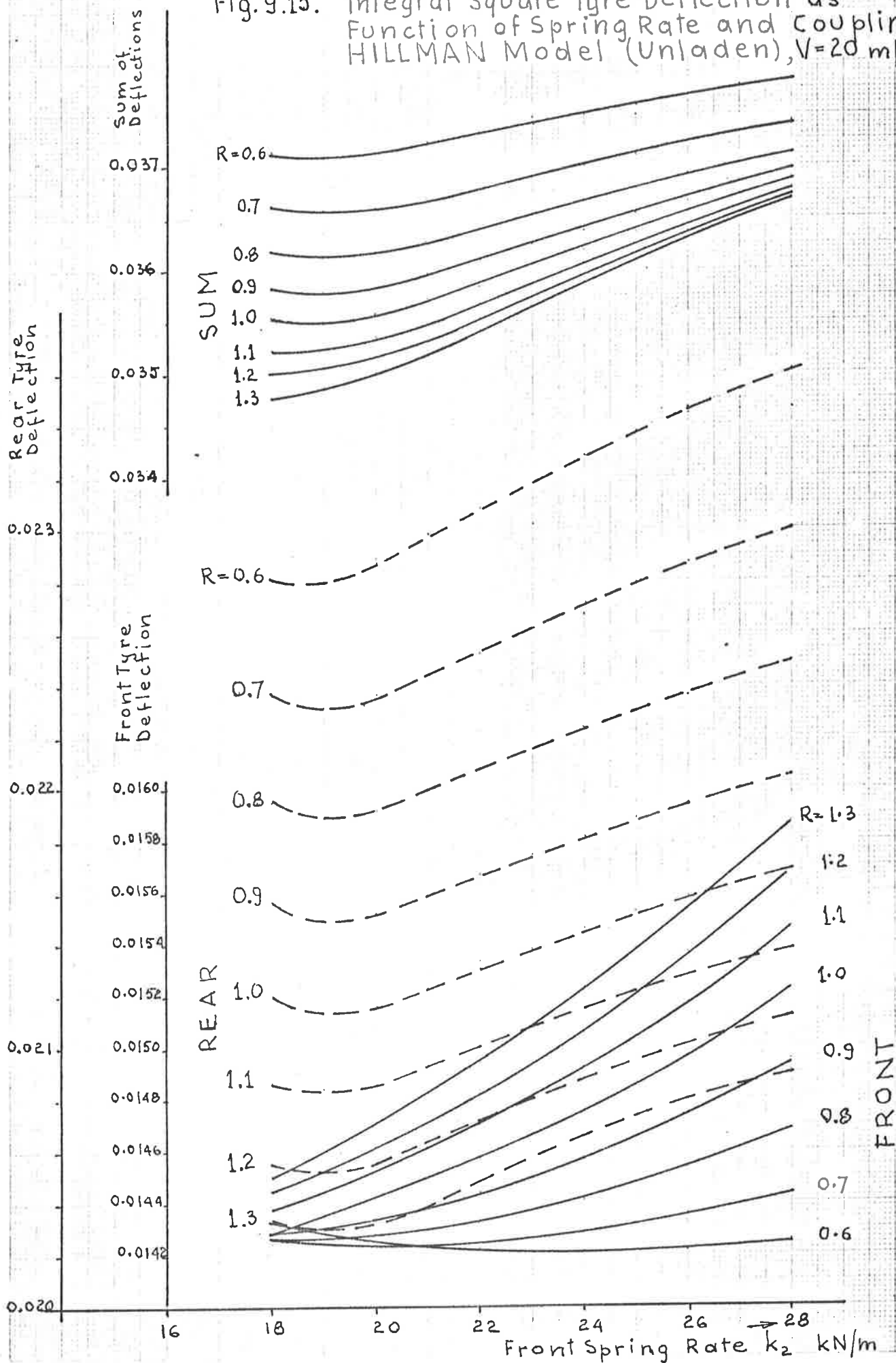


Fig. 9.16. Integral Square Wheel Travel as Function of Spring Rate and Coupling Ratio.
 HILLMAN Model (Unladen), $V=20$ m/s

$$B_2 = B_{2P} = 1800 \text{ Ns/m}$$

$$k_0 = 40812 \text{ N/m}$$

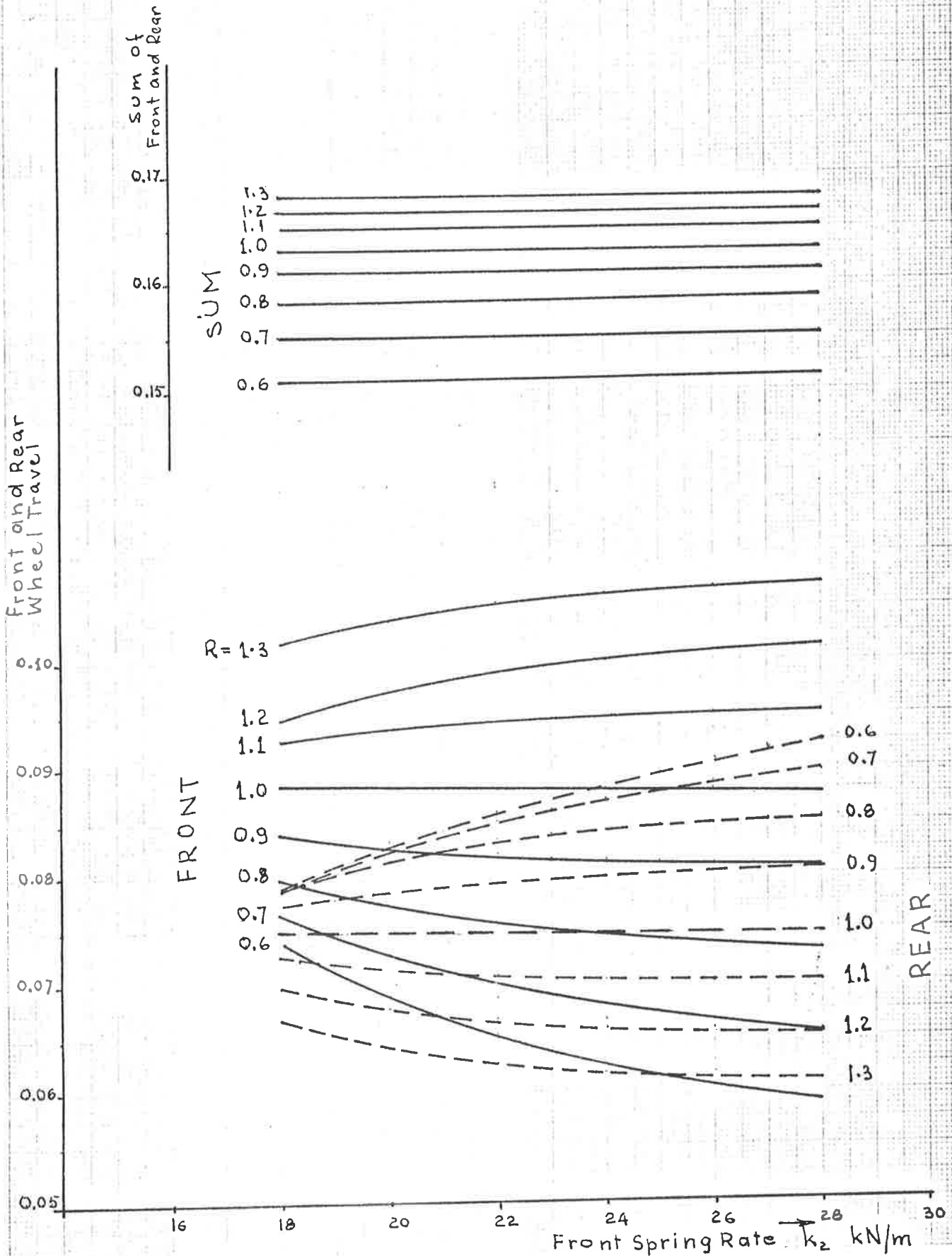


Fig. 9.17. Performance Index as Function of Spring Rate and Coupling Ratio.
 HILLMAN Model (Unladen), $V=20$ m/s.

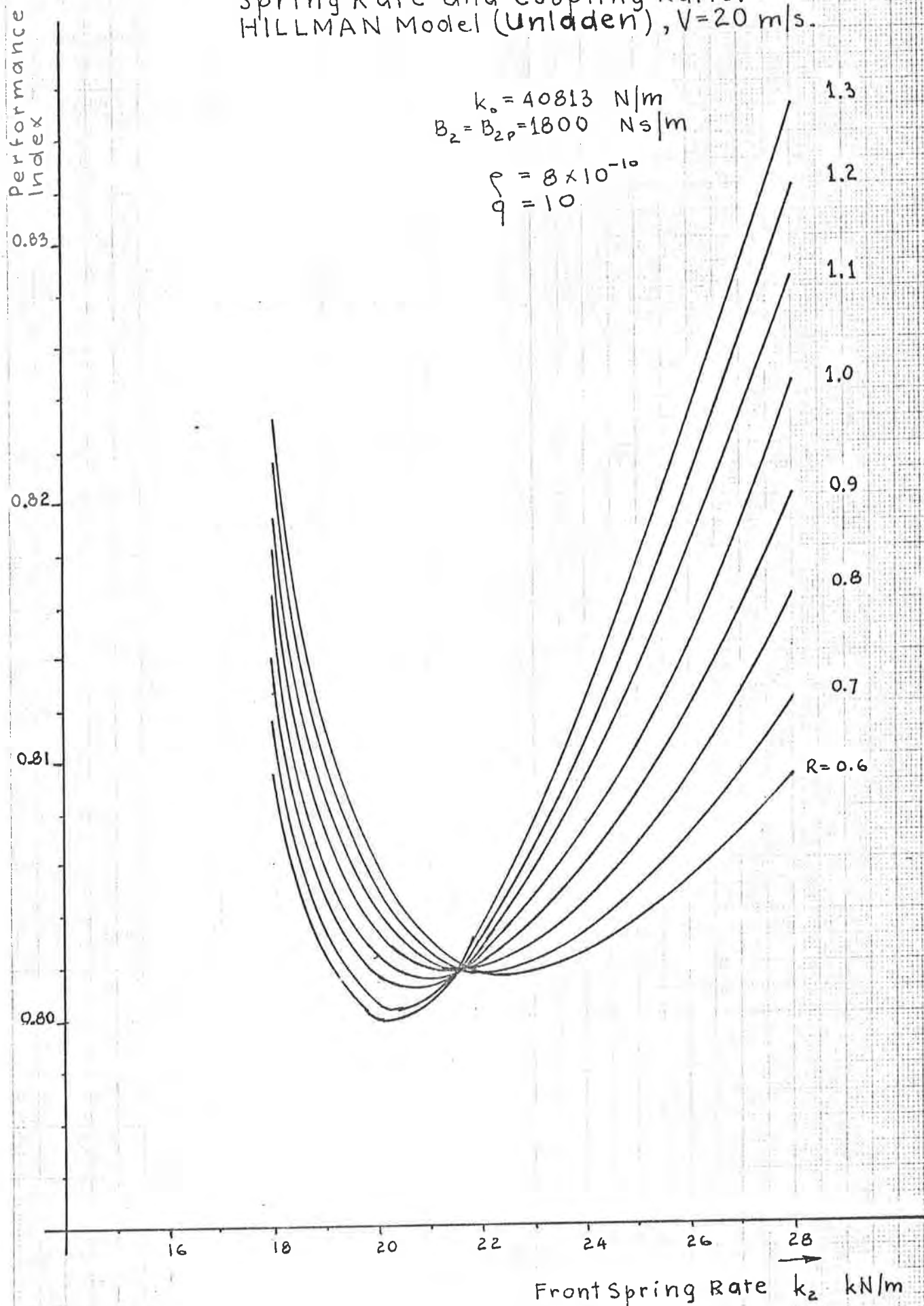


Fig. 9.18. Variation of Body Force with Front Spring Rate, Rear Spring $k_{2P} = \text{Const}$. HILLMAN Model (Unladen), $V = 20 \text{ m/s}$.

$k_{2P} = 22563 \text{ N/m}$
 $B_2 = B_{2P} = 1800 \text{ N/m}$

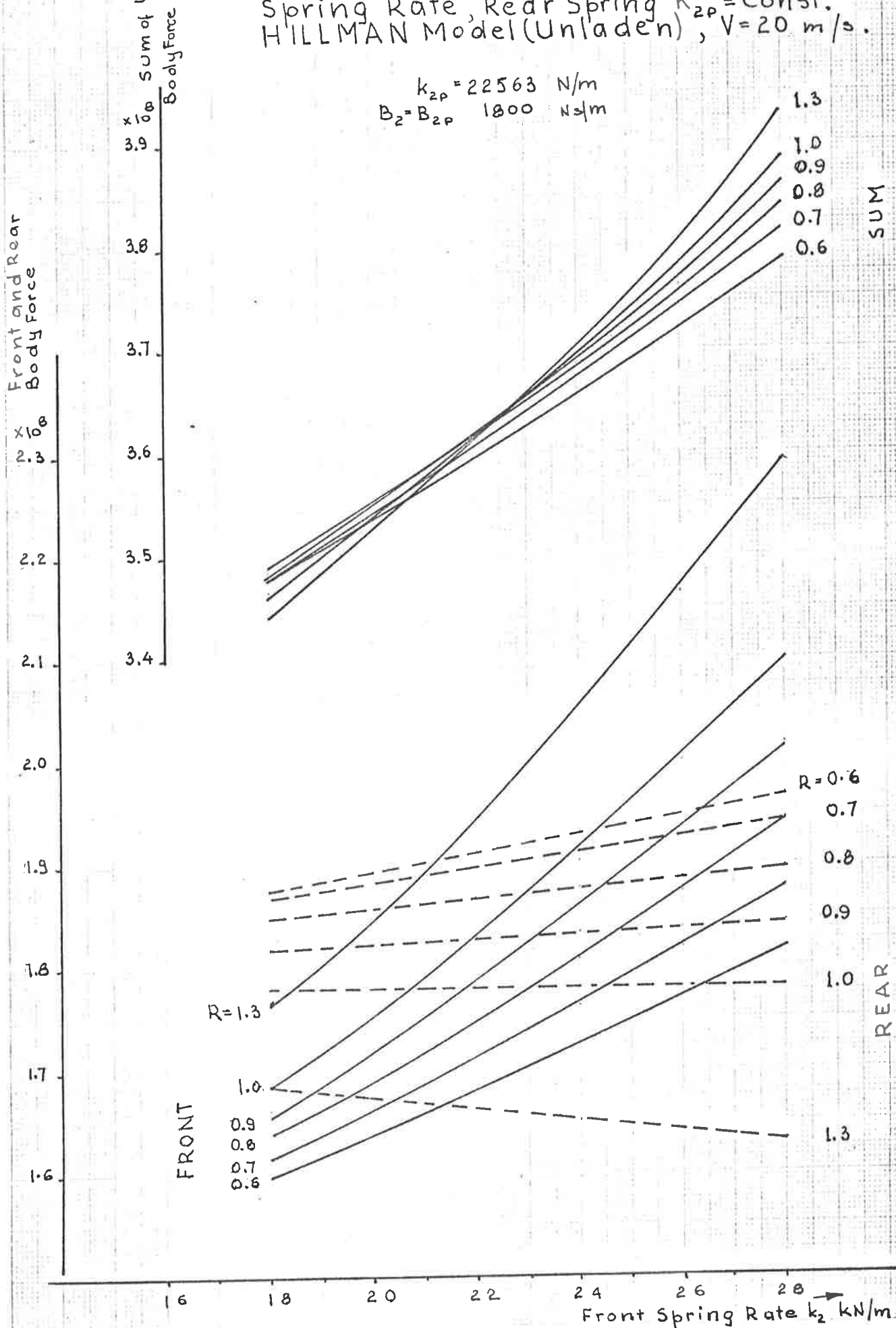


Fig. 9.19. Variation of Tyre Deflection with Front Spring Rate, Rear Spring $k_{2P} = \text{Const.}$
 HILLMAN Model (Unladen), $V = 20 \text{ m/s.}$

$$k_{2P} = 22563 \text{ N/m}$$

$$B_2 = B_{2P} = 1800 \text{ N s/m}$$

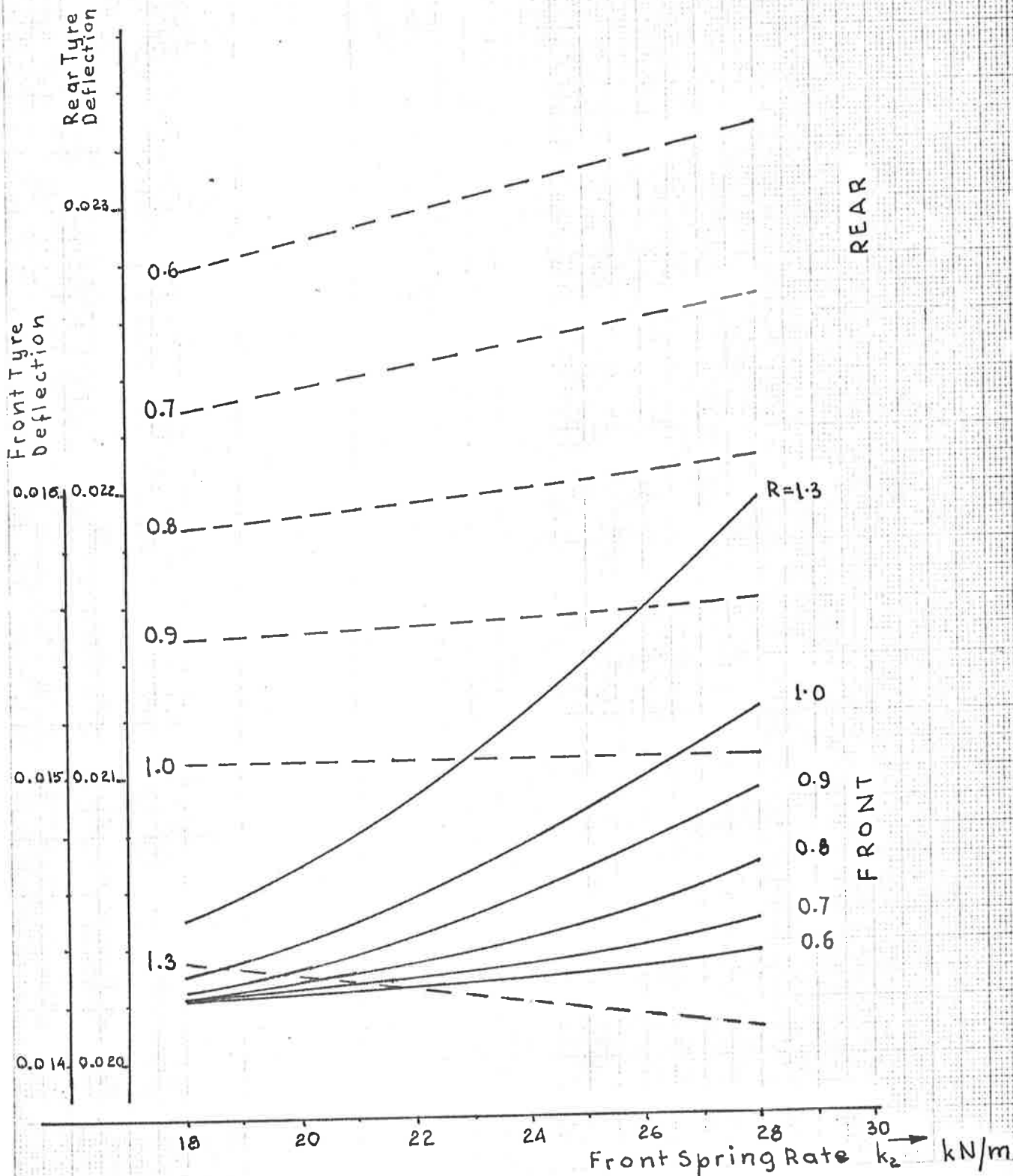


Fig. 9.20. Variation of Relative Wheel Travel with Front Spring Rate, Rear Spring $k_{zR} = \text{Const}$. HLLMAN Model (Unladen), $V = 20 \text{ m/s}$.

$k_{zP} = 22563 \text{ N/m}$
 $B_2 = B_{zP} = 1800 \text{ Ns/m}$

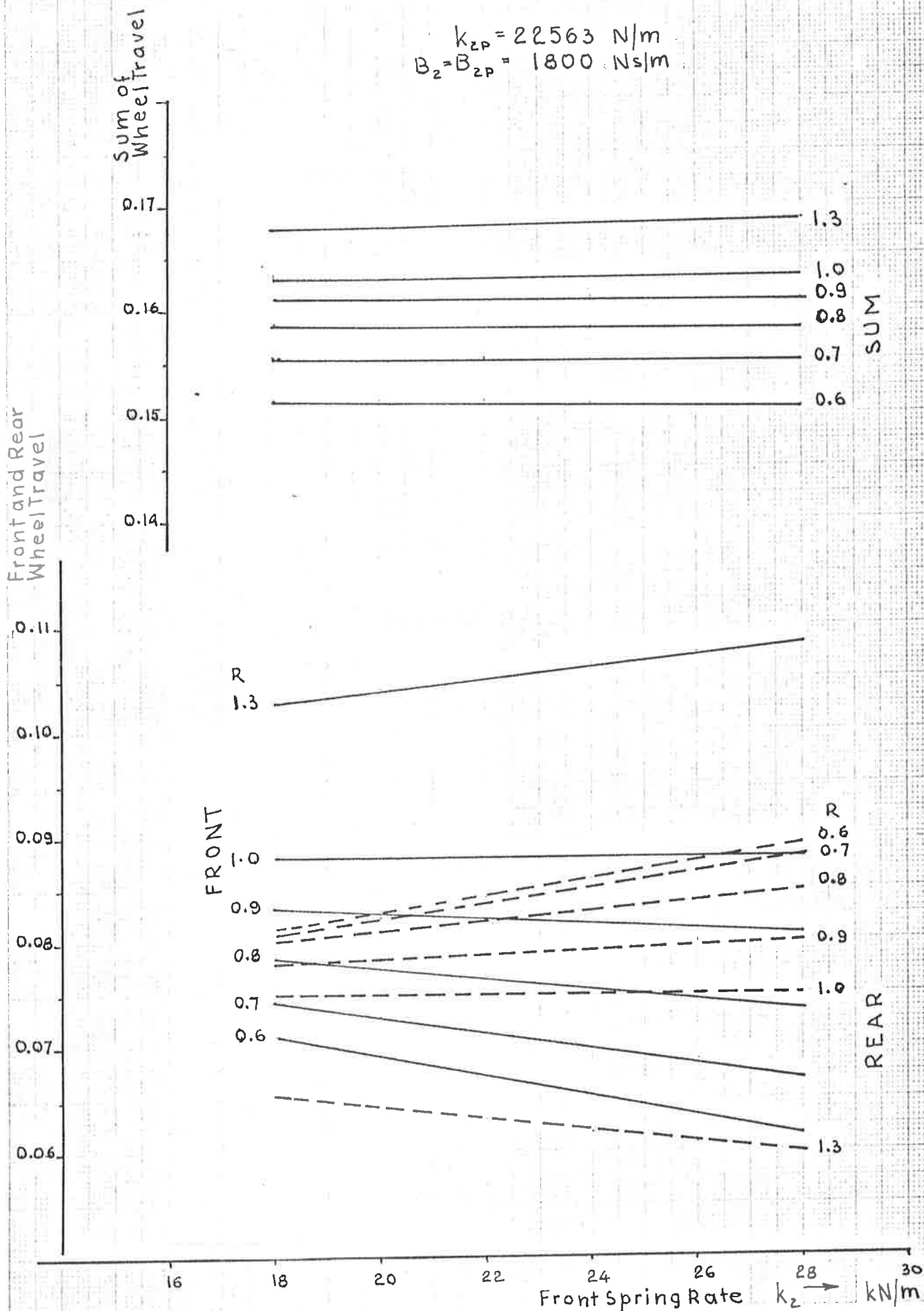


Fig. 9.21. Variation of Body Force with Rear Spring Rate, Front Spring $k_2 = \text{Const}$. HILLMAN Model (Unladen), $V = 20 \text{ m/s}$.

$k_2 = 19972 \text{ N/m}$
 $B_{2P} = B_2 = 1800 \text{ Ns/m}$

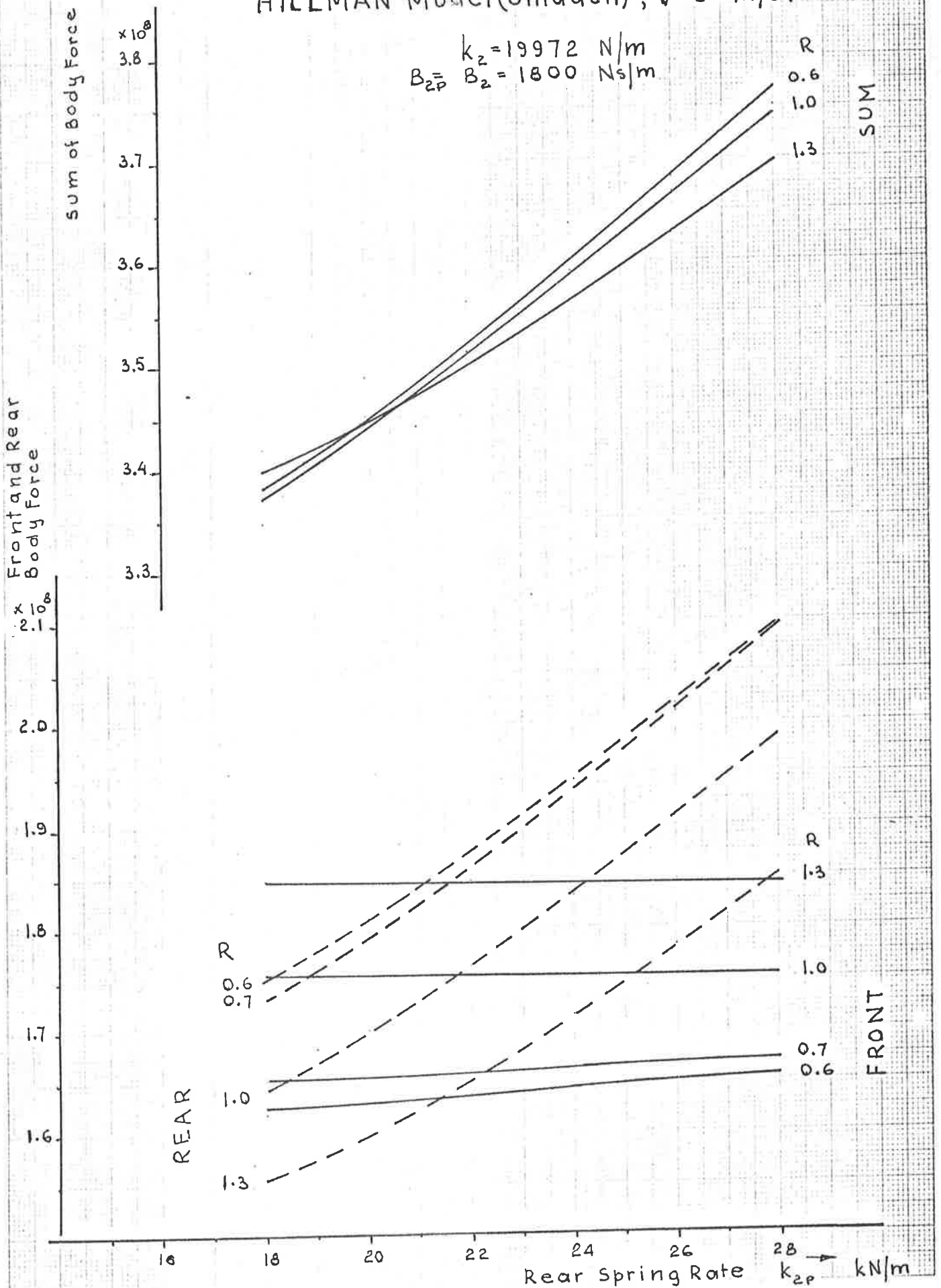


Fig. 9.22. Variation of Tyre Deflection with Rear Spring Rate, Front Spring $k_2 = \text{Const.}$

$$k_2 = 19972 \text{ N/m}$$

$$B_{2P} = B_2 = 1800 \text{ Ns/m}$$

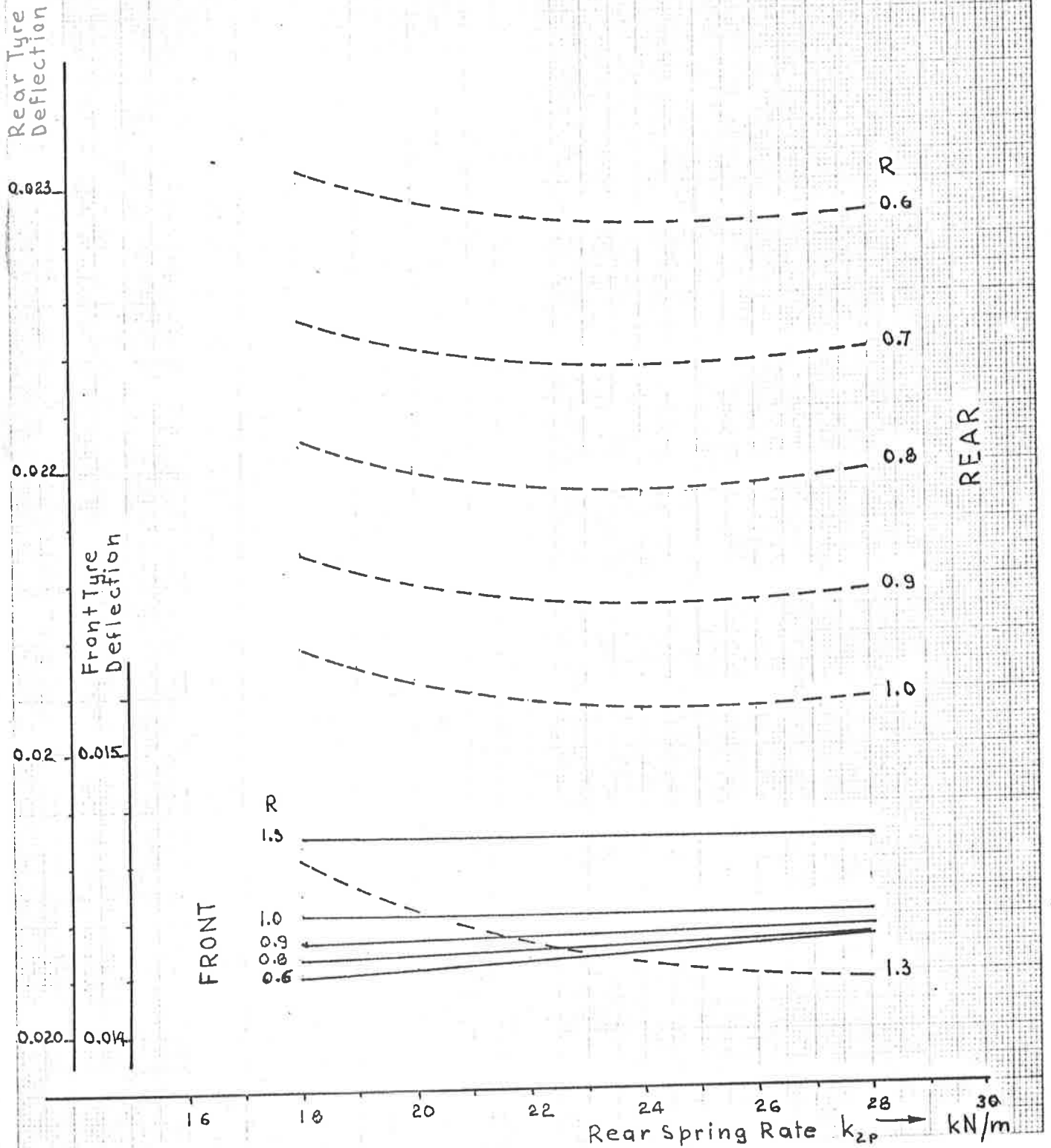


Fig. 9.23. Variation of Relative Wheel Travel with Rear Spring Rate, Front Spring $k_2 = \text{Const.}$ HILLMAN Model (Unaden), $V = 20 \text{ m/s.}$

$k_2 = 19972 \text{ N/m}$
 $B_2 = B_{2P} = 1800 \text{ Ns/m}$

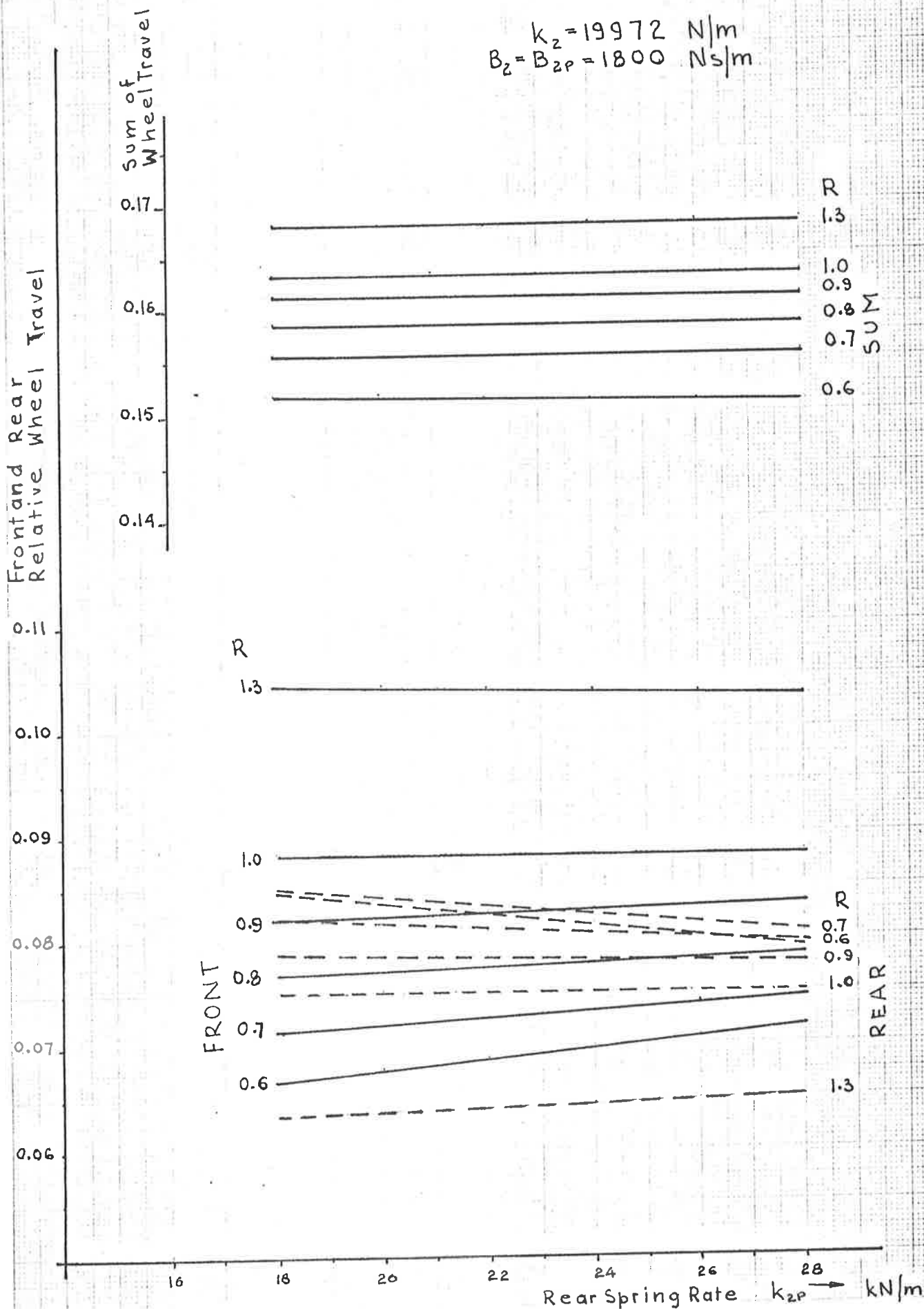
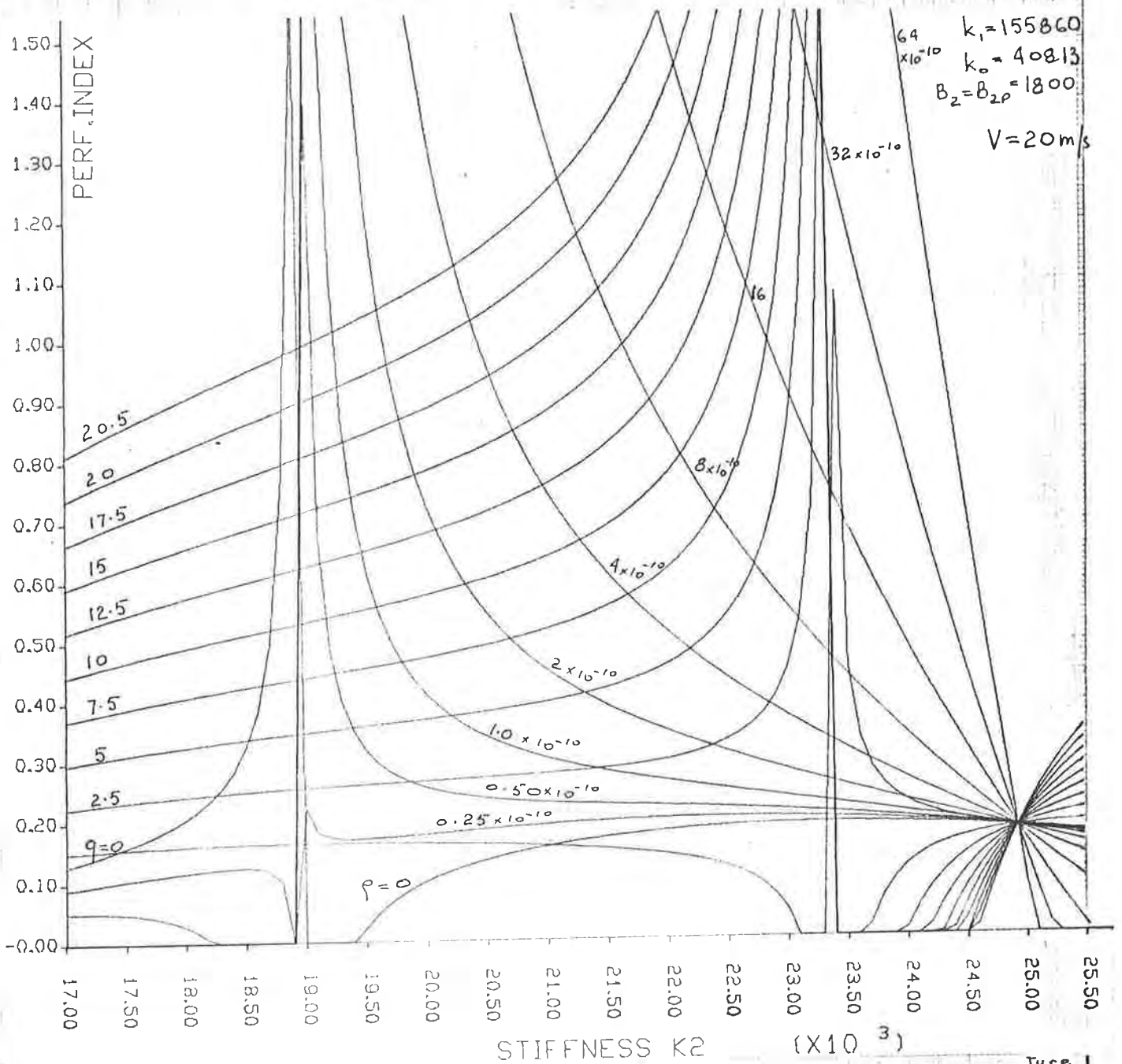


Fig. 9.24. Relationship between min. Performance Index, Spring Stiffness and Weighting Factors. HILLMAN Model (Unladen), $R=0.7$.



$k_1 = 155860$
 $k_0 = 40813$
 $B_2 = B_{2\rho} = 1800$
 $V = 20 \text{ m/s}$

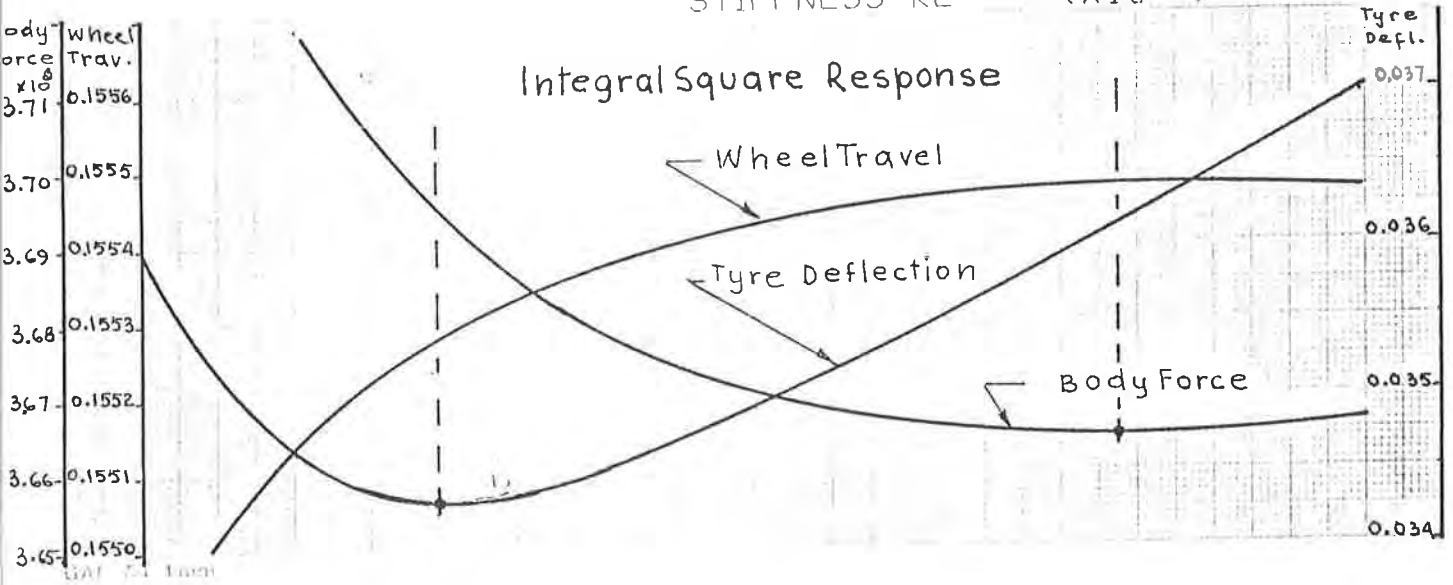
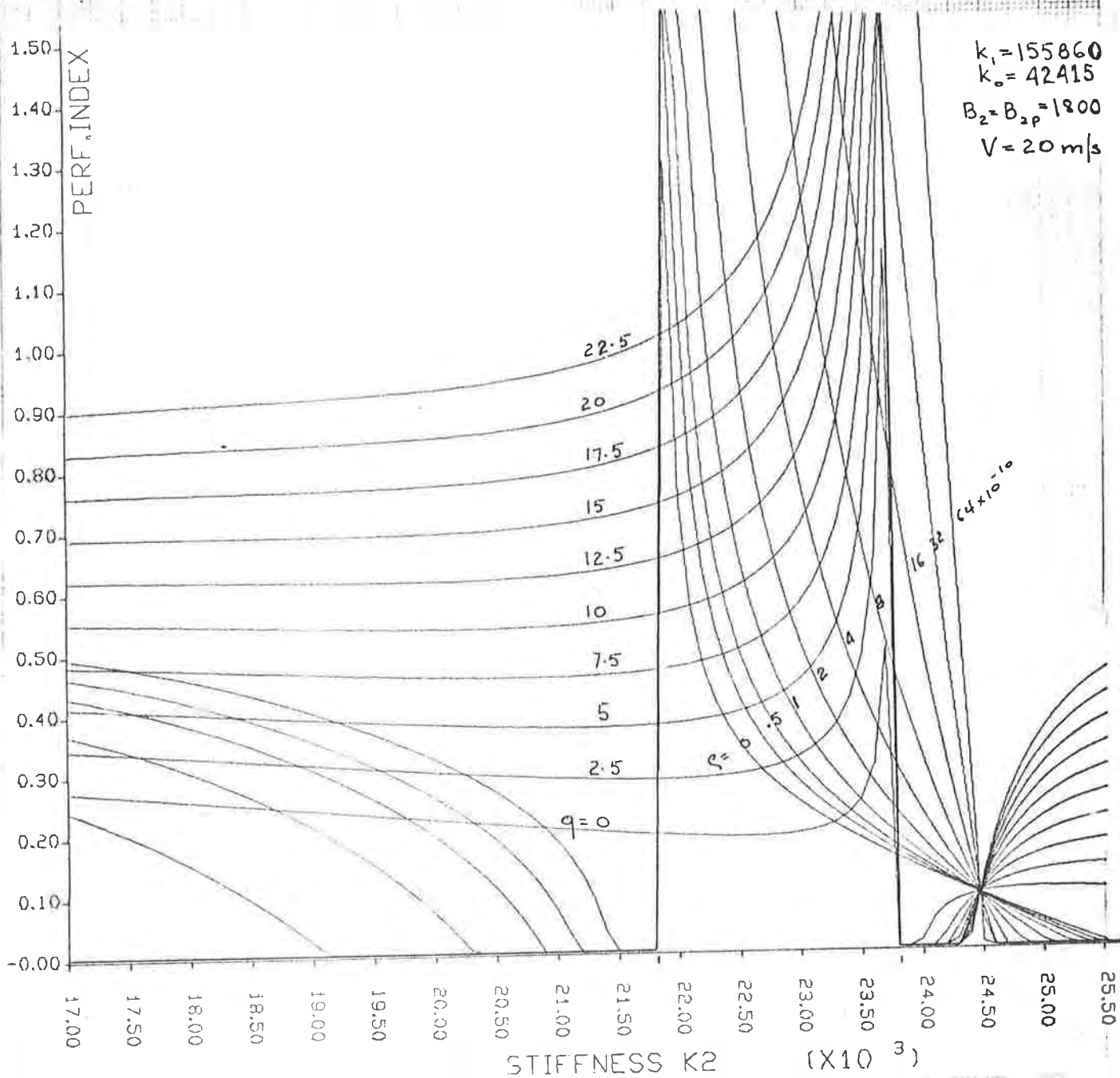


Fig.9.25. Relationship between min. Performance Index, Spring Stiffness and Weighting Factors. HILLMAN Model (Laden), $R=0.7$.



Integral Square Response

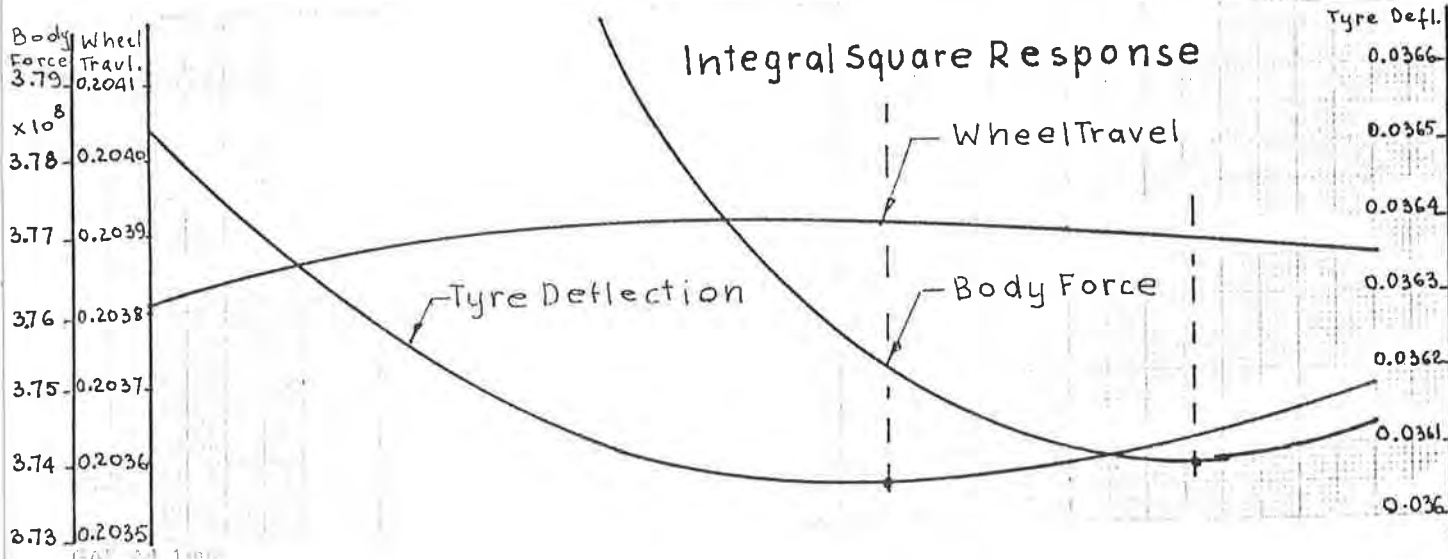


Fig. 9.26. Relationship between min. Performance Index, Spring Stiffness and Weighting Factors. HILLMAN Model (Unladen), $R=1.3$.

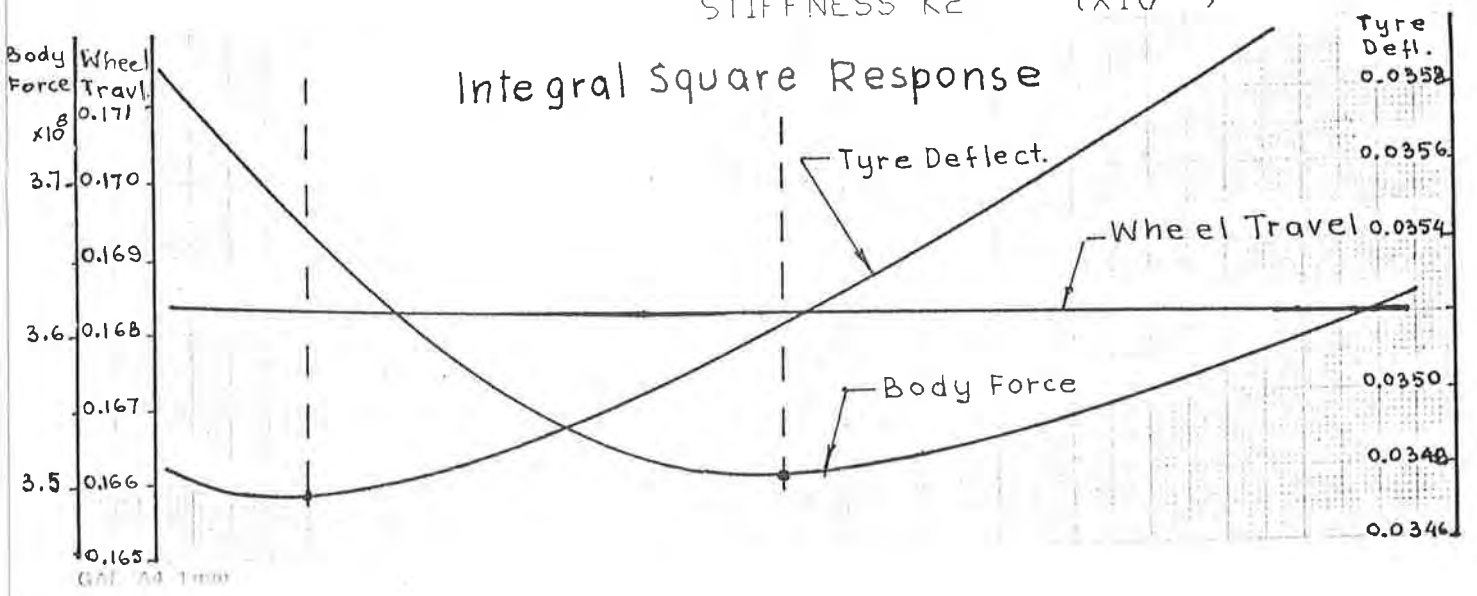
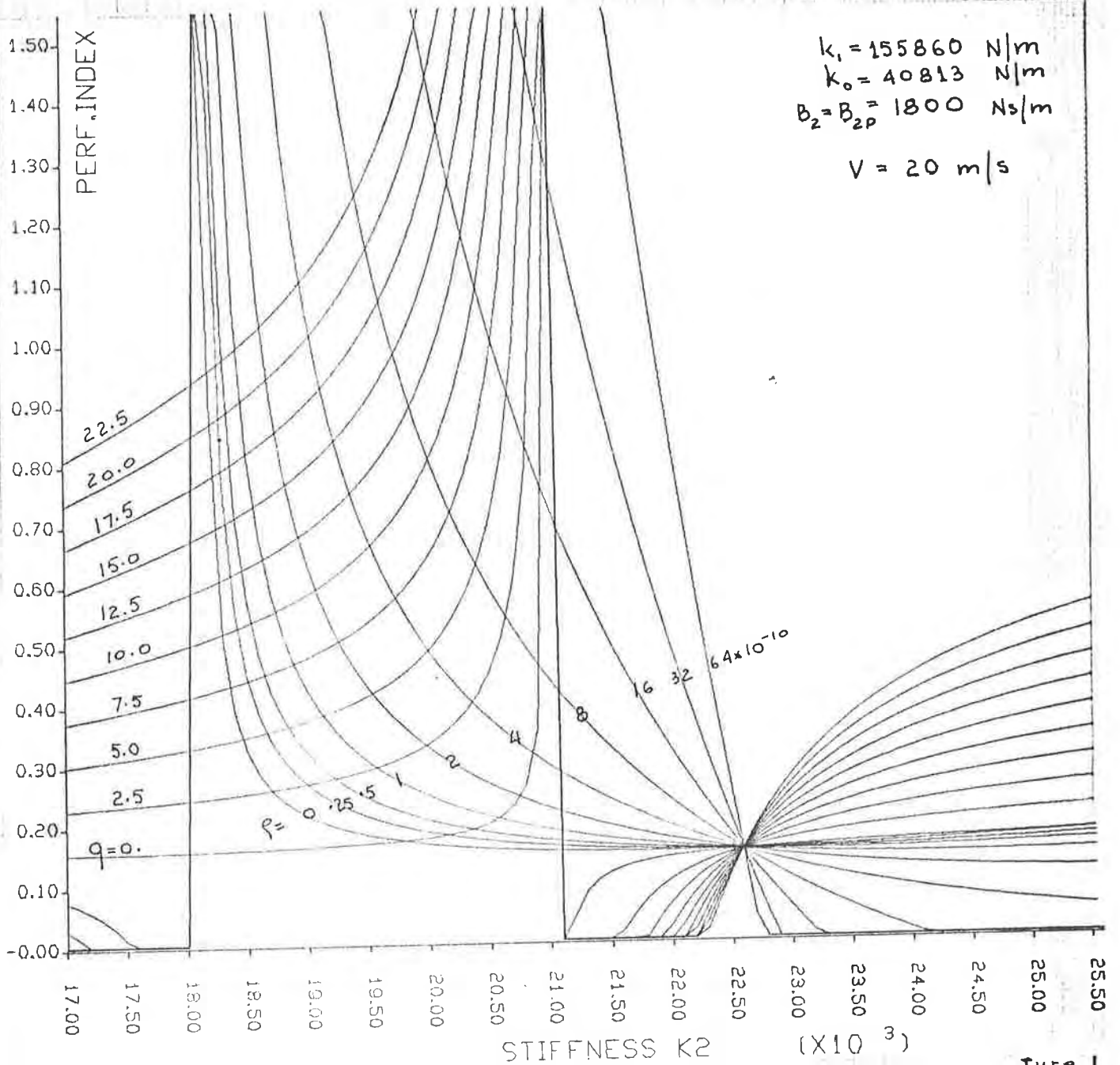


Fig. 9.27. Relationship between min. Performance Index, Spring Stiffness and Weighting Factors. HILLMAN model (Laden), $R=1.3$.

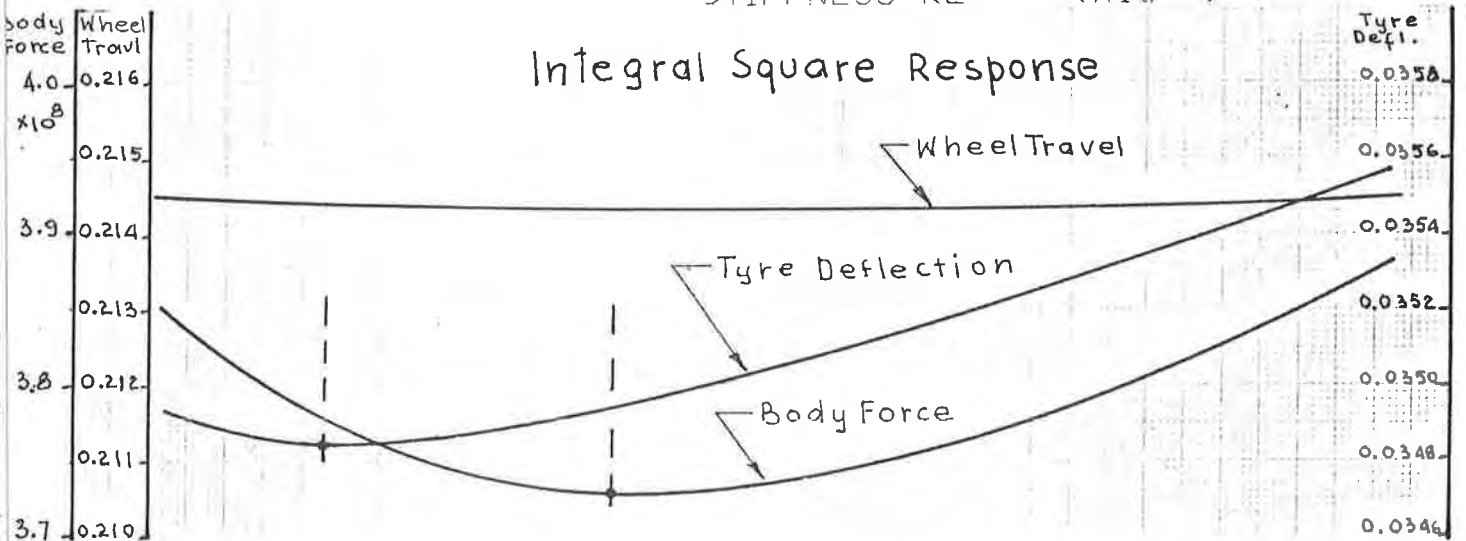
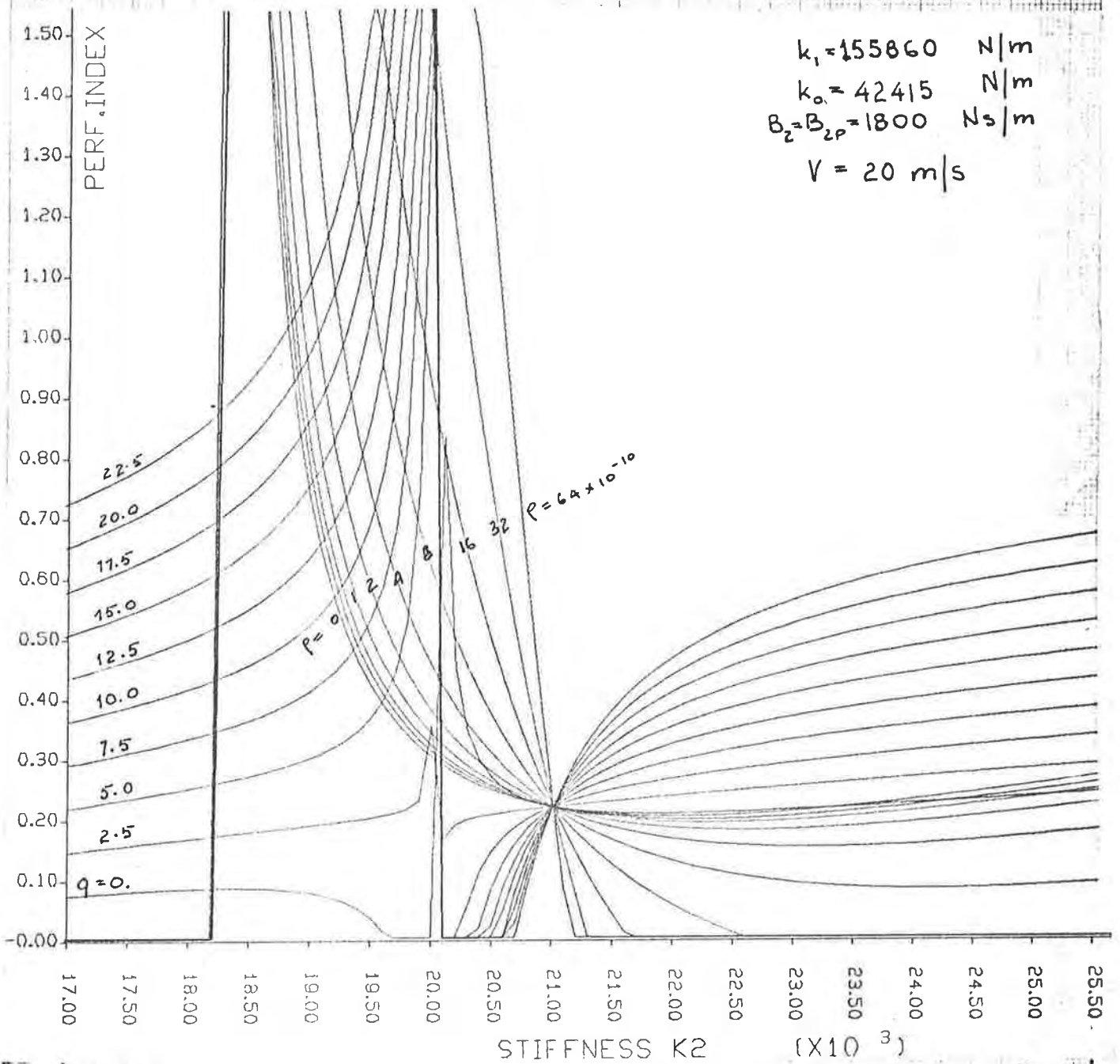




Fig. 9.28. Integral Square Value of Body Force
HILLMAN Model (Unladen)

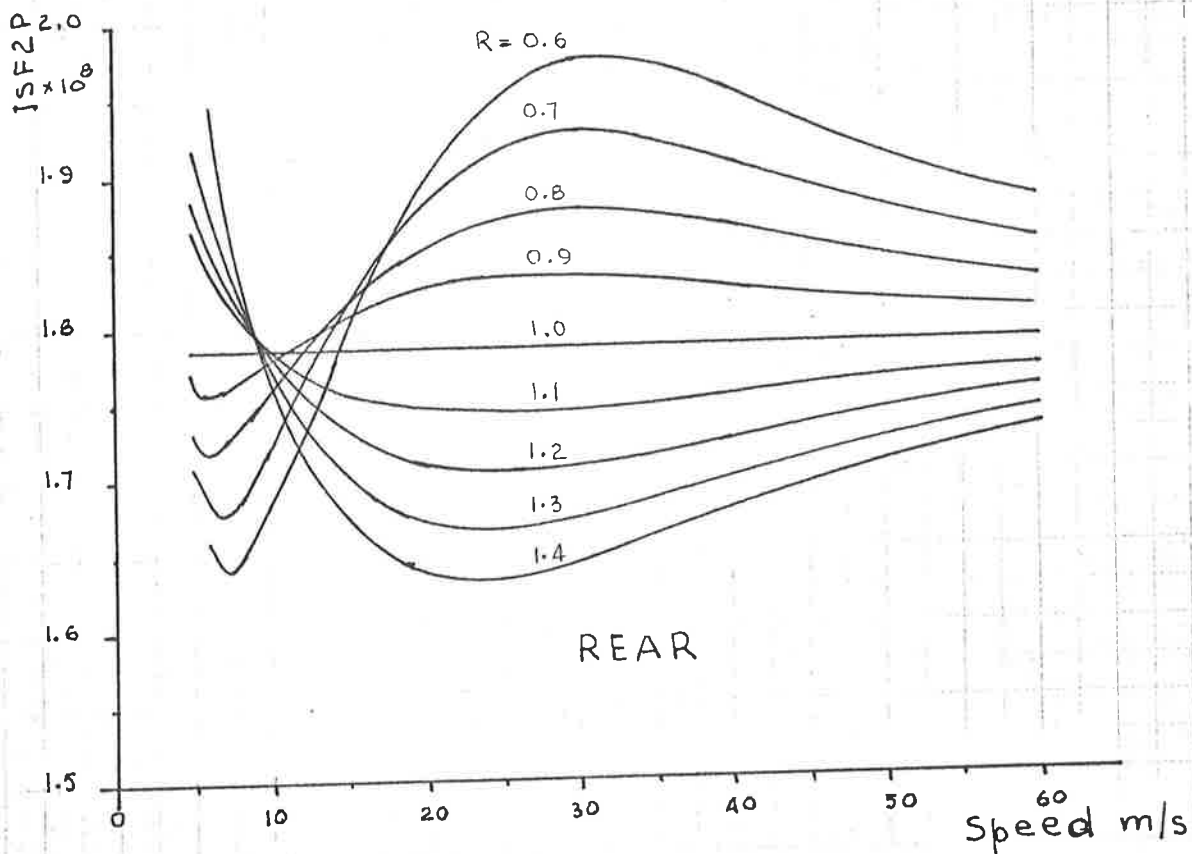
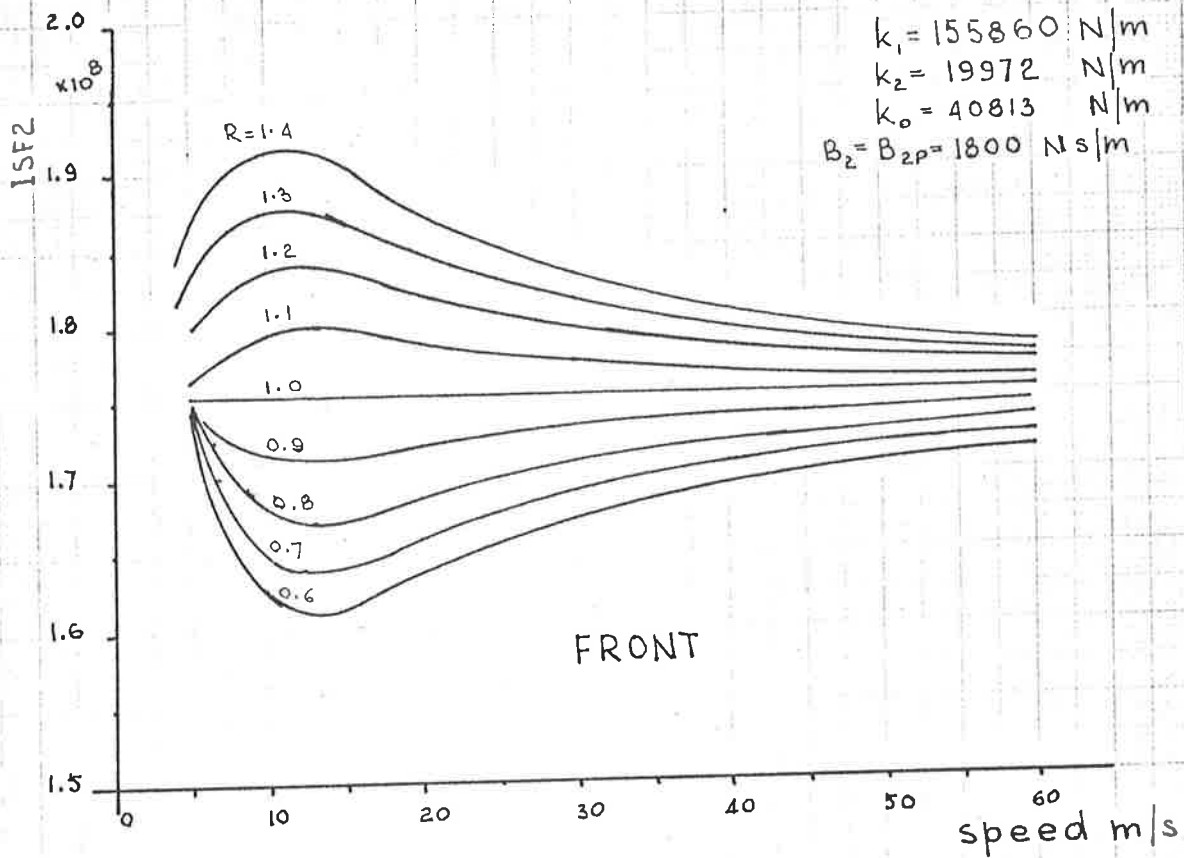




Fig. 9.29. Integral Square Value of Tyre Deflection
HILLMAN Model (Unladen).

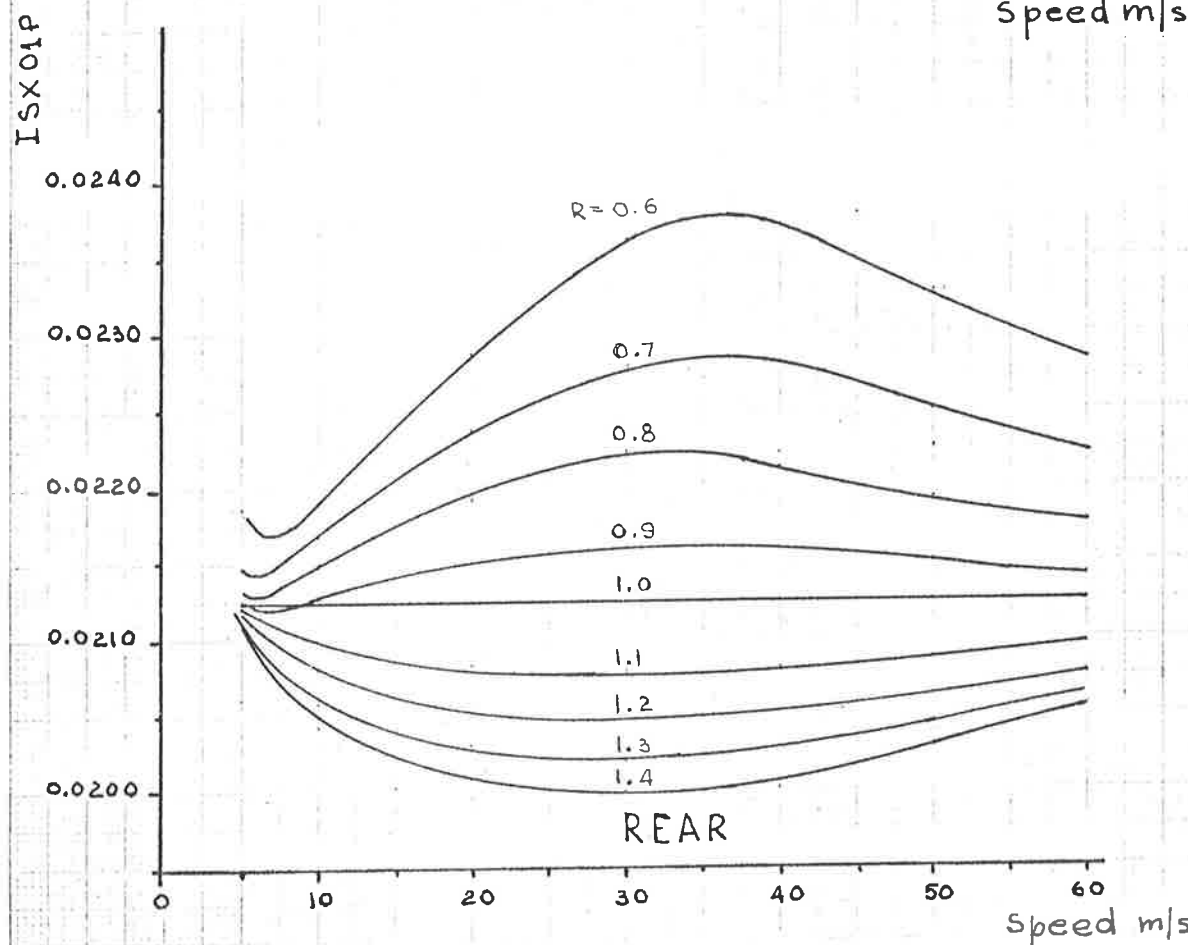
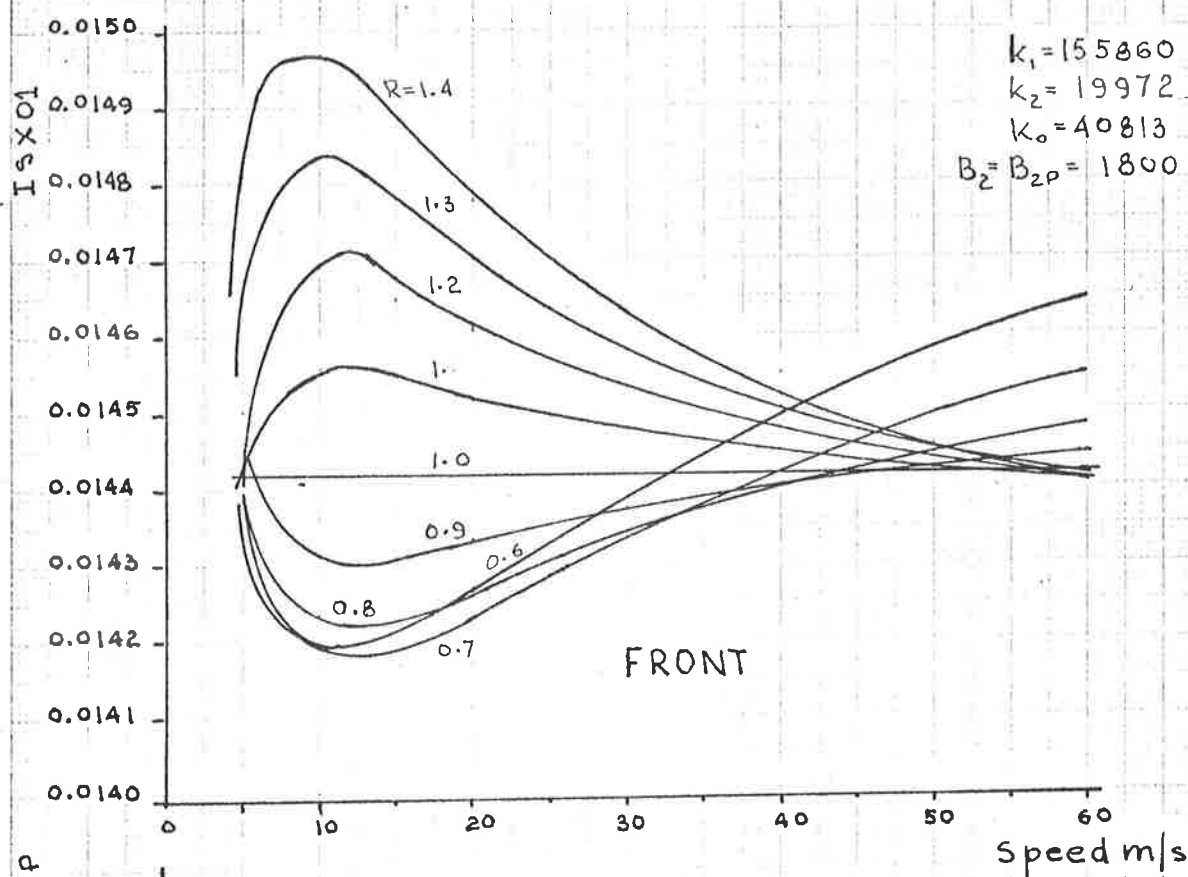




Fig. 9.30. Integral Square Value Wheel Travel
 HILLMAN (Unladen).

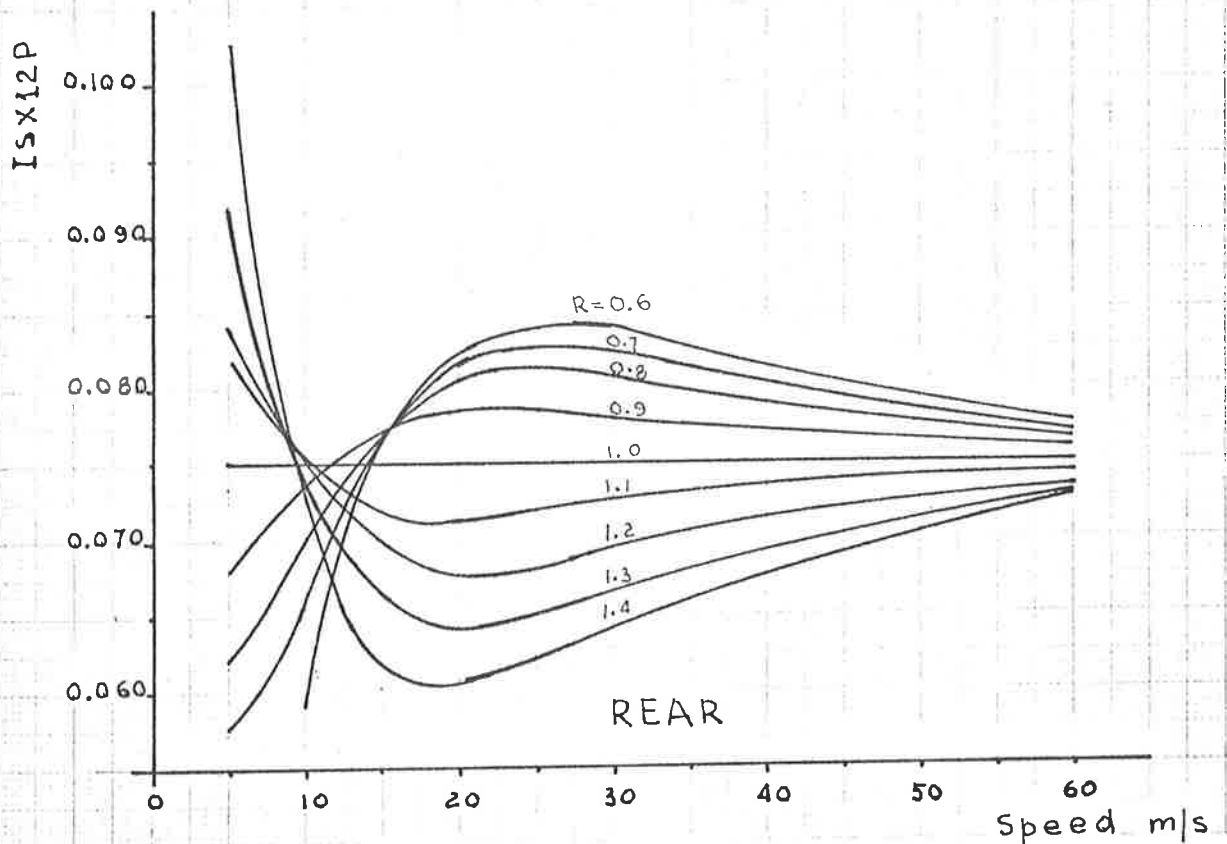
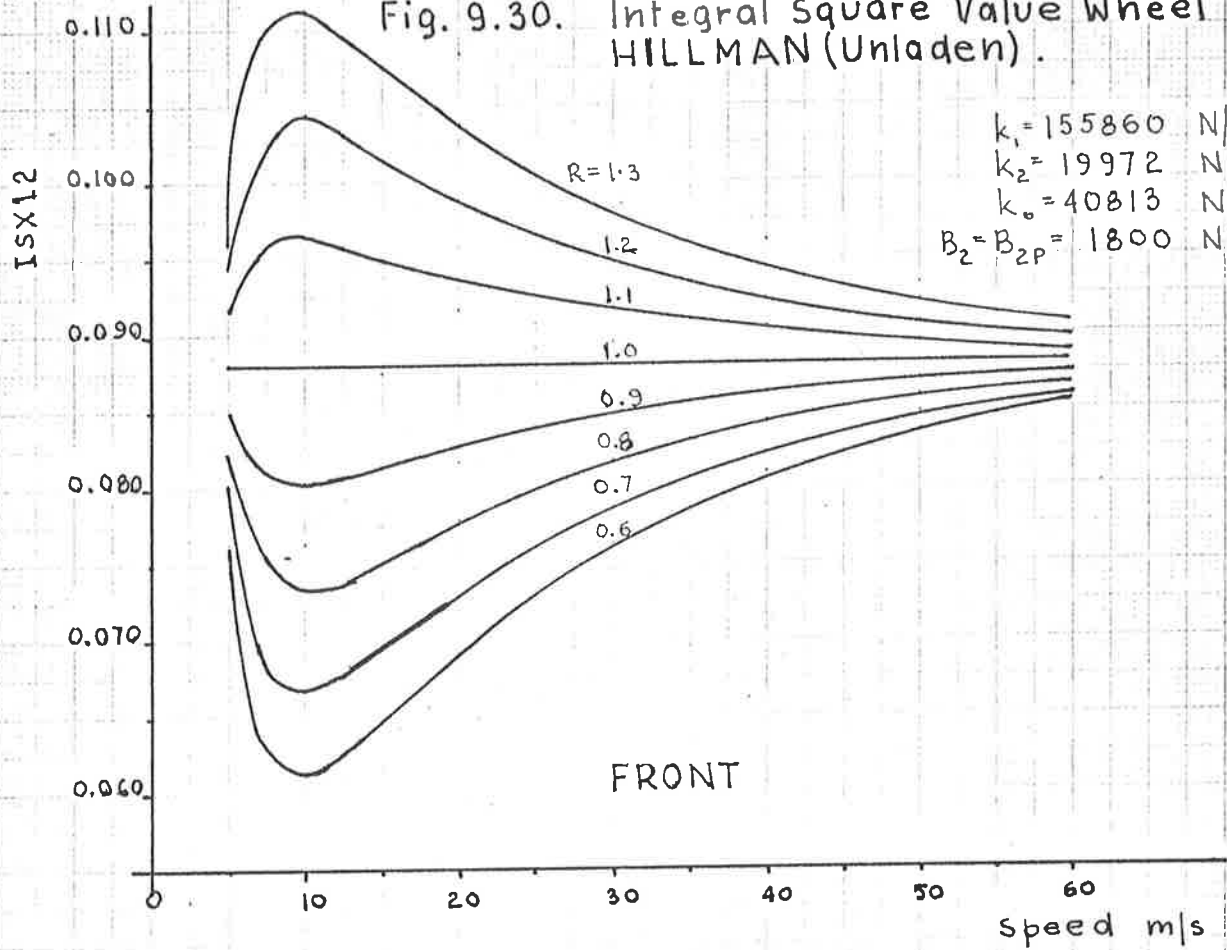




Fig. 9.31. Sum of Integral Square Body Force
HILLMAN Model.

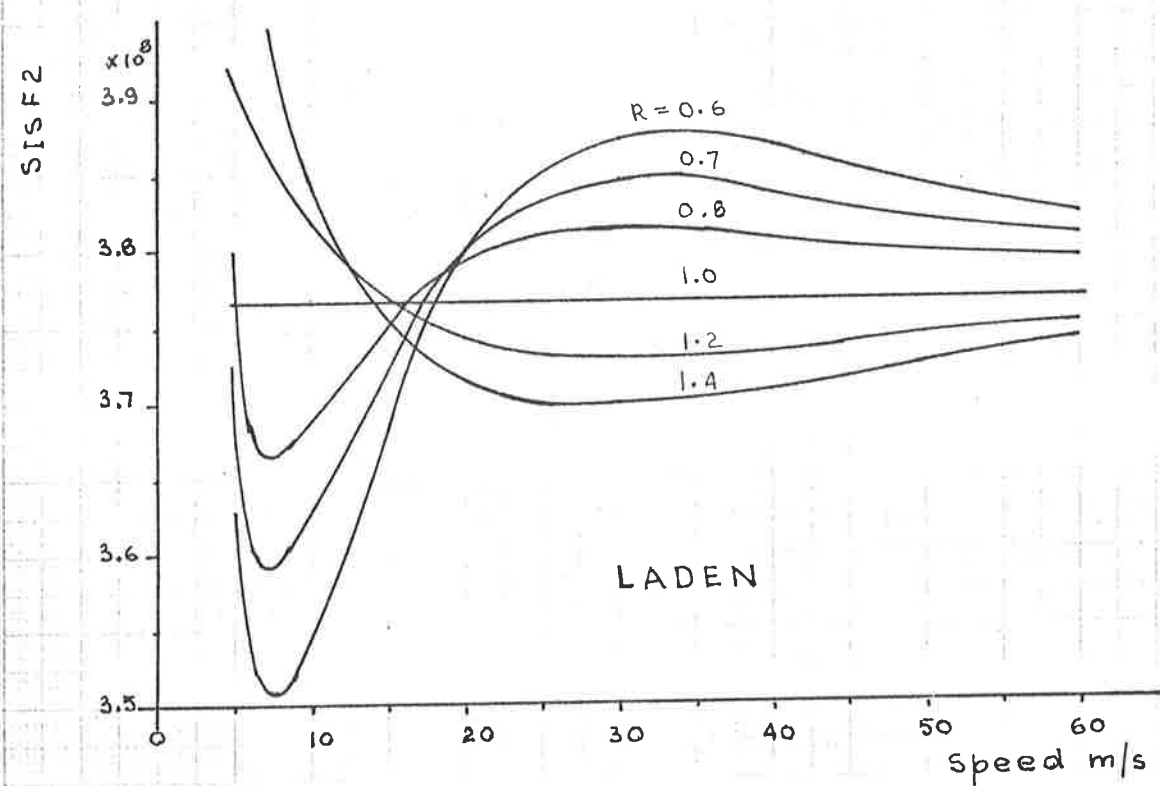
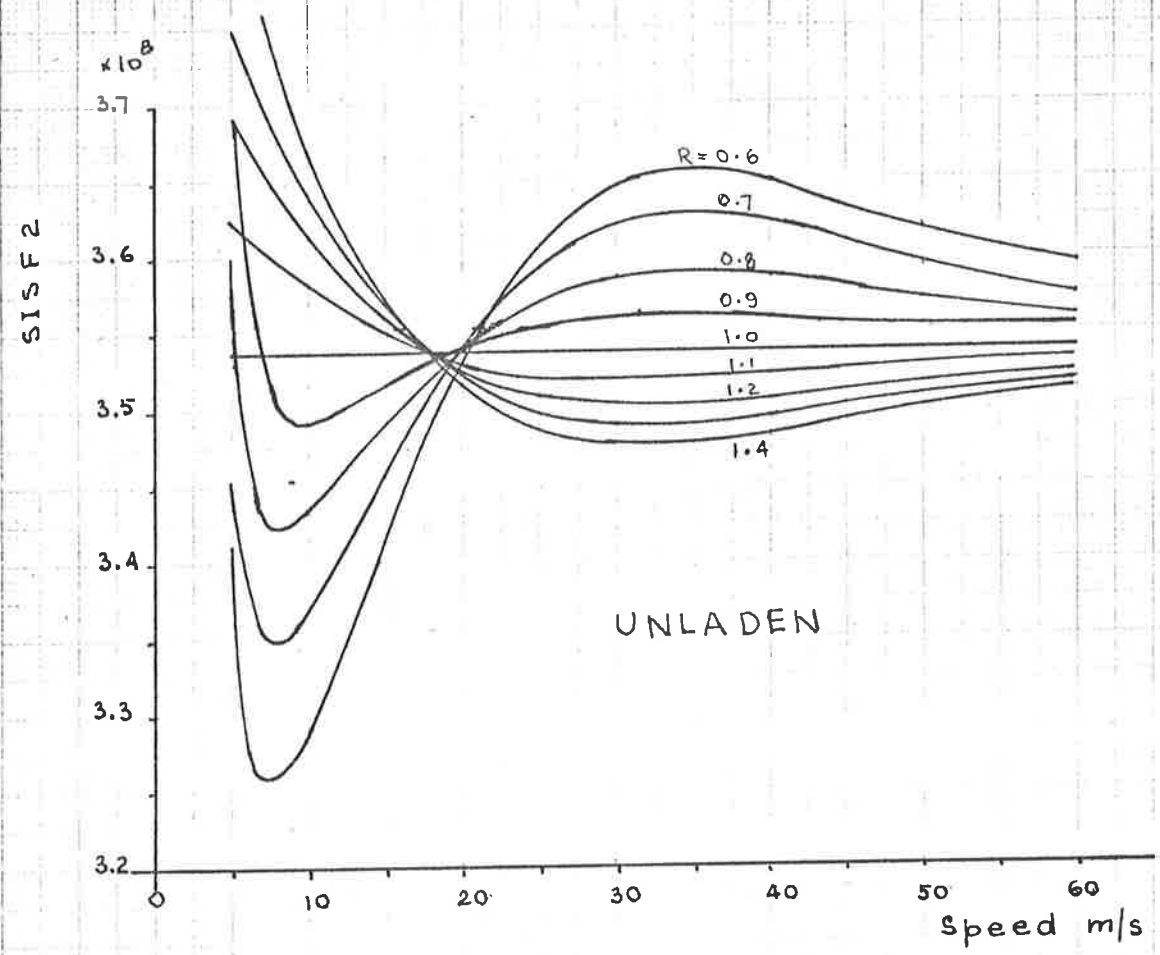




Fig. 9.32. Sum of Integral Square Tyre Deflection
 HILLMAN Model

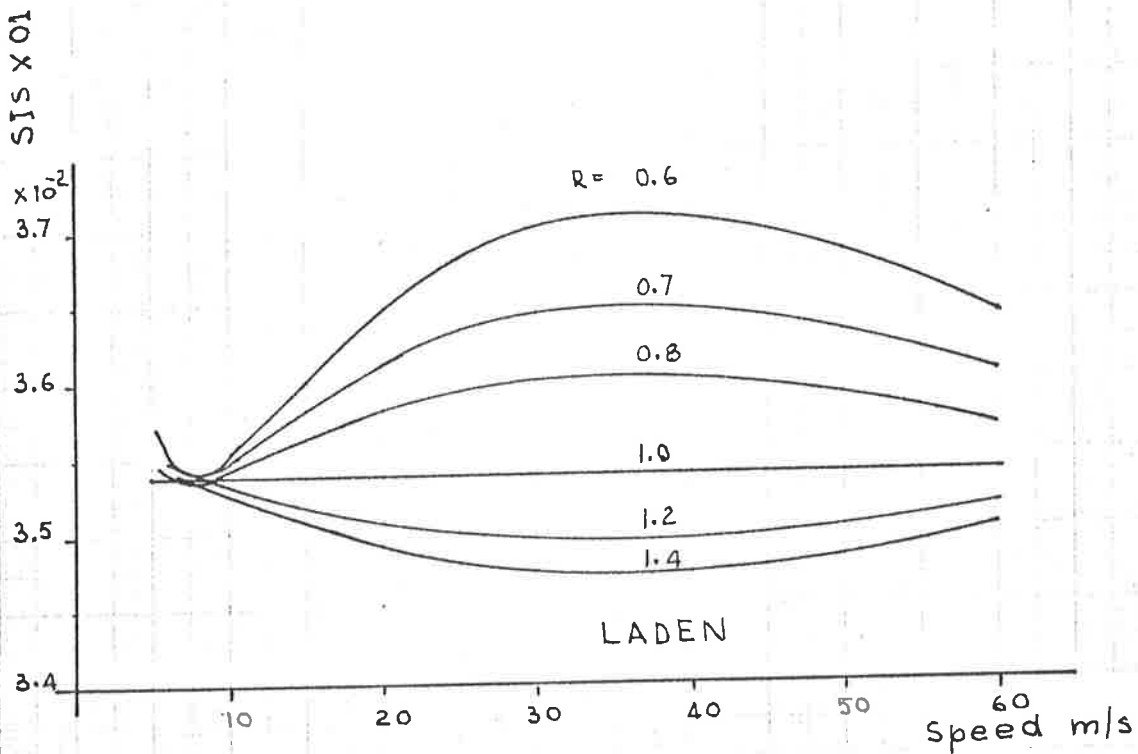
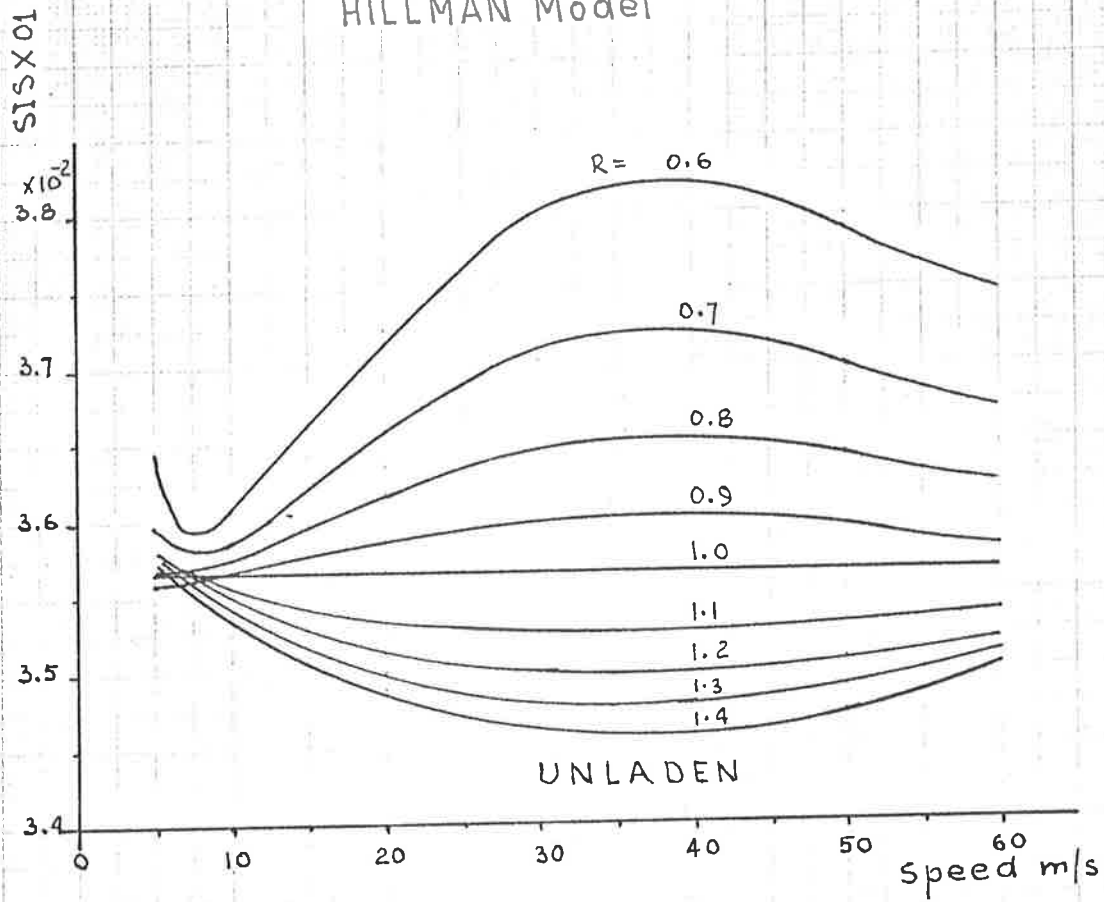




Fig. 9.33. Sum of Integral Square Wheel Travel
HILLMAN Model.

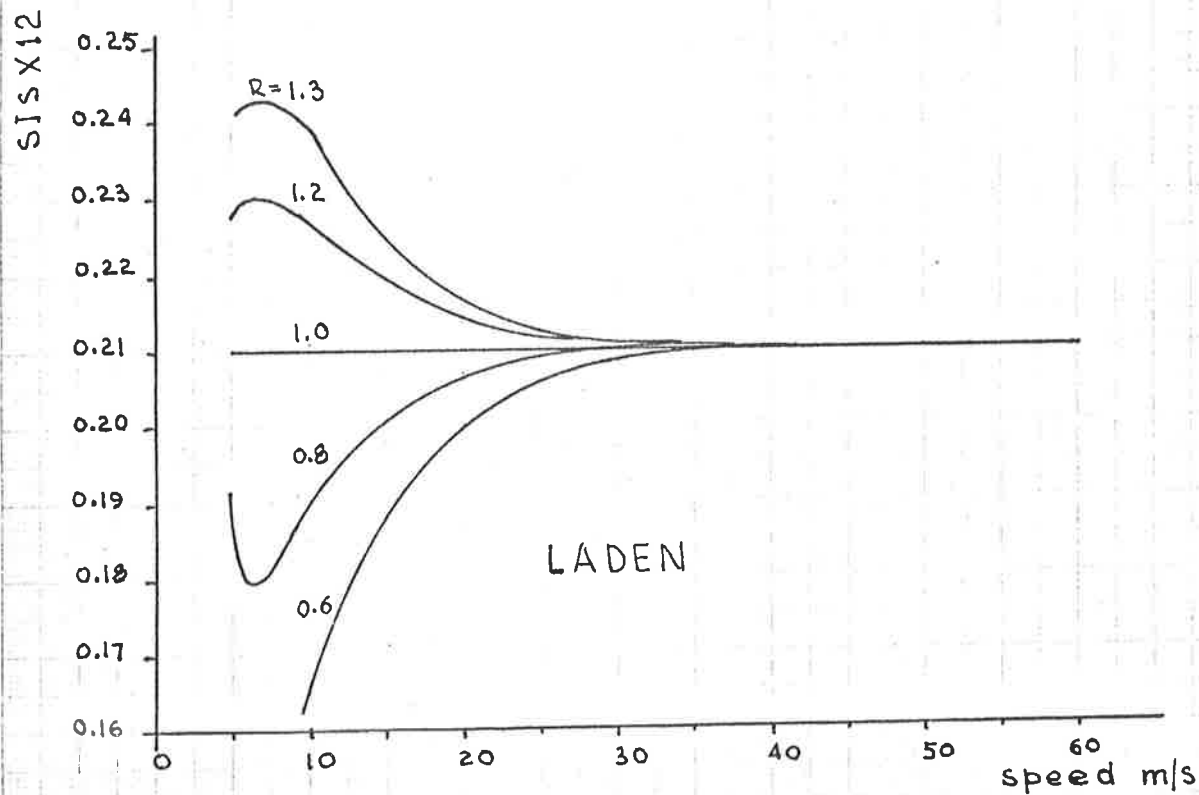
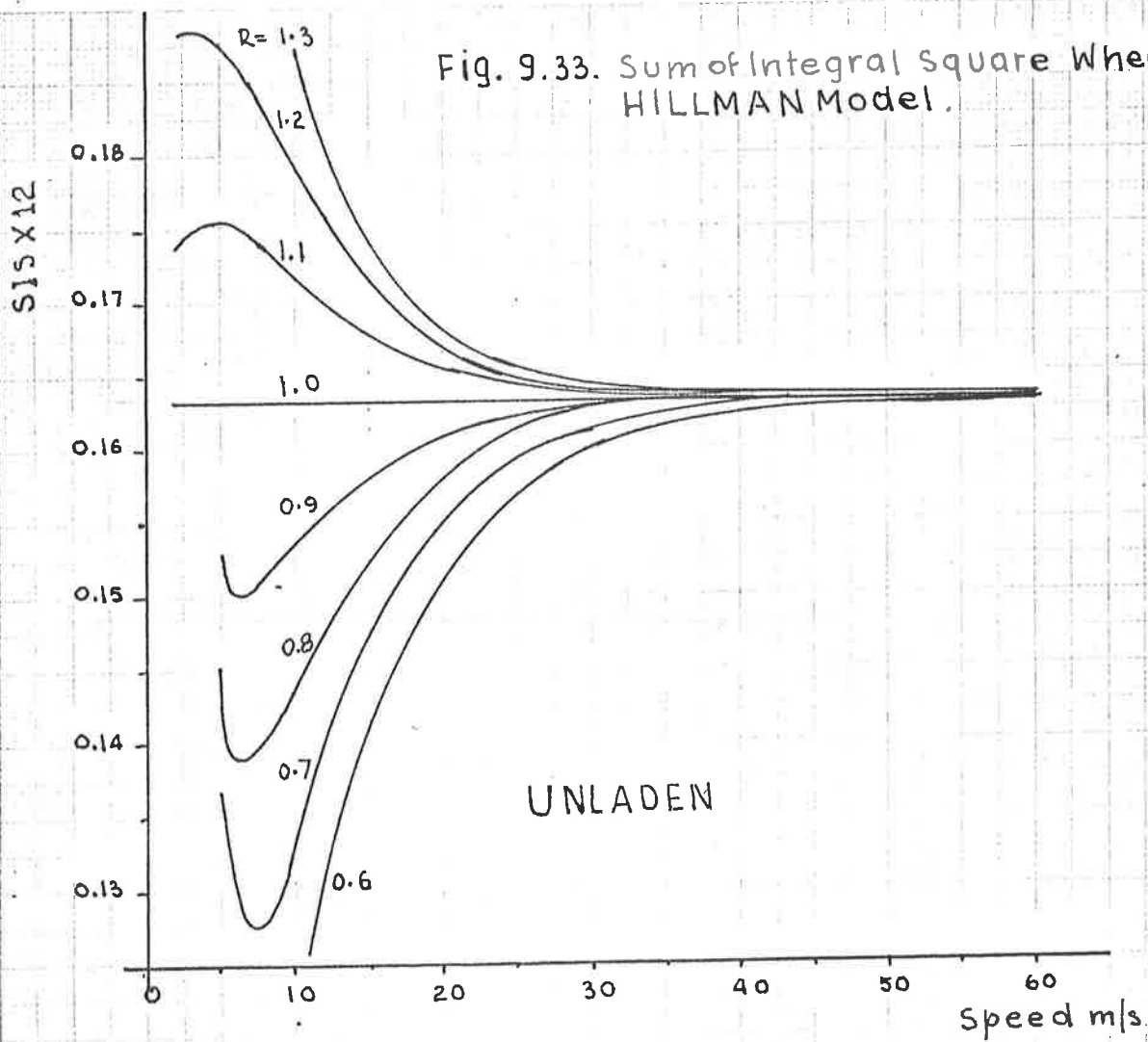
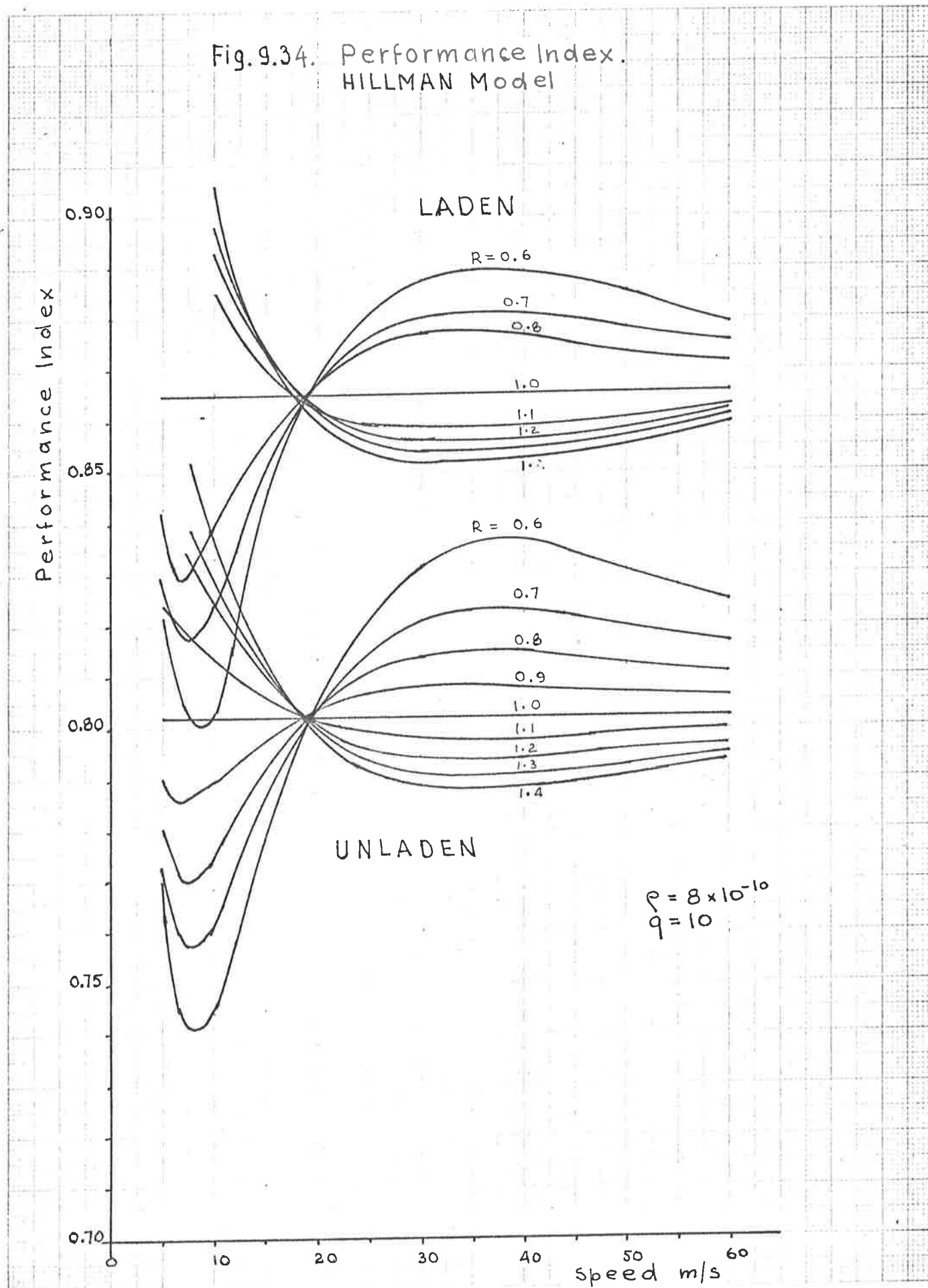




Fig. 9.34. Performance Index.
HILLMAN Model



10. STATE VARIABLES AND COVARIANCE MATRIX METHODS APPLIED TO CALCULATION OF INTEGRAL SQUARE VALUES

10.1 Introduction

The response calculations of vehicle models with a coupling ratio different from unity have been carried out by the use of ACSL digital simulation so far.

ACSL is a special language developed for digital simulation of dynamical systems, and as such is usually not available on general-purpose computing systems normally used in commerce and industry.

It would be an advantage, however, if the model response could be calculated using any of the more common computer languages such as FORTRAN, BASIC or PASCAL for which the compilers are more readily available.

The starting point in each case would be the algorithms based on state variables and processed in the computer by a series of matrix operations. Since BASIC is too limited and inflexible in its applications, and PASCAL is still a relatively new language, this leaves FORTRAN 4 or FORTRAN 5 as the obvious choice.

In Chapter 7 a closed form solution of integral square response was obtained in terms of model parameters for an uncoupled model ($R=1.0$) but owing to much greater complexity of a coupled system, this cannot be expected to be achieved for a model having a coupling ratio R differing from unity, hence only numerical solutions will be feasible.

10.2 State variable analysis of a half-car model

In the analysis that follows, a slightly different, less cumbersome nomenclature will be used, with symbols as under:-

| | |
|--------------------------------|-------------------------------|
| k_1 = front spring stiffness | k_3 = rear spring stiffness |
| c_1 = front damper rate | c_3 = rear damper rate |
| m_1 = front unsprung mass | m_3 = rear unsprung mass |
| k_a = front tyre stiffness | k_b = rear tyre stiffness |

m = total sprung mass

J = body mass moment of inertia

L = length of wheelbase

a = distance of front axle from body centre of mass

b = distance of rear axle from body centre of mass

Vertical and pitching motions are only considered, and body support point forces u_1 and u_3 are assumed to exist between the axles and the body at the front and rear, respectively. The model, shown in Fig. 10.1, has four degrees of freedom and eight state variables. Note that y_1 , y_2 , y_3 , y_4 and y_G represent vertical displacements from static equilibrium position with the vehicle on a level road.

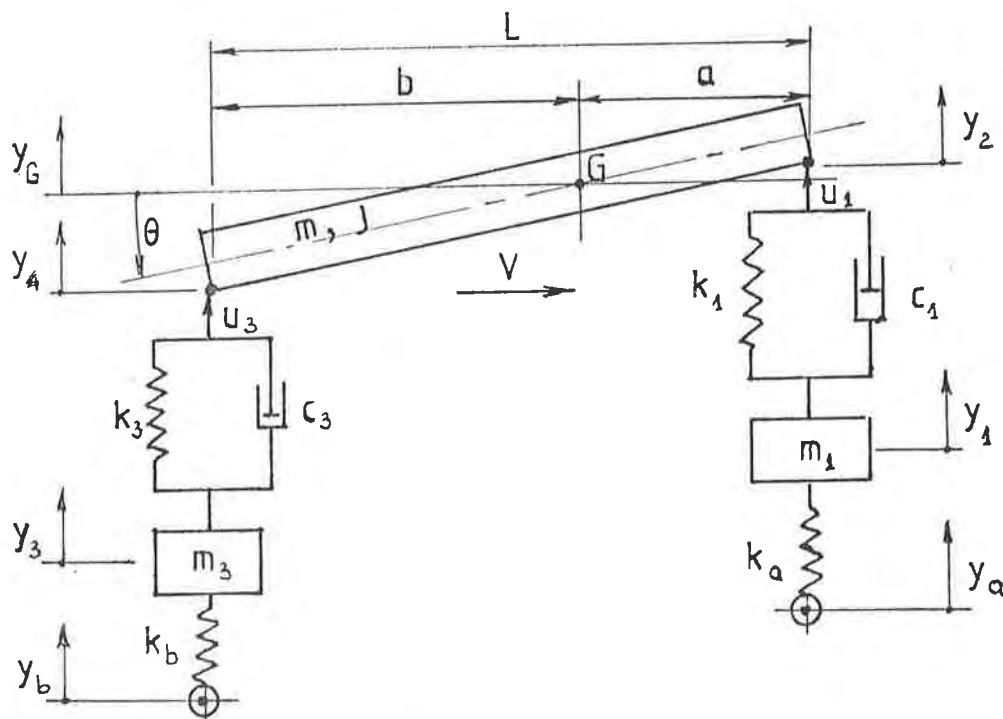


Fig. 10.1 - DYNAMIC VEHICLE MODEL

The equations of motion are:-

$$(y_a - y_1)k_a - u_1 = m_1 \ddot{y}_1 \quad (10.1)$$

$$(y_b - y_3)k_b - u_3 = m_3 \ddot{y}_3 \quad (10.2)$$

$$au_1 - bu_3 = J \ddot{\theta} \quad (10.3)$$

$$u_1 + u_2 = m \ddot{y}_G \quad (10.4)$$

where $\theta = (y_2 - y_4)/L$

$$\text{Also } y_2 = y_G + a\theta = y_G + a(y_2 - y_4)/L \quad (10.5)$$

$$\text{and } y_4 = y_G - b\theta = y_G - b(y_2 - y_4)/L \quad (10.6)$$

which give $y_G = (a y_4 + b y_2)/L$

with the substitutions as above, equations 10.3 and 10.4 can be expressed as

$$a u_1 - b u_3 = J(\ddot{y}_2 - \ddot{y}_4)/L = m r^2(\ddot{y}_2 - \ddot{y}_4)/L \quad (10.7)$$

$$\text{and } u_1 + u_3 = m(a \ddot{y}_4 + b \ddot{y}_2)/L \quad (10.8)$$

$$\text{where } u_1 = (y_1 - y_2)k_1 + (\dot{y}_1 - \dot{y}_2)c_1 \quad (10.9)$$

$$\text{and } u_3 = (y_3 - y_4)k_3 + (\dot{y}_3 - \dot{y}_4)c_3 \quad (10.10)$$

Define the state variables as follows:-

$$\begin{aligned} x_1 &= y_1 - y_a & x_5 &= \dot{y}_1 \\ x_2 &= y_2 - y_1 & x_6 &= \dot{y}_2 \\ x_3 &= y_3 - y_b & x_7 &= \dot{y}_3 \\ x_4 &= y_4 - y_3 & x_8 &= \dot{y}_4 \end{aligned}$$

$$\text{Since } a u_1 - b u_3 = m r^2 (\ddot{y}_2 - \ddot{y}_4)/L$$

$$\text{and } u_1 + u_3 = m(b \ddot{y}_2 + a \ddot{y}_4)/L$$

it follows that

$$\begin{aligned} \ddot{y}_2 = \dot{x}_6 &= u_1(1 + a^2/r^2)/m + u_3(1 - ab/r^2)/m \\ \text{and } \ddot{y}_4 = \dot{x}_8 &= u_1(1 - ab/r^2)/m + u_3(1 + b^2/r^2)/m \end{aligned}$$

$$\text{also } \ddot{y}_1 = \dot{x}_5 = -x_1 k_a/m_1 - u_1/m_1$$

$$\text{and } \ddot{y}_3 = \dot{x}_7 = -x_3 k_b/m_3 - u_3/m_3$$

The state equations may now be expressed in vector-matrix form as follows:-

$$\{\dot{x}\} = A_1 \{x\} + B_1 \{u\} + B \{w\} \quad (10.11)$$

where $\{w\} = [\dot{y}_a \ \dot{y}_b]^T$ denotes the input velocity disturbance vector due to random road profile.

The system matrix A_1 , and coefficient matrices B_1 and B are given by:

$$A_1 = \begin{bmatrix} 0 & 0 & 0 & 0 & 1 & 0 & 0 & 0 \\ 0 & 0 & 0 & 0 & -1 & 1 & 0 & 0 \\ 0 & 0 & 0 & 0 & 0 & 0 & 1 & 0 \\ 0 & 0 & 0 & 0 & 0 & 0 & -1 & 1 \\ -k_a/m_1 & 0 & 0 & 0 & 0 & 0 & 0 & 0 \\ 0 & 0 & 0 & 0 & 0 & 0 & 0 & 0 \\ 0 & 0 & -k_b/m_3 & 0 & 0 & 0 & 0 & 0 \\ 0 & 0 & 0 & 0 & 0 & 0 & 0 & 0 \end{bmatrix}$$

$$B = \begin{bmatrix} 0 & 0 \\ 0 & 0 \\ 0 & 0 \\ 0 & 0 \\ -1/m_1 & 0 \\ (1+a^2/r^2)/m & (1-ab/r^2)/m \\ 0 & -1/m_3 \\ (1-ab/r^2)/m & (1+b^2/r^2)/m \end{bmatrix} \quad B = \begin{bmatrix} -1 & 0 \\ 0 & 0 \\ 0 & -1 \\ 0 & 0 \\ 0 & 0 \\ 0 & 0 \\ 0 & 0 \\ 0 & 0 \end{bmatrix}$$

The disturbance inputs \dot{y}_a and \dot{y}_b are identical for the wheels following the same path, except \dot{y}_b is delayed by time interval $D = L/V$ with respect to \dot{y}_a .

Hence, the disturbance signals can be modelled by the equations

$$\begin{aligned} \dot{y}_a(t) &= v(t+D) \\ \text{and} \quad \dot{y}_b(t) &= v(t) \end{aligned}$$

where $v(t)$ is scalar white noise with intensity cV .

The disturbance vector can now be expressed as

$$\{w\} = \begin{bmatrix} v(t+D) \\ v(t) \end{bmatrix} = \begin{bmatrix} w_1 \\ w_3 \end{bmatrix}$$

The performance index π is defined as the weighted sum of mean square values, or

$$\begin{aligned} \pi = \lim_{T \rightarrow \infty} \frac{1}{T} E \left\{ \int_0^T [\rho_1 u_1^2 + \rho_3 u_3^2 + q_1 (y_1 - y_a)^2 + q_2 (y_2 - y_1)^2 \right. \\ \left. + q_3 (y_3 - y_b)^2 + q_4 (y_4 - y_3)^2] dt \right\} \end{aligned}$$

where ρ_1, ρ_2 and q_1 to q_4 are the weighting factors, and $E\{\cdot\}$ denotes the expectation.

The performance index can be expressed in terms of selected state variables as

$$\pi = \lim_{T \rightarrow \infty} \frac{1}{T} E \left\{ \int_0^T [u^T R_1 u + x^T Q x] dt \right\} \quad (10.12)$$

$$\text{where } R_1 = \begin{bmatrix} \rho_1 & 0 \\ 0 & \rho_3 \end{bmatrix}$$

$$\text{and } Q = \begin{bmatrix} q_1 & 0 & 0 & 0 & 0 & 0 & 0 & 0 \\ 0 & q_2 & 0 & 0 & 0 & 0 & 0 & 0 \\ 0 & 0 & q_3 & 0 & 0 & 0 & 0 & 0 \\ 0 & 0 & 0 & q_4 & 0 & 0 & 0 & 0 \\ 0 & 0 & 0 & 0 & 0 & 0 & 0 & 0 \\ 0 & 0 & 0 & 0 & 0 & 0 & 0 & 0 \\ 0 & 0 & 0 & 0 & 0 & 0 & 0 & 0 \\ 0 & 0 & 0 & 0 & 0 & 0 & 0 & 0 \end{bmatrix}$$

Since the performance index is an average value taken over an infinite time period, it is independent of the initial state of the system. To simplify calculations, the assumption will be made that the initial state is zero.

As the white noise disturbance w_1 and w_3 originate from the same source, and have zero means, the covariance matrix of the disturbance vector according to (63) is

$$W(t_1, t_2) = E \{ w(t_1) \ w(t_2) \}$$

$$= \begin{bmatrix} E \{ w_1(t_1) \ w_1(t_2) \} & E \{ w_1(t_1) \ w_3(t_2) \} \\ E \{ w_3(t_1) \ w_1(t_2) \} & E \{ w_3(t_1) \ w_3(t_2) \} \end{bmatrix}$$

$$= cV \begin{bmatrix} \delta(t_1-t_2) & \delta(t_1-t_2+D) \\ \delta(t_1-t_2-D) & \delta(t_1-t_2) \end{bmatrix} \quad (10.13)$$

$$\text{or } W(t_1, t_2) = cV \begin{bmatrix} 1 & 0 \\ 0 & 1 \end{bmatrix} \delta(t_1-t_2) + cV \begin{bmatrix} 0 & 1 \\ 0 & 0 \end{bmatrix} \delta(t_1-t_2+D) + cV \begin{bmatrix} 0 & 0 \\ 1 & 0 \end{bmatrix} \delta(t_1-t_2-D) \quad (10.14)$$

where δ denotes DIRAC δ -function, and D denotes the time delay L/V . The body forces u_1 and u_3 were given by equations 10.9 and 10.10 as

$$\begin{aligned} u_1 &= (y_1 - y_2)k_1 + (\dot{y}_1 - \dot{y}_2)c_1 \\ \text{and } u_3 &= (y_3 - y_4)k_3 + (\dot{y}_3 - \dot{y}_4)c_3 \end{aligned}$$

which can be expressed in matrix form in terms of state variables as

$$\{u\} = F^T \{x\}$$

$$\text{where } F^T = \begin{bmatrix} 0 & -k_1 & 0 & 0 & c_1 & -c_1 & 0 & 0 \\ 0 & 0 & 0 & -k_3 & 0 & 0 & c_3 & -c_3 \end{bmatrix}$$

The performance index (Eq. 10.12) can now be written as

$$\begin{aligned} \pi &= \lim_{T \rightarrow \infty} \frac{1}{T} E \left\{ \int_0^T [x^T F R_1 F^T x + x^T Q x^T] dt \right\} \\ &= \lim_{T \rightarrow \infty} \frac{1}{T} E \left\{ \int_0^T [x^T (F R_1 F^T + Q) x] dt \right\} \quad (10.15) \\ &= \lim_{T \rightarrow \infty} \frac{1}{T} E \left\{ \int_0^T [x^T R x] dt \right\} \end{aligned}$$

$$\text{where } R = F R_1 F^T + Q$$

and the system can be described in terms of system matrix equation as

$$\{\dot{x}(t)\} = A\{x(t)\} + B\{w(t)\} \quad (10.16)$$

$$\text{where } A = A_1 + B_1 F^T$$

The matrix equation 10.16 has the solution

$$x(t) = \Phi(t) x(0) + \int_0^t \Phi(t, \tau) B(\tau) w(\tau) d\tau \quad (10.17)$$

where $\Phi(t, \tau)$ is the state transition matrix.

Since $x(0) = 0$ by a previous statement regarding the initial state, and B is a constant matrix, equation 10.16 can be written as

$$x(t) = \int_0^t \Phi(t, \tau) B w(\tau) d\tau \quad (10.18)$$

Hence,

$$x^T(t) R x(t) = \int_0^t w^T(\tau) B^T \Phi^T(t, \tau) d\tau R \int_0^t \Phi(t, \tau') B w(\tau') d\tau' \quad (10.19)$$

$$= \int_0^t d\tau \int_0^t \text{tr} [w(\tau') w^T(\tau) B^T \Phi^T(t, \tau) R \Phi(t, \tau') B] d\tau' \quad (10.20)$$

Equation 10.20 is based on the theorem that if x and y are vectors, and M is a matrix, then

$$x^T M y = \text{tr}(y x^T M)$$

Integrating and taking the expectation of both sides of eq. 10.20, the result is

$$\begin{aligned}
E \left\{ \int_0^T x^T(t) R x(t) dt \right\} &= \\
&= \int_0^T dt \int_0^t d\tau \int_0^t \text{tr} \left[E \{ w(\tau') w^T(\tau) \} B^T \Phi^T(t, \tau) R \Phi(t, \tau') B \right] d\tau' \\
&= \text{tr} \left[\int_0^T dt \int_0^t d\tau \int_0^t B w(\tau') B^T \Phi^T(t, \tau) R \Phi(t, \tau') d\tau' \right] \quad (10.21)
\end{aligned}$$

Equation 10.20 is based on the fact that if M and N are compatible matrices then

$$\text{tr} [MN] = \text{tr} [NM]$$

For further development it is advantageous to partition the 8×2 matrix B into two column vectors b_1 and b_2 , i.e. $B = [b_1 \mid b_2]$ as in ref. 69, and to express the covariance matrix of the disturbing vector as in eq. 10.14, i.e.

$$W(\tau', \tau) = cV \left\{ \begin{bmatrix} 1 & 0 \\ 0 & 1 \end{bmatrix} \delta(\tau' - \tau) + \begin{bmatrix} 0 & 1 \\ 0 & 0 \end{bmatrix} \delta(\tau' - \tau + D) + \begin{bmatrix} 0 & 0 \\ 1 & 0 \end{bmatrix} \delta(\tau' - \tau - D) \right\}$$

Hence,

$$\begin{aligned}
B w(\tau', \tau) B^T &= \\
&= cV \left[B B^T \delta(\tau' - \tau) + b_1 b_2^T \delta(\tau' - \tau + D) + b_2 b_1^T \delta(\tau' - \tau - D) \right] \quad (10.22)
\end{aligned}$$

On substituting the right hand side of equation 10.22 into equation 10.21, the result is

$$\begin{aligned}
E \left\{ \int_0^T x^T R x dt \right\} &= \\
&= cV \text{tr} \left[B B^T \int_0^T dt \int_0^t d\tau \int_0^t \delta(\tau' - \tau) \Phi^T(t, \tau) R \Phi(t, \tau') d\tau' \right. \\
&+ b_1 b_2^T \int_0^T dt \int_0^t d\tau \int_0^t b_1 b_2^T \delta(\tau' - \tau + D) \Phi^T(t, \tau) R \Phi(t, \tau') d\tau' \\
&+ b_2 b_1^T \int_0^T dt \int_0^t d\tau \int_0^t b_2 b_1^T \delta(\tau' - \tau - D) \Phi^T(t, \tau) R \Phi(t, \tau') d\tau' \left. \right] \quad (10.23)
\end{aligned}$$

Ref. 69 shows that the integrals of equ. 10.23 can be developed as

$$\begin{aligned}
E \left\{ \int_0^T [x^T R x] dt \right\} &= \\
&= cV \text{tr} \left[B B^T \int_0^T dt \int_{\tau}^T \Phi^T(t, \tau) R \Phi(t, \tau) d\tau \right. \\
&+ b_1 b_2^T \int_D^T dt \int_{\tau}^T \Phi^T(t, \tau) R \Phi(t, \tau - D) d\tau \\
&+ b_2 b_1^T \int_0^{T-D} dt \int_{\tau+D}^T \Phi^T(t, \tau) R \Phi(t, \tau + D) d\tau \left. \right] \quad (10.24)
\end{aligned}$$

From the properties of state transition matrix it follows that

$$\Phi(t, \tau-D) = \Phi(t, \tau) \Phi(\tau, \tau-D)$$

and
$$\Phi(t, \tau+D) = \Phi(t, \tau) \Phi(\tau, \tau+D)$$

With these substitutions equation 10.24 becomes

$$\begin{aligned} E\left\{ \int_0^T [x^T R x] dt \right. &= \\ &= cV \operatorname{tr} \left[\int_0^T B B^T P(t) dt + \int_D^T b_1 b_2^T P(t) \Phi(t, \tau-D) dt \right. \\ &\quad \left. \left. + \int_0^{T-D} b_2 b_1^T \Phi(t+D, t) P(t+D) dt \right] \right. \end{aligned} \quad (10.25)$$

where $P(t)$ represents the symmetric matrix function

$$P(t) = \int_t^T \Phi^T(\tau, t) R \Phi(\tau, t) d\tau \quad (10.26)$$

It may be shown by differentiation (66) that $P(t)$ satisfies the matrix differential equation

$$-\dot{P}(t) = A^T P(t) + P(t) A + R \quad (10.27)$$

For a linear time-invariant system $P(t)$ approaches the constant steady state value \bar{P} as T tends to infinity (Ref. 66), and $\dot{P}(t) \rightarrow 0$.

Eq. 10.27 can now be written as

$$0 = A^T \bar{P} + \bar{P} A + R \quad (10.28)$$

which is the familiar LYAPUNOV equation.

Equ. 10.28 can be solved for \bar{P} which is an 8×8 symmetric matrix, thus involving 36 simultaneous equations. Evidently, only a numerical solution by computer is thus feasible.

For a time-invariant system

$$\Phi(t_1, t_2) = \exp[A(t_1 - t_2)]$$

Hence
$$\Phi(t, t-D) = \Phi(t+D, t) = e^{AD} \quad (10.29)$$

and the performance index can be expressed as

$$\begin{aligned}
 &= \lim_{T \rightarrow \infty} \frac{1}{T} E \left\{ \int_0^T [x^T(t) R x(t)] dt \right\} \\
 &= \lim_{T \rightarrow \infty} \frac{1}{T} cV \operatorname{tr} \left[\int_0^T B B^T \bar{P} dt + b_1 b_2^T \bar{P} \int_D^T \Phi(t, t-D) dt \right. \\
 &\quad \left. + b_2 b_1^T \bar{P} \int_0^{T-D} \Phi^T(t+D, t) dt \right]
 \end{aligned}$$

$$\text{or } \pi = cV \operatorname{tr} [B B^T \bar{P} + b_1 b_2^T \bar{P} e^{AD} + b_2 b_1^T \bar{P} (e^{AD})^T] \quad (10.30)$$

Since b_1 , b_2^T , $b_2 b_1^T$, \bar{P} and $\exp(AD)$ are square matrices, eq. 10.29 can be expressed in the final form as

$$\pi = cV \operatorname{tr} [B B^T + 2 e^{AD} b_1 b_2^T \bar{P}] \quad (10.31)$$

Program INDEX in FORTRAN 5 (Appendix C) was developed to calculate performance indices by state variables and matrix operations as outlined in this chapter.

The program is fairly long, and comprises the subroutines CFCHEN, MATPR, ELIMIN, TRANS, all shown in Appendix C.

The results obtained with this program fully agree with those obtained by ACSL digital simulation, and are listed in Table 10.1 for comparison.

The data used was that corresponding to unladen HILLMAN model having a coupling ratio $R=0.7$.

TABLE 10.1

COMPARISON OF CALCULATED PERFORMANCE INDICES.

HILLMAN Model (UNLADEN), $R=0.7$.

| Vehicle speed m/s | Performance Index | | | | |
|--------------------------------------|-------------------|-----------|-----------|-----------|-----------|
| | 10 | 20 | 30 | 40 | 50 |
| ACSL Simulation | 0.7604842 | 0.8049339 | 0.8215359 | 0.8239172 | 0.8204587 |
| Program INDEX (Covariance Matrix) | 0.76046 | 0.80487 | 0.82161 | 0.82389 | 0.82049 |

The overall computing cost by matrix methods is approximately twice that of ACSL simulation for the same amount of end results. The main cost areas seem to be the setting up and solving the LYAPUNOV equation, also developing the solution for $\exp(AD)$ in the form of a series.

ACSL digital simulation language, on the whole is much more versatile since it also provides the complete time response of the model in addition to mean square values.

11. ANALOGUE COMPUTER SIMULATION

11.1 Introduction

The electronic analogue computer is well known for its versatility, in simulations relating to all types of dynamical systems, and it was used for that purpose almost exclusively before the development of digital simulation languages.

The outstanding feature of the analogue computer is the extreme flexibility associated with the setting of the model parameter values during the simulation process and direct interaction between the machine and the operator so that possible trends in the behaviour of the model are immediately noticed.

However, the analogue computer has its shortcomings also, characteristic to its principle of operation.

Since the signal-to-noise ratio has an economically achievable limit in any electronic device, the accuracy of the analogue machine depends on the quality of components used in its manufacture. In any case, the signal-to-noise ratio is finite, hence the accuracy and repeatability of an analogue machine cannot parallel that of a digital computer.

In direct simulation an accuracy of the order of 0.5% to 1% is typical, but can be considerably worse depending on the type and number of operations in sequence. In order to reduce the percentage error in simulation to as low a value as possible, it is necessary to operate the machine at signal levels approaching the output voltage limit of the machine, hence the magnitude scaling becomes a necessity.

The scaling process is somewhat cumbersome, and not always a straightforward process since the maximum values of model response must be known in advance. In most simulation problems the maximum values of response can only be estimated approximately, and this uncertainty can become embarrassing when suddenly one or more amplifiers will overload during simulation, indicating that the required analogue signal levels exceed the voltage limit of the machine.

The only remedy then is to rescale the whole problem which can be quite tedious, moreover there are no guarantees that it will not happen again if different parameters are varied. Hence interruptions in simulation process are to be expected.

Time scaling is also necessary if the time response of the physical system approaches that of the machine or if the output is to be recorded on a low-speed plotting device such as an X-Y chart recorder.

The problems associated with scaling do not arise in digital simulation since a magnitude does not have to be represented by a voltage, hence the growing popularity of digital simulation. Also the accuracy and repeatability will far exceed the capabilities of any analogue machine.

But the digital simulation process is not as flexible as the analogue simulation since for each model parameter change a new run of calculations would be required with a new set of data cards, also the actual user of the results is somewhat remote from the process, and the direct link of observation as the simulation proceeds is lost.

The analogue machine used to simulate the dynamical behaviour of $\frac{1}{2}$ car model in connection with this thesis was the model EAI-580 Analogue Computer at the School of Electrical Engineering, S.A. Institute of Technology, Levels Campus. The photograph of the computer is shown in Fig. 11.1

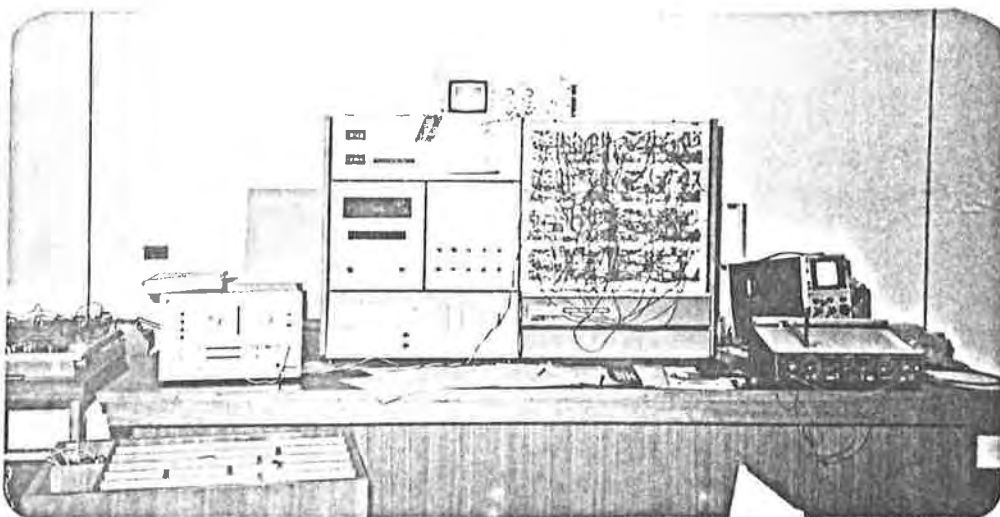


FIG. 11.1 - EAI-580 ANALOGUE COMPUTER

The basic features of the machine are outlined in the operating manual, and will not be discussed here.

The computer has been used for similar simulation studies quite extensively on previous occasions as outlined in references (50) and (70).

11.2 Mathematical Model and Parameter Values

The half-car model shown in Fig. 11.2 was used in analogue computer simulation. The input to the model was a unit step applied to the front wheels at time $t=0$, and a delayed step applied to the rear wheels at time $t=L/V$.

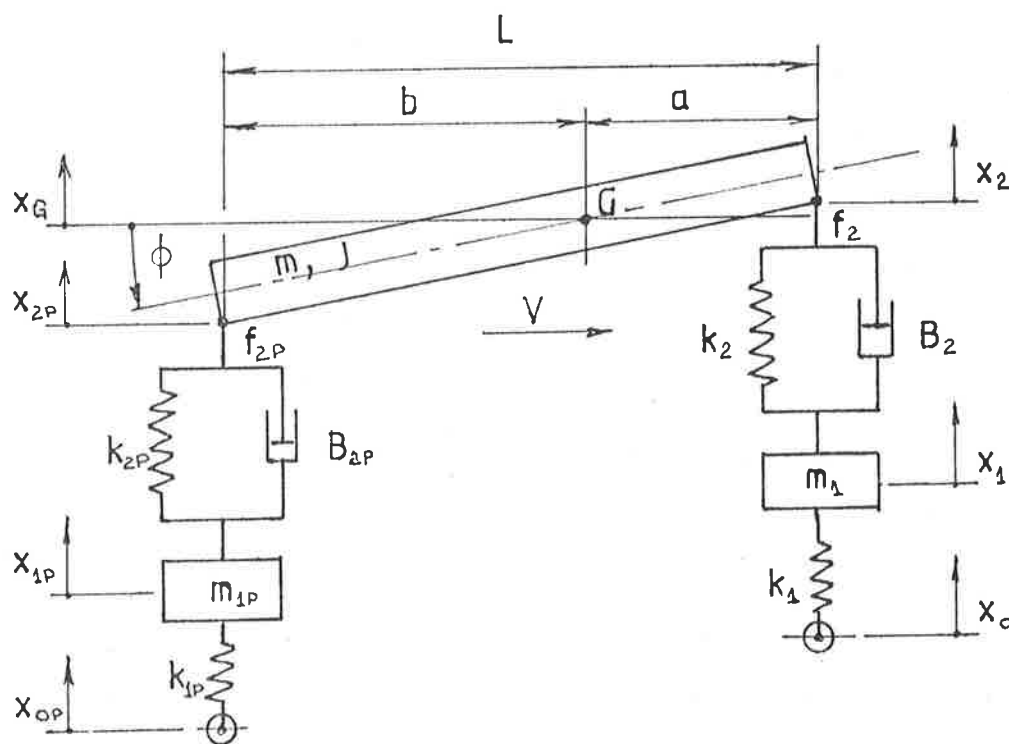


FIG. 11.2 - $\frac{1}{2}$ -CAR MODEL

The equations of motion for the model can be expressed as follows:-

$$f_2 = (x_1 - x_2)k_2 + (\dot{x}_1 - \dot{x}_2)B_2 \quad (11.1)$$

$$f_{2P} = (x_{1P} - x_{2P})k_{2P} + (\dot{x}_{1P} - \dot{x}_{2P})B_{2P} \quad (11.2)$$

$$\ddot{x}_1 = -f_2/m_1 + (x_0 - x_1)k_1/m_1 \quad (11.3)$$

$$\ddot{x}_{1P} = -f_{2P}/m_{1P} + (x_{0P} - x_{1P})k_{1P}/m_{1P} \quad (11.4)$$

$$\ddot{x}_G = (f_2 + f_{2P})/m \quad (11.5)$$

$$\dot{\phi} = (a f_2 - b f_{2P})/J \quad (11.6)$$

Additional relationships are:-

$$x_2 = x_G + a\phi \quad (11.7)$$

$$\dot{x}_2 = \dot{x}_G + a\dot{\phi} \quad (11.8)$$

$$x_{2P} = x_G - b\phi \quad (11.9)$$

$$\dot{x}_{2P} = \dot{x}_G - b\dot{\phi} \quad (11.10)$$

The simulation was based on HILLMAN model with the following initial parameter values:-

| | | | |
|----------|------------------------|-----|-----------------------------|
| m | $= 505.08 \text{ kg}$ | a | $= 1.098 \text{ m}$ |
| m_1 | $= 28.58 \text{ kg}$ | b | $= 1.467 \text{ m}$ |
| m_{1P} | $= 54.43 \text{ kg}$ | L | $= 2.565 \text{ m}$ |
| k_2 | $= 19972 \text{ N/m}$ | R | $= 0.7$ |
| k_0 | $= 40813 \text{ N/m}$ | J | $= 813.75 \text{ R kg m}^2$ |
| k_1 | $= 155860 \text{ N/m}$ | | $= 569.63 \text{ kg m}^2$ |
| k_{1P} | $= 155860 \text{ N/m}$ | | |
| B_2 | $= 1800 \text{ Ns/m}$ | | |
| B_{2P} | $= 1800 \text{ Ns/m}$ | | |

11.3 Scaling, Machine Equations and Patching

Since the maximum output of the machine is one machine unit (10V), and the maximum physical quantity x_{\max} must be represented by a corresponding machine quantity $[X]_{\max}$ less than or equal to one m.u., the scale factor can be expressed simply as:-

Scale factor = Max. physical quantity/1m.u.

$$\text{or S.F.} = x_{\max}/[X]_{\max} = x_{\max}/1\text{m.u.}$$

Now the magnitude of the physical quantity x is given by

$$x = \text{S.F.}[X]$$

where $[X]$ is the corresponding machine quantity in m.u.

Thus it is necessary to estimate the expected maximum values in proposed simulation, and then to rewrite the equations of motion in terms of machine quantities before the problem can be patched on the computer.

The following scaling relationships were found to be suitable for the model:-

$$f_2 = 90000[F_2]$$

$$f_{2P} = 90000[F_{2P}]$$

$$\ddot{x}_G = 360[\ddot{X}_G]$$

$$\dot{x}_G = 16[\dot{X}_G]$$

$$x_G = 1.6[X_G]$$

$$\ddot{\phi} = 240[\ddot{\Phi}]$$

$$\dot{\phi} = 8.0[\dot{\Phi}]$$

$$\phi = 0.8[\Phi]$$

$$\ddot{x}_1 = 5400[\ddot{X}_1]$$

$$\dot{x}_1 = 60[\dot{X}_1]$$

$$x_1 = 1.6[X_1]$$

$$\ddot{x}_{1P} = 3000[\ddot{X}_{1P}]$$

$$\dot{x}_{1P} = 50[\dot{X}_{1P}]$$

$$x_{1P} = 1.6[X_{1P}]$$

$$\dot{x}_2 = 16[\dot{X}_2]$$

$$x_2 = 1.6[X_2]$$

$$\dot{x}_{2P} = 16[\dot{X}_{2P}]$$

$$x_{2P} = 1.6[X_{2P}]$$

$$x_{01} = 1.6[X_{01}]$$

$$x_{01P} = 1.6[X_{01P}]$$

$$\dot{x}_{12} = 50[\dot{X}_{12}]$$

$$x_{12} = 1.2[X_{12}]$$

$$\dot{x}_{12P} = 40[\dot{X}_{12P}]$$

$$x_{12P} = 1.2[X_{12P}]$$

With the scaling relationships shown the machine equations can now be expressed as:-

$$90000[F_2] = 1.2[X_{12}] 19972 + 50 [\dot{X}_{12}]1800 \quad (11.11)$$

$$\text{or } [F_2] = 0.2663[X_{12}] + 1.0000 [\dot{X}_{12}] \quad (11.12)$$

Similarly

$$[F_{2P}] = 0.3008[X_{12P}] + 0.8000[\dot{X}_{12P}] \quad (11.13)$$

$$[\ddot{X}_1] = -0.5832[F_2] + 1.6161[X_{01}] \quad (11.14)$$

$$[\ddot{X}_{1P}] = -0.5512[F_{2P}] + 1.5272[X_{01P}] \quad (11.15)$$

$$[\ddot{X}_G] = 0.4950[F_2] + 0.4950[F_{2P}] \quad (11.16)$$

$$[\ddot{\phi}] = 0.7227[F_2] - 0.9662[F_{2P}] \quad (11.17)$$

$$[\dot{X}_2] = [\dot{X}_G] + 0.5489[\dot{\phi}] \quad (11.18)$$

$$[\dot{X}_{2P}] = [\dot{X}_G] - 0.7338[\dot{\phi}] \quad (11.19)$$

$$[X_2] = [X_G] + 0.5489[\phi] \quad (11.20)$$

$$[X_{2P}] = [X_G] - 0.7338[\phi] \quad (11.21)$$

$$[X_{01P}] = 0.6250[X_{0P}] - [X_{1P}] \quad (11.22)$$

$$[X_{12P}] = 1.3333[X_{1P}] - 1.3333[X_{2P}] \quad (11.23)$$

$$[\dot{X}_{12}] = 1.2000[\dot{X}_1] - 0.3200[\dot{X}_2] \quad (11.24)$$

$$[\dot{X}_{12P}] = 1.2500[\dot{X}_{1P}] - 0.4000[\dot{X}_{2P}] \quad (11.25)$$

If the real time is denoted by t , and the machine time by τ , then the time scale relationship can be expressed as

$$\tau = \beta t$$

$$\text{or } d\tau/dt = \beta$$

When $\beta < 1.0$, the simulation process is faster than the real time, and vice versa.

The integration relationships incorporating the magnitude and time scales are now expressed as:-

$$[\dot{X}_1] = (90/\beta) \int [\ddot{X}_1] d\tau \quad (11.26)$$

$$[X_1] = (37.5/\beta) \int [\dot{X}_1] d\tau \quad (11.27)$$

$$[\dot{X}_{1P}] = (60/\beta) \int [\ddot{X}_{1P}] d\tau \quad (11.28)$$

$$[X_{1P}] = (31.25/\beta) \int [\dot{X}_{1P}] d\tau \quad (11.29)$$

$$[\dot{X}_G] = (22.5/\beta) \int [\ddot{X}_G] d\tau \quad (11.30)$$

$$[X_G] = (10/\beta) \int [\dot{X}_G] d\tau \quad (11.31)$$

$$[\dot{\phi}] = (30/\beta) \int [\ddot{\phi}] d\tau \quad (11.32)$$

$$[\phi] = (10/\beta) \int [\dot{\phi}] d\tau \quad (11.33)$$

The computer patching diagram for simulation of the $\frac{1}{2}$ -car model, together with all potentiometer settings and amplifier gains (for $\beta = 1.0$) is shown in Appendix A.

The time scaling of the simulation was effected by simply altering the integrator gains to suit the needs of computation.

For general simulation and measurement the problem was slowed down 10 times ($\beta = 10$) while for the purposes of plotting on X-Y plotter the problem was slowed down 100 times ($\beta = 100$).

The input excitation to the road wheels was a step of one machine unit, the step to the rear wheels being delayed by a time interval $\Delta\tau = (L/V)\beta$.

The time delay was derived from the computer time base by use of the comparator and the electronic switch on logic panel. The details of patching for the time delay circuit are shown in Fig. 11.2.

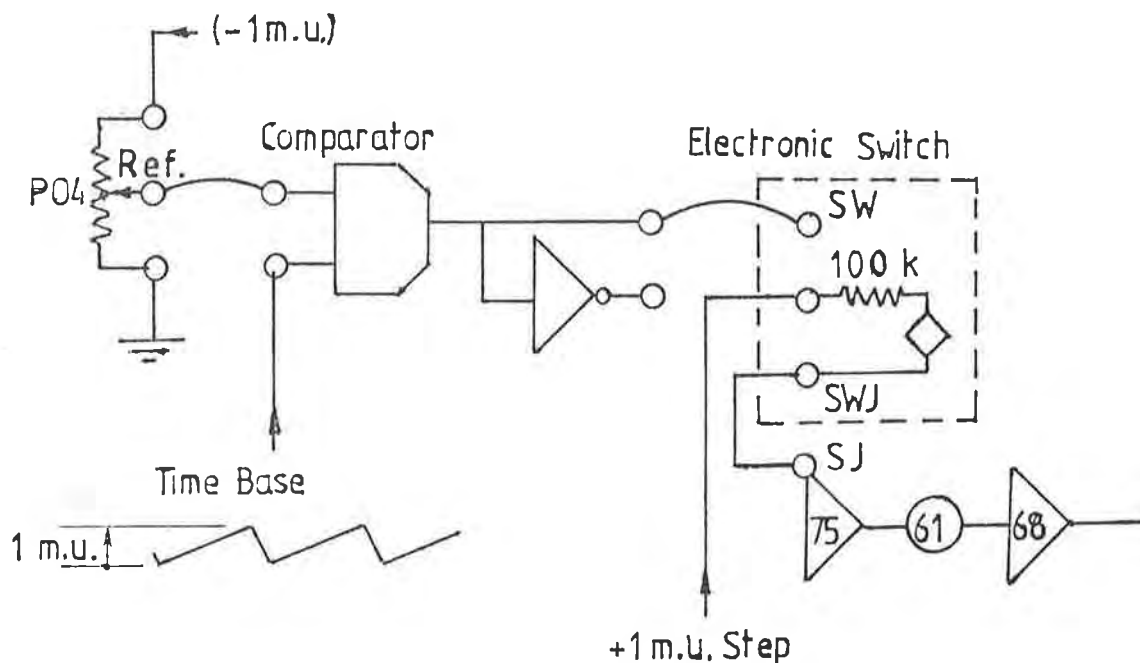


FIG. 11.2 - DIAGRAM OF TIME DELAY CIRCUIT

The operation of the time-delay circuit is as follows:-

For a computer time-base setting of 1 sec the time-base ramp rises linearly from zero volts to 1m.u. (10 volts) in that time interval.

If now the potentiometer P04 is set to value equal to the time delay $D=L/V$, the reference voltage input to the comparator will be $-D$ volts ($D<1$). The time-base voltage will require D sec to reach the same value but of opposite sign. As soon as the sum of the reference voltage and that of the time-base reaches zero, the comparator drives the electronic switch to conduct, thus applying the unit step through the switch to the summing junction of amplifier 75. The output of the amplifier is a delayed step function which is then applied to the rear wheels of the model.

As the computer time base is changed when the simulation is speeded up or slowed down, the circuit will always maintain the correct time-delay relationship relatively to computer integration interval.

To obtain the integrals of mean squared values, the responses were squared and integrated according to patching diagram shown in Fig. 11.3.

Owing to shortage of integrators it was necessary to employ switches for separation of front and rear integral square values.

The scale factors for integral square values were calculated as follows:-

$$\begin{aligned} \langle x_{01}^2 \rangle &= (1/\beta) \int \{1.6[X_{01}]\}^2 d\tau = (2.56/\beta) \int [X_{01}]^2 d\tau \\ \langle x_{01}^2 \rangle &= (1/\beta) \int \{1.2[X_{12}]\}^2 d\tau = (1.44/\beta) \int [X_{12}]^2 d\tau \\ \langle F_2^2 \rangle &= (1/\beta) \int \{9 \times 10^4 [F_2]\}^2 d\tau = (0.81 \times 10^{10}/\beta) \int [F_2]^2 d\tau \end{aligned}$$

The scale factors with $\beta = 10.0$ are thus 0.256, 0.144 and 0.810×10^9 respectively.

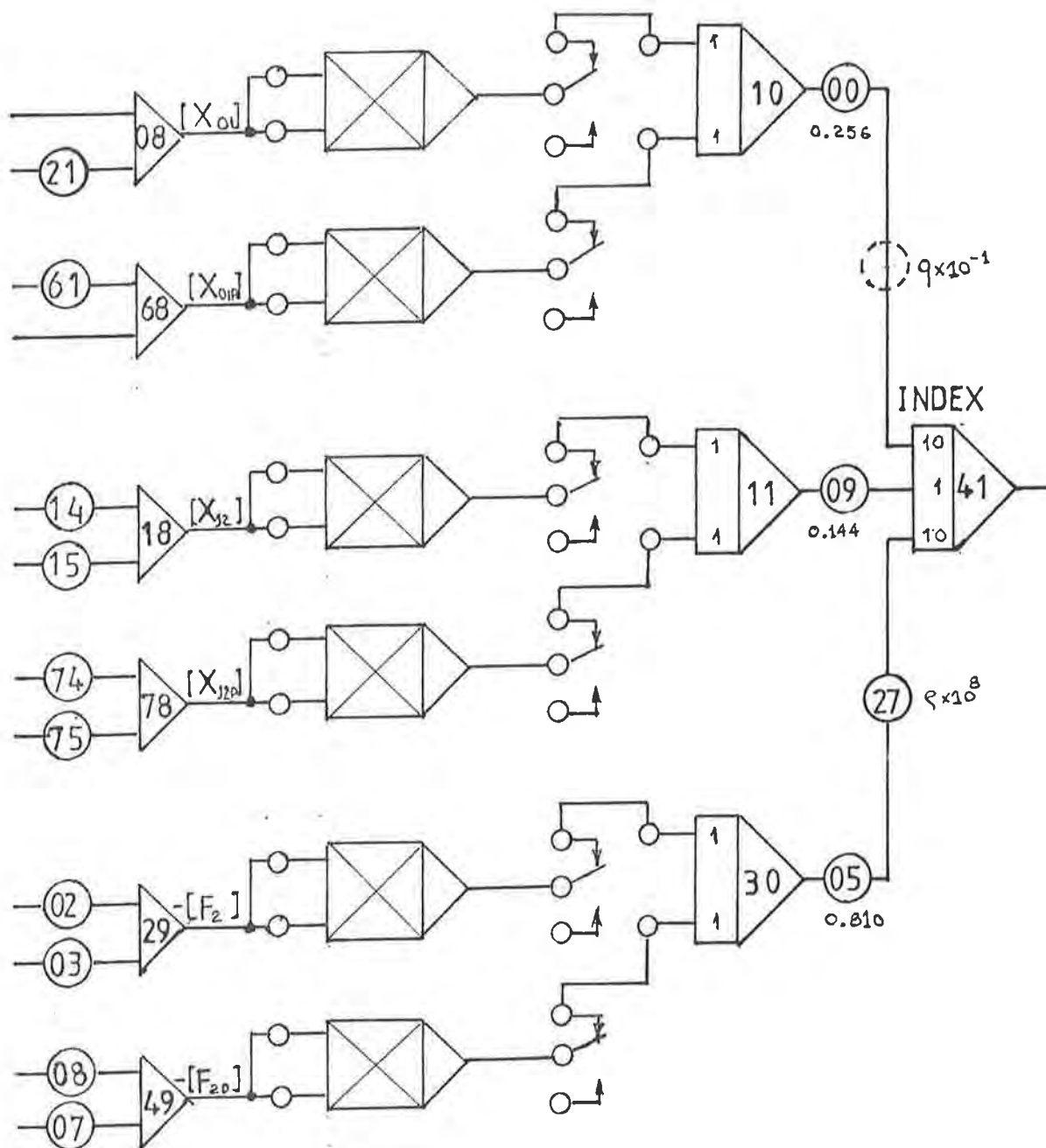


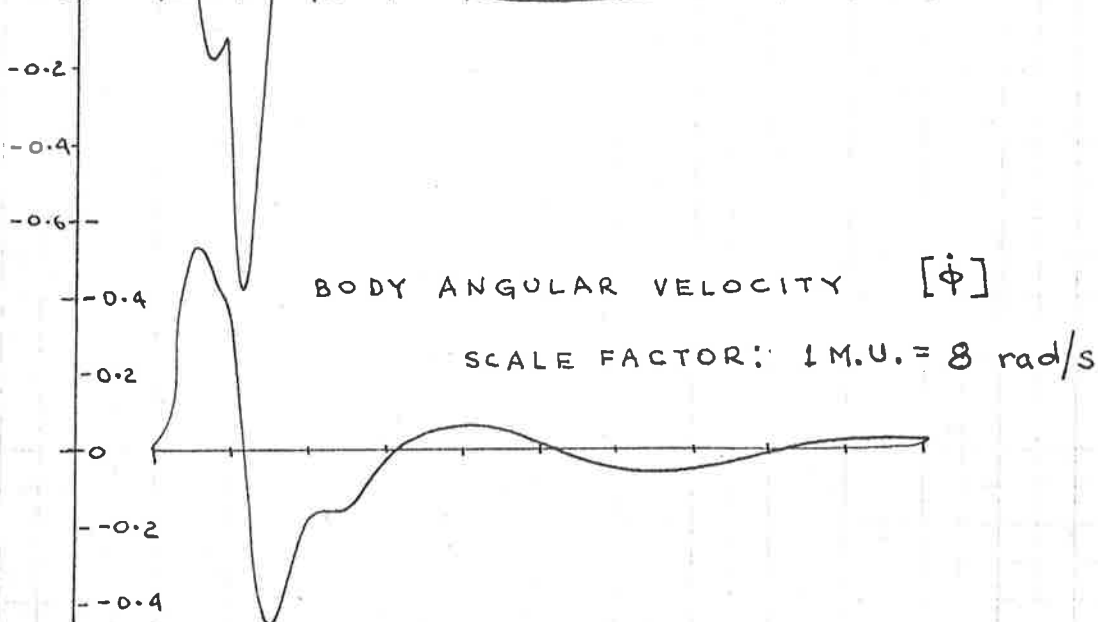
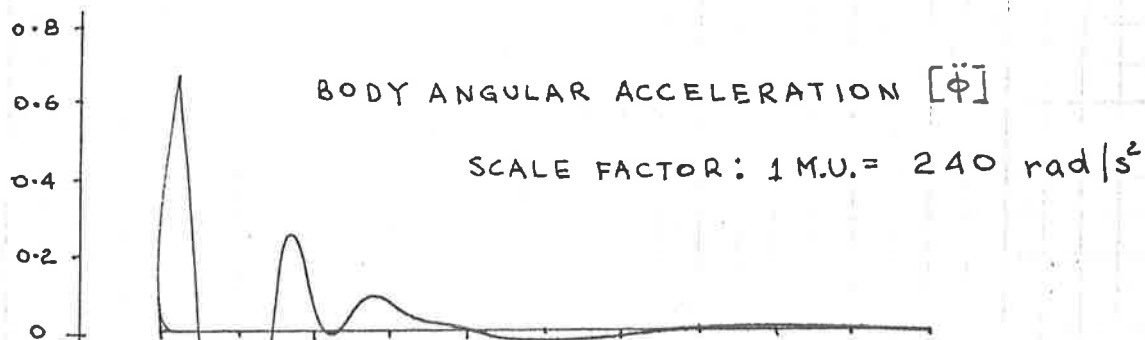
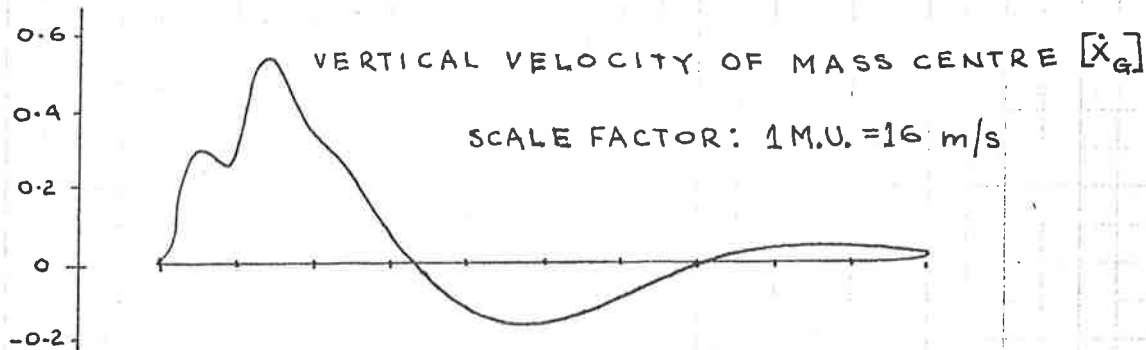
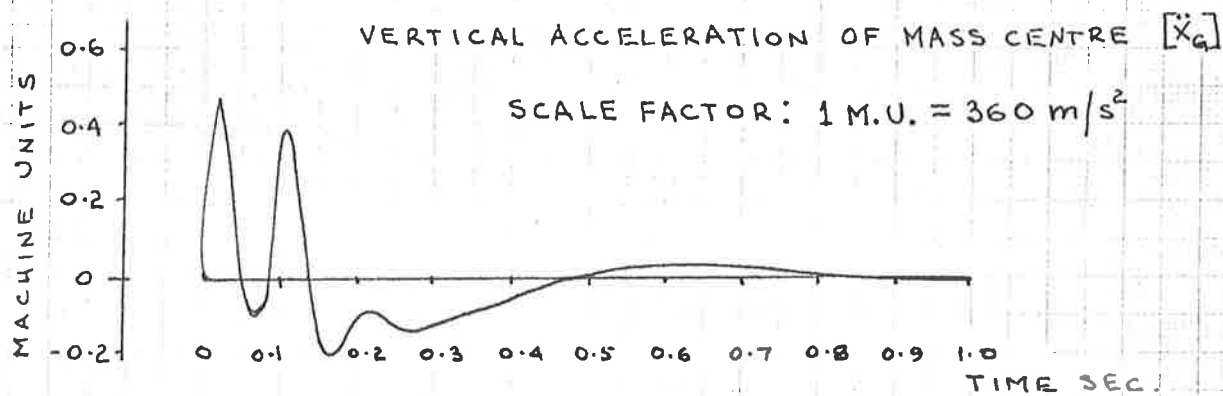
FIG. 11.3 - PATCHING DIAGRAM FOR INTEGRAL SQUARE VALUES

11.4 Results

The response of the model to a unit step input was monitored on C.R.O. screen, and was found to fully agree with the results obtained from digital ACSL simulation.

Typical responses recorded on HEWLETT PACKARD X-Y plotter are shown in Fig. 11.4, corresponding to a road speed of 30 m/s. A more comprehensive set of graphs corresponding to different road speeds is shown in Appendix A.

Fig. 11.4. System Time Response to Unit Step by Analogue Computer Simulation.



HILLMAN $\frac{1}{2}$ Car Model (Unladen), $R=0.7$
 $V=30\text{m/s}$

Fig. 11.5. System Time Response to Unit Step by Digital Computer Simulation.



HILLMAN $\frac{1}{2}$ Car Model (Unladen), $R=0.7$
 $V=30$ m/s

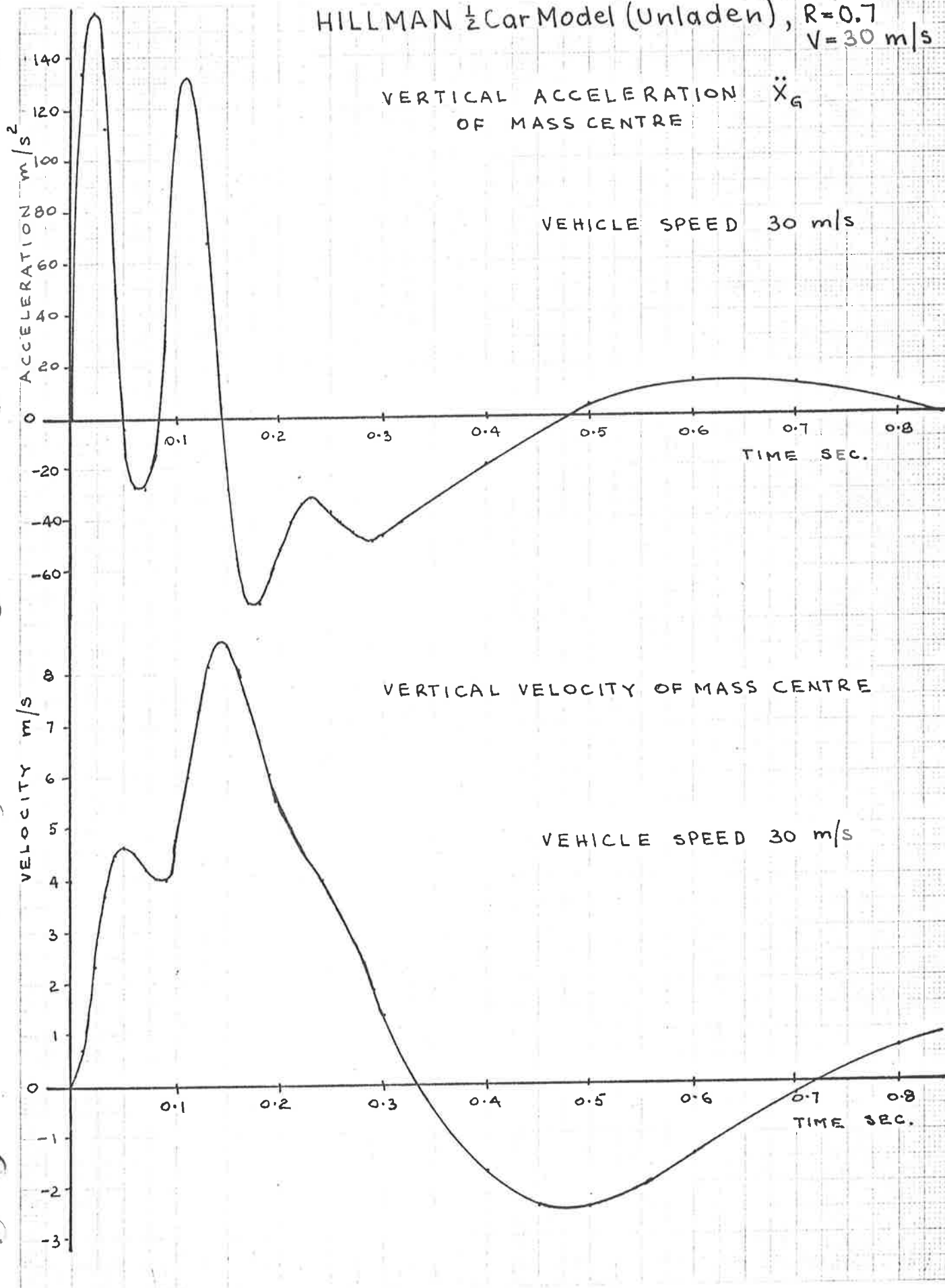
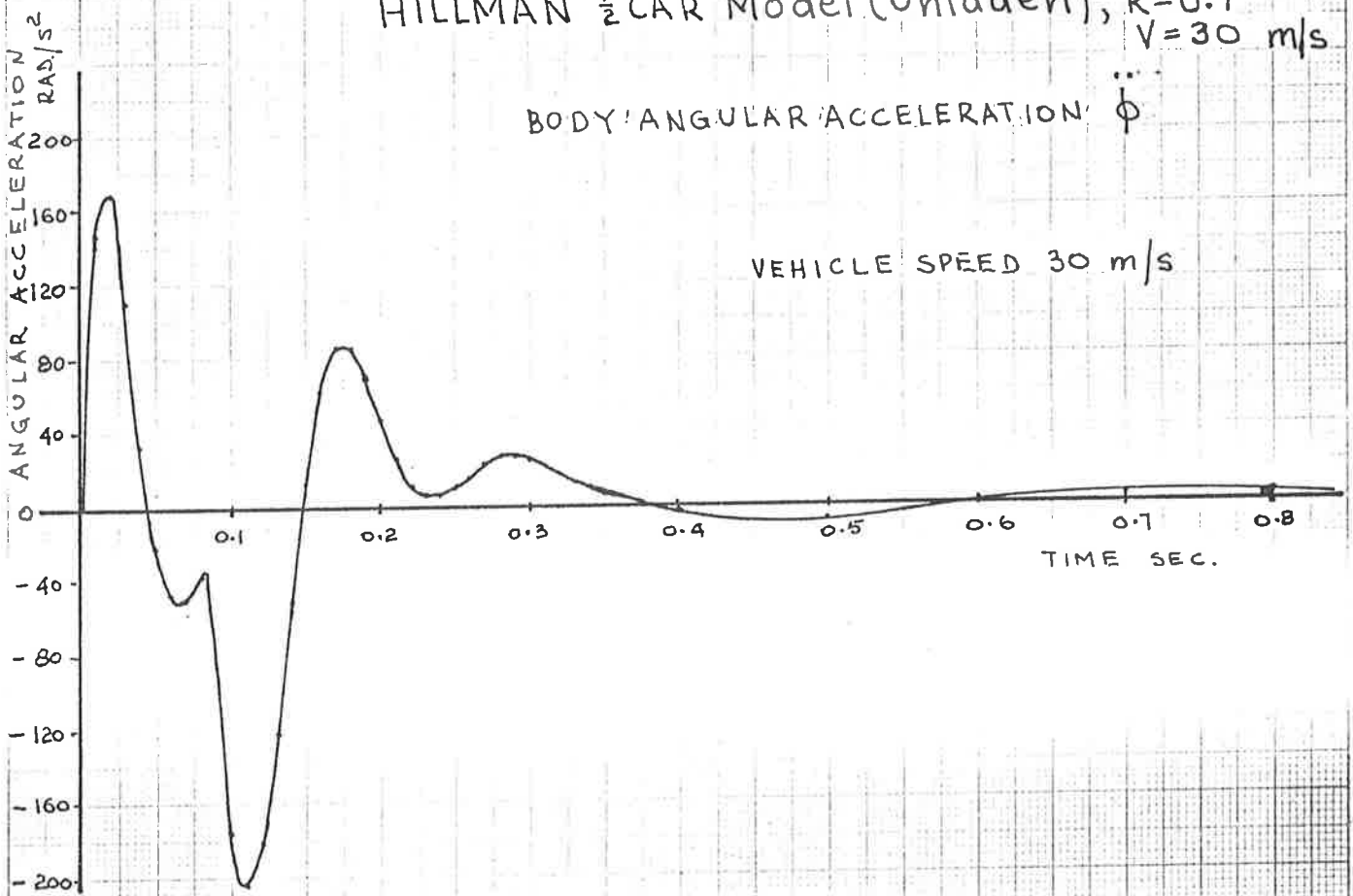


Fig.11.6. System Time Response to Unit Step by Digital Computer Simulation.

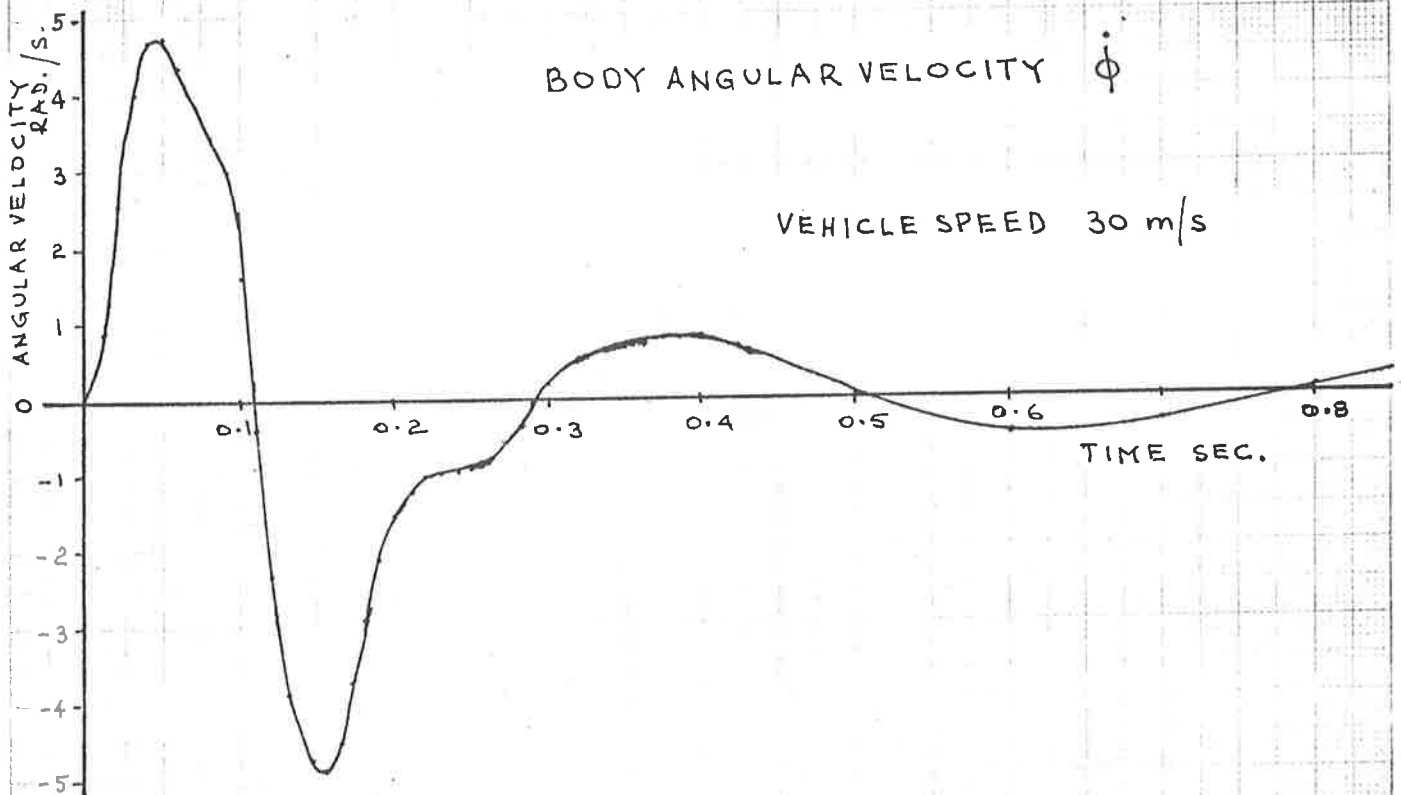


HILLMAN $\frac{1}{2}$ CAR Model (Unladen), $R=0.7$
 $V=30$ m/s

BODY ANGULAR ACCELERATION $\ddot{\phi}$



BODY ANGULAR VELOCITY $\dot{\phi}$



In Fig. 11.4 only the acceleration and velocity of the mass centre as well as the angular acceleration and velocity of the body are shown for comparison with the results from ACSL simulation which are shown in Figs. 11.5 and 11.6.

It can be seen that there is a good agreement between analogue and digital simulation results.

The simulation pertains to $\frac{1}{2}$ -car unladen HILLMAN model with a coupling ratio $R=0.7$, and having the following parameter values:-

$$\begin{array}{ll} k_2 = 19972 \text{ N/m} & B_2 = 1800 \text{ Ns/m} \\ k_{2P} = 22563 \text{ N/m} & B_{2P} = 1800 \text{ Ns/m} \\ k_1 = 155860 \text{ N/m} & \\ k_{1P} = 155860 \text{ N/m} & \end{array}$$

As soon as the agreement between the results of analogue and digital simulations had been confirmed, additional simulation runs were conducted at vehicle speeds and varying suspension parameters.

In these investigations the attention was mainly focussed on integral square values of response and performance index as defined in previous sections of the thesis.

It was soon noticed, however, that significant differences did occur in the values of performance index as demonstrated by graphs in Figs. 11.7, 11.8 and 11.9.

The corresponding analogue and digital computer results are tabulated in Appendix A in Tables A1, A2, A4, A5, A7 and A8.

The integral square values and the performance indices from analogue simulation were significantly lower than the values obtained from digital simulation. It was also observed during analogue simulation that there was a random error associated with repeatability.

To investigate the extent of discrepancies and uncertainties



Fig. 11.7. Comparison of Digital and Analogue Computer Results.
 HILLMAN $\frac{1}{2}$ Car Model (Unladen), $R=0.7$.

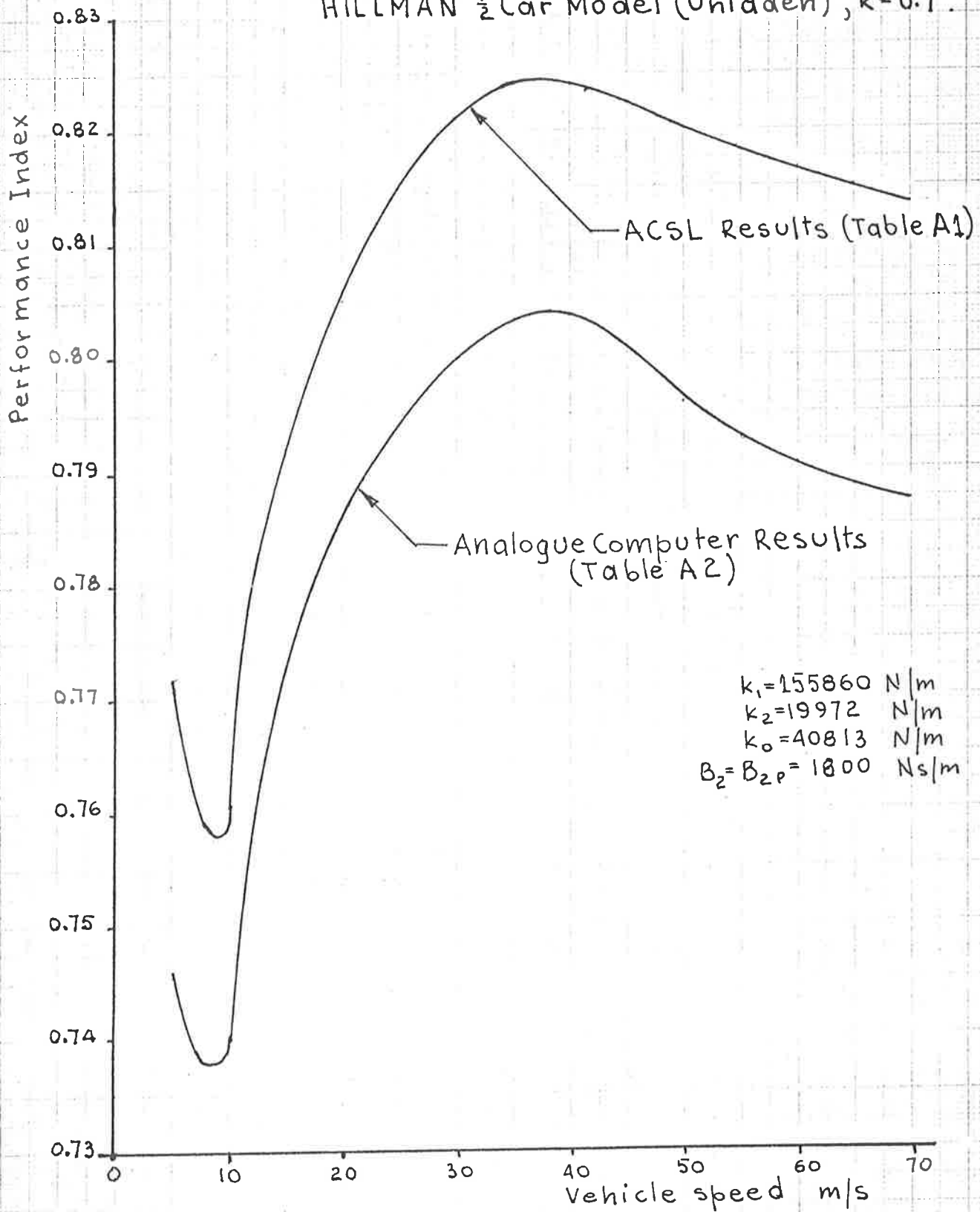




Fig. 11.8. Comparison of Digital and Analogue Computer Results.
 HILLMAN $\frac{1}{2}$ car Model (Unladen), $R=0.7$
 $V=20 \text{ m/s}$

Performance Index

$$k_1 = 155860 \text{ N/m}$$

$$k_0 = 40813 \text{ N/m}$$

$$B_2 = B_{2P} = 1800 \text{ N s/m}$$

0.87
0.86
0.85
0.84
0.83
0.82
0.81
0.80
0.79
0.78
0.77

ACSL Results (Table A4)

Analogue Computer Results
(Table A5)

16 18 20 22 24 26 28 30
 Front spring rate $k_2 \text{ kN/m}$

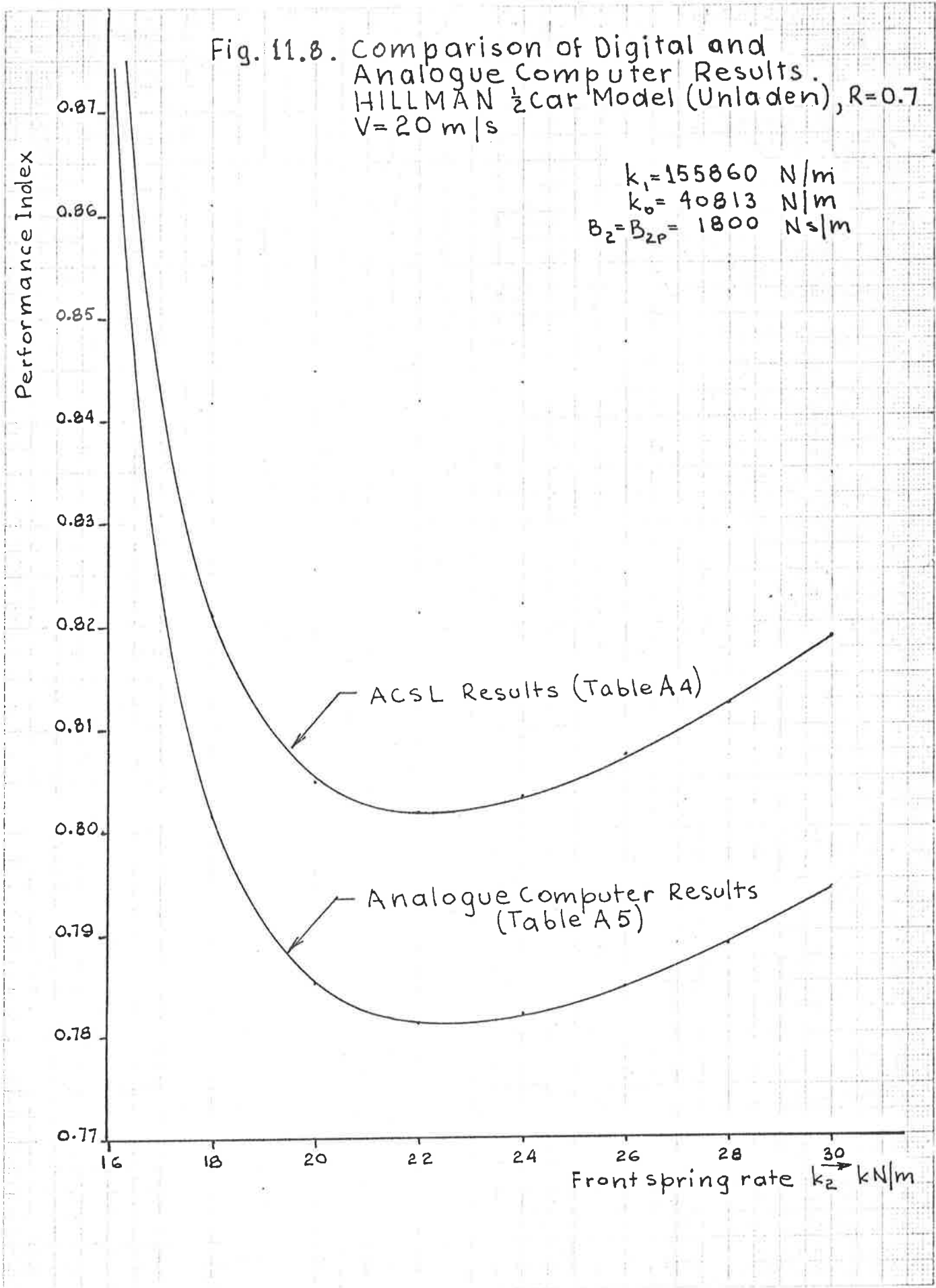
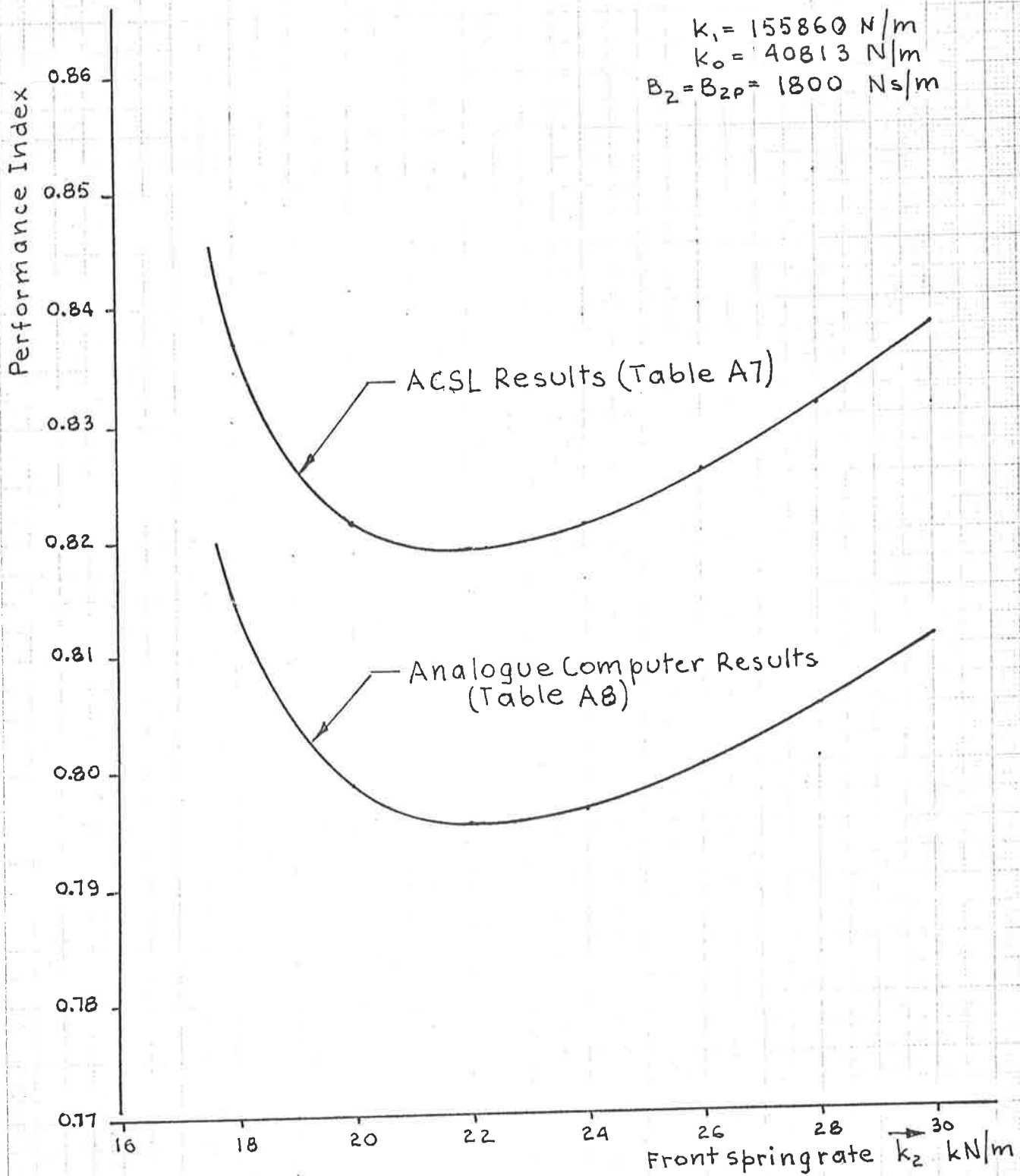




Fig. 11.9. Comparison of Digital and Analogue
Computer Results.
HILLMAN $\frac{1}{2}$ Car Model (Unladen), $R=0.7$
 $V=30$ m/s



involved in analogue simulation, the apparent scale factors for integral square values were calculated from the ratios (I.S.V Digital)/(I.S.V Analogue) for relative tyre deflections, wheel travel and body force respectively. The values are listed in Tables A3, A6 and A9 in Appendix A.

The examination of the calculated ratios in the tables reveals that a large discrepancy exists between the theoretical and actual scale factors for integral square values of tyre deflections, while there are relatively small discrepancies in case of wheel travel and body force.

The theoretical scale factors calculated for integral square responses are listed below which then can be compared with the actual scale factors calculated from comparison of analogue and digital simulation results.

Theoretical scale factors:-

| | |
|--------------------------------|--|
| I.S.V. Dynamic tyre deflection | 0.256 m ² /m.u. |
| I.S.V. Relative wheel travel | 0.144 m ² /m.u. |
| I.S.V. Body Force | 0.81x10 ⁹ N ² /m.u. |
| I.S.V. Body acceleration | 12.96x10 ³ (m/s ²) ² /m.u. |

The mean values and standard deviations of actual scale factors are listed in Table 11.1.

TABLE 11.1
SCALE FACTORS CALCULATED FROM ANALOGUE SIMULATION RESULTS

| SOURCE | TABLE A3 | | TABLE A6 | | TABLE A9 | |
|--|----------------|----------------------|----------------|----------------------|----------------|----------------------|
| | Mean (μ) | $\sigma \times 10^3$ | Mean (μ) | $\sigma \times 10^3$ | Mean (μ) | $\sigma \times 10^3$ |
| $\langle X_{01}^2 \rangle$ | 0.2736 | 2.87 | 0.2762 | 5.99 | 0.2776 | 5.52 |
| $\langle X_{01P}^2 \rangle$ | 0.2661 | 1.83 | 0.2654 | 2.93 | 0.2671 | 2.81 |
| $\langle X_{01}^2 \rangle + \langle X_{01P}^2 \rangle$ | 0.2686 | 2.25 | 0.2698 | 1.33 | 0.2712 | 0.96 |
| $\langle X_{12}^2 \rangle$ | 0.1447 | 0.94 | 0.1441 | 0.39 | 0.1438 | 0.29 |
| $\langle X_{12P}^2 \rangle$ | 0.1465 | 1.20 | 0.1454 | 0.43 | 0.1461 | 0.45 |
| $\langle X_{12}^2 \rangle + \langle X_{12P}^2 \rangle$ | 0.1456 | 0.63 | 0.1448 | 0.37 | 0.1451 | 0.34 |
| $\langle F_2^2 \rangle$ | 0.8181E9 | 1.18E9 | 0.8154E9 | 0.54E9 | 0.8149E9 | 0.88E9 |
| $\langle F_{2P}^2 \rangle$ | 0.8239E9 | 5.56E9 | 0.8168E9 | 0.58E9 | 0.8198E9 | 0.44E9 |
| $\langle F_2^2 \rangle + \langle F_{2P}^2 \rangle$ | 0.8212E9 | 3.08E9 | 0.8160E9 | 1.05E9 | 0.8178E9 | 0.34E9 |
| $\langle \ddot{X}_G^2 \rangle$ | 13200 | 162940 | 12992 | 27258 | 13081 | 62940 |

The data listed in Table 11.1 indicate that there are constant systematic errors as well as random errors associated with integral square values of response. The results shown were taken on different days, and the potentiometers were checked and reset before each simulation run. Also careful static checks were carried out before the actual simulation runs.

The systematic errors can easily be compensated for by applying appropriate correction factors to integral square values, or by adjustment to potentiometers 00, 05 and 09 of the summing amplifier 41, and then in the absence of a random error the summing amplifier output will agree with the performance index as obtained by digital simulation.

On the other hand, if the random error is significant, it is not possible to establish the precise location of minima in performance index characteristics.

Typical characteristics are shown in Figs. 11.7, 11.8 and 11.9. In Fig. 11.7 the suspension parameters are held constant and the road speed is varied while in Figs. 11.8 and 11.9 the road speed is constant and suspension spring stiffness is varied.

It can be seen from Figs. 11.8 and 11.9 that the characteristics are very flat, and near the point of minima the performance index varies only by 0.3% for $\pm 10\%$ variation in spring stiffness about the value that minimises the performance index.

This observation raises two questions:-

- (i) What is the maximum acceptable uncertainty in parameter values that can be tolerated in a parameter optimisation problem.
- (ii) What magnitude random errors can be expected in the values of performance index obtained in analogue simulation.

It is rather difficult to give a precise answer to (i), but a figure of $\pm 5\%$ would be about the maximum error that could be tolerated, which means that the random errors in performance index

should not exceed 0.15%.

It can be said without hesitation that this order of accuracy and repeatability cannot be obtained with a general purpose analogue machine, hence an accurate quantitative analysis on the basis of analogue computer results appears to be impracticable.

It is of interest, however, to examine the accuracy that can be expected in present analogue computer simulation.

The performance index is expressed as

$$I = q\{\langle X_{01}^2 \rangle + \langle X_{01P}^2 \rangle\} + \{\langle X_{12}^2 \rangle + \langle X_{12P}^2 \rangle\} + \rho\{\langle F_2^2 \rangle + \langle F_{2P}^2 \rangle\}$$

or

$$I = q\langle X_{01}^2 \rangle_s + \langle X_{12}^2 \rangle_s + \rho\langle F_2^2 \rangle_s \quad (11.1)$$

where s denotes the sum of the respective integral square values for front and rear suspensions.

The result obtained in the analogue simulation can be expressed as

$$I = q S_1 [X_{01}^2]_s + S_2 [X_{12}^2]_s + \rho S_3 [F_2^2]_s \quad (11.2)$$

$$\text{where } [X_{01}^2]_s = \int [X_{01}]^2 d\tau + \int [X_{01P}]^2 d\tau \quad (11.3)$$

$$[X_{12}^2]_s = \int [X_{12}]^2 d\tau + \int [X_{12P}]^2 d\tau \quad (11.4)$$

$$[F_2^2]_s = \int [F_2]^2 d\tau + \int [F_{2P}]^2 d\tau \quad (11.5)$$

and S_1, S_2, S_3 are the corresponding scale factors.

The variance of I can be obtained by expansion in Taylor series as

$$\sigma_I^2 = \sum_{i=1}^n \left(\frac{\partial I}{\partial S_i} \right)^2 \sigma_{S_i}^2 \quad (11.6)$$

where $\sigma_{S_i}^2$ denotes the variance of scale factors.

This gives

$$\begin{aligned}
\sigma_i^2 &= \{q[X_{10}]_s\}^2 \sigma_{S_1}^2 + \{[X_{12}]_s\}^2 \sigma_{S_2}^2 + \{\rho[F_2^2]_s\}^2 \sigma_{S_3}^2 \\
&= \{q \langle x_{01}^2 \rangle_s \sigma_{S_1} / \bar{S}_1\}^2 + \{\langle x_{12}^2 \rangle_s \sigma_{S_2} / \bar{S}_2\}^2 \\
&\quad + \{\rho \langle F_2^2 \rangle_s \sigma_{S_3} / \bar{S}_3\}^2 \quad (11.7)
\end{aligned}$$

The percentage errors expected in the value of performance indices have been calculated, and are listed in Tables A3, A6 and A9 of Appendix A.

The mean values of expected random errors in performance indices are listed below.

| | From Table A3 | From Table A6 | From Table A9 |
|-------------|---------------|---------------|---------------|
| σ/l | 0.31% | 0.23% | 0.17% |
| $3\sigma/l$ | 0.93% | 0.69% | 0.51% |

It is clear that the random errors will be relatively small, but nevertheless will exceed the desired 0.15%, hence the analogue computer results will be of doubtful value in an accurate parameter optimisation process.

At this point it is also instructive to examine the systematic errors in integral square values listed in Table 11.2.

TABLE 11.2

| Error in | From A3 | From A6 | From A9 |
|------------------|---------|---------|---------|
| ISX01 | 6.82% | 7.90% | 8.45% |
| ISX01P | 3.73% | 3.69% | 4.32% |
| SISX01 | 4.78% | 5.41% | 5.92% |
| ISX12 | 0.51% | 0.083% | 0.11% |
| ISX12P | 1.71% | 0.94% | 1.44% |
| SISX12 | 1.09% | 0.56% | 0.74% |
| ISF2 | 0.94% | 0.66% | 0.61% |
| ISF2P | 1.69% | 0.84% | 1.21% |
| SISF2 | 1.33% | 0.75% | 0.96% |
| ISX _G | 1.85% | 0.25% | 0.94% |

The examination of values listed in Table 11.2 reveals that the errors in integral square values of wheel travel and body force are generally within the range of the accuracy expected from an analogue machine, but overall they seem to be a little high. This is mainly due to multiplier errors, and subsequent integration of errors.

The errors in integral square value of tyre deflections, however, are far in excess of the error usually associated with analogue simulation. The reason for this large error is probably explained by reference to Fig. 11.10 which shows the plots of outputs, from amplifiers 75 (X01) and 76 (X01P) against time.

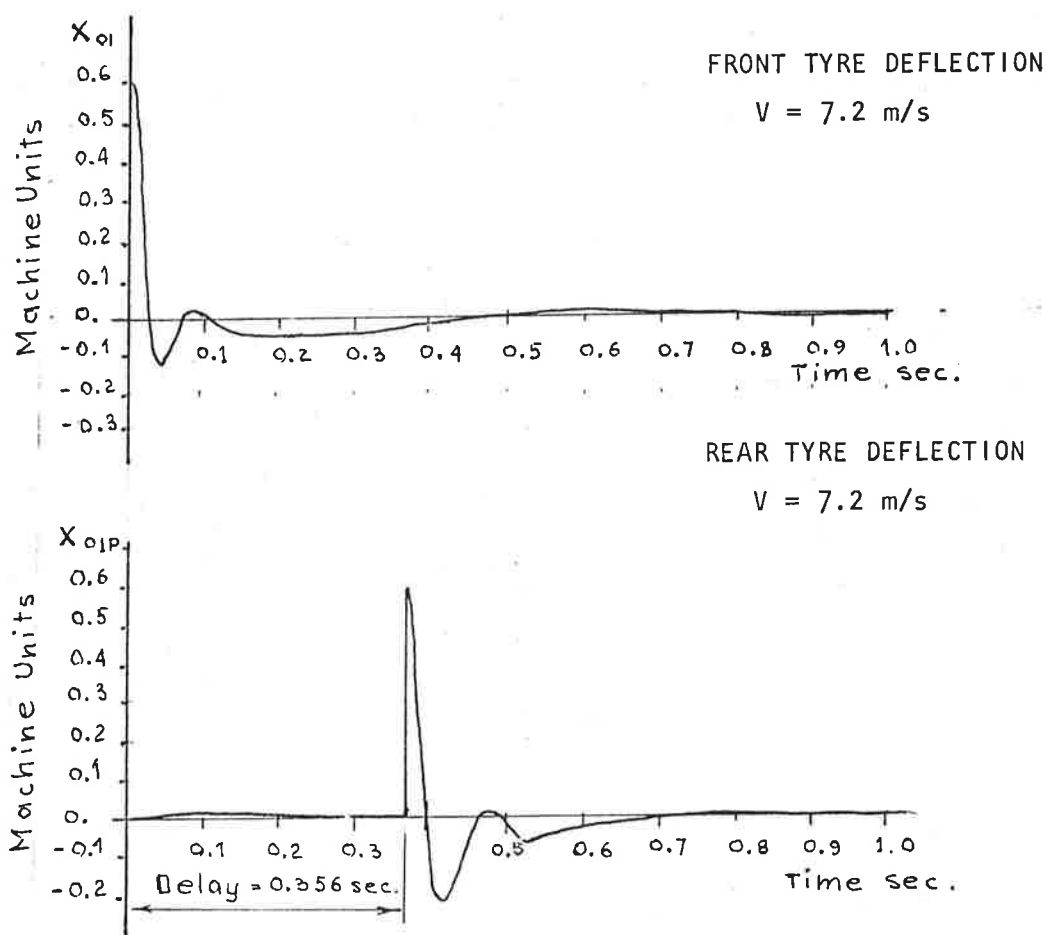


FIG. 11.10 - FRONT AND REAR TYRE DEFLECTIONS
(from amplifiers 75 and 76 respectively)

It can be seen that the signal exists only for a very short period of the total integration interval, and amplifier output is zero for the rest of the interval.

This means that the integrators following the multipliers will be integrating the multiplier errors for the most part of the integrating period, and the error would increase with increasing integrating period.

Hence, the exceptionally large error associated with the integral square value of tyre deflection.

11.5 Summary

The aim of analogue simulation was to establish the suspension parameter values corresponding to minima in performance indices so as to establish the relationships between the weighting factors and corresponding minima of performance indices for different values of coupling ratio.

The process, in principle, would be simple and take much less time and computing effort with associated computing costs than the digital simulation, provided the accuracy of the analogue computer is adequate for this purpose.

The process would be carried out as follows:-

- (i) Set the required weighting factors on potentiometers 00 and 05.
- (ii) Vary spring stiffness for minimum performance index
- (iii) Plot graphs of minimum performance index against spring stiffness with weighting factors as parameters.

During the actual simulation it was found that the situation was much more complicated, mainly because of very flat characteristics of the performance indices in the region of minima, and random errors in computed values of performance indices which tended to mask the location of exact points of minima. Owing to shallowness of the characteristics the analogue computer just has not suffic-

ient repeatability in order to establish the points of minima with adequate reliability unless large numbers of readings are taken for each test point and statistical processing of results is introduced.

The accuracy of direct response of the analogue computer when compared with the results from the digital machine is very good - less than 0.5% error, but after multiplication of signals and subsequent integration, the initial high accuracy is gradually lost along the line of processing so that the errors become significant, especially in the case where the signal occurs only for a very short period of the total integration interval, and the integrators integrate only the multiplier errors for the rest of the interval.

12. SUMMARY AND CONCLUSIONS

In this thesis the techniques of optimal control theory have been applied to the analysis and synthesis of linear, passive suspensions for road vehicles.

The process of optimisation involves the minimisation of the quantity known as the performance index, with the view to obtaining a suspension that has optimum characteristics.

The performance index is a function of several design variables, and is a measure of dynamic behaviour of the suspension with respect to variables such as acceleration, velocity and displacement.

The technique of optimisation, although quite straight-forward in theory, involves some complications when it comes to its practical implementation.

Probably the most difficult and grey area in its application is the representative form of the performance index, i.e. which variables would most appropriately describe the optimum system.

The other aspect of concern is the choice of suitable weighting factors, i.e. which variables need be penalised more heavily than others in order to achieve the best overall characteristics for the suspension.

By optimum performance it is implied that all critical quantities that contribute to the overall response of the system must have optimum values.

In the present analysis of the problem, the mean square values of body acceleration, tyre deformation and relative wheel travel were taken as the critical quantities since they directly relate to ride comfort, road holding and vehicle handling. In an ideal system all these critical quantities should have minimum values when appropriate suspension parameters are chosen.

In the case of passive suspensions some of these responses can be minimised by a suitable choice of suspension parameters, while some have no minima at all.

Furthermore, minima of different responses correspond to different values of suspension parameters.

Hence, the selection and design becomes a compromise, a trade-off of one performance feature against another, often dictated by subjective opinion of the designer or a testing team.

Since the whole aspect of 'optimisation' is rather subjective, it may be expected that different designers will arrive at slightly different solutions for the same basic model since there are no absolute performance standards. As there are no 'exact' solutions, different designers will come up with slightly different 'optimal' systems by accepting different performance criteria. Much will depend on the experience and subjective opinion of a particular designer as to which aspect of performance is considered to be more critical.

Additional uncertainties such as the tyre stiffness and the payload will further complicate the issue. Should the suspension be optimised for tyre stiffness that corresponds to specified inflation pressure or should allowances be made for the spread of stiffness characteristics associated with commercial tyres? Should the temperature effects be considered for a vehicle travelling on a hot bitumen road typical to Australian summer? Should the suspension be optimised for a laden or unladen passenger vehicle?

It is partly to the advantage of the designer that the minima of responses are relatively flat so that the changes in suspension parameters about the nominal values will result in very slight changes to response, hence do not significantly modify the overall behaviour once the basic parameters have been chosen.

It has been demonstrated that the performance index in the form of weighted integral square values of response is not an absolute measure of suspension quality but only serves as a characteristic quantity in computer optimisation process for trade-off studies.

In the process different values of weighting factors will result in different values of minimum performance index but may correspond to exactly the same system, while a specified value of minimum performance index may correspond to vastly different systems as dictated by the

weighting factors.

The situation is demonstrated in Fig. 12.1

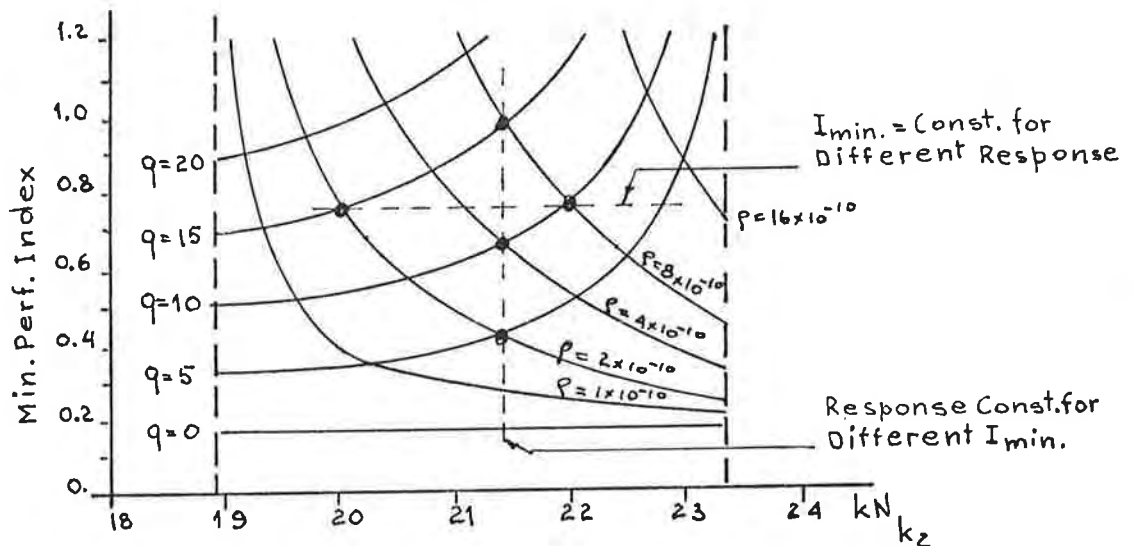


FIG. 12.1 - RELATIONSHIP BETWEEN MIN. PERFORMANCE INDEX AND WEIGHTING FACTORS.

Another complication associated with the optimisation and trade-off studies is the fact that ISO standards specify the recommended limits of maximum acceleration in terms of exposure to vibration without any reference to corresponding road input spectrum.

If it is assumed that continuous 8-hour comfort limit applies to a good motorway for a vehicle travelling at near the maximum permissible road speed (100 km/hr on most Australian principal roads), then some answers must be found for the following questions:-

- (i) What is a reasonable continuous period of exposure to vibration in a vehicle travelling on a poor road (duration of travel)?
- (ii) What road roughness and vehicle speed would adequately describe the conditions of travelling on a typical rough road where the bottoming of suspension and road holding become the limiting criteria of performance.

Computer optimisation routines in literature are often applied to tracked vehicles, and for very good reasons. Here the roughness spectrum of the track is confined to relatively narrow limits, and the accel-

eration limits can be specified in terms of acceleration spectral density. Also the speed of the vehicle is fixed by the design of the system. Thus there are fixed specifications which the system will have to meet, and trade-off studies are carried out to meet the specifications.

The situation for a road vehicle is vastly different since the road roughness varies enormously for different types of road, hence it would be desirable to compare the relative characteristics of different suspensions without any reference to the level of input excitation to the road wheels.

One method of achieving this is to plot the mean square values of body acceleration against tyre deformation for an arbitrary level of random input, with the wheel travel as a constant parameter.

The presentation of vehicle response in this form eliminates the road roughness as a variable. The procedure is discussed at length in Ref. (85) where the simulations were carried out on an analogue machine with random signal input to $\frac{1}{4}$ -car model, and the RMS value of total dynamic body deflection (tyre deflection + wheel travel) was taken as a constant parameter.

The simulation was conducted as follows:-

R.M.S. value of total dynamic deflection was calculated for typical values of spring stiffness and damping. Then the spring stiffness was varied which changed the total deflection. Now the damper was varied to restore the initial value of total deflection. The process was repeated for a whole range of spring stiffnesses and damping, and finally body acceleration was plotted against tyre deflection for a constant value of total deflection as a parameter.

Simulations were repeated for different values of total dynamic deflection, and the results when plotted gave a graph of general form as shown in Fig. 12.2.

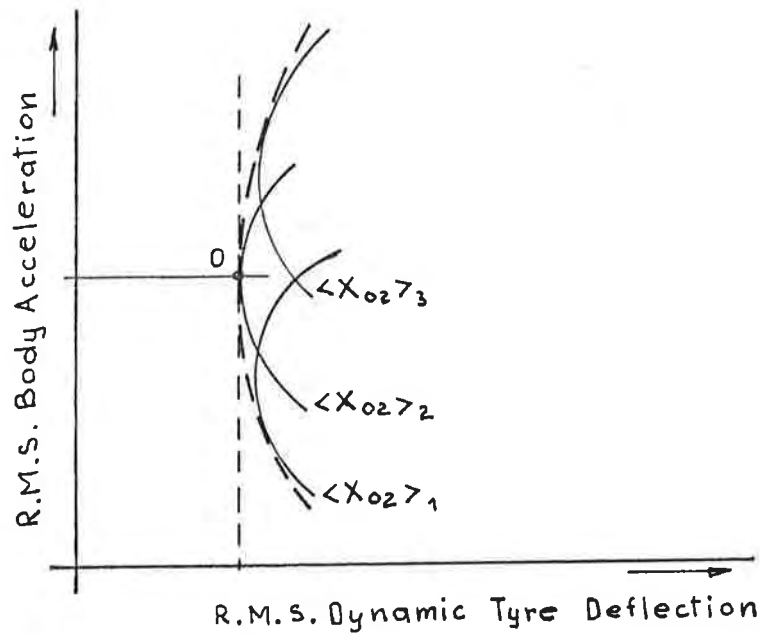


FIG. 12.2 - RELATIONSHIP BETWEEN BODY ACCELERATION AND DYNAMIC TYRE DEFLECTION

After a number of graphs had been plotted, an envelope as shown in dotted lines was drawn, and the optimum suspension was defined as one which resulted in minimum value of tyre deflection indicated by letter 'o' in Fig. 12.2.

Instead of using digital or analogue simulation, the integral square values of responses due to step input can be calculated from model parameter values using Parseval's Theorem.

It was shown in Chapter 5 that for $\frac{1}{4}$ -car model with a unit step input the integral square values of response are given by the expressions:-

$$\langle u_2^2 \rangle = \frac{k_1 B_2}{2} + \frac{k_2 (m_1 + m_2)}{2 B_2}$$

$$\langle x_{01}^2 \rangle = \frac{(m_1 + m_2)^2 B_2}{2 k_1 m_2^2} + \left[\frac{m_1}{2} - \frac{k_2 m_1 (m_1 + m_2)}{k_1 m_2} + \frac{k_2^2 (m_1 + m_2)^3}{2 k_1^2 m_2^2} \right] \frac{1}{B_2}$$

$$\langle x_{12}^2 \rangle = \frac{m_1 + m_2}{2 B_2}$$

It can also be shown that the integral square value of total dynamic deflection is given by:-

$$\langle x_{02}^2 \rangle = \frac{(m_1 + m_2)^2 B_2}{2 k_1 m_2^2} + \left[\frac{m_2}{2} + \frac{k_2 (m_1 + m_2)}{k_1} + \frac{k_2^2 (m_1 + m_2)^3}{2 k_1^2 m_2^2} \right] \frac{1}{B_2} \quad (12.1)$$

For a constant value of total deflection $\langle x_{02}^2 \rangle = \text{CONST.}$, the relationship between damping and suspension spring stiffness is given by

$$\text{CONST.} = \frac{(m_1+m_2)^2 B_2}{2 k_1 m_2^2} + \left[\frac{m_2}{2} + \frac{k_2 (m_1+m_2)}{k_1} + \frac{k_2^2 (m_1+m_2)^3}{2 k_1^2 m_2^2} \right] \frac{1}{B_2} \quad (12.2)$$

If now the spring stiffness is varied the value required of damping for constant total dynamic deflection of the mass centre is given by the solution of the equation

$$B_2^2 - (\text{CONST}) \frac{2 k_1 m_2^2 B_2}{(m_1+m_2)^2} + \left[\frac{m_2^3 k_1}{(m_1+m_2)^2} + \frac{2 k_2 m_2^2}{m_1+m_2} + \frac{k_2^2 (m_1+m_2)}{k_1} \right] = 0$$

The spring stiffness k_2 can now be varied, and corresponding damping calculated from the quadratic such that the integral square value of total dynamic deflection remains constant.

The computer program OPT1 shown in Appendix C was used to calculate the integral square values of response corresponding to $\frac{1}{4}$ -car HILLMAN models. The results of the calculations are plotted in Fig. 12.3 for the front suspension and in Fig. 12.4 for the rear suspension respectively.

The optimum values of suspension spring stiffness and damping rate were obtained from the graphs and are listed in Table 12.1 for comparison.

TABLE 12.1 OPTIMUM SUSPENSION $\frac{1}{4}$ -CAR MODEL
HILLMAN DATA (UNLADEN)

| Suspension Parameters | Front Suspension | Rear Suspension |
|--------------------------------|------------------|-----------------|
| Spring Stiffness k_2, k_{2P} | 12600 N/m | 24700 N/m |
| Damping rate B_2, B_{2P} | 1850 Ns/m | 2100 Ns/m |
| <u>I.S.V. Response</u> | | |
| Total dynamic deflection | 0.100 | 0.085 |
| Tyre deflection | 0.0142 | 0.0209 |
| Body Force | 1.570 E8 | 2.020 E8 |



Fig. 12.3. Relationship between Integral Square Values of Body Force and Tyre Deflection.
 HILLMAN Front Suspension (Unladen),
 1/2 Car Model.

$k_1 = 155.860 \text{ kN/m}$

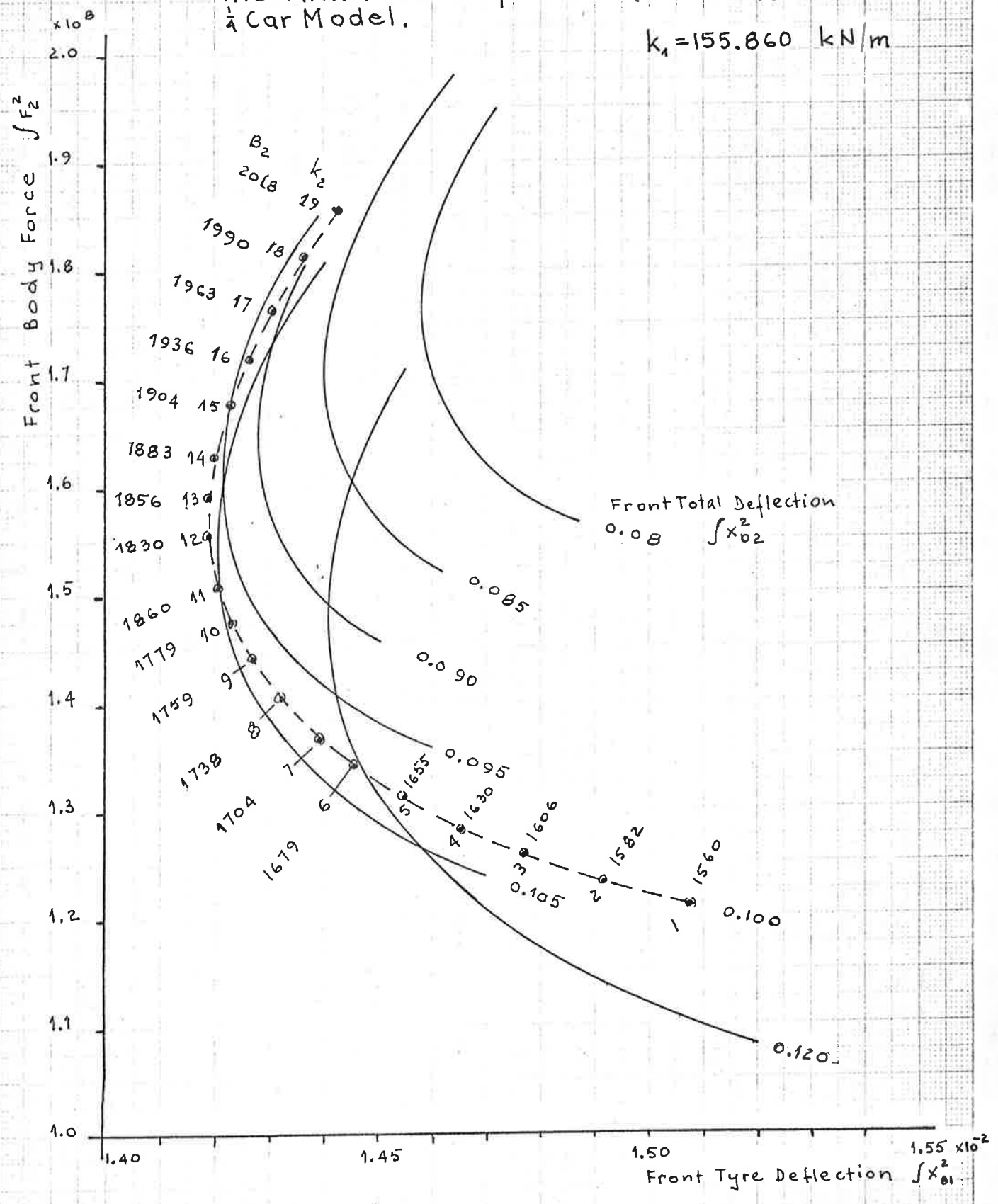
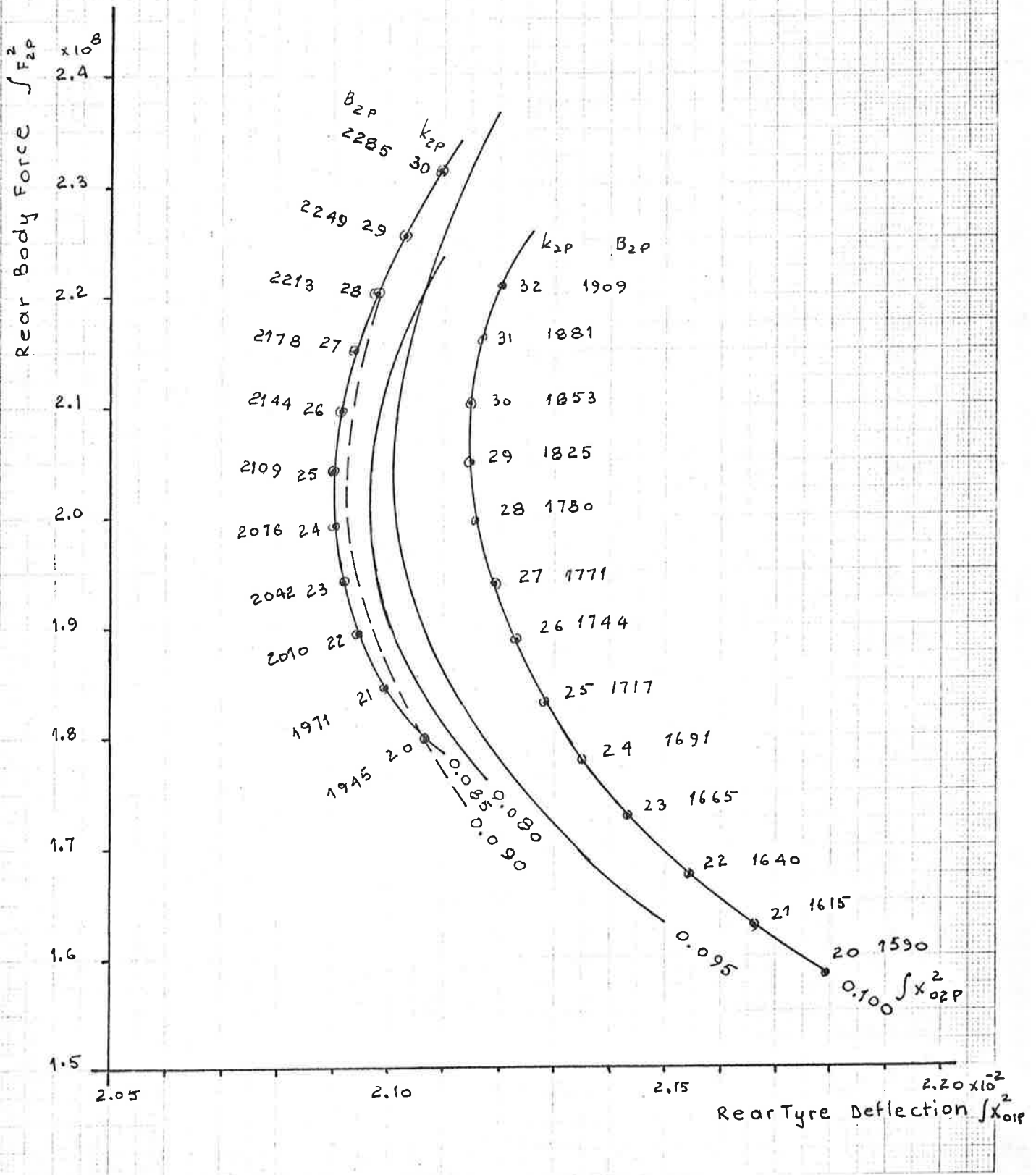




Fig. 12.4. Relationship between Integral Square Values of Body Force and Tyre Deflection. HILLMAN Rear Suspension (Unladen), $\frac{1}{4}$ Car Model.

$k_{1P} = 155.860 \text{ kN/m}$



It is expected that the values listed in Table 12.1 will be close to the values that minimise the integral square value of dynamic tyre deflection.

In Chapter 5 it was shown that for minimum value of dynamic tyre deflection

$$k_{2OPT} = k_1 \frac{m_1 m_2}{(m_1 + m_2)^2}$$

$$\text{and } B_{2OPT} = \frac{m_2}{m_1 + m_2} \sqrt{\frac{k_1 m_1 m_2}{m_1 + m_2}} = m_2 \sqrt{\frac{k_{2OPT}}{m_1 + m_2}}$$

After substituting the values, the result is

$$k_{2OPT} = 12765 \text{ N/m}$$

$$B_{2OPT} = 1832 \text{ Ns/m} \quad \text{for the front suspension}$$

and

$$k_{2OPT} = 25047 \text{ N/m}$$

$$B_{2OPT} = 2080 \text{ Ns/m} \quad \text{for the rear suspension}$$

which are very close to the previous results.

A similar analysis can be extended to $\frac{1}{2}$ -car model with the additional constraint of constant overall static stiffness, i.e. $k_0 = \text{CONST.}$

The integral square values for a coupled model ($R \neq 1.0$) can be obtained by analogue or by digital simulation, but the process would be lengthy and rather expensive in terms of computing costs if carried out on a digital machine.

The computations for an uncoupled model ($R=1.0$) are relatively straight-forward, and can be carried out using equations shown in Chapter 8. The calculations were carried out for $\frac{1}{2}$ -car HILLMAN model ($R=1.0$) using interactive Basic Program OPT2 shown in Appendix C, and the results are plotted in Fig. 12.5 for the model having an overall static stiffness $k_0 = 40813 \text{ N/m}$.

The "optimum" values obtained from Fig. 12.5 are shown in Table 12.2.

Performance index shown was calculated with weighting factors

$$\begin{aligned} \rho &= 8 \times 10^{-10} \\ q_1 &= 10 \\ q_2 &= 1.0 \end{aligned}$$



Fig. 12.5. Relationship between Integral Square Values of Body Force and Tyre Deflection
 HILLMAN $\frac{1}{2}$ Car Model (Unladen), $R=1.0$

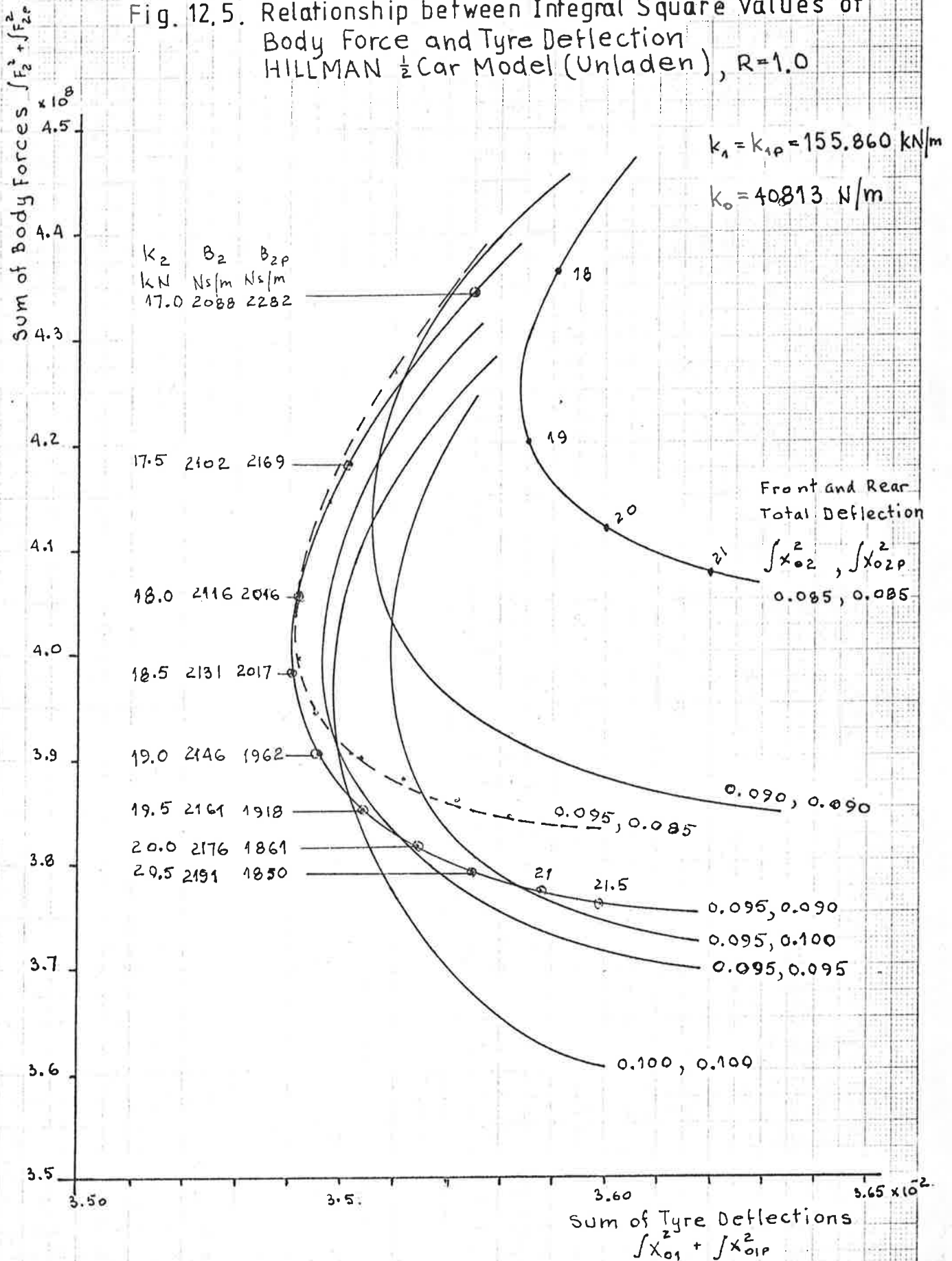


TABLE 12.2 OPTIMUM SUSPENSION $\frac{1}{2}$ -CAR MODEL
HILLMAN DATA (UNLADEN), $R=1.0$, $k_0 = 40813 \text{ N/m}$

| | Front Suspension | Rear Suspension | |
|--------------------------|---------------------|--------------------|-----------|
| Spring Stiffness | 18290 N/m | 27700 N/m | |
| Damping rate | 2125 Ns/m | 2043 Ns/m | |
| Damping ratio ζ | 0.462 | 0.417 | |
| I.S.V. Response | Front | Rear | Sum |
| Total dynamic deflection | 0.095 | 0.090 | 0.1850 |
| Dynamic tyre deflection | 0.014464 | 0.020942 | 0.035406 |
| Relative wheel travel | 0.0747096 | 0.062119 | 0.140929 |
| Body Force | 1.90593E8 | 2.10054E8 | 4.00647E8 |
| Perf. Index | 0.37182 | 0.44368 | 0.81551 |

The suspension parameter values and I.S.V. response for the conditions of minimum dynamic tyre deflection, minimum body force, and minimum performance index were also calculated, and are listed for comparison in Tables 12.3, 12.4 and 12.5 respectively.

TABLE 12.3 SUSPENSION PARAMETERS AND ISV RESPONSE FOR
MINIMUM TYRE DEFLECTION
($R=1.0$, $k_0 = 40813 \text{ N/m}$)

| | Front Suspension | Rear Suspension | |
|--------------------------|---------------------|--------------------|-----------|
| Spring Stiffness | 18563 N/m | 26648 N/m | |
| Damping rate | 1851 Ns/m | 2081 Ns/m | |
| Damping ratio ζ | 0.400 | 0.434 | |
| I.S.V. Response | Front | Rear | Sum |
| Total Dynamic Deflection | 0.107135 | 0.087613 | 0.194748 |
| Dynamic Tyre Deflection | 0.014338 | 0.020920 | 0.035258 |
| Relative Wheel Travel | 0.085783 | 0.065022 | 0.150805 |
| Body Force | 1.7378E8 | 2.0832E8 | 3.82099E8 |
| Perf. Index | 0.36819 | 0.44087 | 0.80906 |

TABLE 12.4 SUSPENSION PARAMETERS AND ISV RESPONSE FOR
MINIMUM BODY FORCE ($R=1.0$, $k_0 = 40813 \text{ N/m}$)

| | Front Suspension | Rear Suspension | |
|--------------------------|---------------------|--------------------|-----------|
| Spring stiffness | 22956 N/m | 17873 N/m | |
| Damping rate | 1036 Ns/m | 745 Ns/m | |
| Damping ratio ζ | 0.201 | 0.190 | |
| I.S.V. Response | Front | Rear | Sum |
| Total dynamic deflection | 0.192597 | 0.194273 | 0.386870 |
| Dynamic tyre deflection | 0.0173543 | 0.033542 | 0.050895 |
| Relative wheel travel | 0.153222 | 0.181669 | 0.33489 |
| Body force | 1.61518E8 | 1.16038E8 | 2.77556E8 |
| Perf. Index | 0.45598 | 0.60992 | 1.0659 |

TABLE 12.5 SUSPENSION PARAMETERS AND ISV RESPONSE FOR
MINIMUM PERFORMANCE INDEX ($R=1.0$, $k_0 = 40813 \text{ N/m}$)

| | Front Suspension | Rear Suspension | |
|--------------------------|---------------------|--------------------|-----------|
| Spring stiffness | 20840 N/m | 20814 N/m | |
| Damping rate | 1860 Ns/m | 1890 Ns/m | |
| Damping ratio ζ | 0.379 | 0.445 | |
| I.S.V. Response | Front | Rear | Sum |
| Total dynamic deflection | 0.109547 | 0.0877983 | 0.197345 |
| Dynamic tyre deflection | 0.144726 | 0.0210871 | 0.035560 |
| Relative wheel travel | 0.0853538 | 0.0715796 | 0.156933 |
| Body force | 1.82019E8 | 1.78296E8 | 3.60316E8 |
| Perf. Index | 0.37569 | 0.42509 | 0.80078 |

In addition, calculations were carried out for further two combinations of suspension springs and dampers as under:-

- (1) Springs selected for minimum body force, and dampers for minimum tyre deflection for the given spring
- (2) Springs selected for minimum tyre deflection, and dampers selected for minimum body force.

The calculations were based on equations developed in Chapters 5 and 8. The results are listed in Tables 12.6 and 12.7 respectively.
(HILLMAN $\frac{1}{2}$ -Car Model, Unladen, $R=1.0$, $k_0 = 40813 \text{ N/m}$)

TABLE 12.6

(Springs selected for min. body force, dampers for min. tyre defl.)

| | Front Suspension | Rear Suspension | |
|--------------------------|---------------------|--------------------|----------|
| Spring stiffness | 21650 N/m | 19511 N/m | |
| Damping rate | 1875 Ns/m | 2092 Ns/m | |
| Damping ratio ζ | 0.375 | 0.509 | |
| I.S.V. Response | Front | Rear | Sum |
| Total dynamic deflection | 0.109786 | 0.0799451 | 0.189731 |
| Dynamic tyre deflection | 0.014530 | 0.021037 | 0.035567 |
| Relative wheel travel | 0.084648 | 0.064660 | 0.149308 |
| Body force | 1.85834E8 | 1.87666E8 | 3.7350E8 |
| Perf. Index | 0.37861 | 0.42516 | 0.80378 |

TABLE 12.7

(Spring selected for min. tyre defl., dampers for min. body force)

| | Front Suspension | Rear Suspension | |
|--------------------------|---------------------|--------------------|-----------|
| Spring stiffness | 18500 N/m | 26883 N/m | |
| Damping rate | 835 Ns/m | 1120 Ns/m | |
| Damping ratio ζ | 0.181 | 0.232 | |
| I.S.V. Response | Front | Rear | Sum |
| Total dynamic deflection | 0.224626 | 0.149419 | 0.374044 |
| Dynamic tyre deflection | 0.019117 | 0.025068 | 0.044185 |
| Relative wheel travel | 0.190129 | 0.120790 | 0.310919 |
| Body force | 1.30143E8 | 1.74576E8 | 3.04719E8 |
| Perf. Index | 0.48541 | 0.51113 | 0.99654 |

The integral square values due to step input excitation are only relative indicators of suspension performance and do not directly display the expected behaviour of the vehicle on the road. A better appreciation could be gained if the model response is referred to some actual road speed and associated road roughness parameter "c".

For a more direct comparison of different suspensions, the response was referred to top speed of 100 km/hr on a good motorway ($c = 1 \times 10^{-6}$) where the performance criterion is mainly the R.M.S. acceleration level as the basic yardstick for ride comfort, and at 35 km/hr on a rough road ($c = 1 \times 10^{-4}$) where road holding and suspension bottoming are the limiting factors.

The following quantities were calculated for each condition:-

- (i) R.M.S. acceleration of centre of mass ($\langle \ddot{x}_G \rangle$)
- (ii) The ratio:- Maximum dynamic tyre force/static wheel load (F_{dyn}/F_{st}).
- (iii) Maximum relative wheel travel ($x_{12 \max}$).

The expected maximum values of response were taken as 3x R.M.S. response.

The results of these calculations are listed in Tables 12.8 and 12.9 for comparison.

TABLE 12.8 EXPECTED RESPONSE AT $V=100$ km/hr, $c=1 \times 10^{-6}$ m
(HILLMAN $\frac{1}{2}$ -CAR, Unladen, $R=1.0$, $k_0 = 40813$ N/m)

| Suspension | $\langle \ddot{x}_G \rangle$ m/s ² | F_{dyn}/F_{st} | | x_{12} max. mm | |
|------------|--|------------------|---------|------------------|--------|
| | | Front | Rear | Front | Rear |
| 12.2 | 0.20887 | 0.10467 | 0.16837 | 4.3218 | 3.9407 |
| 12.3 | 0.20397 | 0.10421 | 0.16828 | 4.6312 | 4.0319 |
| 12.4 | 0.17385 | 0.11465 | 0.15939 | 6.1891 | 6.7393 |
| 12.5 | 0.19808 | 0.10470 | 0.16895 | 4.6196 | 4.2301 |
| 12.6 | 0.20167 | 0.10491 | 0.16875 | 4.6001 | 4.0203 |
| 12.7 | 0.18215 | 0.12033 | 0.18421 | 6.8943 | 5.4950 |

TABLE 12.9 EXPECTED RESPONSE AT $V=35$ km/hr, $c=1 \times 10^{-4}$ m
(HILLMAN $\frac{1}{2}$ -CAR, Unladen, $R=1.0$, $k_0 = 40813$ N/m)

| Suspension | $\langle x_G \rangle$ m/s ² | F_{dyn}/F_{st} | | x_{12} max. mm | |
|------------|---|------------------|--------|------------------|--------|
| | | Front | Rear | Front | Rear |
| 12.2 | 1.2357 | 0.6192 | 0.9961 | 25.568 | 23.314 |
| 12.3 | 1.2067 | 0.6165 | 0.9956 | 27.398 | 23.853 |
| 12.4 | 1.0285 | 0.6783 | 0.9430 | 36.615 | 39.870 |
| 12.5 | 1.1718 | 0.6194 | 0.9995 | 27.330 | 25.025 |
| 12.6 | 1.1931 | 0.6206 | 0.9983 | 27.214 | 23.784 |
| 12.7 | 1.0776 | 0.7119 | 1.0898 | 40.787 | 32.509 |

The comparison of responses listed in Tables 12.8 and 12.9 suggests that there is probably little to choose between the different combinations of suspensions based on different "optima".

The suspensions listed under 12.2, 12.5 and 12.6 exhibit the characteristics very similar to suspension optimised for minimum tyre deflection (12.3), while suspension 12.7 has characteristics similar to suspension that has been optimised for minimum body force (12.4).

The suspension optimised for minimum body force has the lowest possible R.M.S. acceleration as expected, but rather large values of relative wheel travel thus indicating excessive static deflection for a laden vehicle.

Among all the combinations of suspensions listed in Tables 12.8 and 12.9, the maximum variation in vertical R.M.S. acceleration is only 20% while the corresponding variation in relative wheel travel is 60% for the front wheels and 70% for the rear wheels respectively. Hence, a relatively large percentage of wheel travel would have to be traded off for only a small improvement in ride quality.

The tabulated values, in general, agree with the observations of T. DAHLBERG (36, 37, 87) who concludes that optimal road holding is found for suspension parameters lying in the vicinity of those used in today's passenger vehicles, while optimal ride comfort criterion will result in much softer suspensions such that the loading of vehicle would result in excessive static deflection.

The comparisons between different suspension systems so far have been made without any reference to seat dynamics, or more appropriately to the response of passenger/seat interface. This aspect has been investigated by the authors of Ref. (86) quite extensively by studying the input-output spectral densities and transfer functions of the front seat of a typical passenger sedan in actual ride tests.

It was found that the seat acted as a low pass filter to vertical accelerations, with a resonance peaks at 4.9 Hz and 24 Hz respectively. The seat attenuated the frequencies above 6 Hz, with an attenuation of approximately 10 dB at the wheel-hop frequency of 10 Hz.

The general effect of seat dynamics is to filter the higher frequency vertical motions while passing or even amplifying the higher frequency lateral motions.

Since the pass-band for vertical motions is within the frequency range to which the passengers are most sensitive, it can be assumed that the seat input acceleration as measured on the floorboard of the vehicle is a good indicator of the expected ride quality.

These observations were confirmed by the authors of Ref. (27) who observed that the floorboard and passenger/seat interface RMS accelerations were of about the same magnitude. The authors came to the conclusion that the evaluation of ride quality can be based on the acceleration spectra measured either at the floor or at the passenger/seat interface.

The magnitude of RMS acceleration recommended at either of these locations range roughly from 0 to 0.4^0 g for a smooth ride (interstate highway), 0.04 g to 0.06 g for a medium ride, and above 0.06 g for a rough ride.

The authors also proposed a ride indicator R as a measure of ride quality, given in terms of R.M.S. acceleration α (g) measured at the floorboard. The index is expressed by the equation

$$R = 5.55 - 49.4\alpha$$

and varies from $R=1$ to $R=5$ with $R>4$ corresponding to ride in a good automobile on very smooth interstate highway at 80 km/hr, $3 < R < 4$ to an automobile ride on a typical state highway, and $2 < R < 3$ for an automobile ride on a rough secondary road. (In Table 12.8 for comparison, $4.50 < R < 4.67$).

It can be stated, in conclusion, that despite the large number of research papers published on various methods of optimisation of passive suspension systems, there is no unique method that would be a complete answer to the problem. Each of the methods have their own characteristics somewhere in-between the optima for minimum body force and tyre deflection respectively.

Apart from the techniques discussed in this thesis, frequency response methods (15, 38, 42, 88) have been applied quite successfully, but the final conclusion is still the same: there is no uniquely defined optimum suspension, and the final choice will depend on individual subjective judgement.

There is no question however, that the theoretical analysis of the problem and possible computer simulation will go a long way towards selecting an acceptable combination of suspension springs and dampers.

Theoretical analysis will also be very useful in pointing out the directions to be taken even in the case of seat design so as to eliminate the resonant peak, or shift it away from the sensitive low frequency region. This implies a hard seat from the point of view of static behaviour but one which would have improved dynamic response. Apparently manufacturers have realized this and are replacing seat springs by foam

rubber or similar material.

In addition to simulations with random input excitation, the tests with individual road irregularities commonly associated with road construction, such as spoon drains need to be considered in the light of final choice. It is necessary to know how badly the suspension will bottom when crossing a typical drain, and the subsequent behaviour of the vehicle, but again the judgement is subjective.

All in all, the starting point for the design of a suspension can certainly be obtained by calculation or by computer simulation, but the final decision regarding the design would still be subject to individual subjective opinion with due regard to characteristics of the roads over which the vehicle is expected to be driven under normal conditions of usage. Any passive suspension system will be a compromise solution.

APPENDIX A

ANALOGUE COMPUTATION
RESULTS

FIG. A1. ANALOGUE COMPUTER PATCHING DIAGRAM

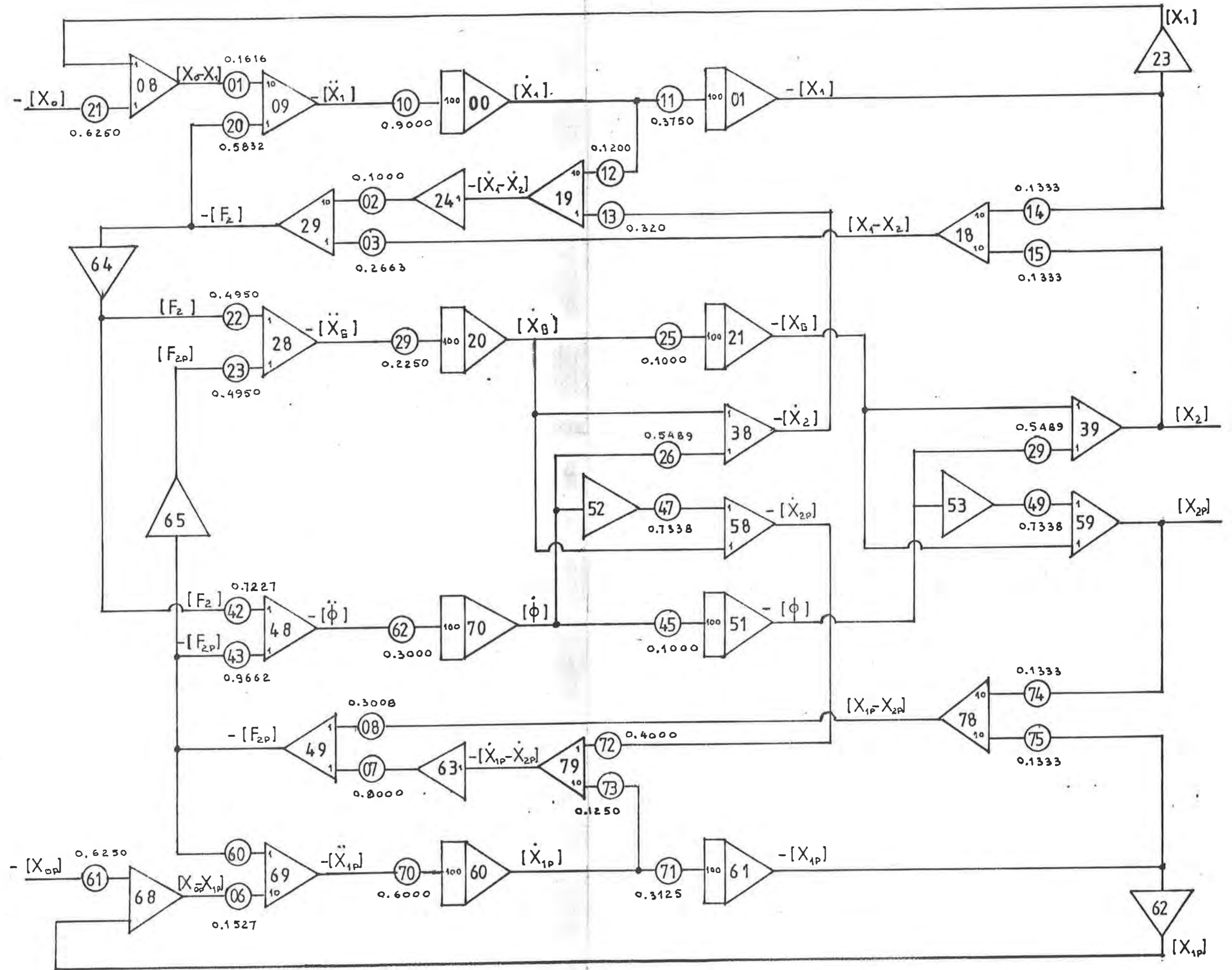


Fig.A 2. Time Response by Analque Computer Simulation.
HILLMAN $\frac{1}{2}$ Car Model, $R=0.7$, $V=30$ m/s

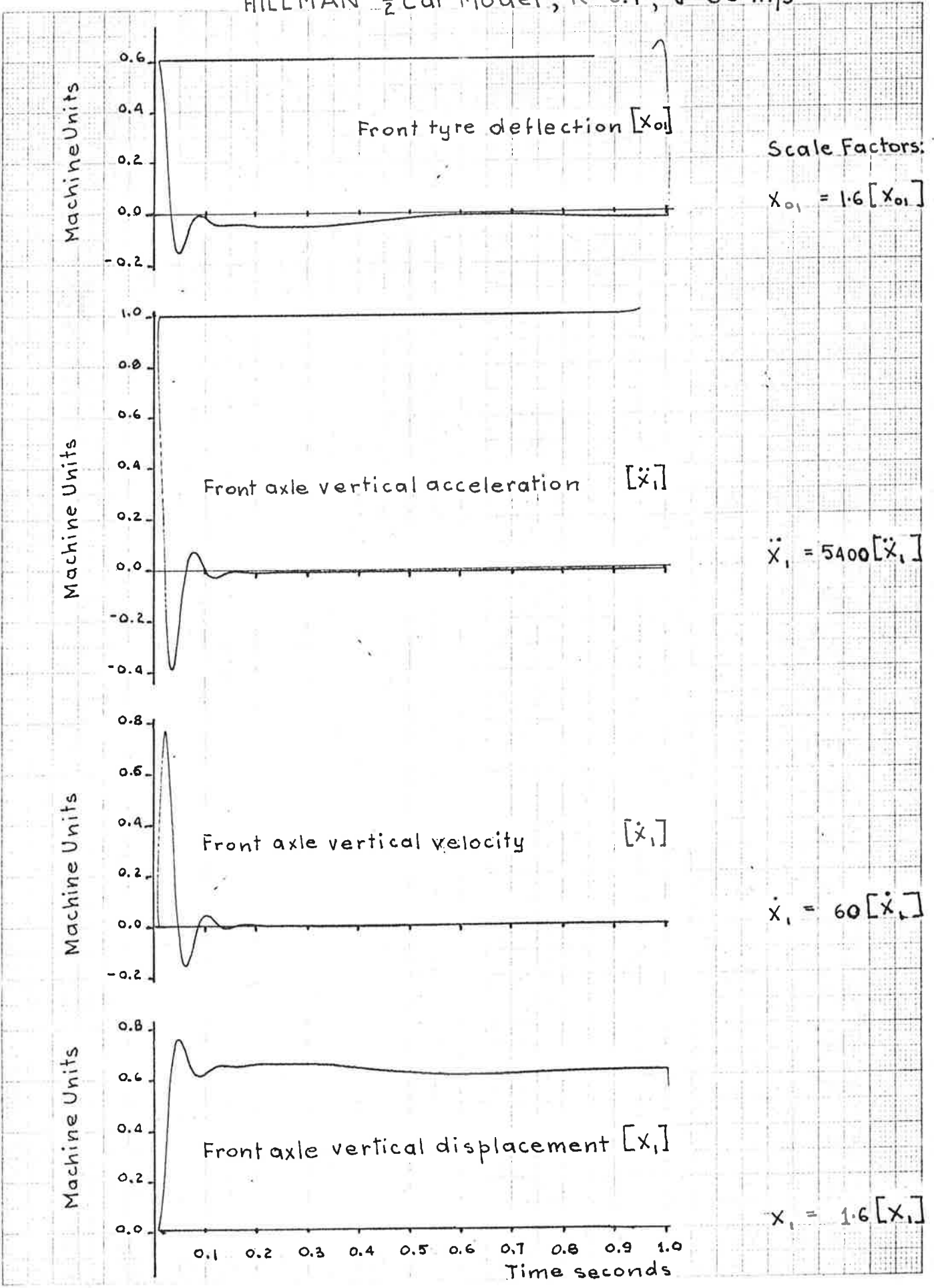


Fig.A 3. Time Response by Analogue Computer Simulation. HILLMAN $\frac{1}{2}$ Car Model, $R=0.7$, $V=30$ m/s

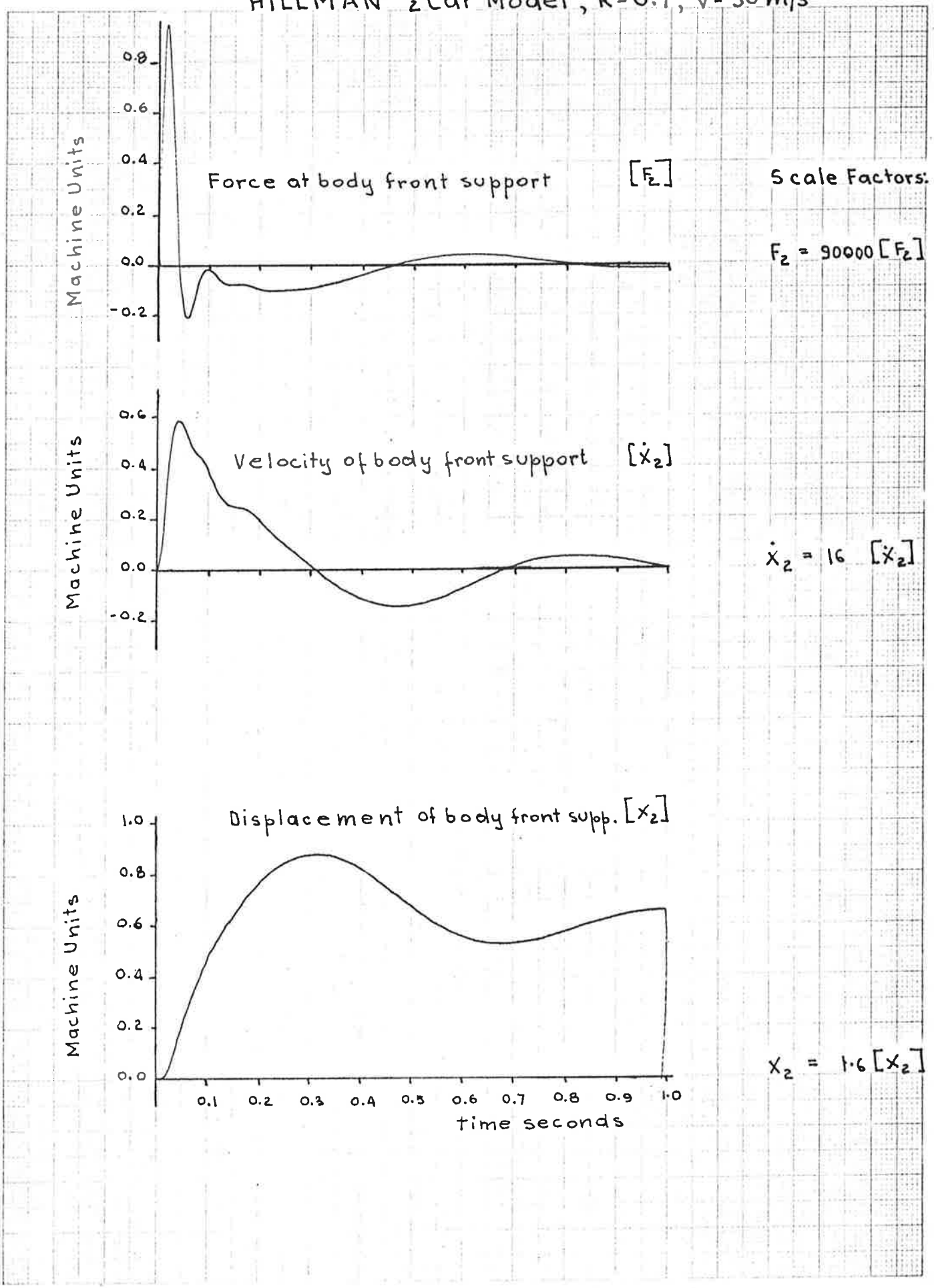
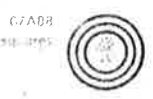


Fig. A 4. Time Response by Analogue Computer Simulation.
 HILLMAN $\frac{1}{2}$ Car Model, $R=0.7$, $V=30$ m/s

Q/ASD

10/10/60

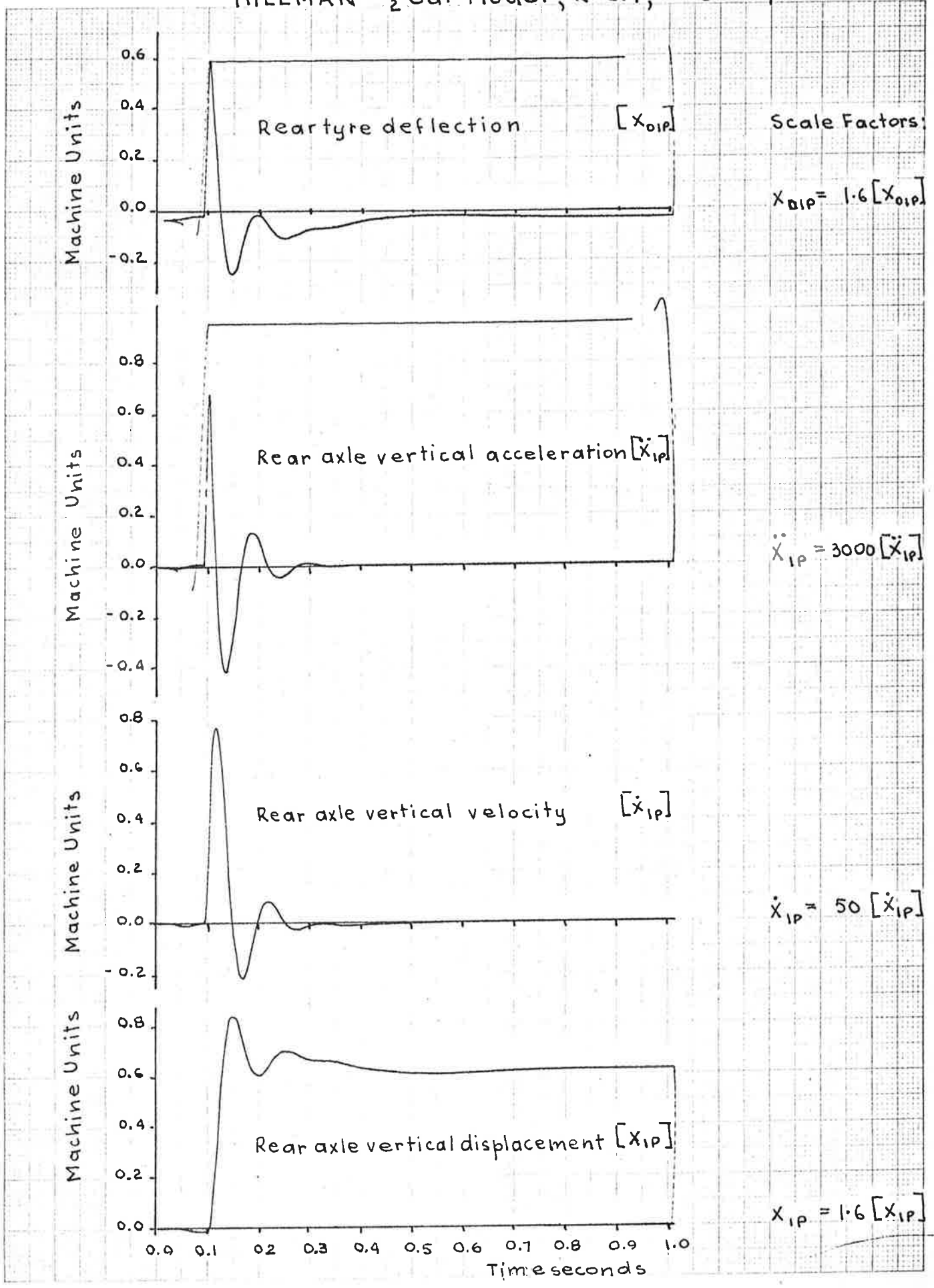


Fig. A 5. Time Response by
Analogue Computer Simulation.
HILLMAN $\frac{1}{2}$ -car Model, $R=0.7$, $V=30$ m/s.

07 APR

7 millimeter squares

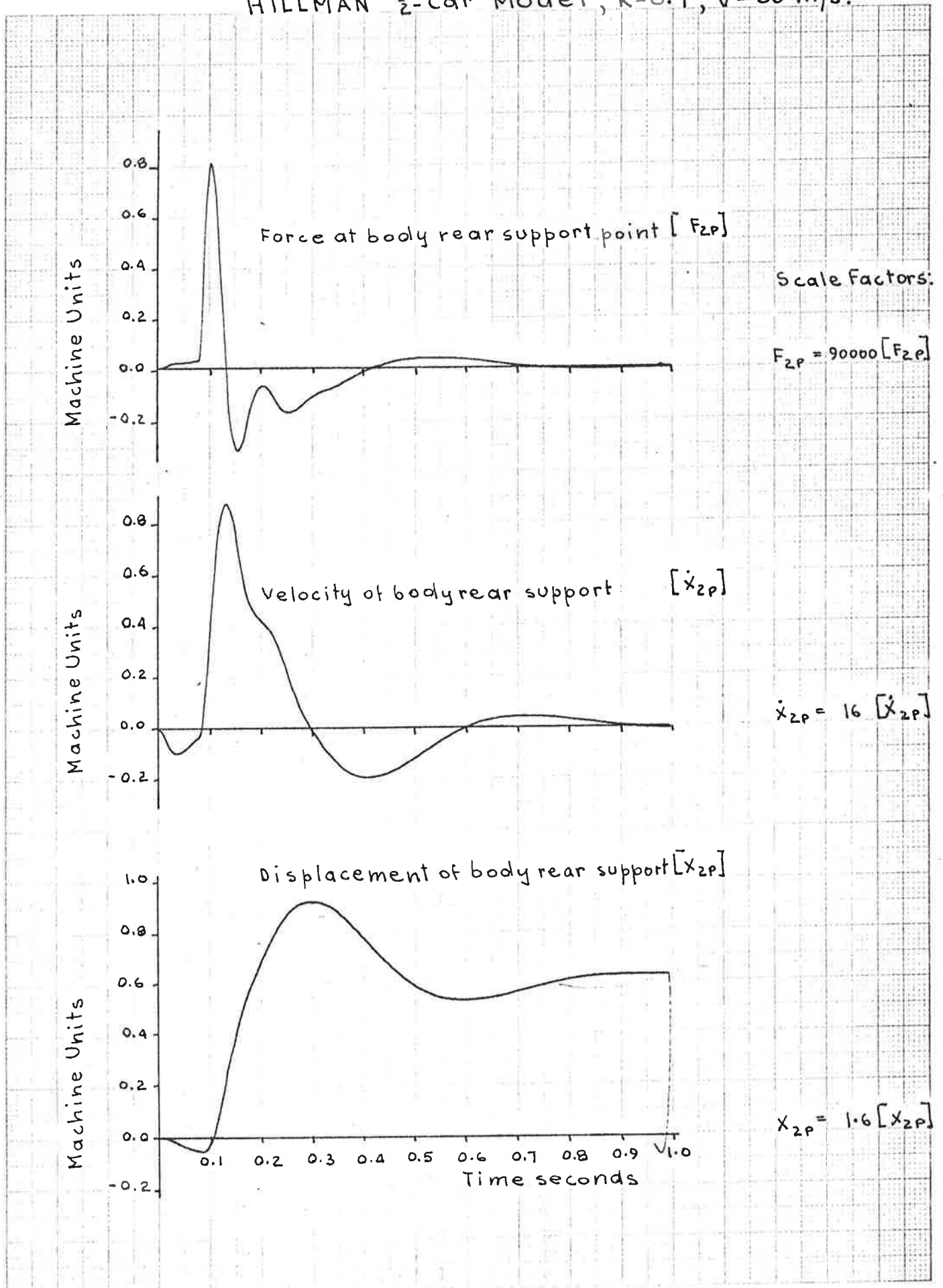


Fig. A 6. Time Response by Analogue Computer Simulation.
 HILLMAN $\frac{1}{2}$ Car Model, $R=0.7$, $V=30$ m/s.

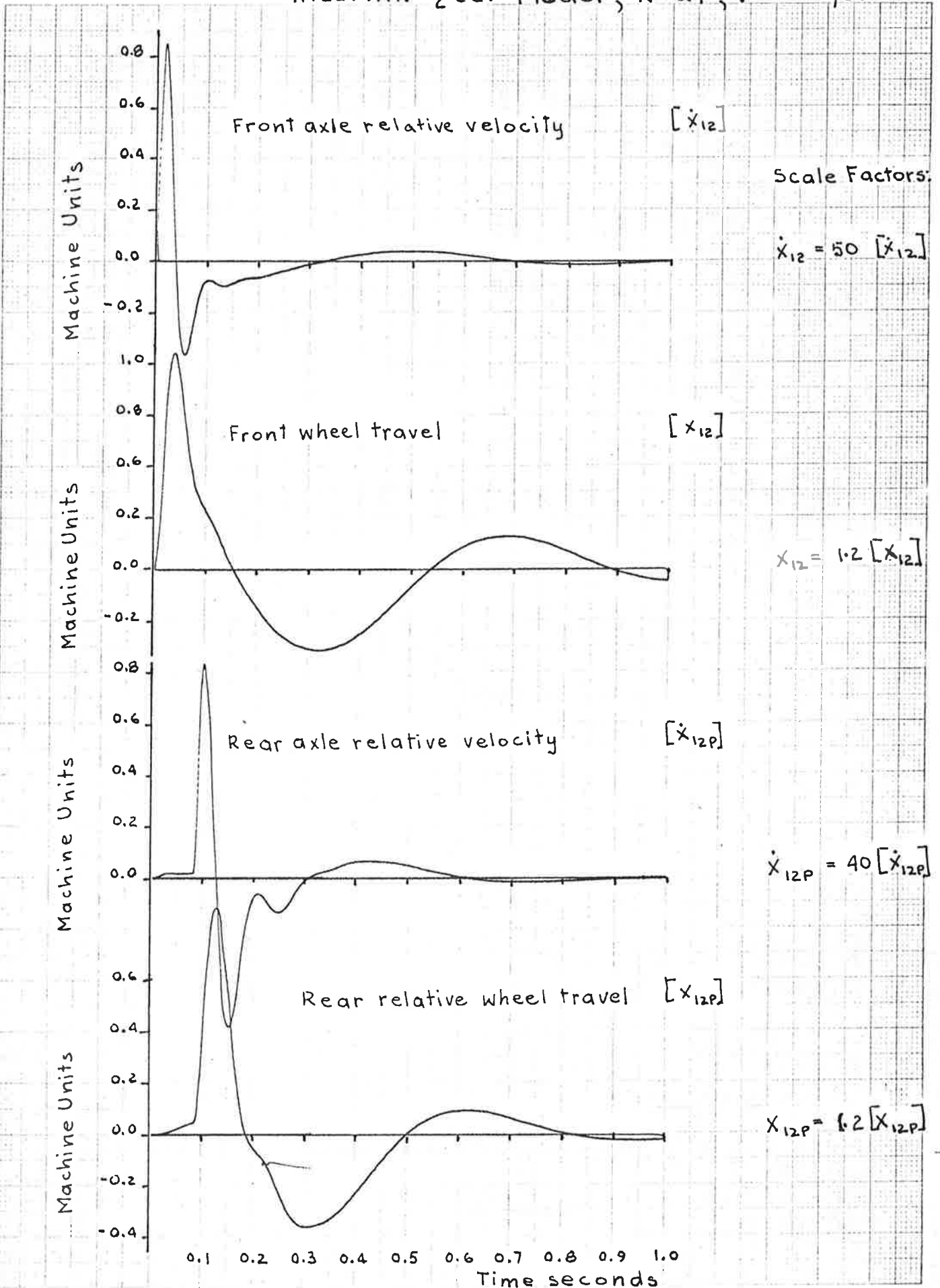
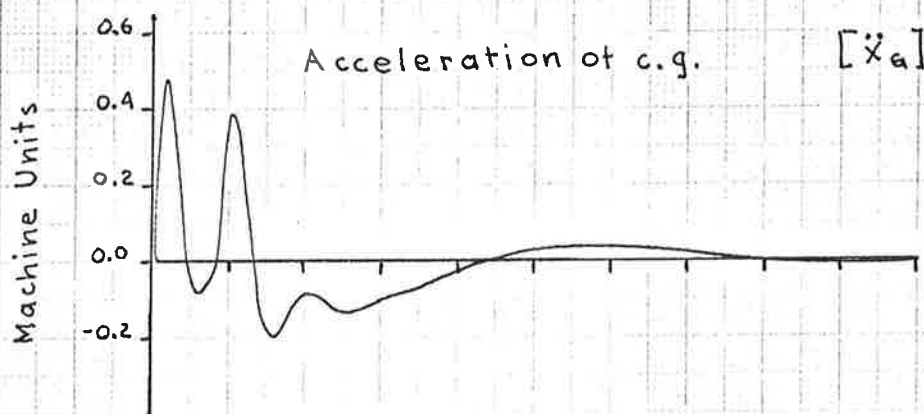
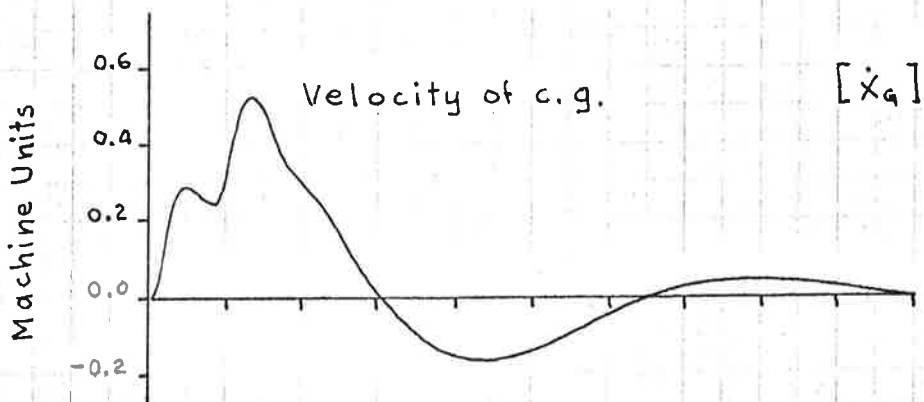


Fig. A7. Time Response by Analogue Computer Simulation. HILLMAN Model, $R=0.7$, $V=30$ m/s.

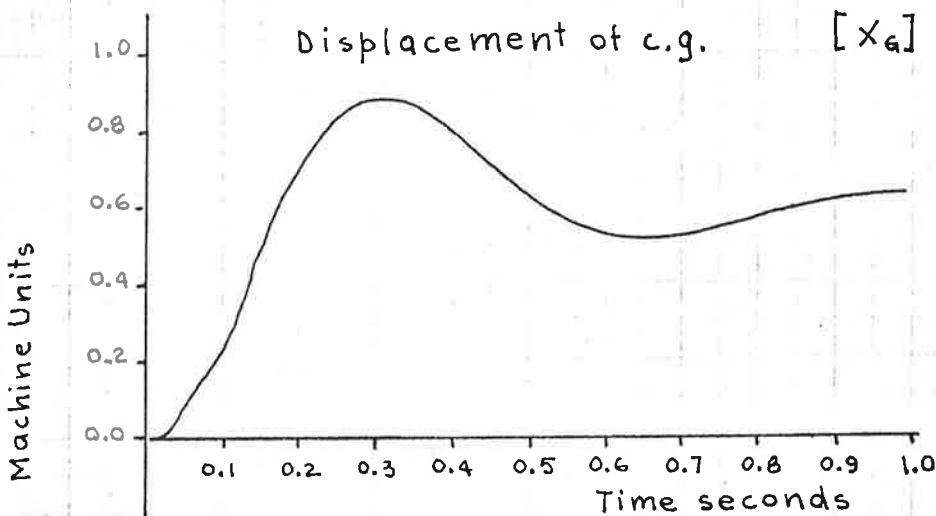


Scale Factors:

$$\ddot{x}_g = 360 [\ddot{x}_g]$$



$$\dot{x}_g = 16 [\dot{x}_g]$$



$$x_g = 1.6 [x_g]$$

Fig. A 8. Time Response by Analogue Computer Simulation.
 HILLMAN $\frac{1}{2}$ Car Model, $R=0.7$, $V=30$ m/s

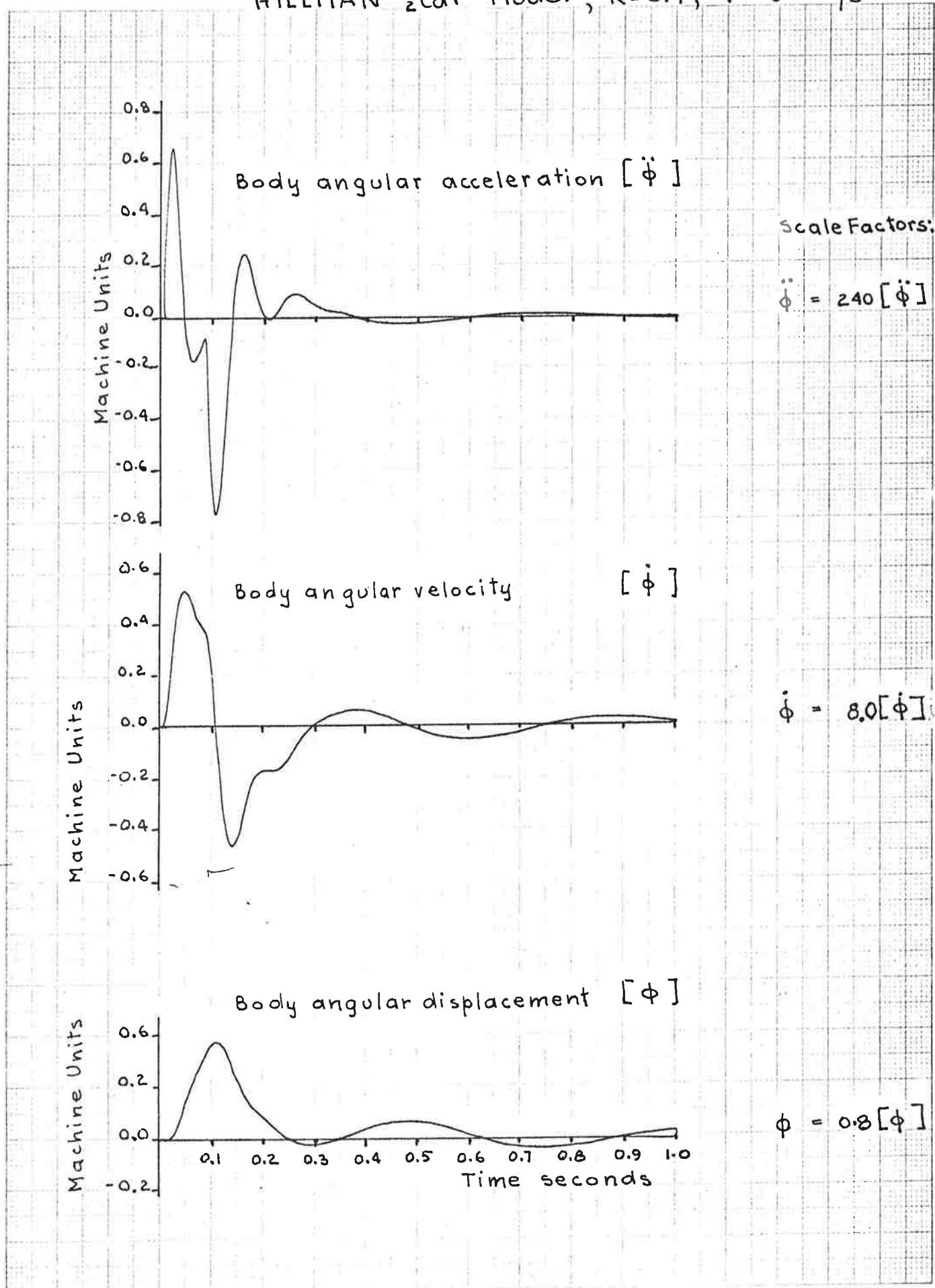


Fig. A 9. Acceleration Square Integrals
by Analogue Computer Simulation.
HILLMAN $\frac{1}{2}$ -Car Model, $R=0.7$, $V=30$ m/s.

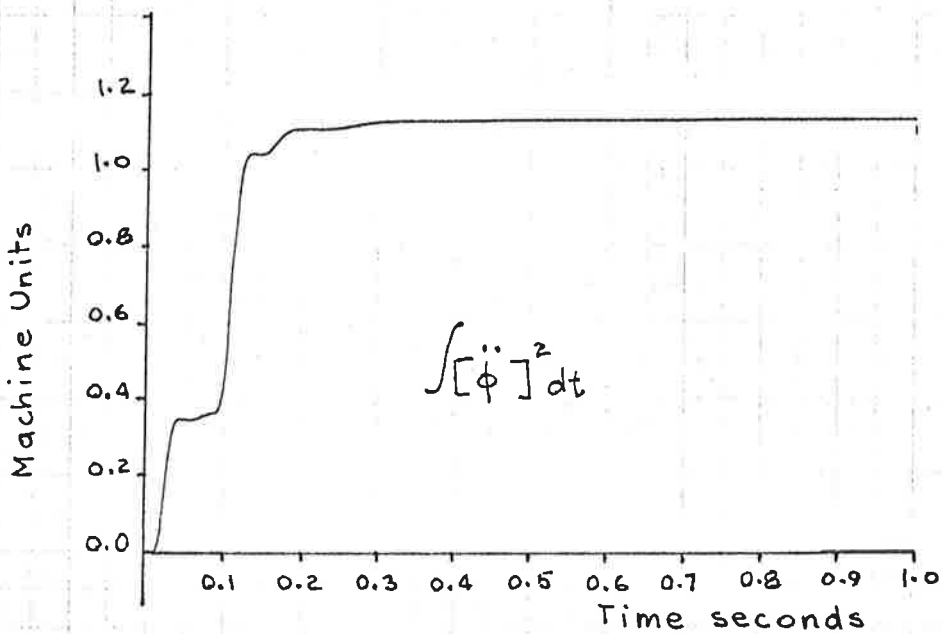
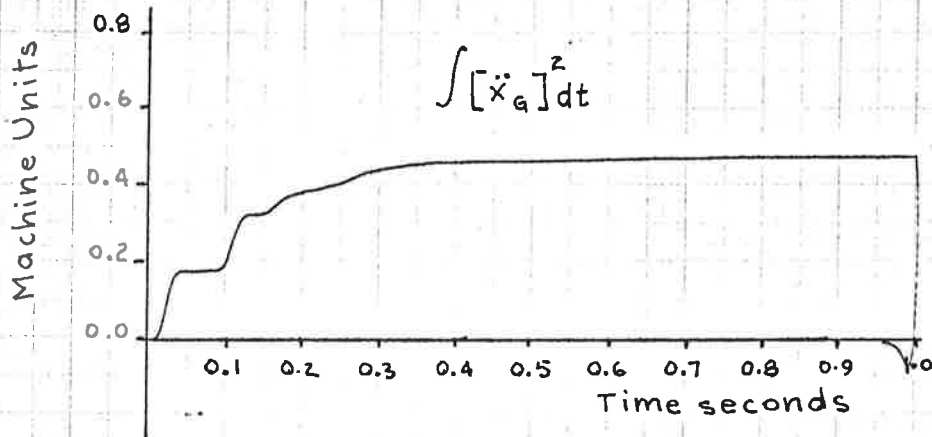
U7 ARE
The square

Fig. A 10. Time Response of Body Acceleration
 by Analogue Computer Simulation.
 HILLMAN $\frac{1}{2}$ Car Model, $R=0.7$, $V=5$ m/s.

SPAS
 SYSTEM

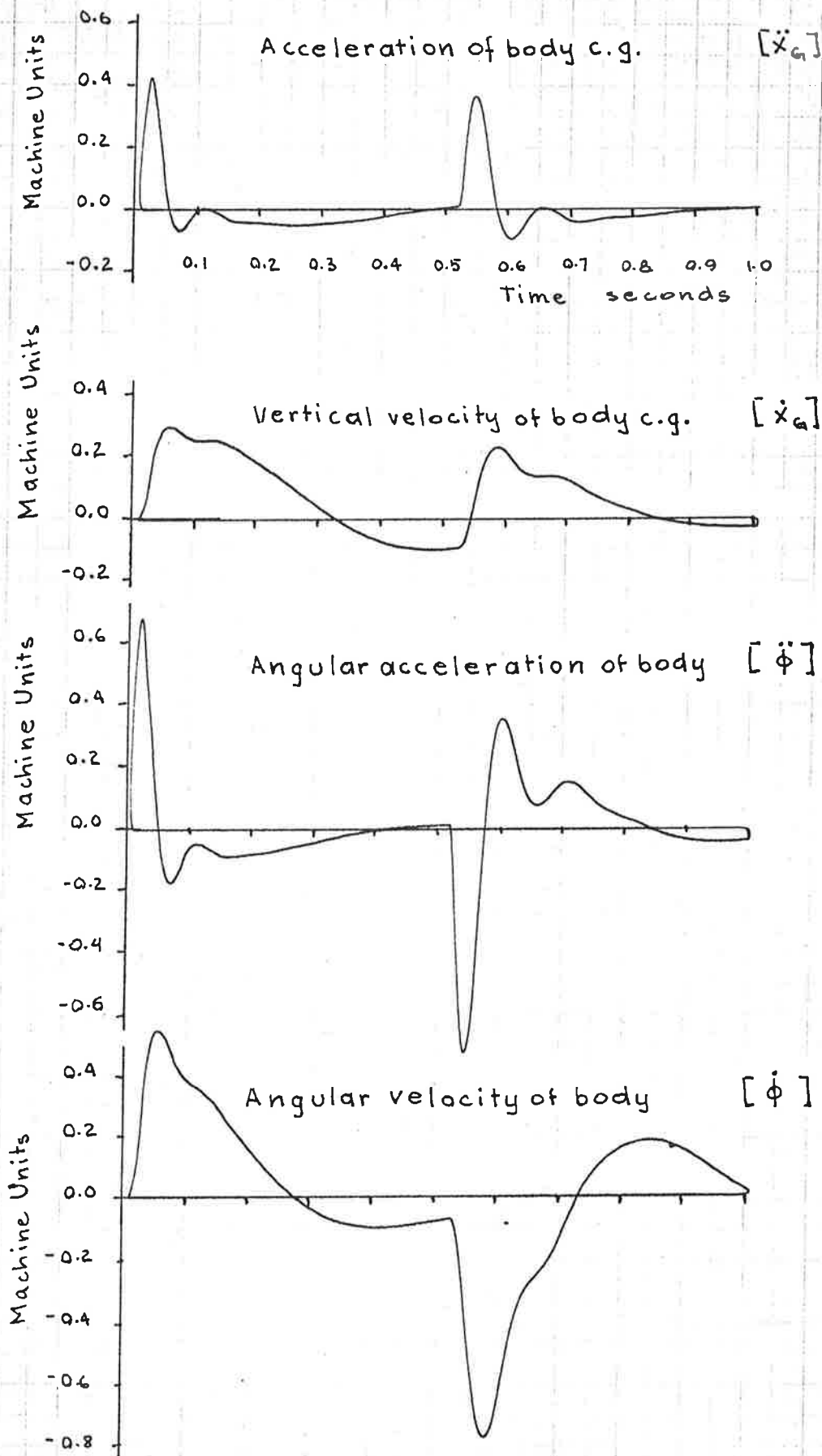


Fig. A 11. Body Acceleration by
 Analogue Computer Simulation.
 HILLMAN $\frac{1}{2}$ Car Model, $R=0.7$, $V=10$ m/s.

07A39

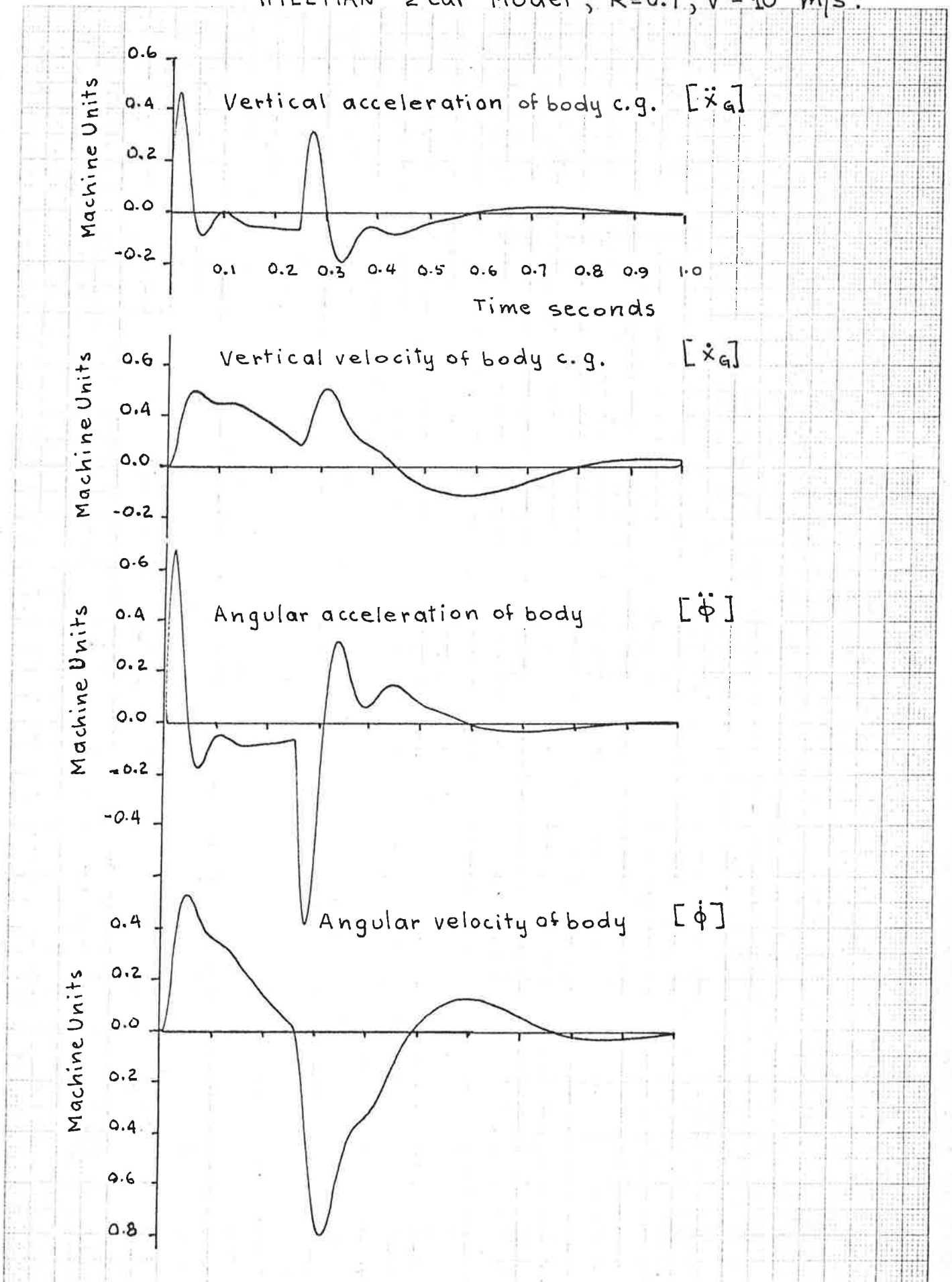


Fig. A 12. Body Acceleration by
Analogue Computer Simulation.
HILLMAN $\frac{1}{2}$ Car Model, $R=0.7$, $V=20$ m/s.

02758

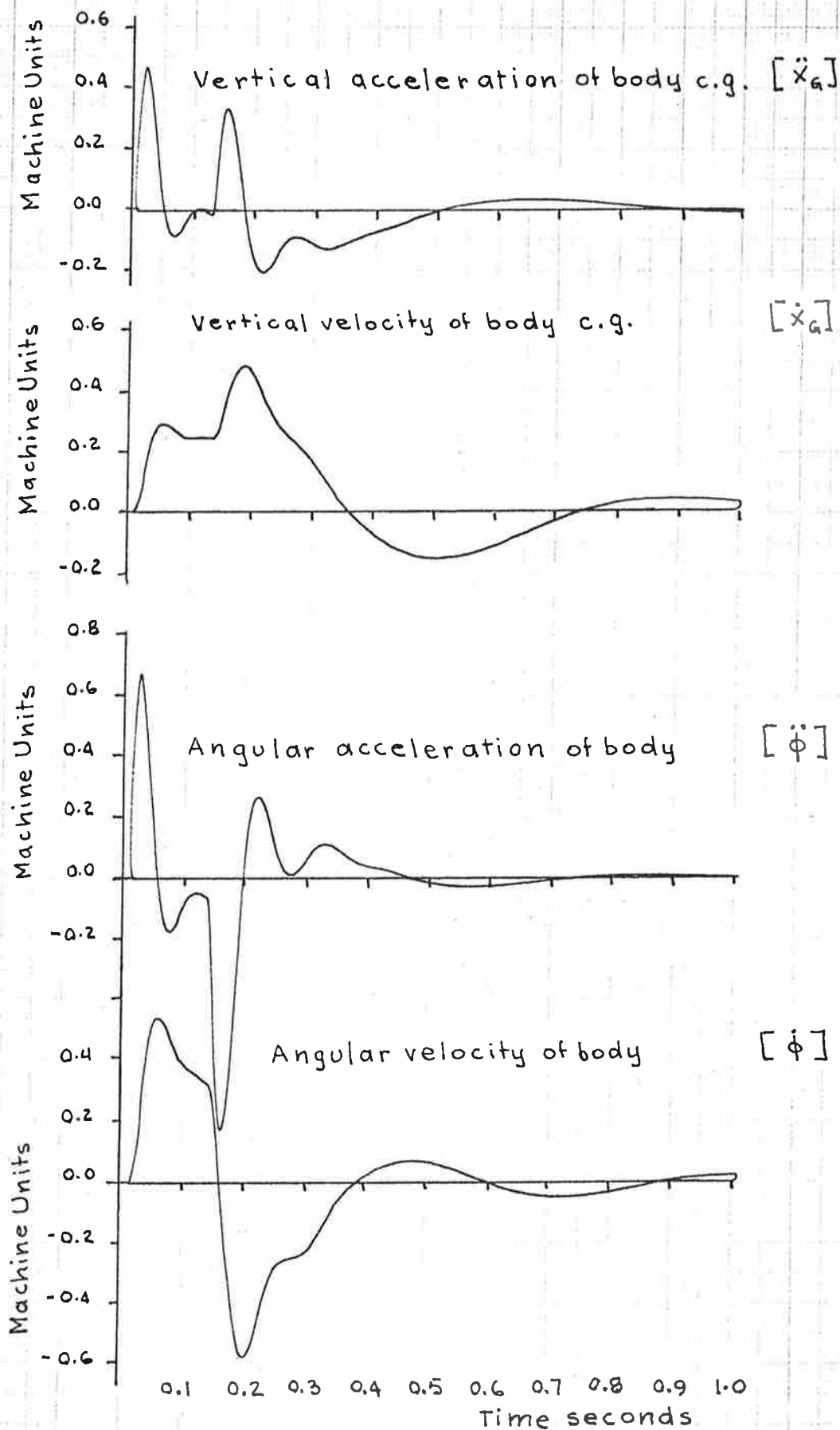


Fig. A 13. Body Acceleration by
Analogue Computer Simulation.
HILLMAN $\frac{1}{2}$ Car Model, $R=0.7$, $V=40$ m/s.

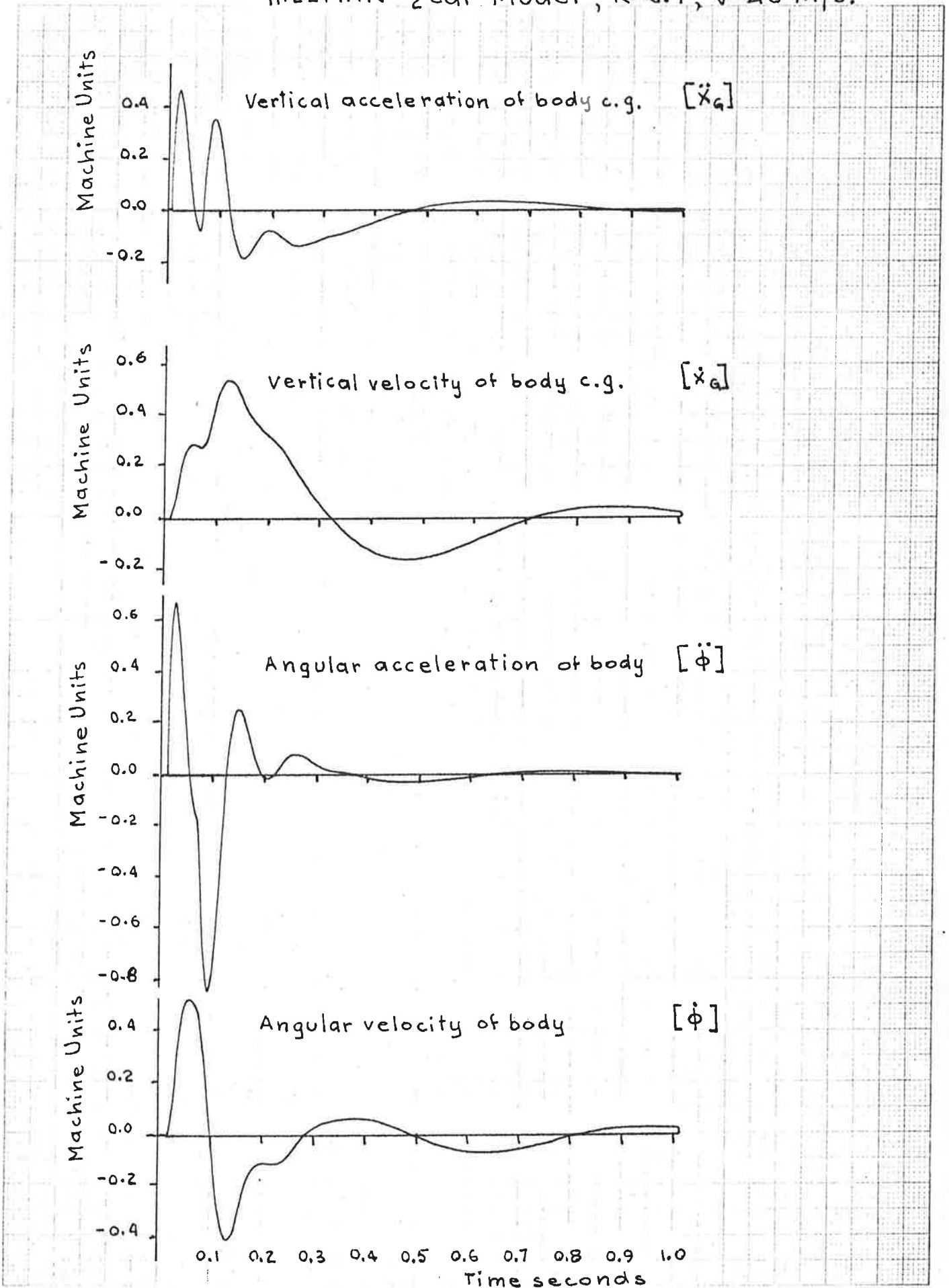


Fig. A14. Body Acceleration by
 Analogue Computer Simulation.
 HILLMAN $\frac{1}{2}$ Car Model, $R=0.7$, $V=50$ m/s.

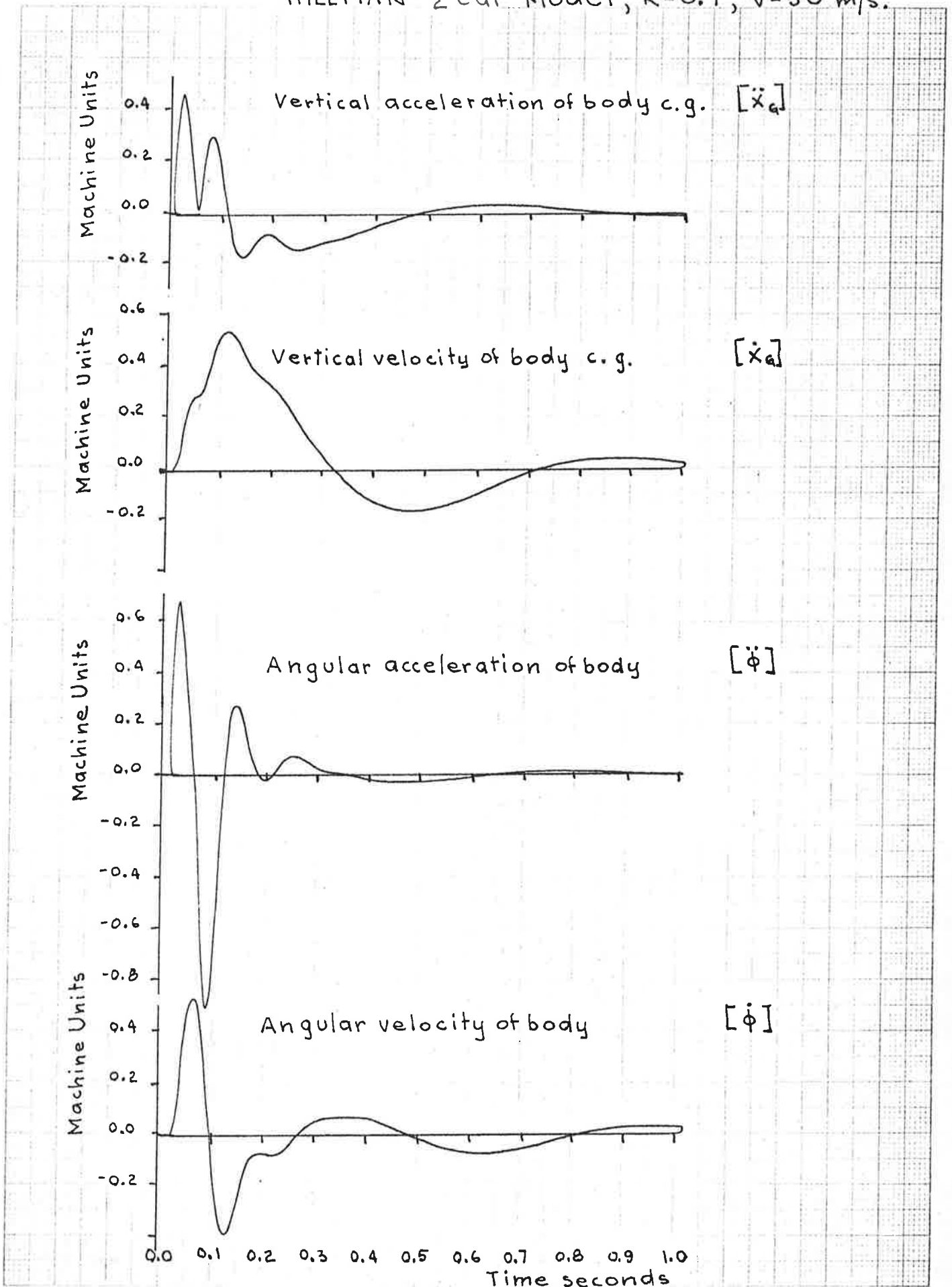


Fig A15. Acceleration and Velocity Square Integrals by Analogue Computer.
 HILLMAN $\frac{1}{2}$ Car Model, $R=0.7$, $V=20\text{m/s}$.

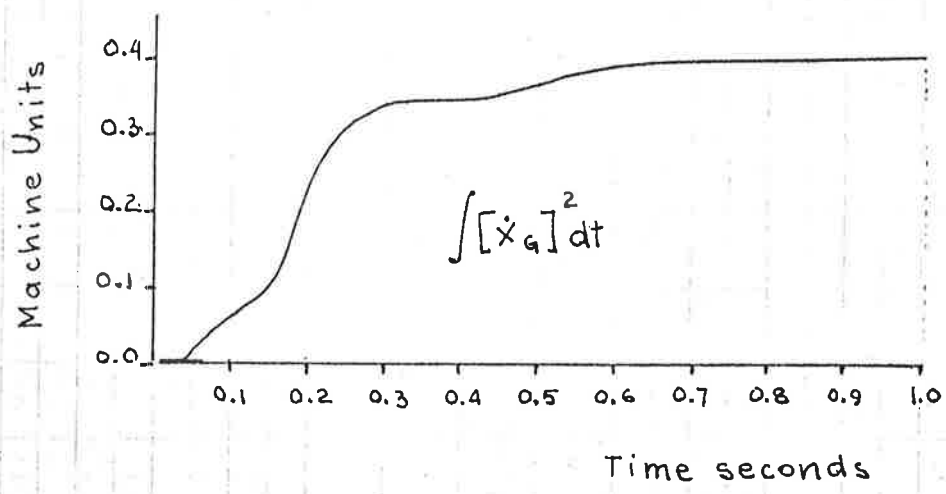
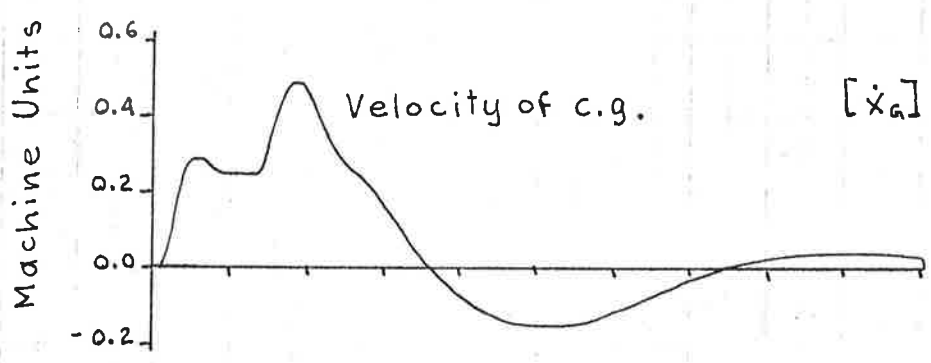
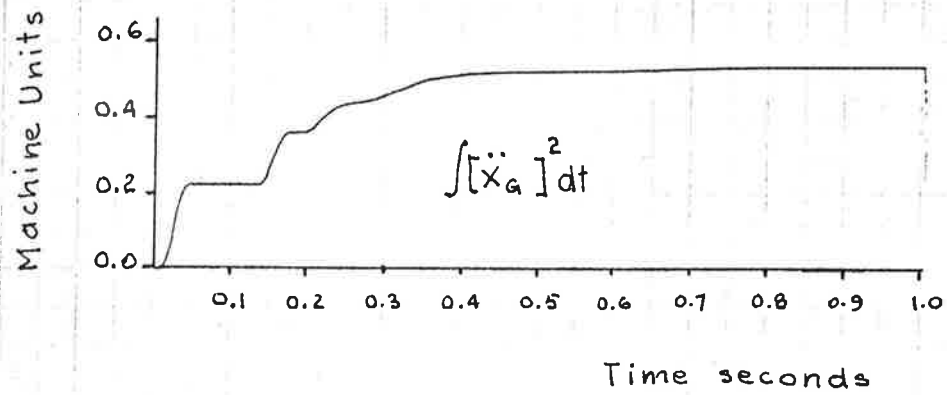
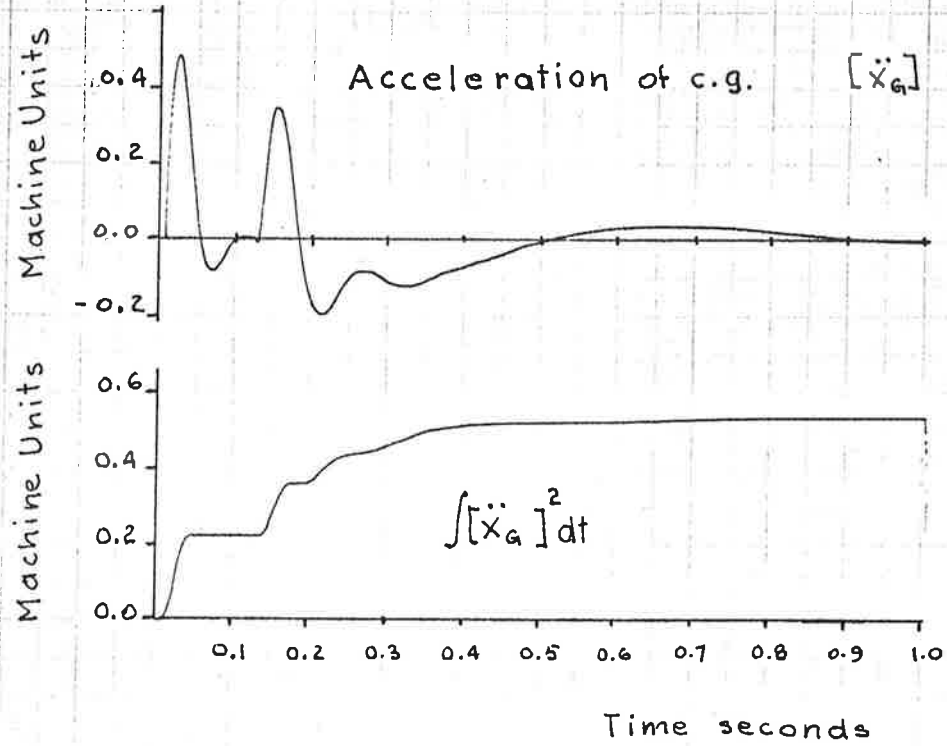


Fig. A16. Acceleration and Velocity Square Integrals by Analogue Computer.
 HILLMAN $\frac{1}{2}$ Car Model, $R=0.7$, $V=20$ m/s.

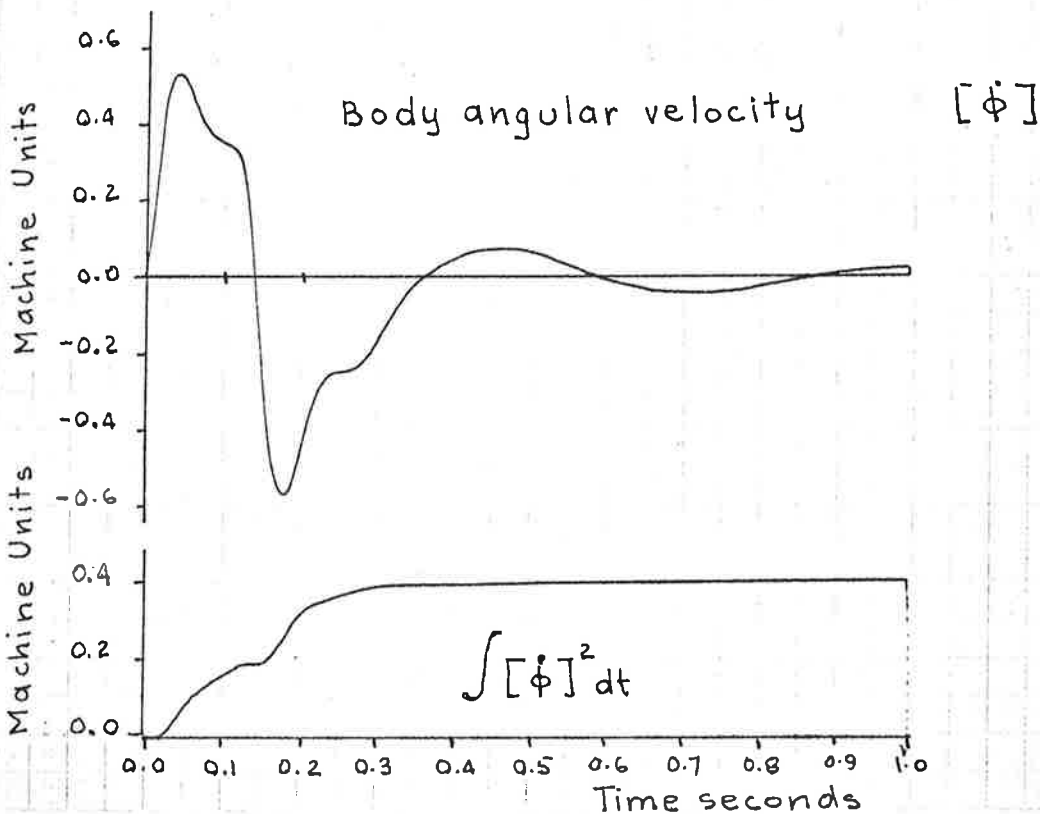
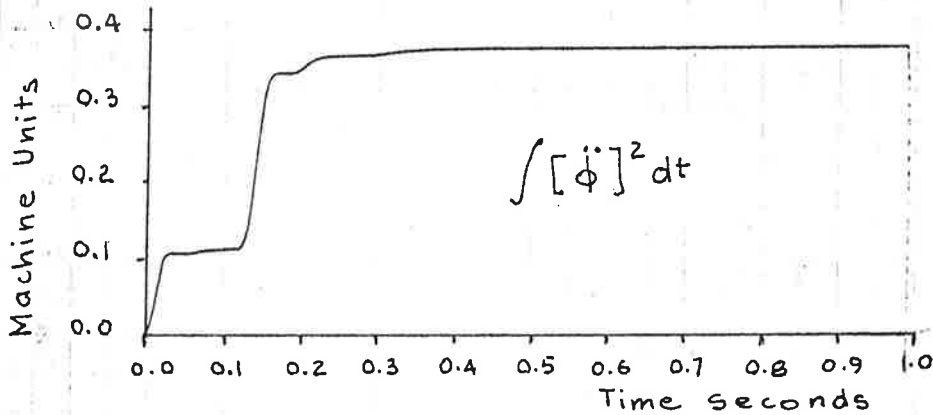
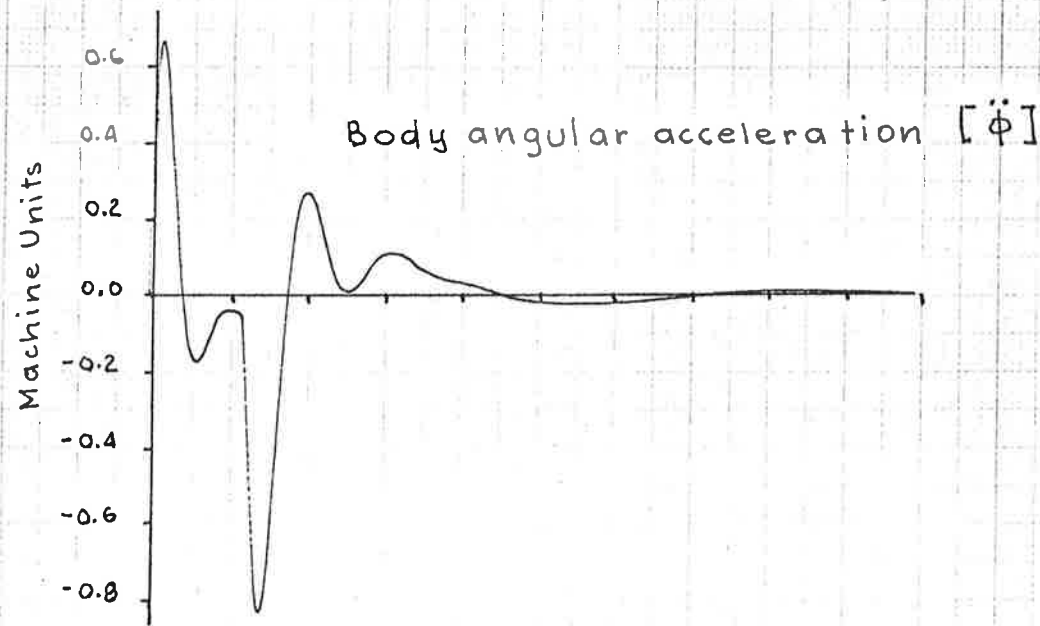


Fig. A 17. Time Response
by Analogue Computer Simulation.
HILLMAN $\frac{1}{2}$ -Car Model, $R=0.7$, $V=7.2$ m/s.

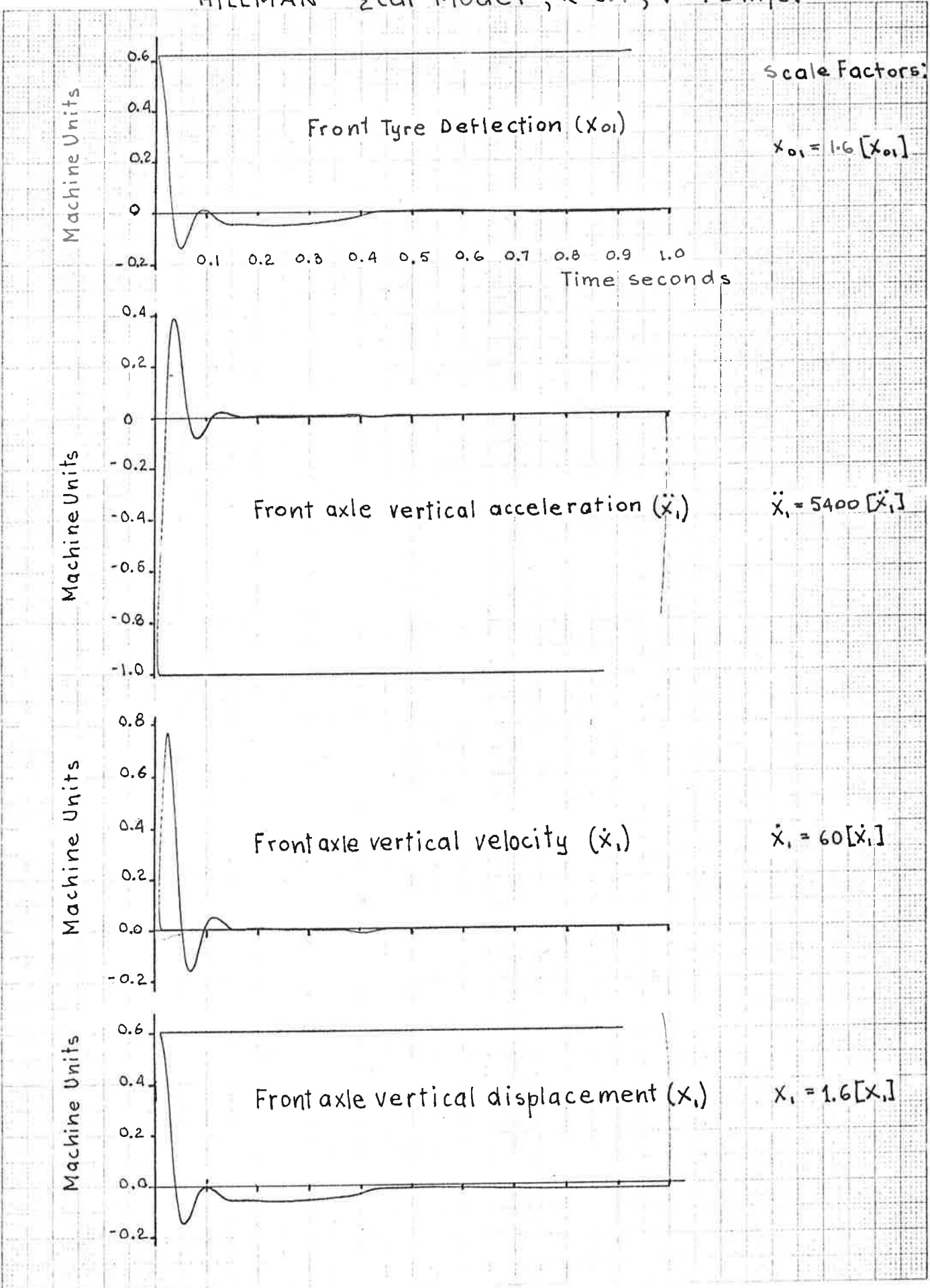
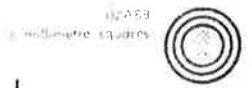


Fig. A 18. Time Response
 by Analogue Computer Simulation.
 HILLMAN $\frac{1}{2}$ -Car Model, $R=0.7$, $V=7.2$ m/s.

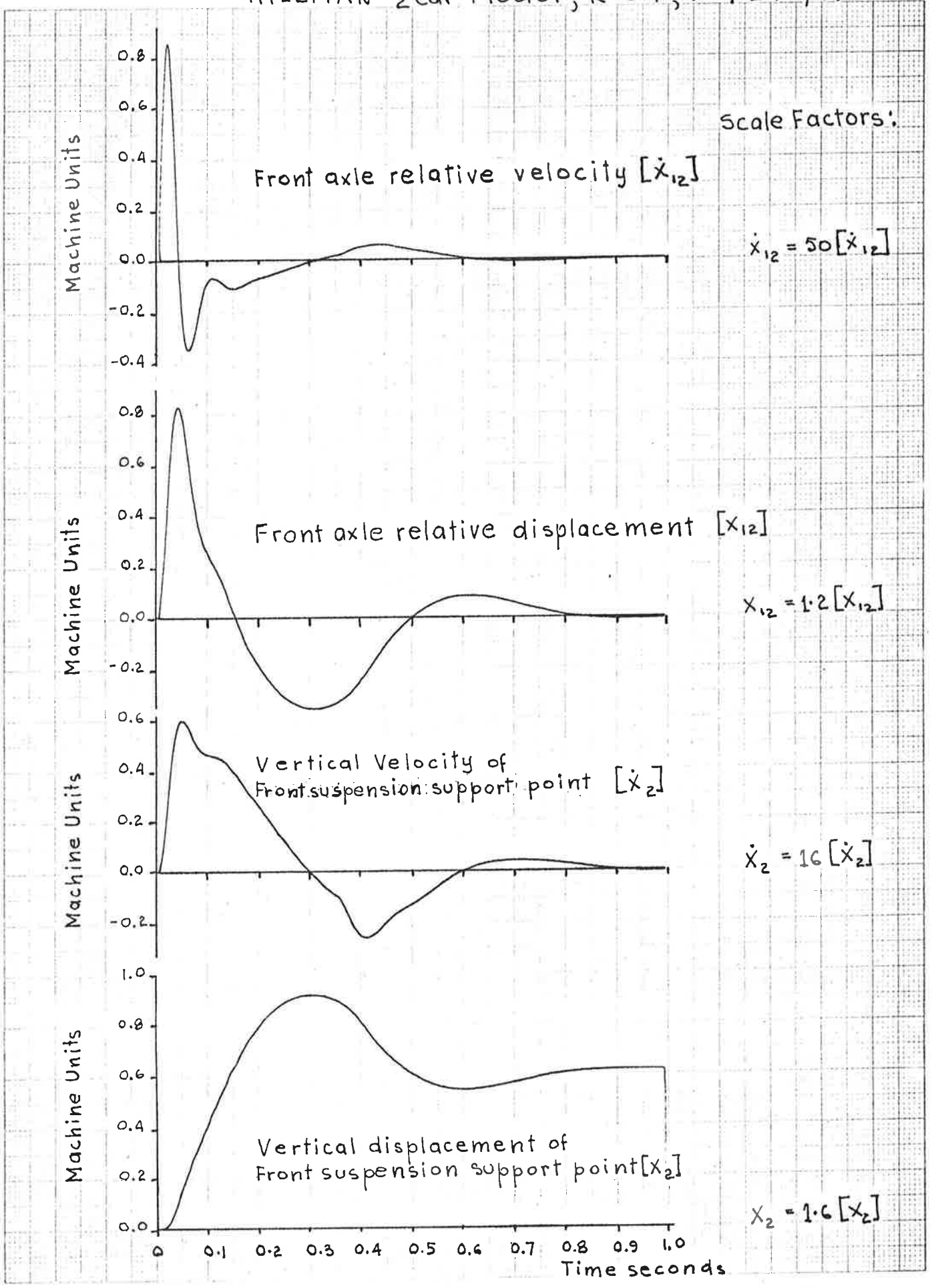


Fig. A 19. Time Response
by Analogue Computer Simulation.
HILLMAN $\frac{1}{2}$ -Car Model, $R=0.7$, $V=7.2$ m/s

GRAPH

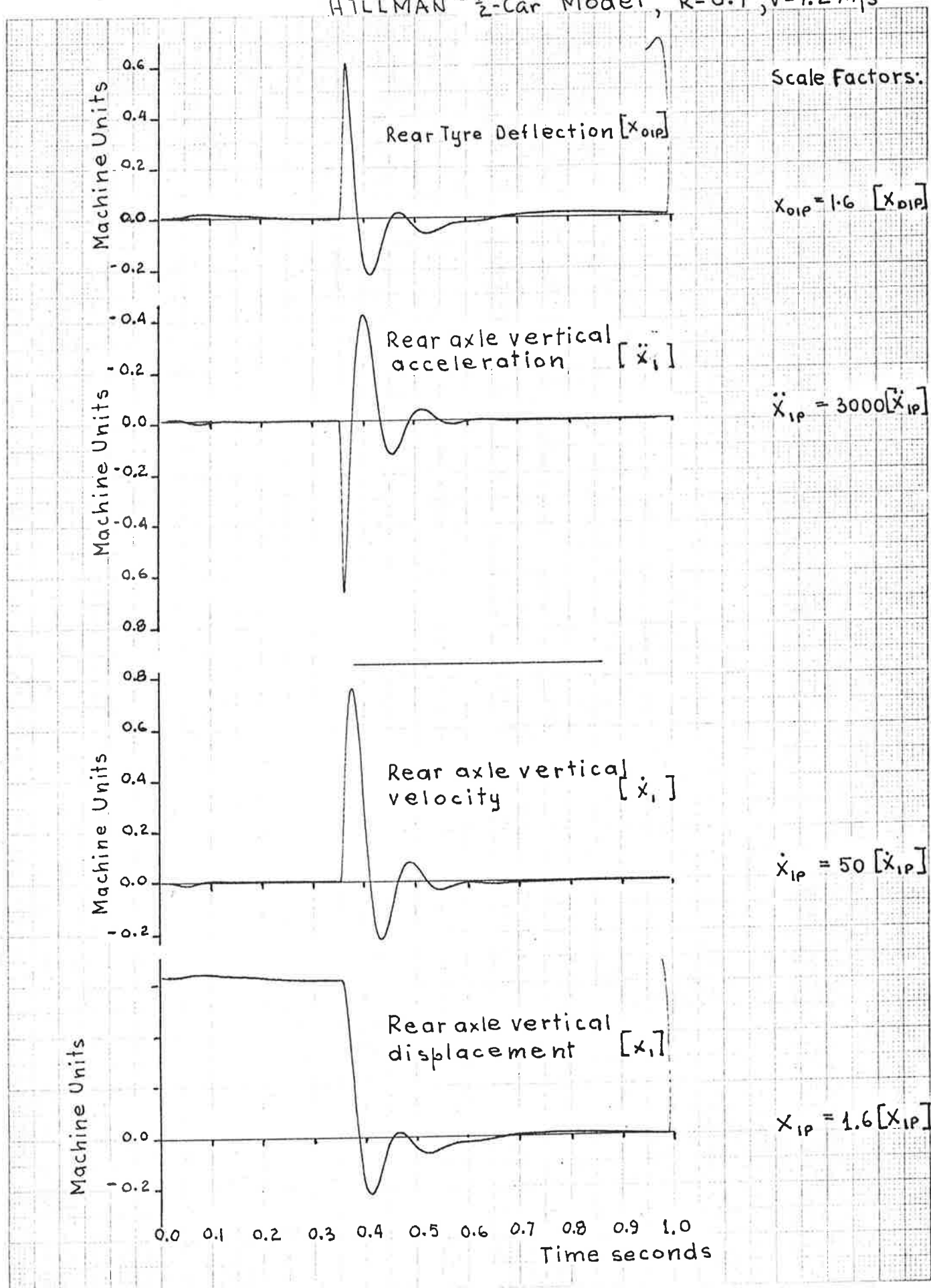


Fig. A 20. Time Response
 by Analogue Computer Simulation.
 HILLMAN $\frac{1}{2}$ -Car Model, $R=0.7$, $V=7.2$ m/s.

07A59

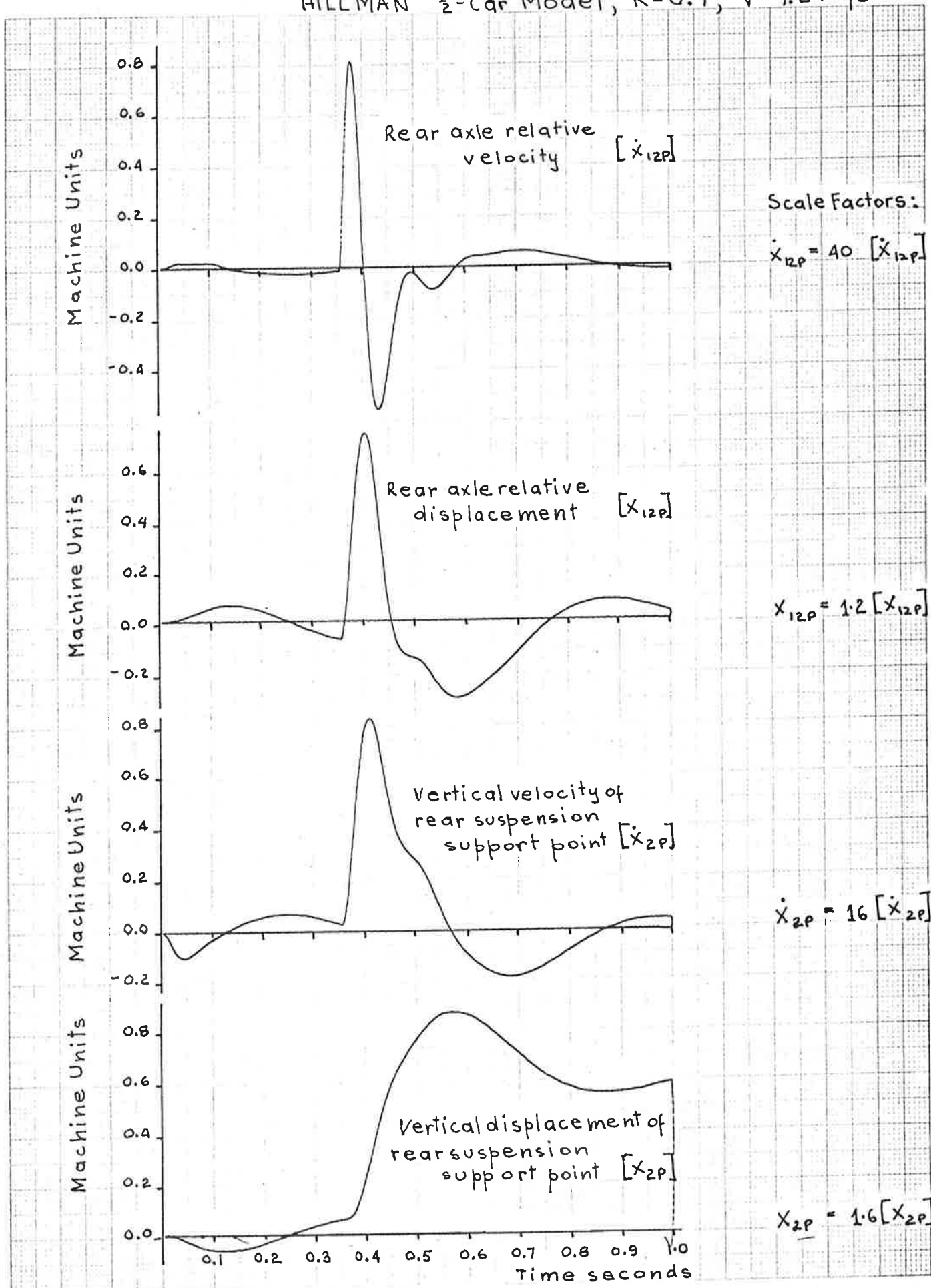


Fig. A21. Time Response
by Analogue Computer Simulation
HILLMAN 1/2-Car Model, $R=0.7$, $V=7.2$ m/s

PZAB9

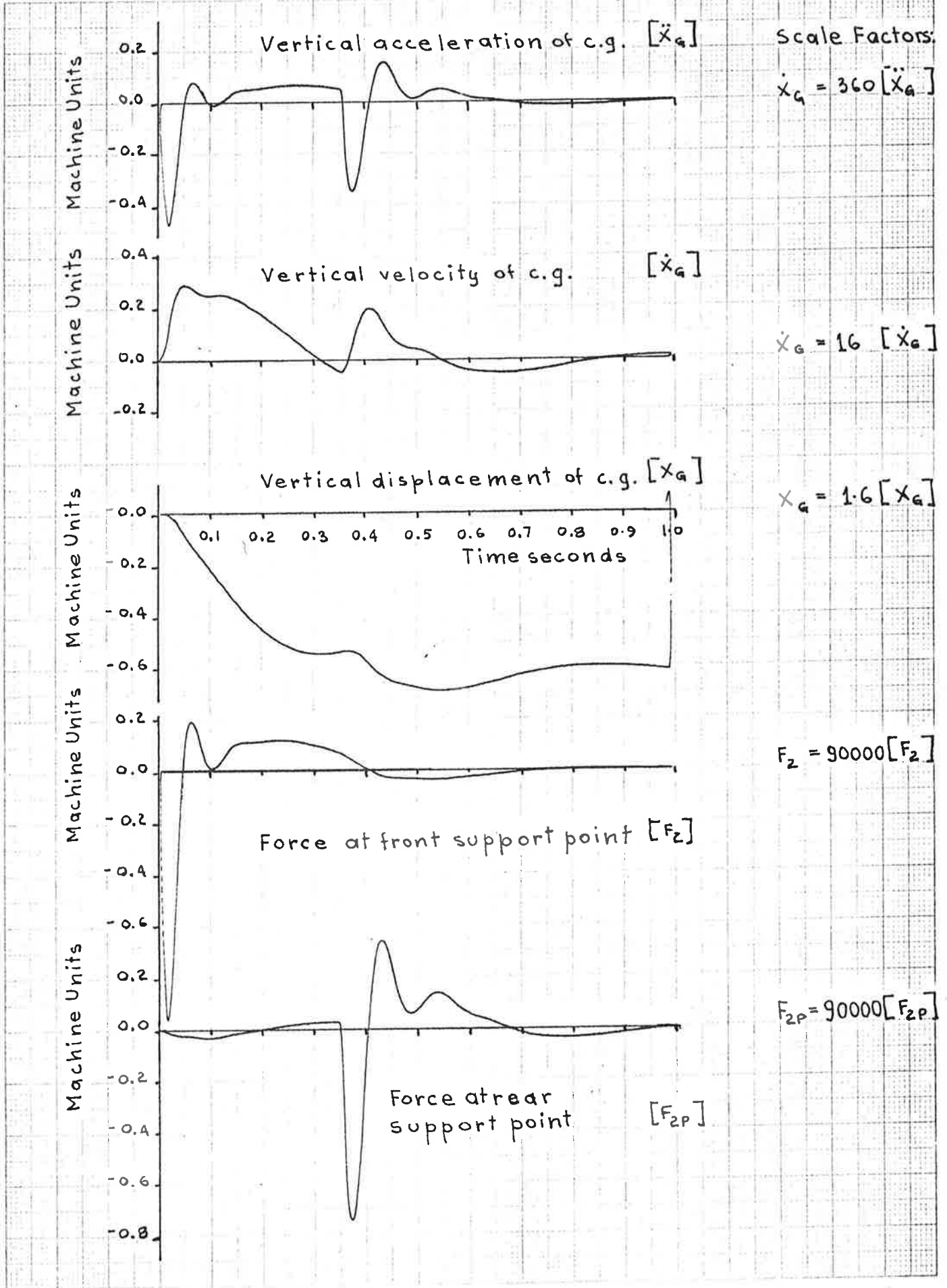


Fig. A22. Time Response
by Analogue Computer Simulation.
HILLMAN $\frac{1}{2}$ -Car Model, $R=0.7, V=7.2$ m/s.

QZAR
THE FACTORY

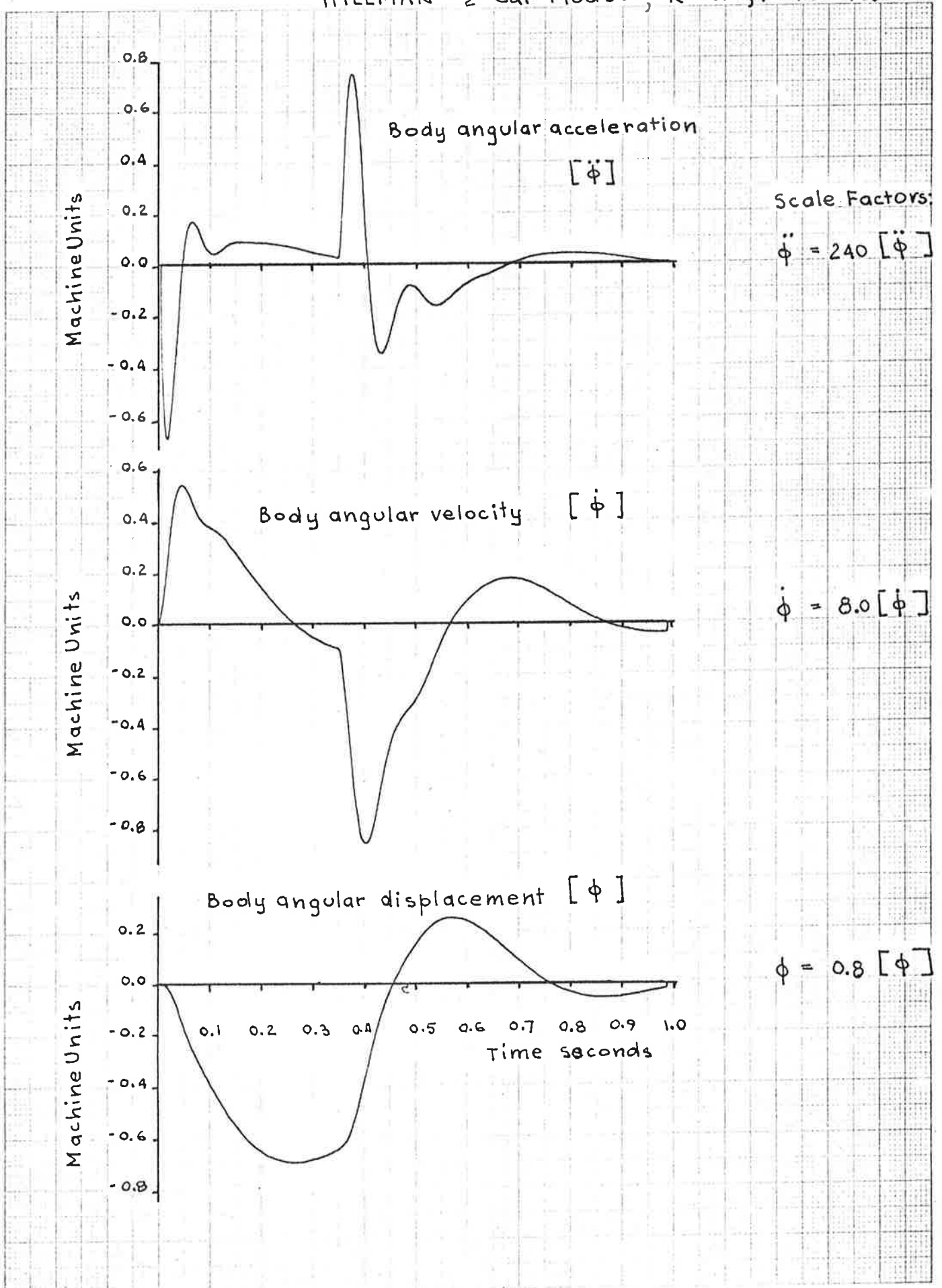


TABLE A1 - VARYING SPEED

MODEL: HILLMAN $\frac{1}{2}$ -CAR; R=0.7.
 $k_2 = 19972 \text{ N/m}$ $B_2 = 1800 \text{ Ns/m}$
 $k_{2P} = 22563 \text{ N/m}$ $B_{2P} = 1800 \text{ Ns/m}$

ANALOGUE COMPUTER SIMULATION RESULTS

| Speed m/s | 5 | 10 | 15 | 20 | 25 | 30 | 40 | 50 | 60 |
|--|--------|--------|--------|--------|--------|--------|--------|--------|--------|
| Pot. setting | 0.5131 | 0.2565 | 0.1710 | 0.1283 | 0.1026 | 0.0855 | 0.0641 | 0.0513 | 0.0428 |
| $\int [X_{01}^2]$ | 0.0525 | 0.0525 | 0.0525 | 0.0526 | 0.0525 | 0.0525 | 0.0525 | 0.0525 | 0.0525 |
| $\int [X_{01P}^2]$ | 0.0810 | 0.0819 | 0.0845 | 0.0841 | 0.0852 | 0.0860 | 0.0855 | 0.0846 | 0.0830 |
| $\int [X_{01}^2] + \int [X_{01P}^2]$ | 0.1334 | 0.1343 | 0.1369 | 0.1367 | 0.1377 | 0.1384 | 0.1379 | 0.1372 | 0.1356 |
| $\int [X_{12}^2]$ | 0.5452 | 0.4581 | 0.4738 | 0.5018 | 0.5288 | 0.5468 | 0.5716 | 0.5877 | 0.5997 |
| $\int [X_{12P}^2]$ | 0.3918 | 0.4425 | 0.5447 | 0.5658 | 0.5693 | 0.5635 | 0.5463 | 0.5328 | 0.5209 |
| $\int [X_{12}^2] \quad \int [X_{12P}^2]$ | 0.9368 | 0.9006 | 1.0185 | 1.0675 | 1.0982 | 1.1103 | 1.1179 | 1.1205 | 1.1207 |
| $\int [F_2^2]$ | 0.2115 | 0.2021 | 0.2010 | 0.2028 | 0.2049 | 0.2066 | 0.2089 | 0.2103 | 0.2113 |
| $\int [F_{2P}^2]$ | 0.2043 | 0.2091 | 0.2259 | 0.2295 | 0.2339 | 0.2346 | 0.2306 | 0.2265 | 0.2236 |
| $\int [F_2^2] \quad \int [F_{2P}^2]$ | 0.4156 | 0.4112 | 0.4267 | 0.4323 | 0.4388 | 0.4412 | 0.4395 | 0.4368 | 0.4350 |
| $\int [\ddot{X}_G^2]$ | 0.1035 | 0.0942 | 0.1041 | 0.1083 | 0.1182 | 0.1219 | 0.1145 | 0.1079 | 0.1085 |
| $\int [\dot{X}_G^2]$ | 0.1738 | 0.1904 | 0.2813 | 0.3252 | 0.3553 | 0.3703 | 0.3855 | 0.3931 | 0.3982 |
| | | | | | | | | | |
| $\int [\ddot{\phi}^2]$ | 0.2993 | 0.3190 | 0.3176 | 0.3113 | 0.2947 | 0.2873 | 0.3043 | 0.3179 | 0.3125 |
| $\int [\dot{\phi}^2]$ | 0.7041 | 0.7312 | 0.5573 | 0.4397 | 0.3425 | 0.2882 | 0.2227 | 0.1843 | 0.1572 |
| $\int [\phi^2]$ | 1.6932 | 0.8716 | 0.4360 | 0.2632 | 0.1582 | 0.1089 | 0.0634 | 0.0462 | 0.0384 |
| | | | | | | | | | |
| I | 0.7457 | 0.7400 | 0.7736 | 0.7838 | 0.7950 | 0.8000 | 0.8039 | 0.7956 | 0.7904 |

TABLE A2

ACSL DIGITAL SIMULATION RESULTS

MODEL: HILLMAN $\frac{1}{2}$ -CAR; R=0.7
 $k_2 = 19972 \text{ N/m}$ $B_2 = 1800 \text{ Ns/m}$
 $k_{2P} = 22564 \text{ N/m}$ $B_{2P} = 1800 \text{ Ns/m}$

| Speed m/s | 5 | 10 | 15 | 20 | 25 | 30 | 40 | 50 | 60 |
|-----------|----------|----------|----------|-----------|----------|-----------|----------|-----------|-----------|
| ISX01 | 0.014541 | 0.014187 | 0.014174 | 0.0142365 | 0.014293 | 0.0143393 | 0.014426 | 0.014497 | 0.014546 |
| ISX01P | 0.021475 | 0.021683 | 0.022350 | 0.022365 | 0.022566 | 0.022785 | 0.022794 | 0.022500 | 0.022202 |
| SISX01 | 0.036015 | 0.035870 | 0.036524 | 0.0366014 | 0.036859 | 0.037124 | 0.037220 | 0.036997 | 0.036748 |
| | | | | | | | | | |
| ISX12 | 0.079478 | 0.066886 | 0.069052 | 0.072939 | 0.076168 | 0.078708 | 0.082321 | 0.084664 | 0.0862302 |
| ISX12P | 0.057142 | 0.065464 | 0.078671 | 0.082435 | 0.083017 | 0.082439 | 0.080370 | 0.078461 | 0.0770313 |
| SISX12 | 0.136620 | 0.132350 | 0.147724 | 0.155374 | 0.159186 | 0.161146 | 0.16269 | 0.1631525 | 0.1632615 |
| | | | | | | | | | |
| ISF2 | 1.7317E8 | 1.6479E8 | 1.6459E8 | 1.6609E8 | 1.6754E8 | 1.6892E8 | 1.7088E8 | 1.7190E8 | 1.7247E8 |
| ISF2P | 1.7042E8 | 1.7200E8 | 1.8448E8 | 1.8839E8 | 1.9142E8 | 1.9252E8 | 1.9040E8 | 1.8730E8 | 1.8503E8 |
| SISF2 | 3.4359E8 | 3.3679E8 | 3.4907E8 | 3.5443E8 | 3.5896E8 | 3.6144E8 | 3.6129E8 | 3.5920E8 | 3.5750E8 |
| ISAX | 1364.422 | 1244.89 | 1365.00 | 1437.85 | 1536.63 | 1603.3911 | 1555.08 | 1431.27 | 142.01 |
| RMSA | 0.082596 | 0.111575 | 0.14309 | 0.16968 | 0.195999 | 0.219321 | 0.24941 | 0.26986 | 0.29189 |
| | | | | | | | | | |
| INDEX | 0.771646 | 0.760484 | 0.792224 | 0.804934 | 0.814945 | 0.821536 | 0.823917 | 0.820459 | 0.81674 |
| | | | | | | | | | |
| | | | | | | | | | |
| | | | | | | | | | |

TABLE A3

CALCULATED SCALE FACTORS FROM ANALOGUE SIMULATION RESULTS

| Speed m/s | 5 | 10 | 15 | 20 | 25 | 30 | 40 | 50 | 60 |
|------------------------|--------|--------|--------|--------|--------|--------|--------|--------|--------|
| ISX01 | 0.2770 | 0.2702 | 0.2700 | 0.2706 | 0.2723 | 0.2731 | 0.2748 | 0.2761 | 0.2770 |
| ISX01P | 0.2651 | 0.2647 | 0.2645 | 0.2659 | 0.2649 | 0.2649 | 0.2666 | 0.2660 | 0.2675 |
| SISX01 | 0.2700 | 0.2671 | 0.2668 | 0.2677 | 0.2677 | 0.2682 | 0.2660 | 0.2697 | 0.2710 |
| ISX12 | 0.1458 | 0.1460 | 0.1457 | 0.1454 | 0.1440 | 0.1439 | 0.1440 | 0.1441 | 0.1438 |
| ISX12P | 0.1458 | 0.1479 | 0.1444 | 0.1457 | 0.1458 | 0.1463 | 0.1471 | 0.1473 | 0.1479 |
| SISX12 | 0.1458 | 0.1470 | 0.1450 | 0.1455 | 0.1449 | 0.1451 | 0.1455 | 0.1456 | 0.1457 |
| ISF2 | 0.8188 | 0.8154 | 0.8189 | 0.8187 | 0.8177 | 0.8176 | 0.8180 | 0.8174 | 0.8162 |
| ISF2P | 0.8342 | 0.8226 | 0.8166 | 0.8209 | 0.8184 | 0.8206 | 0.8257 | 0.8269 | 0.8275 |
| SISF2 | 0.8267 | 0.8190 | 0.8181 | 0.8199 | 0.8180 | 0.8192 | 0.8220 | 0.8223 | 0.8218 |
| ISAX | 13183 | 13215 | 13112 | 13203 | 13000 | 13153 | 13581 | 13265 | 13088 |
| $\sigma_1 \times 10^3$ | 2.431 | 2.404 | 2.468 | 2.487 | 2.510 | 2.528 | 2.548 | 2.522 | 2.507 |
| $\sigma_{1/1} \%$ | 0.315 | 0.312 | 0.312 | 0.309 | 0.308 | 0.308 | 0.309 | 0.307 | 0.307 |
| $3\sigma_{1/1} \%$ | 0.945 | 0.946 | 0.946 | 0.927 | 0.924 | 0.924 | 0.927 | 0.921 | 0.921 |

TABLE A4

VARYING SPRING RATE

MODEL: HILLMAN $\frac{1}{2}$ -CAR; R=0.7

ANALOGUE COMPUTER SIMULATION RESULTS:

Speed $v = 20$ m/s $k_0 = 40812.7$ N/m; $B_2 = B_{2P} = 1800$ Ns/m

| Front Spring Rate | 16000 | 18000 | 20000 | 22000 | 24000 | 26000 | 28000 | 30000 | 32000 |
|--|--------|--------|--------|--------|--------|--------|--------|--------|--------|
| Pot. 03 | 0.2133 | 0.2400 | 0.2667 | 0.2933 | 0.3200 | 0.3467 | 0.3733 | 0.4000 | 0.4267 |
| Rear Spring Rate | 45239 | 28972 | 22500 | 19023 | 16853 | 15369 | 14291 | 13472 | 12828 |
| Pot. 08 | 0.6032 | 0.3863 | 0.3000 | 0.2536 | 0.2247 | 0.2049 | 0.1905 | 0.1796 | 0.1710 |
| $\int [X_{10}^2]$ | 0.0533 | 0.0529 | 0.0525 | 0.0521 | 0.0519 | 0.0516 | 0.0513 | 0.0514 | 0.0516 |
| $\int [X_{10P}^2]$ | 0.0884 | 0.0837 | 0.0842 | 0.0849 | 0.0858 | 0.0866 | 0.0873 | 0.0878 | 0.0883 |
| $\int [X_{10}^2] + \int [X_{10P}^2]$ | 0.1416 | 0.1364 | 0.1364 | 0.1369 | 0.1375 | 0.1379 | 0.1384 | 0.1389 | 0.1397 |
| $\int [X_{12}^2]$ | 0.5642 | 0.5322 | 0.5053 | 0.4868 | 0.4733 | 0.4630 | 0.4551 | 0.4486 | 0.4427 |
| $\int [X_{12P}^2]$ | 0.5043 | 0.5453 | 0.5692 | 0.5861 | 0.5989 | 0.6087 | 0.6166 | 0.6231 | 0.6283 |
| $\int [X_{12}^2] \quad \int [X_{12P}^2]$ | 1.0686 | 1.0774 | 1.0752 | 1.0729 | 1.0722 | 1.0717 | 1.0715 | 1.0712 | 1.0710 |
| $\int [F_2^2]$ | 0.1963 | 0.1992 | 0.2035 | 0.2088 | 0.2148 | 0.2214 | 0.2287 | 0.2367 | 0.2449 |
| $\int [F_{2P}^2]$ | 0.3623 | 0.2596 | 0.2305 | 0.2176 | 0.2107 | 0.2067 | 0.2041 | 0.2024 | 0.2012 |
| $\int [f_2^2] \quad \int [F_{2P}^2]$ | 0.5586 | 0.4586 | 0.4339 | 0.4263 | 0.4253 | 0.4279 | 0.4326 | 0.4388 | 0.4461 |
| $\int [\ddot{X}_G^2]$ | 0.1403 | 0.1168 | 0.1104 | 0.1081 | 0.1075 | 0.1078 | 0.1085 | 0.1096 | 0.1110 |
| $\int [\dot{X}_G]$ | 0.3789 | 0.3451 | 0.3306 | 0.3214 | 0.3154 | 0.3109 | 0.3082 | 0.3063 | 0.3051 |
| $\int [\ddot{\phi}^2]$ | 0.4313 | 0.3345 | 0.3101 | 0.3024 | 0.3076 | 0.3014 | 0.3037 | 0.3075 | 0.3121 |
| $\int [\phi^2]$ | 0.7741 | 0.4986 | 0.4267 | 0.4136 | 0.4213 | 0.4406 | 0.4644 | 0.4921 | 0.5214 |
| $\int [\phi^2]$ | 0.3487 | 0.2594 | 0.2509 | 0.2741 | 0.3082 | 0.3467 | 0.3857 | 0.4221 | 0.4579 |
| I | 0.8784 | 0.8015 | 0.7851 | 0.7812 | 0.7820 | 0.7846 | 0.7889 | 0.7942 | 0.8009 |

TABLE A5

MODEL: HILLMAN $\frac{1}{2}$ CAR, R=0.7

ACSL DIGITAL SIMULATION RESULTS:

Speed $v = 20 \text{ m/s}$ $k_0 = 40812.7 \text{ N/m}$; $B_2 = B_{2P} = 1800 \text{ Ns/m}$

| | | | | | | | | | |
|-------------------|----------|----------|----------|----------|----------|----------|----------|----------|----------|
| Front Spring Rate | 16000 | 18000 | 20000 | 22000 | 24000 | 26000 | 28000 | 30000 | 32000 |
| Rear Spring Rate | 45239 | 28972 | 22500 | 19023 | 16853 | 15369 | 14291 | 13472 | 12828 |
| | | | | | | | | | |
| ISX01 | 0.014340 | 0.014264 | 0.014236 | 0.014243 | 0.014280 | 0.014346 | 0.014439 | 0.014559 | 0.014705 |
| ISX01P | 0.024076 | 0.022364 | 0.022367 | 0.022539 | 0.022714 | 0.022867 | 0.022998 | 0.023112 | 0.023212 |
| SISX01 | 0.038415 | 0.036628 | 0.036603 | 0.036782 | 0.036994 | 0.037213 | 0.037437 | 0.037671 | 0.037917 |
| | | | | | | | | | |
| ISX12 | 0.080888 | 0.076378 | 0.072896 | 0.070284 | 0.068323 | 0.066822 | 0.065647 | 0.064706 | 0.063936 |
| ISX12P | 0.073583 | 0.078763 | 0.082479 | 0.085175 | 0.087153 | 0.088633 | 0.089766 | 0.090652 | 0.091358 |
| SISX12 | 0.154470 | 0.155141 | 0.155375 | 0.155459 | 0.155475 | 0.155455 | 0.155413 | 0.155358 | 0.155294 |
| | | | | | | | | | |
| ISF2 | 1.5996E8 | 1.6256E8 | 1.6610E8 | 1.7031E8 | 1.7513E8 | 1.805E8 | 1.8640E8 | 1.9280E8 | 1.9969E8 |
| ISF2P | 2.9554E8 | 2.1191E8 | 1.8818E8 | 1.7781E8 | 1.7226E8 | 1.6893E8 | 1.6679E8 | 1.6535E8 | 1.6437E8 |
| SISF2 | 4.5550E8 | 3.7447E8 | 3.5428E8 | 3.4813E8 | 3.4739E8 | 3.4943E8 | 3.5319E8 | 3.5816E8 | 3.6406E8 |
| | | | | | | | | | |
| ISAX | 1826.31 | 1519.05 | 1437.19 | 1407.35 | 1398.04 | 1399.49 | 1407.66 | 1420.52 | 1436.95 |
| INDEX | 0.903025 | 0.820992 | 0.804834 | 0.801785 | 0.803326 | 0.807127 | 0.812341 | 0.818598 | 0.825716 |
| | | | | | | | | | |
| | | | | | | | | | |

TABLE A6

Speed $v = 20$ m/s

SCALE FACTORS

MODEL: HILLMAN $\frac{1}{2}$ -CAR MODEL, $R=0.7$

| Front Spring Rate | 16000 | 18000 | 20000 | 22000 | 24000 | 26000 | 28000 | 30000 | 32000 |
|----------------------|--------|--------|--------|--------|--------|--------|--------|--------|--------|
| ISX01 | 0.2690 | 0.2697 | 0.2712 | 0.2734 | 0.2751 | 0.2780 | 0.2815 | 0.2832 | 0.2850 |
| ISX01P | 0.2724 | 0.2672 | 0.2656 | 0.2655 | 0.2647 | 0.2640 | 0.2634 | 0.2632 | 0.2629 |
| SISX01 | 0.2713 | 0.2685 | 0.2684 | 0.2683 | 0.2691 | 0.2699 | 0.2705 | 0.2712 | 0.2714 |
| ISX12 | 0.1434 | 0.1435 | 0.1443 | 0.1444 | 0.1443 | 0.1443 | 0.1442 | 0.1442 | 0.1444 |
| ISX12P | 0.1459 | 0.1444 | 0.1449 | 0.1453 | 0.1455 | 0.1456 | 0.1456 | 0.1454 | 0.1454 |
| SISX12 | 0.1445 | 0.1440 | 0.1445 | 0.1450 | 0.1450 | 0.1450 | 0.1450 | 0.1450 | 0.1450 |
| ISF2 | 0.8149 | 0.8161 | 0.8162 | 0.8157 | 0.8153 | 0.8153 | 0.8150 | 0.8145 | 0.8154 |
| ISF2P | 0.8157 | 0.8163 | 0.8164 | 0.8171 | 0.8176 | 0.8173 | 0.8172 | 0.8169 | 0.8169 |
| SISF2 | 0.8154 | 0.8165 | 0.8165 | 0.8166 | 0.8168 | 0.8166 | 0.8134 | 0.8162 | 0.8161 |
| ISAX | 13017 | 13006 | 13018 | 13019 | 13005 | 12982 | 12974 | 12961 | 12945 |
| $\sigma_1 \times 10$ | 1.990 | 1.888 | 1.883 | 1.890 | 1.900 | 1.911 | 1.922 | 1.934 | 1.947 |
| $\sigma_1 / 1 \%$ | 0.220 | 0.230 | 0.234 | 0.236 | 0.237 | 0.237 | 0.237 | 0.236 | 0.236 |
| $3 \sigma_1 / 1 \%$ | 0.660 | 0.690 | 0.702 | 0.708 | 0.711 | 0.711 | 0.711 | 0.708 | 0.708 |

TABLE A7 - VARYING SPRING RATE

MODEL: HILLMAN $\frac{1}{2}$ -CAR, R=0.7, $k_0 = 40812.7$ N/m; $B_2 = B_{2P} = 1800$ Ns/m

ANALOGUE COMPUTER SIMULATION RESULTS:

Speed $v = 30$ m/s

| | | | | | | | | | |
|--------------------------------------|--------|--------|--------|--------|--------|--------|--------|--------|--------|
| Front Spring Rate | 16000 | 18000 | 20000 | 22000 | 24000 | 26000 | 28000 | 30000 | 32000 |
| Pot. 03 | .2133 | .2400 | .2667 | .2933 | .3200 | .3467 | .3733 | .4000 | .4267 |
| Rear Spring Rate | 45239 | 28972 | 22500 | 19023 | 16853 | 15369 | 14291 | 13472 | 12828 |
| Pot. 08 | .6032 | .3863 | .3000 | .2536 | .2247 | .2049 | .1905 | .1796 | .1710 |
| $\int [X_{01}^2]$ | 0.0534 | 0.0529 | 0.0525 | 0.0522 | 0.0518 | 0.0517 | 0.0517 | 0.0519 | 0.0523 |
| $\int [X_{01}^2]$ | 0.0893 | 0.0846 | 0.0852 | 0.0862 | 0.0869 | 0.0879 | 0.0885 | 0.0889 | 0.0894 |
| $\int [X_{01}^2] + \int [X_{01P}^2]$ | 0.1427 | 0.1374 | 0.1375 | 0.1382 | 0.1387 | 0.1395 | 0.1401 | 0.1407 | 0.1415 |
| $\int [X_{12}^2]$ | 0.6061 | 0.5745 | 0.5473 | 0.5268 | 0.5111 | 0.4982 | 0.4882 | 0.4797 | 0.4723 |
| $\int [X_{12P}^2]$ | 0.5046 | 0.5424 | 0.5656 | 0.5837 | 0.5986 | 0.6110 | 0.6214 | 0.6301 | 0.6373 |
| $\int [X_{12}^2] + \int [X_{12P}^2]$ | 1.1105 | 1.1165 | 1.1129 | 1.1101 | 1.1092 | 1.1093 | 1.1094 | 1.1095 | 1.1095 |
| $\int [F_2^2]$ | 0.1990 | 0.2025 | 0.2079 | 0.2127 | 0.2190 | 0.2261 | 0.2337 | 0.2421 | 0.2509 |
| $\int [F_{2P}^2]$ | 0.3667 | 0.2637 | 0.2348 | 0.2221 | 0.2153 | 0.2113 | 0.2087 | 0.2071 | 0.2059 |
| $\int [F_2^2] + \int [F_{2P}^2]$ | 0.5657 | 0.4661 | 0.4419 | 0.4345 | 0.4342 | 0.4374 | 0.4423 | 0.4490 | 0.4567 |
| $\int [\ddot{X}_G^2]$ | 0.1501 | 0.1274 | 0.1221 | 0.1208 | 0.1212 | 0.1225 | 0.1244 | 0.1266 | 0.1290 |
| $\int [\dot{X}_G^2]$ | 0.4063 | 0.3792 | 0.3711 | 0.3665 | 0.3639 | 0.3639 | 0.3632 | 0.3641 | 0.3657 |
| $\int [\ddot{\phi}^2]$ | 0.4129 | 0.3139 | 0.2874 | 0.2776 | 0.2733 | 0.2716 | 0.2716 | 0.2729 | 0.2750 |
| $\int [\dot{\phi}^2]$ | 0.6662 | 0.3717 | 0.2879 | 0.2628 | 0.2603 | 0.2708 | 0.2859 | 0.3065 | 0.3282 |
| $\int [\phi^2]$ | 0.2682 | 0.1437 | 0.1102 | 0.1144 | 0.1350 | 0.1621 | 0.1930 | 0.2235 | 0.2519 |
| I | 0.8918 | 0.8145 | 0.7986 | 0.7952 | 0.7962 | 0.8003 | 0.8050 | 0.8109 | 0.8179 |

TABLE A8

ACSL DIGITAL SIMULATION RESULTS:

Speed $v = 30$ m/sMODEL: HILLMAN $\frac{1}{2}$ -CAR, $R=0.7$. $k_0 = 40812.7$ N/m, $B_2 = B_{2P} = 1800$ Ns/m

| | | | | | | | | | |
|-------------------|----------|----------|----------|----------|----------|----------|----------|----------|----------|
| Front Spring Rate | 16000 | 18000 | 20000 | 22000 | 24000 | 26000 | 28000 | 30000 | 32000 |
| Rear Spring Rate | 45239 | 28972 | 22500 | 19023 | 16853 | 15369 | 14291 | 13472 | 12828 |
| ISX01 | 0.014412 | 0.014353 | 0.014339 | 0.014359 | 0.014410 | 0.014490 | 0.014596 | 0.014729 | 0.014888 |
| ISX01P | 0.024416 | 0.022746 | 0.022787 | 0.022980 | 0.023164 | 0.023321 | 0.023453 | 0.023565 | 0.023662 |
| SISX01 | 0.038828 | 0.037099 | 0.037126 | 0.037339 | 0.037574 | 0.037811 | 0.038049 | 0.038295 | 0.038550 |
| ISX12 | 0.086965 | 0.082379 | 0.078662 | 0.075764 | 0.073516 | 0.071745 | 0.070320 | 0.069145 | 0.068158 |
| ISX12P | 0.073989 | 0.078718 | 0.082485 | 0.085401 | 0.087653 | 0.089421 | 0.090840 | 0.092005 | 0.092981 |
| SISX12 | 0.160954 | 0.161097 | 0.161146 | 0.161165 | 0.161169 | 0.161166 | 0.161160 | 0.161150 | 0.161139 |
| ISF2 | 1.6216E8 | 1.6511E8 | 1.6898E8 | 1.7351E8 | 1.7864E8 | 1.8432E8 | 1.9052E8 | 1.9723E8 | 2.0442E8 |
| ISF2P | 3.0065E8 | 2.1600E8 | 1.9231E8 | 1.8204E8 | 1.7656E8 | 1.7329E8 | 1.7120E8 | 1.6980E8 | 1.6886E8 |
| SISF2 | 4.6281E8 | 3.8111E8 | 3.6129E8 | 3.5555E8 | 3.5520E8 | 3.5761E8 | 3.6172E8 | 3.6704E8 | 3.7328E8 |
| ISAX | 1975.86 | 1673.63 | 1602.89 | 1584.81 | 1587.40 | 1600.87 | 1621.16 | 1646.26 | 1675.02 |
| INDEX | 0.919480 | 0.836972 | 0.821445 | 0.818997 | 0.821072 | 0.825361 | 0.831034 | 0.837729 | 0.845269 |

TABLE A9

MODEL: HILLMAN $\frac{1}{2}$ -CAR, R=0.7Speed $v = 30$ m/s

| Front Spring Rate | 16000 | 18000 | 20000 | 22000 | 24000 | 26000 | 28000 | 30000 | 32000 |
|------------------------|--------|--------|--------|--------|--------|--------|--------|--------|--------|
| ISX01 | 0.2699 | 0.2713 | 0.2731 | 0.2751 | 0.2782 | 0.2803 | 0.2823 | 0.2838 | 0.2847 |
| ISX01P | 0.2734 | 0.2694 | 0.2675 | 0.2666 | 0.2666 | 0.2653 | 0.2650 | 0.2651 | 0.2647 |
| SISX01 | 0.2721 | 0.2700 | 0.2700 | 0.2702 | 0.2709 | 0.2710 | 0.2716 | 0.2722 | 0.2724 |
| ISX12 | 0.1435 | 0.1434 | 0.1437 | 0.1438 | 0.1438 | 0.1440 | 0.1440 | 0.1441 | 0.1443 |
| ISX12P | 0.1466 | 0.1451 | 0.1458 | 0.1463 | 0.1464 | 0.1464 | 0.1462 | 0.1460 | 0.1459 |
| SISX12 | 0.1449 | 0.1443 | 0.1448 | 0.1452 | 0.1453 | 0.1453 | 0.1453 | 0.1452 | 0.1452 |
| ISF2 | 0.8149 | 0.8154 | 0.8128 | 0.8157 | 0.8157 | 0.8152 | 0.8152 | 0.8147 | 0.8147 |
| ISF2P | 0.8199 | 0.8191 | 0.8190 | 0.8196 | 0.8201 | 0.8201 | 0.8203 | 0.8199 | 0.8201 |
| SISF2 | 0.8181 | 0.8177 | 0.8175 | 0.8183 | 0.8181 | 0.8176 | 0.8178 | 0.8175 | 0.8173 |
| ISAX | 13164 | 13137 | 13128 | 13119 | 13097 | 13068 | 13032 | 13004 | 12985 |
| $\sigma_1 \times 10^3$ | 1.438 | 1.376 | 1.376 | 1.383 | 1.391 | 1.400 | 1.407 | 1.416 | 1.425 |
| σ_1 / I % | 0.156 | 0.164 | 0.168 | 0.169 | 0.169 | 0.169 | 0.169 | 0.169 | 0.169 |
| $3 \sigma_1 / I$ % | 0.468 | 0.492 | 0.504 | 0.507 | 0.507 | 0.507 | 0.507 | 0.507 | 0.507 |

APPENDIX B

TABLES OF CALCULATED
COEFFICIENTS

APPENDIX B

TABLE B.1

COEFFICIENTS FOR
HILLMAN FRONT RESPONSE,
(UNLADEN)

$$k_2 = 19972 \text{ N/m}$$

$$k_0 = 40813 \text{ N/m}$$

$$V = 20 \text{ m/s}$$

| COUPLING RATIO | COEFFICIENTS FOR | | |
|-------------------|--------------------------------|--------------------------------|---------------------------------|
| | ISF2 | ISX01 | ISX12 |
| 0.6 | $C_1 = 7.52646 \times 10^4$ | $C_3 = 3.96448 \times 10^{-6}$ | $C_5 = -6.06689 \times 10^{-7}$ |
| | $C_2 = 5.10931 \times 10^{10}$ | $C_4 = 12.8346$ | $C_6 = 126.471$ |
| 0.7 | $C_1 = 7.57031 \times 10^4$ | $C_3 = 3.90854 \times 10^{-6}$ | $C_5 = -4.86919 \times 10^{-7}$ |
| | $C_2 = 5.36152 \times 10^{10}$ | $C_4 = 12.9626$ | $C_6 = 132.896$ |
| 0.8 | $C_1 = 7.63556 \times 10^4$ | $C_3 = 3.88205 \times 10^{-6}$ | $C_5 = -3.46911 \times 10^{-7}$ |
| | $C_2 = 5.66554 \times 10^{10}$ | $C_4 = 13.1057$ | $C_6 = 140.779$ |
| 0.9 | $C_1 = 7.71344 \times 10^4$ | $C_3 = 3.87325 \times 10^{-6}$ | $C_5 = -1.72551 \times 10^{-7}$ |
| | $C_2 = 5.99039 \times 10^{10}$ | $C_4 = 13.2568$ | $C_6 = 149.531$ |
| 1.0 | $C_1 = 7.7930 \times 10^4$ | $C_3 = 3.87487 \times 10^{-6}$ | $C_5 = 0$ |
| | $C_2 = 6.33263 \times 10^{10}$ | $C_4 = 13.4085$ | $C_6 = 158.755$ |
| 1.1 | $C_1 = 7.87357 \times 10^4$ | $C_3 = 3.88037 \times 10^{-6}$ | $C_5 = 2.70302 \times 10^{-7}$ |
| | $C_2 = 6.65929 \times 10^{10}$ | $C_4 = 13.5619$ | $C_6 = 167.693$ |
| 1.2 | $C_1 = 7.94925 \times 10^4$ | $C_3 = 3.89145 \times 10^{-6}$ | $C_5 = 6.41781 \times 10^{-7}$ |
| | $C_2 = 6.97013 \times 10^{10}$ | $C_4 = 13.6961$ | $C_6 = 176.006$ |
| 1.3 | $C_1 = 8.02242 \times 10^4$ | $C_3 = 3.90352 \times 10^{-6}$ | $C_5 = 9.98644 \times 10^{-7}$ |
| | $C_2 = 7.18271 \times 10^{10}$ | $C_4 = 13.7923$ | $C_6 = 182.738$ |
| 1.4 | $C_1 = 8.09144 \times 10^4$ | $C_3 = 3.91630 \times 10^{-6}$ | $C_5 = 14.6205 \times 10^{-7}$ |
| | $C_2 = 7.39530 \times 10^{10}$ | $C_4 = 13.8885$ | $C_6 = 189.123$ |
| 1.5 | $C_1 = 8.15342 \times 10^4$ | $C_3 = 3.93350 \times 10^{-6}$ | $C_5 = 19.8118 \times 10^{-7}$ |
| | $C_2 = 7.57696 \times 10^{10}$ | $C_4 = 13.9558$ | $C_6 = 194.566$ |

APPENDIX B

TABLE B.2

COEFFICIENTS FOR
HILLMAN REAR RESPONSE
(UNLADEN)

$k_{2P} = 22563$
 $k_0 = 40813 \text{ N/m}$
 $V = 20 \text{ m/s}$

| COUPLING RATIO | COEFFICIENTS FOR | | |
|-------------------|--------------------------------|---------------------------------|----------------------------------|
| | ISF2P | ISX01P | ISX12P |
| 0.6 | $C_1 = 8.06778 \times 10^4$ | $C_3 = 6.07009 \times 10^{-6}$ | $C_5 = -1.41621 \times 10^{-6}$ |
| | $C_2 = 7.94489 \times 10^{10}$ | $C_4 = 21.5038$ | $C_6 = 152.609$ |
| 0.7 | $C_1 = 8.03139 \times 10^4$ | $C_3 = 5.72151 \times 10^{-6}$ | $C_5 = -1.350172 \times 10^{-6}$ |
| | $C_2 = 7.88444 \times 10^{10}$ | $C_4 = 21.7171$ | $C_6 = 152.892$ |
| 0.8 | $C_1 = 7.95666 \times 10^4$ | $C_3 = 5.44100 \times 10^{-6}$ | $C_5 = -1.07574 \times 10^{-6}$ |
| | $C_2 = 7.66933 \times 10^{10}$ | $C_4 = 21.8220$ | $C_6 = 149.467$ |
| 0.9 | $C_1 = 7.87333 \times 10^4$ | $C_3 = 5.21329 \times 10^{-6}$ | $C_5 = -6.08022 \times 10^{-7}$ |
| | $C_2 = 7.32267 \times 10^{10}$ | $C_4 = 21.8400$ | $C_6 = 143.2792$ |
| 1.0 | $C_1 = 7.79300 \times 10^4$ | $C_3 = 5.02725 \times 10^{-6}$ | $C_5 = 0$ |
| | $C_2 = 6.88746 \times 10^{10}$ | $C_4 = 21.79431$ | $C_6 = 135.284$ |
| 1.1 | $C_1 = 7.72240 \times 10^4$ | $C_3 = 4.87500 \times 10^{-6}$ | $C_5 = 7.39048 \times 10^{-7}$ |
| | $C_2 = 6.40826 \times 10^{10}$ | $C_4 = 21.71245$ | $C_6 = 126.368$ |
| 1.2 | $C_1 = 7.65800 \times 10^4$ | $C_3 = 4.74608 \times 10^{-6}$ | $C_5 = 1.47000 \times 10^{-6}$ |
| | $C_2 = 5.93600 \times 10^{10}$ | $C_4 = 21.6180$ | $C_6 = 117.345$ |
| 1.3 | $C_1 = 7.60181 \times 10^4$ | $C_3 = 4.641161 \times 10^{-6}$ | $C_5 = 2.19513 \times 10^{-6}$ |
| | $C_2 = 5.46417 \times 10^{10}$ | $C_4 = 21.5058$ | $C_6 = 108.486$ |
| 1.4 | $C_1 = 7.54982 \times 10^4$ | $C_3 = 4.54914 \times 10^{-6}$ | $C_5 = 2.81557 \times 10^{-6}$ |
| | $C_2 = 5.04525 \times 10^{10}$ | $C_4 = 21.4089$ | $C_6 = 100.409$ |
| 1.5 | $C_1 = 7.49913 \times 10^4$ | $C_3 = 4.46901 \times 10^{-6}$ | $C_5 = 3.33460 \times 10^{-6}$ |
| | $C_2 = 4.68542 \times 10^{10}$ | $C_4 = 21.3255$ | $C_6 = 93.2137$ |

APPENDIX B

TABLE B.3

HILLMAN FRONT DAMPER OPTIMISATION DATA

| COUPLING RATIO | $q_{V.S.}$ | B_2 for min. ISF2 | minimum ISF2 $\times 10^{-8}$ | $\rho_{H.S.} \times 10^{10}$ | B for minimum ISX01 | Minimum ISX01 $\times 10^2$ |
|----------------|------------|---------------------|-------------------------------|------------------------------|---------------------|-----------------------------|
| 0.6 | -12.509 | 823.9 | 1.240 | 6.669 | 1799.3 | 1.427 |
| 0.7 | -13.039 | 837.9 | 1.270 | 6.787 | 1821.1 | 1.424 |
| 0.8 | -13.793 | 861.4 | 1.316 | 7.058 | 1837.4 | 1.427 |
| 0.9 | -14.609 | 881.5 | 1.360 | 7.358 | 1850.2 | 1.433 |
| 1.0 | -15.474 | 901.5 | 1.405 | 7.694 | 1860.7 | 1.442 |
| 1.1 | -16.289 | 919.7 | 1.448 | 7.992 | 1869.5 | 1.451 |
| 1.2 | -17.053 | 936.4 | 1.488 | 8.267 | 1876.0 | 1.460 |
| 1.3 | -17.659 | 946.2 | 1.517 | 8.468 | 1879.7 | 1.468 |
| 1.4 | -18.216 | 956.0 | 1.545 | 8.636 | 1883.2 | 1.475 |
| 1.5 | -18.710 | 964.0 | 1.570 | 8.784 | 1883.6 | 1.482 |

TABLE B.4

HILLMAN REAR DAMPER OPTIMISATION DATA

| COUPLING RATIO | $q_{V.S.}$ | B for min. ISF2P | Minimum ISF2P $\times 10^{-8}$ | $\rho_{4.5} \times 10^{10}$ | B for minimum ISX01P | Minimum ISX01P $\times 10^2$ |
|----------------|------------|------------------|--------------------------------|-----------------------------|----------------------|------------------------------|
| 0.6 | -9.919 | 992.4 | 1.601 | 7.639 | 1882.2 | 2.215 |
| 0.7 | -9.579 | 990.8 | 1.592 | 6.992 | 1948.3 | 2.229 |
| 0.8 | -9.079 | 981.8 | 1.562 | 6.344 | 2002.7 | 2.179 |
| 0.9 | -8.478 | 966.9 | 1.519 | 5.720 | 2046.8 | 2.134 |
| 1.0 | -7.797 | 940.1 | 1.465 | 5.030 | 2082.1 | 2.094 |
| 1.1 | -7.118 | 910.9 | 1.407 | 4.398 | 2110.4 | 2.058 |
| 1.2 | -6.490 | 880.4 | 1.348 | 3.800 | 2134.2 | 2.026 |
| 1.3 | -5.884 | 847.8 | 1.289 | 3.304 | 2152.6 | 1.998 |
| 1.4 | -5.364 | 817.5 | 1.234 | 2.859 | 2169.4 | 1.974 |
| 1.5 | -4.917 | 790.4 | 1.186 | 2.486 | 2184.5 | 1.953 |

APPENDIX B

TABLE B.5.

RESPONSE COEFFICIENTS FOR HILLMAN MODEL (UNLADEN) $V = 20 \text{ m/2}$

| R | $A_1 \times 10^6$ | X_1 | $Y_1 \times 10^4$ | $Z_1 \times 10^9$ |
|-----|-------------------|----------|-------------------|-------------------|
| 0.6 | 3.96448 | 16.5416 | -3.148171 | 6.49152 |
| 0.7 | 3.90854 | 15.8586 | -2.80094 | 6.77484 |
| 0.8 | 3.88205 | 15.2735 | -2.51838 | 7.17840 |
| 0.9 | 3.87325 | 14.7543 | -2.26246 | 7.57440 |
| 1.0 | 3.87487 | 14.2880 | -2.01510 | 7.89221 |
| 1.1 | 3.88036 | 13.8656 | -1.76918 | 8.09820 |
| 1.2 | 3.89140 | 13.4772 | -1.52460 | 8.18400 |
| 1.3 | 3.90350 | 13.1324 | -1.28762 | 8.16825 |
| 1.4 | 3.91630 | 13.4162 | -1.45156 | 8.87135 |
| 1.5 | 3.93350 | 13.4718 | -1.52806 | 9.40100 |
| R | $A_2 \times 10^6$ | X_2 | $Y_2 \times 10^4$ | $Z_2 \times 10^9$ |
| 0.6 | 6.07009 | 28.2395 | -5.15961 | 9.63658 |
| 0.7 | 5.72151 | 27.8427 | -4.82887 | 9.36333 |
| 0.8 | 5.44099 | 27.5550 | -4.59796 | 9.11707 |
| 0.9 | 5.21329 | 27.3485 | -4.45025 | 8.90330 |
| 1.0 | 5.02725 | 27.2155 | -4.37179 | 8.72713 |
| 1.1 | 4.87500 | 27.1531 | -4.34901 | 8.58802 |
| 1.2 | 4.74608 | 27.1533 | -4.36620 | 8.47822 |
| 1.3 | 4.64116 | 27.1850 | -4.40986 | 8.38896 |
| 1.4 | 4.54914 | 27.6616 | -4.57897 | 8.46346 |
| 1.5 | 4.46901 | 27.8079 | -4.62507 | 8.34034 |
| R | $A_3 \times 10^7$ | X_3 | $Y_3 \times 10^3$ | $Z_3 \times 10^9$ |
| 0.6 | -6.06689 | 267.3550 | -10.40282 | 16.76707 |
| 0.7 | -4.86919 | 238.0018 | -7.81869 | 12.79800 |
| 0.8 | -3.46911 | 209.4920 | -5.15530 | 8.58611 |
| 0.9 | -1.72551 | 182.7793 | -2.51793 | 4.27198 |
| 1.0 | 0 | 158.7595 | 0 | 0 |
| 1.1 | 2.70302 | 138.9282 | 2.20841 | -3.84616 |
| 1.2 | 6.41781 | 122.4418 | 4.15404 | -7.37074 |
| 1.3 | 9.98644 | 108.7387 | 5.79602 | -10.4689 |
| 1.4 | 14.62045 | 49.1672 | 12.89480 | -27.9559 |
| 1.5 | 28.30710 | 37.1311 | 14.61180 | -31.8327 |

CONT'D:

APPENDIX B

TABLE B.5 (cont'd)

| R | $A_4 \times 10^7$ | X_4 | $Y_4 \times 10^4$ | $Z_4 \times 10^9$ |
|-----|----------------------|-----------------------|----------------------|-------------------|
| 0.6 | -14.16211 | 221.522 | -43.3393 | 56.7186 |
| 0.7 | -13.50172 | 201.277 | -30.1149 | 38.4289 |
| 0.8 | -10.75738 | 178.718 | -17.9377 | 22.0044 |
| 0.9 | -6.08022 | 156.152 | -7.7158 | 8.9106 |
| 1.0 | 0 | 135.284 | 0 | 0 |
| 1.1 | 7.39048 | 117.313 | 5.0349 | -4.5269 |
| 1.2 | 14.70200 | 102.918 | 7.5204 | -4.9927 |
| 1.3 | 21.95126 | 91.948 | 7.7943 | -2.0593 |
| 1.4 | 28.15570 | 82.961 | 11.1577 | -8.3405 |
| 1.5 | 33.34620 | 75.155 | 12.0263 | -8.64441 |
| R | $A_5 \times 10^{-4}$ | $X_5 \times 10^{-10}$ | $Y_5 \times 10^{-5}$ | Z_5 |
| 0.6 | 7.52646 | 4.48521 | -19.460 | 113.006 |
| 0.7 | 7.57031 | 3.28472 | -14.751 | 125.888 |
| 0.8 | 7.63533 | 2.15319 | -10.204 | 139.106 |
| 0.9 | 7.71344 | 1.05537 | -5.344 | 150.469 |
| 1.0 | 7.79300 | 0 | 0 | 158.760 |
| 1.1 | 7.87357 | -1.03613 | 5.940 | 163.200 |
| 1.2 | 7.94925 | -1.95667 | 11.727 | 165.150 |
| 1.3 | 8.02242 | -2.09477 | 14.027 | 169.781 |
| 1.4 | 8.09144 | -2.24434 | 14.586 | 178.507 |
| 1.5 | 8.15342 | -2.12583 | 12.844 | 190.987 |
| R | $A_6 \times 10^{-4}$ | $X_6 \times 10^{-9}$ | $Y_6 \times 10^{-4}$ | Z_6 |
| 0.6 | 8.06777 | 32.57035 | -144.435 | 156.285 |
| 0.7 | 8.03139 | 21.15191 | -82.725 | 149.983 |
| 0.8 | 7.95666 | 11.88366 | -36.592 | 143.517 |
| 0.9 | 7.87333 | 4.84395 | -9.412 | 138.989 |
| 1.0 | 7.79300 | 0 | 0 | 135.284 |
| 1.1 | 7.72240 | -2.62278 | -8.254 | 134.846 |
| 1.2 | 7.65800 | -3.26610 | -29.050 | 135.884 |
| 1.3 | 7.60181 | -2.99930 | -52.305 | 136.583 |
| 1.4 | 7.43254 | 3.86805 | -89.3223 | 138.397 |
| 1.5 | 7.34345 | 6.19988 | -107.2620 | 137.146 |

APPENDIX B

TABLE B.6

RESPONSE COEFFICIENTS FOR HILLMAN MODEL (LADEN)

V = 20 m/s

| R | $A_1 \times 10^6$ | X_1 | $Y_1 \times 10^4$ | $Z_1 \times 10^9$ |
|-----|-------------------|----------|-------------------|-------------------|
| 0.6 | 3.89522 | 16.5782 | -3.21991 | 6.59063 |
| 0.7 | 3.83412 | 15.9424 | -2.91272 | 7.15238 |
| 0.8 | 3.80118 | 15.3196 | -2.57557 | 7.66575 |
| 0.9 | 3.78471 | 14.7850 | -2.28629 | 8.28900 |
| 1.0 | 3.77893 | 14.2880 | -1.98987 | 8.81317 |
| 1.1 | 3.78073 | 13.8239 | -1.68768 | 9.19350 |
| 1.2 | 3.78880 | 13.3200 | -1.38890 | 9.42581 |
| 1.3 | 3.80163 | 13.0075 | -1.10707 | 9.53381 |
| 1.4 | 3.81779 | 12.6689 | -0.85406 | 9.55237 |
| 1.5 | 3.83597 | 12.3854 | -0.64013 | 9.52200 |
| R | $A_2 \times 10^6$ | X_2 | $Y_2 \times 10^4$ | $Z_2 \times 10^9$ |
| 0.6 | 5.05531 | 29.1261 | -5.05153 | 12.05715 |
| 0.7 | 4.79723 | 28.1294 | -4.26441 | 10.89466 |
| 0.8 | 4.59744 | 27.4929 | -3.87482 | 10.38539 |
| 0.9 | 4.43931 | 27.2110 | -3.82886 | 10.4402 |
| 1.0 | 4.31680 | 27.2155 | -4.05115 | 10.9286 |
| 1.1 | 4.22198 | 27.4377 | -4.44920 | 11.67667 |
| 1.2 | 4.14632 | 26.6997 | -4.45425 | 12.54836 |
| 1.3 | 4.08387 | 28.2370 | -5.48489 | 13.40417 |
| 1.4 | 4.03046 | 28.6891 | -5.93487 | 14.15096 |
| 1.5 | 3.98346 | 29.1204 | -6.35139 | 14.74242 |
| R | $A_3 \times 10^7$ | X_3 | $Y_3 \times 10^3$ | $Z_3 \times 10^8$ |
| 0.6 | 11.76655 | 342.3652 | -16.04618 | 30.48615 |
| 0.7 | 10.35838 | 300.2879 | -13.02658 | 23.84876 |
| 0.8 | 7.51705 | 258.7270 | -8.78276 | 16.38478 |
| 0.9 | 3.71494 | 218.8841 | -4.37809 | 8.32455 |
| 1.0 | 0 | 181.7550 | 0 | 0 |
| 1.1 | -2.29679 | 148.3040 | +4.14498 | -8.16204 |
| 1.2 | -2.39665 | 119.1374 | 7.90369 | -15.81216 |
| 1.3 | +0.0769 | 94.6467 | 11.5583 | -22.64119 |
| 1.4 | +5.03140 | 75.3599 | 13.8348 | -28.44169 |
| 1.5 | 12.08697 | 60.9856 | 15.9194 | -33.10589 |

CONT'D:

APPENDIX B

TABLE B.6 (cont'd)

| R | $A_4 \times 10^7$ | X_4 | $Y_4 \times 10^4$ | $Z_4 \times 10^9$ |
|-----|----------------------|-----------------------|----------------------|-------------------|
| 0.6 | -10.5822 | 329.041 | -43.154 | 6.177 |
| 0.7 | -15.2919 | 282.561 | -13.109 | -38.647 |
| 0.8 | -14.9068 | 249.249 | + 3.399 | -51.709 |
| 0.9 | -9.3067 | 214.722 | + 8.093 | -39.302 |
| 1.0 | 0 | 197.288 | 0 | 0 |
| 1.1 | +11.7054 | 190.835 | -17.963 | 58.541 |
| 1.2 | 23.7202 | 194.051 | -43.035 | 129.873 |
| 1.3 | 34.6897 | 204.248 | -71.510 | 205.372 |
| 1.4 | 44.1065 | 218.230 | -100.617 | 278.970 |
| 1.5 | 51.4762 | 234.980 | -128.581 | 347.142 |
| R | $A_5 \times 10^{-4}$ | $X_5 \times 10^{-10}$ | $Y_5 \times 10^{-5}$ | Z_5 |
| 0.6 | 7.58557 | 5.3253 | -27.450 | 127.125 |
| 0.7 | 7.61564 | 3.7818 | -19.845 | 138.375 |
| 0.8 | 7.66777 | 2.4363 | -13.455 | 154.125 |
| 0.9 | 7.72827 | 1.1626 | -6.705 | 168.750 |
| 1.0 | 7.79300 | 0 | 0 | 181.755 |
| 1.1 | 7.86229 | -1.1385 | 7.380 | 190.125 |
| 1.2 | 8.00933 | -2.1467 | 14.197 | 196.313 |
| 1.3 | 8.08584 | -3.0660 | 20.790 | 197.125 |
| 1.4 | 8.17888 | -3.8933 | 26.955 | 199.125 |
| 1.5 | 8.31240 | -4.5802 | 32.018 | 198.563 |
| R | $A_6 \times 10^{-4}$ | $X_6 \times 10^{-9}$ | $Y_6 \times 10^{-4}$ | Z_6 |
| 0.6 | 8.3435 | 29.1324 | 15.899 | 168.954 |
| 0.7 | 8.1790 | 13.0016 | 97.538 | 164.044 |
| 0.8 | 8.0232 | 2.1989 | 125.278 | 165.857 |
| 0.9 | 7.8943 | -1.5811 | 85.467 | 178.423 |
| 1.0 | 7.7930 | 0 | 0 | 197.288 |
| 1.1 | 7.7207 | +5.0755 | -110.112 | 218.465 |
| 1.2 | 7.6633 | 14.6246 | -251.168 | 244.772 |
| 1.3 | 7.6164 | 24.6000 | -383.224 | 267.754 |
| 1.4 | 7.5740 | 35.3337 | -509.025 | 288.062 |
| 1.5 | 7.5343 | 44.9061 | -612.635 | 303.245 |

APPENDIX C

DIGITAL COMPUTER PROGRAMS

FILE C1 (FORTRAN)

Calculates I_{\min} for varying B_2 and ρ as parameters. Front and Rear $\frac{1}{4}$ -Car Model.

PROGRAM B2OPT

```

00100 PROGRAM B2OPT (OUTPUT,TAPE 2=OUTPUT)
00110 DIMENSION B2(10),PR(10,10),PQ(10,10),Q1(10,10)
00115 DIMENSION QR(10),RQ(10),RK(10,10)
00120 DATA AM1,AM2,SK1,SK2/ 28.58, 288.94, 155860., 19972.0/
00185 B=700.
00190 DO 20 I=1,10
00195 B=B+100.
00200 B2(I)=B
00210 20 CONTINUE
00212 PRINT 25
00213 25 FORMAT(16X,11HDAMPER RATE)
00214 PRINT 30,(B2(I),I=1,10)
00216 30 FORMAT(15X,10G11.5)
00220 DO 90 J=1,10
00224 DO 80 I=1,10
00230 R=.25E-10*2.0**(J-2)
00240 IF(J-2.LT.0) GO TO 5
00250 GO TO 10
00260 5 R=0.
00270 10 CONTINUE
00275 RQ(J)=R
00276 B=B2(I)
00300 R0=SK1/2.
00310 R1=(AM1+AM2)/2.
00320 R2=(SK2**2)*R1
00330 R3=((AM1+AM2)**2)/(2.0*SK1*AM2*AM2)
00340 R4=AM1/2.-SK2*AM1*(AM1+AM2)/(SK1*AM2)
00350 R5=(SK2*SK2*(AM1+AM2)**3)/(2.0*(SK1*AM2)**2)
00360 Q=(R*(R0*B*B-R2)-R1)/(R4+R5-R3*B*B)
00370 U=R0*B+R2/B
00380 X01=R3*B+(R4+R5)/B
00390 X12=R1/B
00400 PR(I,J)=R*U+Q*X01+X12
00415 Q1(I,J)=Q
00620 QJ=(J-1)
00630 Q=2.5*QJ
00635 QR(J)=Q
00640 R=(Q*(R4+R5-R3*B*B)+R1)/(R0*B*B-R2)
00645 RK(I,J)=R
00650 PQ(I,J)=R*U+Q*X01+X12
00680 80 CONTINUE
00690 90 CONTINUE
00700 PRINT 95

```

PROGRAM B2OPT (continued)....

```
00710 95 FORMAT(/, 6H "RHO", 20X, 34HPERF. INDEX WITH "RHO" AS PARAMETER)
00720 DO 100 J=1, 10
00730 PRINT 110, RQ(J), (PR(I, J), I=1, 10)
00740 100 CONTINUE
00750 110 FORMAT(1X, 1G11. 3, 2X, 10G11. 5)
00760 PRINT 115
00770 115 FORMAT(/, 5H "Q1", 21X, 33HPERF. INDEX WITH "Q1" AS PARAMETER)
00780 DO 120 J=1, 10
00790 PRINT 110, QR(J), (PQ(I, J), I=1, 10)
00800 120 CONTINUE
00810 PRINT 130
00820 130 FORMAT(/, 6H "RHO", 20X, 38HVALUES OF "Q1" WITH "RHO" AS PARAMETER)
00830 DO 140 J=1, 10
00850 PRINT 110, RQ(J), (Q1(I, J), I=1, 10)
00855 140 CONTINUE
00860 PRINT 150
00870 150 FORMAT(/, 5H "Q1", 21X, 38HVALUES OF "RHO" WITH "Q1" AS PARAMETER)
00880 DO 160 J=1, 10
00890 PRINT 110, QR(J), (RK(I, J), I=1, 10)
00895 160 CONTINUE
00900 STOP
00910 END
```

FILE C2 (FORTRAN)

The program plots I_{\min} against damping rate B_2 for different damping rates of p and q as parameters $\frac{1}{4}$ -Car Model.

PROGRAM B2PLT

```

00100 PROGRAM B2OPT (OUTPUT, TAPE 2=OUTPUT)
00110 DIMENSION B2(90), PR(90,10), PQ(90,10), Q1(90,10)
00115 DIMENSION QR(10), RQ(10), RK(90,10)
00120 DATA AM1, AM2, SK1, SK2 / 28.58, 288.94, 155860., 19972.0 /
00130 CALL PLOTS(5HCAL25)
00140 CALL AXIS(0.0, 0.0, 10HPERF. INDEX, 10, 16., 90., 0.0, 0.1, -1)
00150 CALL AXIS(0.0, 0.0, 10HDAMPING B2, -10, 18., 0.0, 800., 100., -1)
00180 B=780.0
00190 DO 20 I=1, 90
00195 B=B+20.0
00200 B2(I)=B
00210 20 CONTINUE
00220 DO 90 J=1, 10
00225 DO 80 I=1, 90
00230 RJ=J-1
00240 R=4.0E-10*RJ
00250 RQ(J)=R
00260 B=B2(I)
00300 R0=SK1/2.
00310 R1=(AM1+AM2)/2.
00320 R2=(SK2**2)*R1
00330 R3=((AM1+AM2)**2)/(2.0*SK1*AM2*AM2)
00340 R4=AM1/2. -SK2*AM1*(AM1+AM2)/(SK1*AM2)
00350 R5=(SK2*SK2*(AM1+AM2)**3)/(2.0*(SK1*AM2)**2)
00360 Q=(R*(R0*B*B-R2)-R1)/(R4+R5-R3*B*B)
00370 U=R0*B+R2/B
00380 X01=R3*B+(R4+R5)/B
00390 X12=R1/B
00400 Q1(I, J)=Q
00410 PR(I, J)=R*U+Q*X01+X12
00420 IF(PR(I, J).GT.1.6) GO TO 40
00430 IF(PR(I, J).LT.0.0) GO TO 45
00440 GO TO 50
00450 40 PR(I, J)=1.6
00460 GO TO 50
00470 45 PR(I, J)=0.0
00480 50 CONTINUE
00620 QJ=(J-1)
00630 Q=2.5*QJ
00635 QR(J)=Q
00640 R=(Q*(R4+R5-R3*B*B)+R1)/(R0*B*B-R2)
00645 RK(I, J)=R
00650 PQ(I, J)=R*U+Q*X01+X12
00660 IF(PQ(I, J).GT.1.6) GO TO 60
00670 IF(PQ(I, J).LT.0.0) GO TO 65
00680 GO TO 80
00690 60 PQ(I, J)=1.6
00700 GO TO 80
00710 65 PQ(I, J)=0.0
00720 80 CONTINUE
00750 CALL LINE(B2, 800., 100., PR(1, J), 0.0, 0.1, 90, 0)
00760 CALL LINE(B2, 800., 100., PQ(1, J), 0.0, 0.1, 90, 0)
00770 90 CONTINUE
00780 CALL PLOTE
00790 STOP
00800 END

```

FILE C3 (ACSL)

*****ADVANCED CONTINUOUS SIMULATION LANGUAGE*****
 ACSL S.A.I.T. VERSION 1 LEVEL 5B 81/03/10. 10.49.36. PAGE 1

```

PROGRAM PERFORMANCE INDEX
"DETERMINATION OF QUADRATIC INTEGRAL PERFORMANCE INDEX"
CONSTANT M1 = 28.576 , K1 = 1.55860E05 , B2 = 1.8000E03 , ...
          M1P = 54.431 , K2 = 1.99720E04 , B2P = 1.8000E03 , ...
          M = 500.080 , K0 = 4.03127E04 , WB = 2.5654 , ...
          R = 1.0 , RHO = 8.0000 E-10 , A = 1.0978
CONSTANT V = 20.0 , TF = 2.49
CINTERVAL CINT = .01
TD = WB/V
B = WB - A
MA = M*B / WB + M1
MB = M*A / WB + M1P
STF1 = 9.8*MA
STF1P = 9.8*MB
J = R*M*A*B
K2P = A*A / (WB*WB / K0 - 3*B / K2)
X0 = 0.0
X01 = X0 - X1
X12 = X1 - X2
F1 = K1*X01
VX12 = VX1 - VX2
AX1 = (F1 - F2) / M1
VX1 = INTEG(AX1, 0.)
X1 = INTEG(VX1, -1.0)
F2 = K2*X12 + B2*VX12
AX2 = AX + A*APHI
VX2 = INTEG(AX2, 0.)
X2 = INTEG(VX2, -1.0)
XOP = FCNSW(T - TD, -1.0, 0., 0.)
X01P = XOP - X1P
X12P = X1P - X2P
F1P = K1*X01P
VX12P = VX1P - VX2P
AX1P = (F1P - F2P) / M1P
VX1P = INTEG(AX1P, 0.)
X1P = INTEG(VX1P, -1.0)
F2P = K2P*X12P + B2P*VX12P
AX2P = AX - B*APHI
VX2P = INTEG(AX2P, 0.)
X2P = INTEG(VX2P, -1.0)
AX = (F2 + F2P) / A
APHI = (A*F2 - B*F2P) / J
VPHI = (VX2 - VX2P) / WB
ISX01 = INTEG(X01*X01, 0.)
ISX01P = INTEG(X01P*X01P, 0.)
ISX12 = INTEG(X12*X12, 0.)
ISX12P = INTEG(X12P*X12P, 0.)
ISVX12 = INTEG(VX12*VX12, 0.)
IVX12P = INTEG(VX12P*VX12P, 0.)
ISF2 = INTEG(F2*F2, 0.)
ISF2P = INTEG(F2P*F2P, 0.)
ISVPHI = INTEG(VPHI*VPHI, 0.)
ISAX = INTEG(AX*AX, 0.)
RMSA = SORT(ISAX*V*1.0E-06)
PR = 5.55 - 49.4*RMSA/9.8

```

The program calculates complete time response and integral square values for $\frac{1}{2}$ -car model by digital simulation.

PERFORMANCE INDEX (continued).....

*****ADVANCED CONTINUOUS SIMULATION LANGUAGE*****
 ACSL S.A.I.T. VERSION 1 LEVEL 5B 81/03/10. 10.49.36. PAGE 2

RMSF1 =K1*SQRT(ISX01*V*1.0E-06)
 RMSF1P =K1*SQRT(ISX01P*V*1.0E-06)
 RMS12 =SQRT(ISX12*V*1.0E-05)
 RMS12P =SQRT(ISX12P*V*1.0E-06)
 SISX01 =ISX01+ISX01P
 SISX12 =ISX12+ISX12P

SISF2 =ISF2+ISF2P
 INDEX =SISX12+10.*SISX01+RHO*SISF2
 CINT =RSW(T-.29.LT.0.0,CINT,0.1)

TERMT(T.GE.TF)
 END

TRANSLATION TIME = 5.410

ACSL RUN-TIME EXEC VERSION 1 LEVEL 5B 81/03/10. 10.56.38. PAGE 1

SET TITLE ="QUADRATIC PERFORMANCE INDEX"
 OUTPUT T,ISX01,ISX12,ISF2,ISAX,K2P,ISX01P,ISX12P,ISF2P,RMSA,...
 INDEX,SISX01,SISX12,SISF2,PR,"NCIOUT"=60

START

| | | | | | |
|-------|------------|--------|------------|--------|------------|
| T | 0. | ISX01 | 0. | ISX12 | 0. |
| K2P | 22563.4965 | ISX01P | 0. | ISX12P | 0. |
| INDEX | 0. | SISX01 | 0. | SISX12 | 0. |
| | | ISF2 | 0. | ISAX | 0. |
| | | ISF2P | 0. | RMSA | 0. |
| | | SISF2 | 0. | PR | 5.55000000 |
| T | 2.50000000 | ISX01 | 0.01442420 | ISX12 | 0.08819963 |
| K2P | 22563.4965 | ISX01P | 0.02115820 | ISX12P | 0.07515896 |
| INDEX | 0.80238787 | SISX01 | 0.03558241 | SISX12 | 0.16335859 |
| | | ISF2 | 1.7546E+08 | ISAX | 1443.81928 |
| | | ISF2P | 1.7455E+08 | RMSA | 0.16993053 |
| | | SISF2 | 3.5401E+08 | PR | 4.69341140 |

FILE C4 (BASIC)

PROGRAM INDEX1

```

00100 PRINT "          ", "B2", "B2P"
00110 PRINT "          ", "K2", "K2P"
00120 PRINT "          ", "ISF2", "ISF2P", "SISF2"
00130 PRINT "          ", "ISX01", "ISX01P", "SISX01"
00140 PRINT "          ", "ISX12", "ISX12P", "SISX12"
00150 PRINT
00160 READ M1, M2, M3, M4, K1
00170 READ A, B, L, K3, B1, B2
00180 FOR K2=16000 TO 32000 STEP 500
00190 C1=K1*B1+K2*K2*(M1+M2)/B1
00200 D=K2/K3-(B/L)^2
00210 K4=(K2*(A/L)^2)/D
00220 C2=K1*B2+K4*K4*(M3+M4)/B2
00230 S1=(C1+C2)/2
00240 C3=((((M1+M2)/M2)^2/K1)*B1/2
00250 C4=((((M3+M4)/M4)^2/K1)*B2/2
00260 C5=(M1/2-K2*M1*(M1+M2)/(K1*M2))/B1
00270 C6=(M3/2-K4*M3*(M3+M4)/(K1*M4))/B2
00280 C7=((((K2^2)*(M1+M2)^3)/(2*(K1*M2)^2))/B1
00290 C8=((((K4^2)*(M3+M4)^3)/(2*(K1*M4)^2))/B2
00300 S2=C3+C4+C5+C6+C7+C8
00310 S3=((M1+M2)/B1+(M3+M4)/B2)/2
00320 I1=10. *(C3+C5+C7)+8. E-10*C1/2+. 5*(M1+M2)/B1
00330 I2=10. *(C4+C6+C8)+8. E-10*C2/2+. 5*(M3+M4)/B2
00340 I=8. E-10*S1+10. *S2+S3
00350 PRINT "          ", "FRONT", "REAR", "SUM"
00360 PRINT "DAMPERS", B1, B2
00370 PRINT "SPRINGS", K2, K4
00380 PRINT "FORCE", C1/2, C2/2, S1
00390 PRINT "TYRE DEFL", C3+C5+C7, C4+C6+C8, S2
00400 PRINT "WHEEL TRVL", . 5*(M1+M2)/B1, . 5*(M3+M4)/B2, S3
00410 PRINT "INDEX", I1, I2, I
00420 PRINT
00430 NEXT K2
00440 DATA 40. 82, 435. 52, 70. 31, 471. 55, 210000
00450 DATA 1. 466, 1. 354, 2. 820, 41146. , 1600. , 1600.
00460 END

```

The program calculates the integral square response and Perf.

Index with $\rho = 3 \times 10^{-10}$, $q = 10$ for varying k_2 . Complete response, uncoupled system ($R=1.0$), $k_0 = \text{const.}$

FILE C5 (BASIC)

PROGRAM INDEX2

```

00100 PRINT "          ", "B2", "B2P"
00110 PRINT "          ", "K2", "K2P"
00120 PRINT "          ", "ISF2", "ISF2P", "SISF2"
00130 PRINT "          ", "ISX01", "ISX01P", "SISX01"
00140 PRINT "          ", "ISX12", "ISX12P", "SISX12"
00150 PRINT
00160 READ M1, M2, M3, M4, K1
00170 READ A, B, L, K3, K2, B2
00180 FOR B1=1600 TO 2400 STEP 100
00190 C1=K1*B1+K2*K2*(M1+M2)/B1
00200 D=K2/K3-(B/L)^2
00210 K4=(K2*(A/L)^2)/D
00220 C2=K1*B2+K4*K4*(M3+M4)/B2
00230 S1=(C1+C2)/2
00240 C3=((M1+M2)/M2)^2/K1)*B1/2
00250 C4=((M3+M4)/M4)^2/K1)*B2/2
00260 C5=(M1/2-K2*M1*(M1+M2)/(K1*M2))/B1
00270 C6=(M3/2-K4*M3*(M3+M4)/(K1*M4))/B2
00280 C7=((K2^2)*(M1+M2)^3)/(2*(K1*M2)^2))/B1
00290 C8=((K4^2)*(M3+M4)^3)/(2*(K1*M4)^2))/B2
00300 S2=C3+C4+C5+C6+C7+C8
00310 S3=((M1+M2)/B1+(M3+M4)/B2)/2
00320 I1=10. *(C3+C5+C7)+8. E-10*C1/2+. 5*(M1+M2)/B1
00330 I2=10. *(C4+C6+C8)+8. E-10*C2/2+. 5*(M3+M4)/B2
00340 I=8. E-10*S1+10. *S2+S3
00350 PRINT "          ", "FRONT", "REAR", "SUM"
00360 PRINT "DAMPERS", B1, B2
00370 PRINT "SPRINGS", K2, K4
00380 PRINT "FORCE", C1/2, C2/2, S1
00390 PRINT "TYRE DEFL", C3+C5+C7, C4+C6+C8, S2
00400 PRINT "WHEEL TRVL", . 5*(M1+M2)/B1, . 5*(M3+M4)/B2, S3
00410 PRINT "INDEX", I1, I2, I
00420 PRINT
00430 NEXT B1
00440 DATA 28.576, 334.935, 54.431, 340.145, 155860
00450 DATA 1.2926, 1.2728, 2.5654, 42415, 19972, 1800
00460 END

```

The program calculates complete integral square response and Perf. Index with $\gamma = 8 \times 10^{-10}$, $q = 10$ for varying B_2 or B_{2P} . Uncoupled system ($R=1.0$), $k_0 = \text{const.}$

The program calculates Integral Square Response for $\frac{1}{2}$ -car uncoupled ($R=1.0$), model for varying front or rear damper rate.

PROGRAM DAMP

```

10 PRINT "B2P", "BODY FORCE", "TYRE DEFL", "WHEEL TRVL", "PERF INDEX"
20 READ M1, M2, M3, M4, K1
30 READ A, B, L, K3, K2, B1
35 FOR B2=1200 TO 2400 STEP 20
40 C1=K1*B1+K2*K2*(M1+M2)/B1
50 D=K2/K3-(B/L)^2
60 K4=(K2*(A/L)^2)/D
70 C2=K1*B2+K4*K4*(M3+M4)/B2
80 S1=(C1+C2)/2
90 C3=((((M1+M2)/M2)^2/K1)*B1/2
100 C4=((((M3+M4)/M4)^2/K1)*B2/2
110 C5=(M1/2-K2*M1*(M1+M2)/(K1*M2))/B1
120 C6=(M3/2-K4*M3*(M3+M4)/(K1*M4))/B2
130 C7=((K2^2)*(M1+M2)^3)/(2*(K1*M2)^2)/B1
140 C8=((K4^2)*(M3+M4)^3)/(2*(K1*M4)^2)/B2
150 S2=C3+C4+C5+C6+C7+C8
160 S3=((M1+M2)/B1+(M3+M4)/B2)/2
170 I=8. E-10*S1+10. *S2+S3
180 PRINT B2, S1, S2, S3, I
190 NEXT B2
200 DATA 40. 82, 435. 52, 70. 31, 471. 55, 210000
210 DATA 1. 466, 1. 354, 2. 820, 41146, 19270, 1600
220 END

```

The program calculates I_{\min} and B_{2OPT} for given q and a series of values of ρ ($\frac{1}{4}$ -car model).

PROGRAM OPTI

```

100 READ M1, M2, K1, K2
110 INPUT Q
120 PRINT "M1=", M1, "M2=", M2
130 PRINT "K1=", K1, "K2=", K2
140 PRINT "Q1=", Q
150 PRINT
160 PRINT "B2 OPT", "PERF INDEX", "BODY FORCE", "TYRE DEFL", "WHEEL TRVL"
170 FOR R=0 TO 30E-10 STEP 2E-10
180 A=K2*K2*(M1+M2)/2
190 C=M1/2-K2*M1*(M1+M2)/(K1*M2)
200 D=(K2*K2*(M1+M2)^3)/(2*(K1*M2)^2)
220 E=((M1+M2)^2)/(2*K1*M2*M2)
230 G=(M1+M2)/2
240 X=R*K1/2+Q*E
250 Y=R*A+Q*(C+D)+G
260 B=SQR(Y/X)
270 F=K1*B/2+A/B
280 T=E*B+(C+D)/B
290 W=G/B
300 I=R*F+Q*T+W
310 PRINT B, I, F, T, W
320 NEXT R
330 DATA 28. 58, 334. 94, 155860, 19972
340 END

```

FILE C7 (FORTRAN 5)

The program calculates the Integral Square Response and Performance Index for $\frac{1}{2}$ -Car Model, using state variable algorithms and matrices.

```

M INDEX      73/173  OPT=0                               FTN 5.0+518  8
PROGRAM INDEX
THIS PROGRAM CALCULATES THE PERFORMANCE INDEX OF A HALF-CAR MODEL
HAVING FOUR DEGREES OF FREEDOM
SYMBOLS USED ARE:
TKA  FRONT TYRE STIFFNESS
TKB  REAR TYRE STIFFNESS
BM   BODY MASS
BJ   BODY MASS MOMENT OF INERTIA ABOUT ITS CENTRE OF MASS
FM1  FRONT UNSPRUNG MASS
RM3  REAR UNSPRUNG MASS
WB   LENGTH OF WHEELBASE
AG   DISTANCE OF CM FROM THE FRONT WHEELS
BG   DISTANCE OF CM FROM THE REAR WHEELS
SK1  FRONT SPRING STIFFNESS
SK3  REAR SPRING STIFFNESS
C1   FRONT DAMPER RATIO
C3   REAR DAMPER RATIO
DIMENSION A(8,8),A1(8,8),A2(8,8),FRFT(8,8),P(8,8),Q(8,8),R(8,8)
DIMENSION B(8,2),B1(8,2),FT(2,8),FR(8,2),F(8,2),F1(2,2),PP(36,37)
DIMENSION AD(8,8),BBT(8,8),B1B2T(8,8),C(8,8),CB(8,8),L(8,8)
DIMENSION RM(8,8),SM(8,8),TM(8,8),G(36)
OPEN(1,FILE='INPUT',STATUS='OLD')
OPEN(2,FILE='OUTPUT',STATUS='OLD')
INITIALISE ARRAYS
DO 10 I=1,2
DO 10 J=1,2
10  R1(I,J)=0.0
DO 14 I=1,8
DO 14 J=1,2
14  B(I,J)=0.0
    R1(I,J)=0.0
    F(I,J)=0.0
    FR(I,J)=0.0
DO 16 I=1,8
DO 16 J=1,8
    A(I,J)=0.0
    A1(I,J)=0.0
    A2(I,J)=0.0
    FRFT(I,J)=0.0
    P(I,J)=0.0
    Q(I,J)=0.0
    R(I,J)=0.0
16  LIST THE DESIGN DATA
    READ(1,20) TKA,TKB,BM,BJ,FM1,RM3,WB,AG
20  FORMAT(8F10.4)
    R2=BJ/BM
    BG=WB-AG
    CR=R2/(AG*BG)
21  PRINT 21
    FORMAT(1H1,5X,27H MODEL PARAMETER VALUES ARE,/)
    PRINT 22,TKA,TKB,BM,BJ,FM1,RM3,WB,AG,BG,CR
22  FORMAT(//5X,30H FRONT TYRE STIFFNESS =,G11.5,5H N/M /
25X,30H REAR TYRE STIFFNESS =,G11.5,5H N/M /
35X,30H BODY MASS =,G11.5,4H KG /
45X,30H BODY INERTIA ABOUT C.O.F.M. =,G11.5,6H KGM2 /
55X,30H FRONT UNSPRUNG MASS =,G11.5,4H KG /
65X,30H REAR UNSPRUNG MASS =,G11.5,4H KG /
M INDEX      73/173  OPT=0                               FTN 5.0+518
75X,30H WHEEL BASE LENGTH =,G11.5,2H M /
85X,30H DISTANCE OF CM FROM FRONT =,G11.5,2H M /
95X,30H DISTANCE OF CM FROM REAR =,G11.5,3H M /
$5X,30H COUPLING RATIO R2/A*B =,G11.5)

```

Program INDEX (continued).....

```

24 READ(1,24)SK1,SK3,C1,C3
   FFORMAT(4F10.3)
   PRINT 26,SK1,SK3,C1,C3
26 FFORMAT(//5X,30H FRONT SPRING STIFFNESS      =,G11.5,5H N/M /
   25X,30H REAR SPRING STIFFNESS                =,G11.5,5H N/M /
   35X,30H FRONT DAMPER RATE                     =,G11.5,6H NS/M /
   45X,30H REAR DAMPER RATE                      =,G11.5,6H NS/M /)
C ASSEMBLE MATRICES
  DC 28 I=1,4
  J=I+4
28 A1(I,J)=1.0
  A1(2,5)=-1.0
  A1(4,7)=-1.0
  A1(5,1)=-TKA/PM1
  A1(7,3)=-TKB/RM3
  PRINT 30
30 FFORMAT(//5X,17H SYSTEM MATRIX A1,/)
  CALL MATPR(A1,8,8,8,8)
  ASSEMBLE B-MATRIX
  B(1,1)=-1.0
  B(3,2)=-1.0
  PRINT 32
32 FFORMAT(//5X,10H B MATRIX,/)
  CALL MATPR(B,8,2,8,2)
  ASSEMBLE B1-MATRIX
  B1(5,1)=-1.0/PM1
  B1(6,1)=(1.0+AG*AG/R2)/BM
  B1(6,2)=(1.0-AG*BG/R2)/BM
  B1(7,2)=-1.0/RM3
  B1(8,1)=B1(6,2)
  B1(8,2)=(1.0 + BG*BG/R2)/BM
  PRINT 42
42 FFORMAT(//5X,10H B1 MATRIX,/)
  CALL MATPR(B1,8,2,8,2)
  READ(1,44)(F1(I,1),I=1,2)
44 FFORMAT(2G10.4)
  READ(1,46)(C(I,1),I=3,4)
46 FFORMAT(4G10.4)
  PRINT 48
48 FFORMAT(//5X,11H RHC MATRIX,/)
  CALL MATPR(R1,2,2,2,2)
  PRINT 50
50 FFORMAT(//5X,10H Q MATRIX,/)
  CALL MATPR(Q,8,8,8,8)
  ASSEMBLE F-MATRIX
  F(2,1)=-SK1
  F(4,2)=-SK3
  F(5,1)=C1
  F(6,1)=-C1
  F(7,2)=C3
  F(8,2)=-C3
  PRINT 52
52 FFORMAT(//5X,10H F MATRIX,/)

```

M INDEX 73/173 (PT=0)

FTN 5.0+518

```

C CALL MATPR(F,8,2,8,2)
  FORM TRANSPOSE OF F-MATRIX
  DC 54 I=1,2
  DC 54 J=1,2
54 FT(I,J)=F(J,I)
  PRINT 56
56 FFORMAT(//5X,10H FT MATRIX,/)
  CALL MATPR(FT,2,8,2,8)
  DC 60 I=1,8
  DC 60 J=1,8
  SUM = 0.0
  DO 58 K=1,2
58 SUM = SUM +B1(I,K)*FT(K,J)
60 A2(I,J)=SUM
  PRINT 62
62 FFORMAT(//5X,10H A2 MATRIX,/)
  CALL MATPR(A2,8,8,8,8)
  PRINT 64
64 FFORMAT(//5X,10H A MATRIX,/)

```

Program INDEX (continued).....

```

DC 66 I=1,8
DC 66 J=1,8
A(I,J)=A1(I,J)+A2(I,J)
66 CONTINUE
CALL MATPR(A,8,8,8,8)
DO 70 I=1,8
DO 70 J=1,2
SUM=0.0
DO 68 K=1,2
68 SUM=SUM+F(I,K)*R1(K,J)
70 FR(I,J)=SUM
DO 80 I=1,8
DO 80 J=1,8
SUM=0.0
DO 78 K=1,2
78 SUM=SUM+FR(I,K)*FT(K,J)
80 FRFT(I,J)=SUM
PRINT 8?
82 FORMAT(//5X,12H FRFT MATRIX,/)
CALL MATPR(FRFT,8,8,8,8)
DO 84 I=1,8
DO 84 J=1,8
84 R(I,J)=FRFT(I,J)+Q(I,J)
PRINT 86
86 FORMAT(//5X,10H R MATRIX,/)
CALL MATPR(R,8,8,8,8)
CALL CFCHEN(PP,A,R,NI,NJ,H)
CALL MATPR(PP,36,37,NI,NJ)
NR=NI
NC=NJ
DO 90 I=1,NR
90 G(I)=C.
CONTINUE
T=NR
N=(SQRT(8*T+1)-1)/2
CALL ELIMIN(PP,P,G,NR,NC,DETA,RATIO)
IF(DETA) 121,119,121
119 WRITE(2,139)

```

M INDEX

73/173 DET=0

FTN 5.0+518

121 CONTINUE

C
C

```

OUTPUT THE RESULTS
WRITE(2,116)
116 FORMAT(//5X,23H THE SOLUTION VECTOR IS//)
WRITE(2,117) (G(I),I=1,NR)
117 FORMAT(5X,G12.5)
WRITE(2,118) DETA,RATIO
118 FORMAT(//5X,13H DETERMINANT=,E12.5,10X,7H RATIO=,E12.5//)
DO 95 I=1,N
RN=N
RI=I
KS=(RI-1)*(RN-(RI-2)/2)+1
KF=RI*(RN-(RI-1)/2)
DO 92 K=KS,KF
J=I+K-KS
92 P(I,J)=G(K)
P(J,I)=P(I,J)
95 CONTINUE
WRITE(2,120)
120 FORMAT(//5X,39H SYSTEM COVARIANCE MATRIX (P MATRIX) IS//)
DO 96 I=1,N
WRITE(2,130) (P(I,J),J=1,N)
130 FORMAT(5X,(8(1X,G12.5)))
96 CONTINUE
CALL TRANS(A,AD,B,BBT,B1B21,P,C,CB,E,PM,SM,TM,N,WB)
139 FORMAT(46H THE EQUATIONS ARE ILL CONDITIONED OR SINGULAR/)
STOP
END

```

Subroutine CFCHEN

Subroutine MATPR

CFCHEN 73/173 OPT=0

FTN 5.0+518

80

```

SUBROUTINE CFCHEN(P,A,C,NJ,NJ,M)
SOLVING LYAPUNOV EQUATION  $AP + PA + Q = 0$ 
DIMENSION P(36,37),A(8,8),Q(8,8)
M=M+1
NI=N*(N+1)/2
NJ=NJ+1
DO 20 I=1,N
DO 20 J=1,N
M=M+1
P(M,NJ)=-Q(I,J)
IF(I.EQ.J) P(M,NJ)=-Q(I,J)/2.
LM=C
DO 20 K=1,N
DO 20 L=K,N
LM=LM+1
IF(K.EQ.I.AND.L.NE.J) GO TO 21
IF(K.NE.I.AND.L.EQ.J) GO TO 22
IF(K.NE.I.AND.L.NE.J.AND.K.EQ.J.AND.L.NE.I) GO TO 23
IF(K.NE.I.AND.L.NE.J.AND.K.NE.J.AND.L.EQ.I) GO TO 24

IF(K.NE.J.AND.L.NE.J.AND.K.NE.J.AND.L.NE.I) GO TO 25
IF(K.EQ.I.AND.L.EQ.J.AND.K.EQ.J.AND.L.EQ.J) GO TO 26
IF(K.EQ.I.AND.L.EQ.J.AND.K.NE.J.AND.L.NE.I) GO TO 27
21 P(M,LM)=A(L,J)
GO TO 20
22 P(M,LM)=A(K,I)
GO TO 20
23 P(M,LM)=A(L,I)
GO TO 20
24 P(M,LM)=A(K,J)
GO TO 20
25 P(M,LM)=0.
GO TO 20
26 P(M,LM)=A(K,I)
GO TO 20
27 P(M,LM)=A(K,I)+A(L,J)
20 CONTINUE
PRINT 100
100 FORMAT(///5X,40H THE REQUIRED SIMULTANEOUS EQUATIONS ARE,10X, 61H
THE SEQUENCE OF P IS P(1,1)...P(1,N),P(2,2)...P(2,N)...P(N,N)///)
RETURN
END

```

MATPR 73/173 OPT=0

FTN 5.0+518

80

The program prints out matrices arranged in rows and columns.

```

SUBROUTINE MATPR(B,NR,NC,I,J)
DIMENSION B(NR,NC)
CHARACTER *50,IFORM

JB=J
1 JA=J-JB+1
IF(JB.LT.11)GO TO 4
JC=JA+9
2 PRINT 2,JA,JC,(N,(B(I,M),M=JA,JC),N=1,I)
FORMAT(79H COLUMNS ,13,4H TO ,13//((14,3X,10G12.5)))
PRINT 3
3 FORMAT(1H-)
JB=JB-10
GO TO 1
4 IF(JB-2)5,7,9
5 WRITE(IFORM,6)
GO TO 11
6 FORMAT(37H(78H COLUMN ,13,T9,13//((14,3X,612.5)))
7 WRITE(IFORM,8)
GO TO 11
8 FORMAT(44H(79H COLUMNS ,13,5H AND ,13//((14,3X,2G12.5)))
9 WRITE(IFORM,10) JB
10 FORMAT(35H(79H COLUMNS ,13,4H TO ,13//((14,3X,,12,7HG12.5)))
11 PRINT IFORM,JA,J,(N,(B(N,M),M=JA,J),N=1,I)
RETURN
END

```

Subroutine ELIMIN

```

LIMIN      73/173  OPT=0                      FTN 5.0+518      6
SUBROUTINE LELIMIN(A,G,X,NEQN,JMAX,DET,RATIO)
SUBROUTINE FOR SOLVING SIMULTANEOUS EQUATIONS BY GAUSSIAN
ELIMINATION WITH PARTIAL PIVOTING
DIMENSION A(36,37),G(8,8),X(36)
FIND MEAN COEFFICIENT MAGNITUDE
1  AMEAN=0.
DO 2 I=1,NEQN
DO 2 J=1,NEQN
2  AMEAN=AMEAN+ABS(A(I,J))
AMEAN=AMEAN/FLCAT(NEQN*NEQN)
COMMENCE ELIMINATION PROCESS
NEQNMI=NEQN-1
DO 6 IEQN=1,NEQNMI
SEARCH LEADING COLUMN FOR LARGEST ELEMENT
IMIN=IEQN+1
IMAX=IEQN
DO 3 I=IMIN,NEQN
IF(ABS(A(I,IEQN)).GT.ABS(A(IMAX,IEQN))) IMAX=I
3 CONTINUE
IF(IMAX.EC.IEQN) GO TO 5
DO 4 J=IEQN,JMAX
4  AA=A(IEQN,J)
A(IEQN,J)=A(IMAX,J)
A(IMAX,J)=AA
ELIMINATE X(IEQN) FROM EQUATIONS, TEST FOR NONZERO PIVOT
5  IF(ABS(A(IEQN,IEQN)/AMEAN).LT.1.E-8) GO TO 10
DO 6 I=IMIN,NEQN
FACT=A(I,IEQN)/A(IEQN,IEQN)
DO 6 J=IMIN,JMAX
6  A(I,J)=A(I,J)-FACT*A(IEQN,J)
CONTINUE
SOLVE THE UPPER-TRIANGULAR SET OF EQUATIONS BY BACK SUBSTITUTION
IF(ABS(A(NEQN,NEQN)/AMEAN).LT.1.E-8) GO TO 10
X(NEQN)=A(NEQN,JMAX)/A(NEQN,NEQN)
DO 8 L=2,NEQN
I=NEQN+1-L
SUM=A(I,JMAX)
IP1=I+1
DO 7 J=IP1,NEQN
7  SUM=SUM-A(I,J)*X(J)
8  X(I)=SUM/A(I,I)
EVALUATE DET OF COEFFICIENT MATRIX, AND COMPARE WITH ORIGINAL
DETA=1.
DO 9 I=1,NEQN
9  DETA=DETA*A(I,I)
CONTINUE
DET=DETA
RATIO=DETA/AMEAN**NEQN
RETURN
LIMIN      73/173  OPT=0                      FTN 5.0+518      1
10 DET=0
RETURN
END

```


SUBROUTINE TRANS (continued)....

TRANS 73/172 OPT=0

FTN 5.0+518

80/

```

WRITE(2,52)((E(I,J),J=1,N),I=1,N)
DO 16 I=1,N
DO 16 J=1,N
R(I,J)=0.0
DO 15 K=1,N
15 R(I,J)=R(I,J)+E(I,K)*B1B2T(K,J)
16 CONTINUE
WRITE(2,53)
53 FORMAT(//5X,20H R MATRIX = EXP(AD)*B1B2T//)
WRITE(2,52)((R(I,J),J=1,N),I=1,N)
52 FORMAT(8(2X,G12.5))
DO 17 I=1,N
DO 17 J=1,N
S(I,J)=BBT(I,J)+2.0*R(I,J)
17 CONTINUE
WRITE(2,56)
56 FORMAT(//5X,20H S MATRIX = BBT + 2*R//)
WRITE(2,52)((S(I,J),J=1,N),I=1,N)
DO 19 I=1,N
DO 19 J=1,N
T(I,J)=0.0
DO 18 K=1,N
18 T(I,J)=T(I,J)+S(I,K)*P(K,J)
19 CONTINUE
WRITE(2,59)
59 FORMAT(//5X,20H T MATRIX = (BBT + 2*R)*P//)
WRITE(2,52)((T(I,J),J=1,N),I=1,N)
PI=C.0
DO 20 I=1,N
J=I
PI=PI+T(I,J)
20 CONTINUE
WRITE(2,60) PI
60 FORMAT(//5X,20H PERFORMANCE INDEX= ,G12.5//)
25 CONTINUE
RETURN
END

```

MODEL PARAMETER VALUES ARE

| | | | |
|----------------------------|---|----------|------------------|
| FRONT TYRE STIFFNESS | = | .155E+06 | N/M |
| REAR TYRE STIFFNESS | = | .155E+06 | N/M |
| BODY MASS | = | 505.08 | KG |
| BODY INERTIA ABOUT C.OF M. | = | 569.63 | KGM ² |
| FRONT UNSPRUNG MASS | = | 28.576 | KG |
| REAR UNSPRUNG MASS | = | 34.431 | KG |
| WHEEL BASE LENGTH | = | 2.5654 | M |
| DISTANCE OF CM FROM FRONT | = | 1.0978 | M |
| DISTANCE OF CM FROM REAR | = | 1.4676 | M |
| COUPLING RATIO R2/A*B | = | .70000 | |
| FRONT SPRING STIFFNESS | = | 19972. | N/M |
| REAR SPRING STIFFNESS | = | 22564. | N/M |
| FRONT DAMPER RATE | = | 1800.0 | NS/M |
| REAR DAMPER RATE | = | 1800.0 | NS/M |

FILE C3 (FORTRAN)

The program calculates l_{\min} for varying values of damping with p and q as parameters. $\frac{1}{2}$ -Car Model.

PROGRAM B2MIN

```

00100 PROGRAM B2MIN (OUTPUT, TAPE 2=OUTPUT)
00110 DIMENSION B2(10), PR(10, 10), PQ(10, 10), Q1(10, 10)
00115 DIMENSION QR(10), RQ(10), RK(10, 10)
00118 DATA B3, CR/1800., .7/
00120 DATA C1, C3, C5/7.58055E4, 3.908616E-6, -4.83683E-7/
00130 DATA C2, C4, C6/5.321777E10, 12.96269, 132.899/
00140 DATA P1, P3, P5/8.03139E4, 5.721513E-6, -1.35017E-6/
00150 DATA P2, P4, P6/7.88444E10, 21.71708, 152.8918/
00160 B=700.
00170 DO 20 I=1, 10
00180 B=B+100.
00190 B2(I)=B
00200 20 CONTINUE
00210 PRINT 25
00220 25 FORMAT(16X, 11HDAMPER RATE)
00230 PRINT 30, (B2(I), I=1, 10)
00240 30 FORMAT(15X, 10G11.5)
00250 DO 90 J=1, 10
00260 DO 80 I=1, 10
00270 R=.25E-10*2.0**(J-2)
00280 IF(J-2.LT.0) GO TO 5
00290 GO TO 10
00300 5 R=0.
00310 10 CONTINUE
00320 RQ(J)=R
00330 B=B2(I)
00340 Q=-((C5-C6/(B*B))+R*((C1-C2/(B*B))))/(C3-C4/(B*B))
00350 F2=C1*B+C2/B
00360 X01=C3*B+C4/B
00370 X12=C5*B+C6/B
00380 F2P=P1*B3+P2/B3
00390 X01P=P3*B3+P4/B3
00400 X12P=P5*B3+P6/B3
00410 PR(I, J)=R*(F2+F2P)+Q*(X01+X01P)+(X12+X12P)
00420 Q1(I, J)=Q
00620 QJ=(J-1)
00630 Q=2.5*QJ
00635 QR(J)=Q
00640 R=-((C5-C6/(B*B))+Q*(C3-C4/(B*B)))/(C1-C2/(B*B))
00645 RK(I, J)=R
00650 PQ(I, J)=R*(F2+F2P)+Q*(X01+X01P)+(X12+X12P)
00680 80 CONTINUE
00690 90 CONTINUE
00700 PRINT 95
00710 95 FORMAT(/, 6H "RHO", 20X, 34HPERF. INDEX WITH "RHO" AS PARAMETER)
00720 DO 100 J=1, 10
00730 PRINT 110, RQ(J), (PR(I, J), I=1, 10)
00740 100 CONTINUE

```

FILE C3 (FORTRAN) continued.....

```
00750 110 FORMAT(1X,1G11.3,2X,10G11.5)
00760 PRINT 115
00770 115 FORMAT(/,5H "Q1",21X,33HPERF. INDEX WITH "Q1" AS PARAMETER)
00780 DO 120 J=1,10
00790 PRINT 110,QR(J), (PQ(I,J), I=1,10)
00800 120 CONTINUE
00810 PRINT 130
00820 130 FORMAT(/,6H "RHO",20X,38HVALUES OF "Q1" WITH "RHO" AS PARAMETER)
00830 DO 140 J=1,10
00850 PRINT 110,RQ(J), (Q1(I,J), I=1,10)
00855 140 CONTINUE
00860 PRINT 150
00870 150 FORMAT(/,5H "Q1",21X,38HVALUES OF "RHO" WITH "Q1" AS PARAMETER)
00880 DO 160 J=1,10
00890 PRINT 110,QR(J), (RK(I,J), I=1,10)
00895 160 CONTINUE
00900 STOP
00910 END
```

FILE C9 (BASIC)

The program calculates coefficients A,X,Y,Z from ACSL output for $\frac{1}{2}$ -Car Model.

$$(I.S.V. = AB_2 + (X + Y k_2 + Z k_2^2)/B_2)$$

PROGRAM COEF

```

00100 INPUT X1,X2,X3,X4
00110 READ B1,B2,B3,B4
00120 READ K1,K2,K3,K4
00130 R1=(X1*B2-X2*B1)*B1*B2/(B2^2-B1^2)
00140 R2=(X2*B3-X3*B2)*B2*B3/(B3^2-B2^2)
00150 R3=(X3*B4-X4*B3)*B3*B4/(B4^2-B3^2)
00160 P1=(K1*B2*B2-K2*B1*B1)/(B2*B2-B1*B1)
00170 P2=(K2*B3*B3-K3*B2*B2)/(B3*B3-B2*B2)
00180 P3=(K3*B4*B4-K4*B3*B3)/(B4*B4-B3*B3)
00190 Q1=((K1*B2)^2-(K2*B1)^2)/(B2*B2-B1*B1)
00200 Q2=((K2*B3)^2-(K3*B2)^2)/(B3*B3-B2*B2)
00210 Q3=((K3*B4)^2-(K4*B3)^2)/(B4*B4-B3*B3)
00220 S1=P1-P2
00230 S2=P2-P3
00240 S3=Q1-Q2
00250 S4=Q2-Q3
00260 R4=(R1-R2)/S1
00270 R5=(R2-R3)/S2
00280 R6=(Q1-Q2)/S1
00290 R7=(Q2-Q3)/S2
00300 Z=(R4-R5)/(R6-R7)
00310 Y1=R4-Z*R6
00320 Y2=R5-Z*R7
00330 Y=(Y1+Y2)/2
00340 Z1=R1-Y*P1-Z*Q1
00350 Z2=R2-Y*P2-Z*Q2
00360 Z3=R3-Y*P3-Z*Q3
00370 X=(Z1+Z2+Z3)/3
00380 A1=X1/B1-(X+Y*K1+Z*K1*K1)/(B1*B1)
00390 A2=X2/B2-(X+Y*K2+Z*K2*K2)/(B2*B2)
00400 A3=X3/B3-(X+Y*K3+Z*K3*K3)/(B3*B3)
00410 A4=X4/B4-(X+Y*K4+Z*K4*K4)/(B4*B4)
00420 A=(A1+A2+A3+A4)/4
00430 PRINT "Y1", "Y2"
00440 PRINT Y1, Y2
00450 PRINT "X1", "X2", "X3"
00460 PRINT Z1, Z2, Z3
00470 PRINT "A1", "A2", "A3", "A4"
00480 PRINT A1, A2, A3, A4
00490 PRINT "A", "X", "Y", "Z"
00500 PRINT A, X, Y, Z
00510 DATA 1800, 2000, 1700, 2082.5
00520 DATA 22563.5, 17825.3, 22563.5, 28972.2
00530 END

```

FILE C10 (BASIC)

The program calculates Integral Square Response:

$$I.S.V. = AB_2 + (X + Y k_2 + Z k_2^2)/B_2 \text{ for front and rear.}$$

PROGRAM PERF3

```

00160 READ A, B, L, K3, R
00170 INPUT B1, B2, K2
00180 READ A1, X1, Y1, Z1
00190 READ A2, X2, Y2, Z2
00200 READ A3, X3, Y3, Z3
00210 READ A4, X4, Y4, Z4
00220 READ A5, X5, Y5, Z5
00230 READ A6, X6, Y6, Z6
00240 D=K2/K3-(B/L)^2
00250 K4=((A/L)^2)*K2/D
00260 S1=A1*B1+(X1+Y1*K2+Z1*K2*K2)/B1
00270 S2=A2*B2+(X2+Y2*K4+Z2*K4*K4)/B2
00280 S3=A3*B1+(X3+Y3*K2+Z3*K2*K2)/B1
00290 S4=A4*B2+(X4+Y4*K4+Z4*K4*K4)/B2
00300 S5=A5*B1+(X5+Y5*K2+Z5*K2*K2)/B1
00310 S6=A6*B2+(X6+Y6*K4+Z6*K4*K4)/B2
00320 I1=10. *S1+8. E-10*S5+S3
00330 I2=10. *S2+8. E-10*S6+S4
00340 I=I1+I2
00350 PRINT " COUPLING R =", R
00360 PRINT "          ", "FRONT", "REAR", "SUM"
00370 PRINT "DAMPERS", B1, B2
00380 PRINT "SPRINGS", K2, K4
00390 PRINT "FORCE", S5, S6, S5+S6
00400 PRINT "TYRE DEFL", S1, S2, S1+S2
00410 PRINT "WHEEL TRVL", S3, S4, S3+S4
00420 PRINT "INDEX", I1, I2, I
00430 PRINT
00440 DATA 1. 0978, 1. 4676, 2. 5654, 40812. 7, . 7
450 DATA 3. 908842E-6, 15. 9867, -2. 9316E-4, 7. 096945E-9
460 DATA 5. 733392E-6, 27. 5252, -4. 58323E-4, 8. 83832E-9
470 DATA -4. 711301E-7, 244. 305, -8. 461616E-3, 1. 4423E-7
480 DATA -1. 874146E-6, 212. 702, -3. 941066E-3, 6. 00406E-8
490 DATA 75711. 5, 3. 686526E10, -1. 8469E6, 134. 4
500 DATA 79995. 5, 2. 55695E10, -1. 0378E6, 152. 4737
00510 END

```

FILE C11 (BASIC)

The program calculates k_2 that minimises the Performance Index for specified values of q and ρ .

HILLMAN, $R=0.7$, (Laden) $V = 20$ m/s.

PROGRAM MIN

```

00100 READ A, B, L, K3
00110 READ A0, B0, C0
00120 READ A1, B1, C1
00130 READ A2, B2, C2
00140 READ D0, E0, F0
00150 READ D1, E1, F1
00160 READ D2, E2, F2
00170 DATA 1. 2926, 1. 2728, 2. 5654, 42415.
00180 DATA . 01575850, -1. 618175E-7, 3. 973542E-12
00190 DATA . 1687339, -7. 236988E-6, 1. 324931E-10
00200 DATA 1. 58100E8, -1. 1025E3, . 076875
00210 DATA . 02426182, -2. 369117E-7, 6. 052588E-12
00220 DATA . 1542265, -7. 282867E-7, -2. 147053E-11
00230 DATA 1. 544557E8, 541. 8804, . 09113548
00240 INPUT K2, Q, R, C
00250 PRINT "COUPLING RATIO =", C
00260 GO TO 00280
00270 K2=K2-. 25*53/I3
00280 D=K2/K3-(B/L)^2
00290 K4=((A/L)^2)*K2/D
00300 D4=-((K4/K2)*(B/A))^2
00310 D5=2*D4*(D4*K2/K4-1)/K2
00320 R0=B0+2*K2*C0
00330 R1=B1+2*K2*C1
00340 R2=B2+2*K2*C2
00350 R3=(E0+2*K4*F0)*D4
00360 R4=(E1+2*K4*F1)*D4
00370 R5=(E2+2*K4*F2)*D4
00380 S0=R0+R3
00390 S1=R1+R4
00400 S2=R2+R5
00410 S3=Q*S0+S1+R*S2
00420 T4=2*C0+D5*R3+2*D4*F0*D4
00430 T5=2*C1+D5*R4+2*D4*F1*D4
00440 T6=2*C2+D5*R5+2*D4*F2*D4
00450 I3=T4*Q+T5*1. +T6*R
00460 IF ABS(S3)>1. E-12 THEN 00270
00470 S4=A0+B0*K2+C0*K2*K2
00480 S5=A1+B1*K2+C1*K2*K2
00490 S6=A2+B2*K2+C2*K2*K2
00500 S7=D0+E0*K4+F0*K4*K4
00510 S8=D1+E1*K4+F1*K4*K4
00520 S9=D2+E2*K4+F2*K4*K4

```

Program MIN (continued).....

```
00530 I1=R*S6+Q*S4+S5
00540 I2=R*S9+Q*S7+S8
00550 I=I1+I2
00560 T1=S4+S7
00570 T2=S5+S8
00580 T3=S6+S9
00590 PRINT
00600 PRINT "RHO", "Q", "K2", "K2P", "DI/DK2"
00610 PRINT R, Q, K2, K4, S3
00620 PRINT
00630 PRINT "          ", "DX01/DK2", "DX12/DK2", "DF2/DK2"
00640 PRINT "FRONT", R0, R1, R2
00650 PRINT "REAR", R3, R4, R5
00660 PRINT "SUM", S0, S1, S2
00670 PRINT
00680 PRINT "          ", "TYRE DEFL", "WHEEL TRVL", "BODY FORCE", "PERF INDEX"
00690 PRINT "FRONT", S4, S5, S6, I1
00700 PRINT "REAR", S7, S8, S9, I2
00710 PRINT "SUM", T1, T2, T3, I
00720 PRINT
00730 GO TO 00240
00740 END
```

FILE C12 (BASIC)

The program calculates Min. Perf. Index as function of q and p for a given value of k_2 .

Data: HILLMAN, $\frac{1}{2}$ -Car Model, $R=0.7$ (Unladen).

PROGRAM MINIQ

```

00100 READ A, B, L, K3
00110 READ A0, B0, C0
00120 READ A1, B1, C1
00130 READ A2, B2, C2
00140 READ D0, E0, F0
00150 READ D1, E1, F1
00160 READ D2, E2, F2
00170 DATA 1. 0978, 1. 4676, 2. 5654, 40812. 7
00180 DATA . 0158457, -1. 556078E-7, 3. 7638E-12
00190 DATA . 131529, -4. 343718E-6, 7. 11E-11
00200 DATA 1. 54514E8, -819. 5, 6. 99375E-2
00210 DATA . 02576962, -2. 682707E-7, 5. 201849E-12
00220 DATA . 1093146, -1. 673051E-6, 2. 134936E-11
00230 DATA1. 563412E8, -459. 5847, . 08332405
00240 INPUT K2, C
00250 PRINT "COUPLING RATIO =", C
00260 D=K2/K3-(B/L)^2
00270 K4=((A/L)^2)*K2/D
00280 D4=-((K4/K2)*(B/A))^2
00290 D5=2*D4*(D4*K2/K4-1)/K2
00300 R0=B0+2*K2*C0
00310 R1=B1+2*K2*C1
00320 R2=B2+2*K2*C2
00330 R3=(E0+2*K4*F0)*D4
00340 R4=(E1+2*K4*F1)*D4
00350 R5=(E2+2*K4*F2)*D4
00360 S0=R0+R3
00370 S1=R1+R4
00380 S2=R2+R5
00390 FOR Q = 0 TO 5 STEP 1.
00400 R=-(Q*S0+S1)/S2
00410 S3=Q*S0+S1+R*S2
00420 T4=2*C0+D5*R3+2*D4*F0*D4
00430 T5=2*C1+D5*R4+2*D4*F1*D4
00440 T6=2*C2+D5*R5+2*D4*F2*D4
00450 I3=T4*Q+T5*1. +T6*R
00460 S4=A0+B0*K2+C0*K2*K2
00470 S5=A1+B1*K2+C1*K2*K2
00480 S6=A2+B2*K2+C2*K2*K2
00490 S7=D0+E0*K4+F0*K4*K4
00500 S8=D1+E1*K4+F1*K4*K4
00510 S9=D2+E2*K4+F2*K4*K4
00520 I1=R*S6+Q*S4+S5
00530 I2=R*S9+Q*S7+S8

```

PROGRAM MINIQ (continued).....

```

00540 I=I1+I2
00550 T1=54+57
00560 T2=55+58
00570 T3=56+59
00580 PRINT
00590 PRINT "RHO", "Q", "K2", "K2P", "DI/DK2"
00600 PRINT R, Q, K2, K4, S3
00610 PRINT
00620 PRINT " ", "DX01/DK2", "DX12/DK2", "DF2/DK2"
00630 PRINT "FRONT", R0, R1, R2
00640 PRINT "REAR", R3, R4, R5
00650 PRINT "SUM", S0, S1, S2
00660 PRINT
00670 PRINT " ", "TYRE DEFL", "WHEEL TRVL", "BODY FORCE", "PERF INDEX"
00680 PRINT "FRONT", S4, S5, S6, I1
00690 PRINT "REAR", S7, S8, S9, I2
00700 PRINT "SUM", T1, T2, T3, I
00710 PRINT
00720 NEXT Q
00730 END

```

FILE C13 (BASIC)

The Program calculates k_2 that minimises the Performance Index for given values of weighting factors. HILLMAN, $R=0.7$, (Unladen).

PROGRAM MINI

```

00100 READ A, B, L, K3
00110 READ A0, B0, C0
00120 READ A1, B1, C1
00130 READ A2, B2, C2
00140 READ D0, E0, F0
00150 READ D1, E1, F1
00160 READ D2, E2, F2
00170 DATA 1. 0978, 1. 4676, 2. 5654, 40812. 7
00180 DATA . 0158457, -1. 556078E-7, 3. 7638E-12
00190 DATA . 131529, -4. 343718E-6, 7. 11E-11
00200 DATA 1. 54514E8, -819. 5, 6. 99375E-2
00210 DATA . 02576962, -2. 682707E-7, 5. 201849E-12
00220 DATA . 1093146, -1. 673051E-6, 2. 134936E-11
00230 DATA 1. 563412E8, -459. 5847, . 08332405
00240 INPUT K2, Q, R, C
00250 PRINT "COUPLING RATIO =", C
00260 GO TO 00280
00270 K2=K2-. 25*S3/I3
00280 D=K2/K3-(B/L)^2
00290 K4=((R/L)^2)*K2/D
00300 D4=-((K4/K2)*(B/R))^2
00310 D5=2*D4*(D4*K2/K4-1)/K2
00320 R0=B0+2*K2*C0

```

PROGRAM MINI (continued).....

```

00330 R1=B1+2*K2*C1
00340 R2=B2+2*K2*C2
00350 R3=(E0+2*K4*F0)*D4
00360 R4=(E1+2*K4*F1)*D4
00370 R5=(E2+2*K4*F2)*D4
00380 S0=R0+R3
00390 S1=R1+R4
00400 S2=R2+R5
00410 S3=Q*S0+S1+R*S2
00420 T4=2*C0+D5*R3+2*D4*F0*D4
00430 T5=2*C1+D5*R4+2*D4*F1*D4
00440 T6=2*C2+D5*R5+2*D4*F2*D4
00450 I3=T4*Q+T5*1. +T6*R
00460 IF ABS(S3)>1. E-12 THEN 00270
00470 S4=R0+B0*K2+C0*K2*K2
00480 S5=R1+B1*K2+C1*K2*K2
00490 S6=R2+B2*K2+C2*K2*K2
00500 S7=D0+E0*K4+F0*K4*K4
00510 S8=D1+E1*K4+F1*K4*K4
00520 S9=D2+E2*K4+F2*K4*K4
00530 I1=R*S6+Q*S4+S5
00540 I2=R*S9+Q*S7+S8
00550 I=I1+I2
00560 T1=S4+S7
00570 T2=S5+S8
00580 T3=S6+S9
00590 PRINT
00600 PRINT "RHO", "Q", "K2", "K2P", "DI/DK2"
00610 PRINT R, Q, K2, K4, S3
00620 PRINT
00630 PRINT " ", "DX01/DK2", "DX12/DK2", "DF2/DK2"
00640 PRINT "FRONT", R0, R1, R2
00650 PRINT "REAR", R3, R4, R5
00660 PRINT "SUM", S0, S1, S2
00670 PRINT
00680 PRINT " ", "TYRE DEFL", "WHEEL TRVL", "BODY FORCE", "PERF INDEX"
00690 PRINT "FRONT", S4, S5, S6, I1
00700 PRINT "REAR", S7, S8, S9, I2
00710 PRINT "SUM", T1, T2, T3, I
00720 PRINT
00730 GO TO 00240
00740 END

```

FILE C14 (BASIC)

The program calculates I_{\min} and q for series values of k_2 and ρ . $\frac{1}{2}$ -car Model.

PROGRAM MINIR

```

00100 READ A, B, L, K3
00110 READ A0, B0, C0
00120 READ A1, B1, C1
00130 READ A2, B2, C2
00140 READ D0, E0, F0
00150 READ D1, E1, F1
00160 READ D2, E2, F2
00170 DATA 1. 0978, 1. 4676, 2. 5654, 40812. 7
00180 DATA . 0158457, -1. 556078E-7, 3. 7638E-12
00190 DATA . 131529, -4. 343718E-6, 7. 11E-11
00200 DATA 1. 54514E8, -819. 5, 6. 99375E-2
00210 DATA . 02576962, -2. 682707E-7, 5. 201849E-12
00220 DATA . 1093146, -1. 673051E-6, 2. 134936E-11
00230 DATA 1. 563412E8, -459. 5847, . 08332405
00240 INPUT R, C
00250 PRINT "COUPLING RATIO =", C
00260 PRINT "RHO", "Q1", "K2", "K2P", "DI/DK2"
00270 FOR K2=16000 TO 24000 STEP 100
00280 D=K2/K3-(B/L)^2
00290 K4=((A/L)^2)*K2/D
00300 D4=-((K4/K2)*(B/A))^2
00310 D5=2*D4*(D4*K2/K4-1)/K2
00320 R0=B0+2*K2*C0
00330 R1=B1+2*K2*C1
00340 R2=B2+2*K2*C2
00350 R3=(E0+2*K4*F0)*D4
00360 R4=(E1+2*K4*F1)*D4
00370 R5=(E2+2*K4*F2)*D4
00380 S0=R0+R3
00390 S1=R1+R4
00400 S2=R2+R5
00410 Q=-((R*S2+S1)/S0)
00420 S3=Q*S0+S1+R*S2
00430 T4=2*C0+D5*R3+2*D4*F0*D4
00440 T5=2*C1+D5*R4+2*D4*F1*D4
00450 T6=2*C2+D5*R5+2*D4*F2*D4
00460 I3=T4*Q+T5*1. +T6*R
00470 S4=A0+B0*K2+C0*K2*K2
00480 S5=A1+B1*K2+C1*K2*K2
00490 S6=A2+B2*K2+C2*K2*K2
00500 S7=D0+E0*K4+F0*K4*K4
00510 S8=D1+E1*K4+F1*K4*K4
00520 S9=D2+E2*K4+F2*K4*K4
00530 I1=R*S6+Q*S4+S5
00540 I2=R*S9+Q*S7+S8
00550 I=I1+I2
00560 T1=S4+S7
00570 T2=S5+S8
00580 T3=S6+S9
00590 PRINT R, Q, K2, K4, S3
00600 NEXT K2
00620 END

```

FILD C15 (FORTRAN)

The program calculates I_{\min} for series of k_2 with p and q as parameters.

HILLMAN $\frac{1}{2}$ -Car Model (Unladen) $R=0.7$.

PROGRAM MINIF2

```

00100 PROGRAM MINIF (OUTPUT, TAPE 2=OUTPUT)
00110 DIMENSION SKF(10), PR(10, 10), PQ(10, 10), Q1(10, 10)
00115 DIMENSION QR(10), RQ(10), RK(10, 10)
00120 DATA A, B, WB, SK3/ 1. 0978, 1. 4676, 2. 5654, 40812. 7/
00130 DATA A0, B0, C0/ . 0158457, -1. 556078E-7, 3. 7638E-12/
00140 DATA A1, B1, C1/ . 131529, -4. 343718E-6, 7. 11E-11/
00150 DATA A2, B2, C2/ 1. 54514E8, -819. 5, 6. 99375E-2/
00160 DATA D0, E0, F0/ . 02576962, -2. 682707E-7, 5. 201849E-12/
00170 DATA D1, E1, F1/ . 1093146, -1. 673051E-6, 2. 134936E-11/
00180 DATA D2, E2, F2/ 1. 563412E8, -459. 5847, . 08332405/
00185 SK=16000.
00190 DO 20 I=1, 10
00195 SK=SK+1000.
00200 SKF(I)=SK
00210 20 CONTINUE
00212 PRINT 25
00213 25 FORMAT(16X, 17HFRONT SPRING RATE)
00214 PRINT 30, (SKF(I), I=1, 10)
00216 30 FORMAT(15X, 10G11. 5)
00220 DO 90 J=1, 10
00224 DO 80 I=1, 10
00230 R=. 25E-10*2. 0**(J-2)
00240 IF(J-2. LT. 0) GO TO 5
00250 GO TO 10
00260 5 R=0.
00270 10 CONTINUE
00275 RQ(J)=R
00276 SK2=SKF(I)
00280 D=SK2/SK3-(B/WB)**2
00290 SK4=((A/WB)**2)*SK2/D
00300 D4=-((SK4/SK2)*(B/A))**2
00320 R0=B0+2. *SK2*C0
00330 R1=B1+2. *SK2*C1
00340 R2=B2+2. *SK2*C2
00350 R3=(E0+2. *SK4*F0)*D4
00360 R4=(E1+2. *SK4*F1)*D4
00370 R5=(E2+2. *SK4*F2)*D4
00380 S0=R0+R3
00390 S1=R1+R4
00400 S2=R2+R5
00410 Q=- (R*S2+S1)/S0
00415 Q1(I, J)=Q
00470 S4=A0+B0*SK2+C0*SK2*SK2
00480 S5=A1+B1*SK2+C1*SK2*SK2
00490 S6=A2+B2*SK2+C2*SK2*SK2
00500 S7=D0+E0*SK4+F0*SK4*SK4
00510 S8=D1+E1*SK4+F1*SK4*SK4
00520 S9=D2+E2*SK4+F2*SK4*SK4
00550 PR(I, J)=R*(S6+S9)+Q*(S4+S7)+(S5+S8)

```

PROGRAM MINIF2 (continued).....

```
00620 QJ=(J-1)
00630 Q=2.5*QJ
00635 QR(J)=Q
00640 R=-(Q*50+51)/52
00645 RK(I,J)=R
00650 PQ(I,J)=R*(56+59)+Q*(54+57)+(55+58)
00680 80 CONTINUE
00690 90 CONTINUE
00700 PRINT 95
00710 95 FORMAT(/,6H "RHO",20X,34HPERF. INDEX WITH "RHO" AS PARAMETER)
00720 DO 100 J=1,10
00730 PRINT 110,RQ(J),(PR(I,J),I=1,10)
00740 100 CONTINUE
00750 110 FORMAT(1X,10G11.3,2X,10G11.5)
00760 PRINT 115
00770 115 FORMAT(/,5H "Q1",21X,33HPERF. INDEX WITH "Q1" AS PARAMETER)
00780 DO 120 J=1,10
00790 PRINT 110,QR(J),(PQ(I,J),I=1,10)
00800 120 CONTINUE
00810 PRINT 130
00820 130 FORMAT(/,6H "RHO",20X,38HVALUES OF "Q1" WITH "RHO" AS PARAMETER)
00830 DO 140 J=1,10
00850 PRINT 110,RQ(J),(Q1(I,J),I=1,10)
00855 140 CONTINUE
00860 PRINT 150
00870 150 FORMAT(/,5H "Q1",21X,38HVALUES OF "RHO" WITH "Q1" AS PARAMETER)
00880 DO 160 J=1,10
00890 PRINT 110,QR(J),(RK(I,J),I=1,10)
00895 160 CONTINUE
00900 STOP
00910 END
```

FILE C16 (FORTRAN)

The program plots l_{\min} against k_2 with p and q as parameters. HILLMAN, $\frac{1}{2}$ -Car Model.

```

00100 PROGRAM MINIPLT (OUTPUT, TAPE 2=OUTPUT)
00110 DIMENSION SKF(100), PR(100, 10), PQ(100, 10), Q1(100, 10)
00120 DIMENSION QR(10), RQ(10), RK(100, 10)
00130 DATA A, B, WB, SK3/ 1. 0978, 1. 4676, 2. 5654, 40812. 7/
00140 DATA A0, B0, C0/ . 0158457, -1. 556078E-7, 3. 7638E-12/
00150 DATA A1, B1, C1/ . 131529, -4. 343718E-6, 7. 11E-11/
00160 DATA A2, B2, C2/ 1. 54514E8, -819. 5, 6. 99375E-2/
00170 DATA D0, E0, F0/ . 02576962, -2. 682707E-7, 5. 201849E-12/
00180 DATA D1, E1, F1/ . 1093146, -1. 673051E-6, 2. 134936E-11/
00190 DATA D2, E2, F2/ 1. 563412E8, -459. 5847, . 08332405/
00200 CALL PLOTS(5HCAL25)
00210 CALL AXIS(0. 0, 0. 0, 10HPERF. INDEX, 10, 16. , 90. , 0. 0, 0. 1, -1)
00220 CALL AXIS(0. 0, 0. 0, 12HSTIFFNESS K2, -12, 20. , 0. 0, 17000. , 500. , -1)
00230 SK=16900.
00240 DO 20 I=1, 100
00250 SK=SK+100.
00260 SKF(I)=SK
00270 20 CONTINUE
00280 DO 90 J=1, 10
00290 DO 80 I=1, 100
00300 R=. 25E-10*2. 0**(J-2)
00310 IF(J-2. LT. 0) GO TO 5
00320 GO TO 10
00330 5 R=0.
00340 10 CONTINUE
00350 RQ(J)=R
00360 SK2=SKF(I)
00370 D=SK2/SK3-(B/WB)**2
00380 SK4=((A/WB)**2)*SK2/D
00390 D4=-((SK4/SK2)*(B/A))**2
00400 R0=B0+2. *SK2*C0
00410 R1=B1+2. *SK2*C1
00420 R2=B2+2. *SK2*C2
00430 R3=(E0+2. *SK4*F0)*D4
00440 R4=(E1+2. *SK4*F1)*D4
00450 R5=(E2+2. *SK4*F2)*D4
00460 S0=R0+R3
00470 S1=R1+R4
00480 S2=R2+R5
00490 Q=-(R*S2+S1)/S0
00500 Q1(I, J)=Q
00510 S4=A0+B0*SK2+C0*SK2*SK2
00520 S5=A1+B1*SK2+C1*SK2*SK2
00530 S6=A2+B2*SK2+C2*SK2*SK2
00540 S7=D0+E0*SK4+F0*SK4*SK4
00550 S8=D1+E1*SK4+F1*SK4*SK4
00560 S9=D2+E2*SK4+F2*SK4*SK4

```

Program MINIPLT (continued).....

```
00570 PR(I, J)=R*(S6+S9)+Q*(S4+S7)+(S5+S8)
00580 IF<PR(I, J). GT. 1. 6) GO TO 40
00590 IF<PR(I, J). LT. 0. 0) GO TO 45
00600 GO TO 50
00610 40 PR(I, J)=1. 6
00620 GO TO 50
00630 45 PR(I, J)=0. 0
00640 50 CONTINUE
00650 QJ=(J-1)
00660 Q=2. 5*QJ
00670 QR(J)=Q
00680 R=-<Q*S0+S1>/S2
00690 RK(I, J)=R
00700 PQ(I, J)=R*(S6+S9)+Q*(S4+S7)+(S5+S8)
00710 IF<PQ(I, J). GT. 1. 6) GO TO 60
00720 IF<PQ(I, J). LT. 0. 0) GO TO 65
00730 GO TO 80
00740 60 PQ(I, J)=1. 6
00750 GO TO 80
00760 65 PQ(I, J)=0. 0
00770 80 CONTINUE
00780 CALL LINE<SKF, 17000. , 500. , PR(1, J), 0. 0, 0. 1, 100, 0)
00790 CALL LINE<SKF, 17000. , 500. , PQ(1, J), 0. 0, 0. 1, 100, 0)
00800 90 CONTINUE
00810 CALL PLOTE
00820 STOP
00830 END
```

FILE C17

The program calculates the spring and damper rates for a given total deflection C.
 HILLMAN $\frac{1}{2}$ -Car Model, Front Suspension.
 PROGRAM OPT1

```

00100 READ M1,M2,K1
00110 DATA 28.576,288.94,155860
00120 INPUT C
00130 FOR K2= 14000 TO 32000 STEP 1000
00140 A=((M1+M2)^2)/(2*K1*M2*M2)
00150 B=K2*(M1+M2)/K1
00160 D=K2*A*B
00170 X=B*K2*K1/2
00180 Y=M1/2-B*M1/M2+D
00190 Z=M2/2+B+D
00200 P=.5*C/A
00210 R=P*P-Z/A
00220 IF R<0 GO TO 330
00230 Q=SQR(R)
00240 B2=P+Q
00250 B3=P-Q
00260 X2=A*B2+Y/B2
00270 X3=A*B3+Y/B3
00280 F2=K1*B2/2+X/B2
00290 F3=K1*B3/2+X/B3
00300 PRINT K2,B2,X2,F2,Q
00310 PRINT K2,B3,X3,F3
00320 NEXT K2
00330 STOP
00340 END

```

FILE C18

The program determines the suspension spring rate for minimum tyre deflection, and damper rates for minimum body force. HILLMAN $\frac{1}{2}$ -Car Model, R=1.0.

PROGRAM SPRG

```

00100 READ A,B,L,K1,K3
00110 READ M1,M2,M3,M4
00120 DATA 1.0978,1.4676,2.5654,155860,40813
00130 DATA 28.58,288.94,54.43,216.14
00140 FOR K2= 21645 TO 21650 STEP 1
00150 R1=(A/L)^2
00160 R2=(B/L)^2
00170 R3=K2/K3
00180 K4=K2*R1/(R3-R2)
00190 R4=2*K1*((M2/(M1+M2))^2)
00200 R5=((K2*(M1+M2)/(K1*M2))^2)*((M1+M2)/2)
00210 R6=2*K1*((M4/(M3+M4))^2)
00220 R7=((K4*(M3+M4)/(K1*M4))^2)*((M3+M4)/2)
00230 R8=(M3+M4)/(M1+M2)
00240 S1=(M1/2-K2*M1*(M1+M2)/(K1*M2)+R5)*R4
00250 S2=(M3/2-K4*M3*(M3+M4)/(K1*M4)+R7)*R6
00260 B2=SQR(S1)
00270 B4=SQR(S2)
00280 S3=(R1*R1*R2/((R3-R2)^3))*R8*B2/B4
00290 PRINT K2,K4,B2,B4,S3
00300 NEXT K2
00310 END

```

FILE C19.

The program calculates the spring and damper rates for constant front deflection C_1 and rear deflection C_2 .

Also calculates I.S.V. of Body Force and Tyre Deflection. HILLMAN $\frac{1}{2}$ -Car Model.
(Unladen) $R=1.0$.

PROGRAM OPT2

```

00090 INPUT C1,C2
00100 READ M1,M2,M3,M4,K1
00110 READ A,B,L,K3
00120 DATA 28.576, 288.94, 54.431, 216.14, 155860
00130 DATA 1.0978, 1.4676, 2.5654, 40812.7
00140 FOR K2=15000 TO 30000 STEP 500
00150 D=K2/K3-(B/L)^2
00160 K4=((A/L)^2)*K2/D
00170 A1=((M1+M2)^2)/(2*K1*M2*M2)
00180 A2=((M3+M4)^2)/(2*K1*M4*M4)
00190 B1=K2*(M1+M2)/K1
00200 B2=K4*(M3+M4)/K1
00210 D1=K2*A1*B1
00220 D2=K4*A2*B2
00230 X1=B1*K2*K1/2
00240 X2=B2*K4*K1/2
00250 Y1=M1/2-B1*M1/M2+D1
00260 Y2=M3/2-B2*M3/M4+D2
00270 Z1=M2/2+B1+D1
00280 Z2=M4/2+B2+D2
00290 P1=.5*C1/A1
00300 P2=.5*C2/A2
00310 R1=P1*P1-Z1/A1
00320 R2=P2*P2-Z2/A2
00330 Q1=SQR(R1)
00340 Q2=SQR(R2)
00350 B3=P1-Q1
00360 B4=P2-Q2
00370 X3=A1*B3+Y1/B3
00380 X4=A2*B4+Y2/B4
00390 F3=K1*B3/2+X1/B3
00400 F4=K1*B4/2+X2/B4
00410 PRINT K2,B3,X3,F3,(X3+X4)
00420 PRINT K4,B4,X4,F4,(F3+F4)
00430 NEXT K2
00440 END

```

BIBLIOGRAPHY

1. ISO/TC 108/WG 9 (BSI Panel MEE/158/3/1)
Generalised Terrain - Dynamic Inputs to Vehicles, June 1972.
2. C.J. DODDS and J.D. ROBSON
"The Description of Road Surface Roughness"
Journal of Sound and Vibration, 31, (1973), pp175-183.
3. J.D. ROBSON and C.J. DODDS
"Stochastic Road Inputs and Vehicle Response"
Vehicle System Dynamics 5 (1975/76), pp.1-13.
4. C.J. DODDS
"The Laboratory Simulation of Vehicle Service Stress"
Journal of Engineering for Industry, May 1974, pp.391-398.
5. J.D. ROBSON, K.M.A. KAMASH
"Road Surface Description in Relation to Vehicle Response"
Vehicle System Dynamics Vol. 6, Nos. 2 & 3, Sept. 1977.
6. J.D. ROBSON
"Road Surface Description and Vehicle Response"
Int. Journal of Vehicle Design, Vol.1, No. 1, 1979, pp.25-35
7. J.D. ROBSON
"The Role of Parkhilovskii Model in Road Description"
Vehicle System Dynamics 7 (1978), pp.153-162.

8. A.J. HEALEY, E. NATHMAN, C.C. SMITH
"An Analytical and Experimental Study of Automobile Dynamics with Random Roadway Inputs"
Journal of Dynamic Systems, Measurement and Control, Dec. 1977, pp.284-292.

9. V. BORMANN
"Messungen von Fahrbahn Unebenheiten Paralleler Fahrspuren und Anwendung der Ergebnisse" (German)
Vehicle System Dynamics 7 (1978), pp.65-81.

10. A. SATTARIPOUR
"The Effect of Road Roughness on Vehicle Behaviour"
Vehicle System Dynamics Vol. 6, No. 2-3, Sept. 1977, pp.157-161.

11. M.A. DOKAINISH, M.M. ELMADANY
"Random Response of Tractor-Semitrailer System"
Vehicle System Dynamics 9 (1980), pp.187-212.

12. J.C. WAMBOLD, W.H. PARK, R.G. VASHLISHAN
"A New Random Data Description and its Use in Transferring Road Roughness to Vehicle Response"
Journal of Engineering for Industry, May 1974, pp.676-681.

13. J.Y. WONG
Theory of Ground Vehicles (Book)
J. WILEY & SONS, 1978.

14. N.S. NATHOO, A.J. HEALEY
"Coupled Vertical-Lateral Dynamics of a Pneumatic Tired Vehicle"
Journal of Dynamic Systems, Measurement and Control, Dec. 1978,
Vol.100, pp.319-325.

15. D. RYBA
"Possible Improvements in Ride Comfort"
Vehicle System Dynamics 2 (1973), pp.1-32.

16. P.R. BELANGER, R. GUILLEMETTE
"Passive Suspension Design for a Magnetically Levitated Vehicle".
Journal of Dynamic Systems, Measurement and Control, Dec. 1977.
pp.277-282.

17. J.K. HEDRICK, G.E. BILLINGTON, D.A. DREESBACH
"Analysis, Design and Optimisation of High Speed Vehicle Suspensions
Using State Variable Techniques".
Journal of Dynamic Systems, Measurement and Control, June 1974,
pp.193-203.

18. D.E. NEWLAND
An Introduction to Random Vibrations and Spectral Analysis (Book)
LONGMAN (1975)

19. I. McCAUSLAND
Introduction to Optimal Control (Book)
J. WILEY & SONS INC. (1969)

20. B. ETKIN
"A Simple Method for the Analogue Computation of the Mean-Square Response of Airplanes to Atmospheric Turbulence".
UTIA Technical Note No. 32,
Institute of Aerophysics, University of Toronto, January, 1960.

21. W.G. BRADFORD
"On Errors in Published Formulas for the Noise-Response Integrals"
Proceedings of the I.E.E., Nov. 1971, pp.1614-1615.

22. C.G. NEWTON, L.A. GOULD & J.F. KAISER
Analytical Design of Linear Feedback Controls (Book)
J. WILEY & SONS, 1957.

23. J.K. HEDRICK
"Some Optimal Control Techniques Applicable to Suspension System Design".
Trans. ASME Paper No. 73-ICT-55.

24. A.G. THOMPSON
"Digital Simulation Techniques for Optimising Automobile Suspension Design".
Presented at the Inter Society Symposium
"Computers in Automotive Design and Analysis" held in Melbourne,
October, 1978.

25. M.M. ELMADANY, M.A. DOKAINISH, A.B. ALLAN
"Ride Dynamics of Articulated Vehicles - A Literature Survey"
Vehicle System Dynamics 8 (1979) pp.287-316.

26. R.N. JANEWAY
"Passenger Vibration Limits"
SAE Journal, August 1948.

27. C.C. SMITH, D.Y. McGEHEE, A.J. HEALEY
"The Prediction of Passenger Riding Comfort From Acceleration Data".
Transactions A.S.M.E., Vol.100, March 1978, pp.34-41.

28. R.A. LEE, F. PRADKO
"Analytical Analysis of Human Vibration"
S.A.E. Transactions, Vol. 77, paper No. 680091, Jan. 1968.

29. W.H. PARK, J.C. WAMBOLD, R.G. VASHLISHAN
"Prediction of Objective Passenger Comfort from Road Profile"
Journal of Engineering for Industry, May 1974, pp.503-508.

30. Dept. of Transport Specification, 1972.
Performance Specifications and Engineering Design Requirements
for the UTACV.

31. A.A. BUTKUNAS
"Power Spectral Density and Ride Evaluation"
S.A.E. Paper No. 660138, 1966.

32. International Organisation for Standardisation.
"Guide for the Evaluation of Human Exposure to Whole Body Vibration"
International Standard ISO2631-1974.

33. C.C. SMITH
"On Using I.S.O. Standards to Evaluate the Ride Quality of Broad-Band Vibration Spectra in Transportation Vehicles".
Journal of Dynamic Systems, Measurement and Control, Vol.98, No. 4,
Dec. 1976, pp.440-449.

34. M.J. CLARKE
"A Study of the Available Evidence on Duration Effects on Comfort and Task Proficiency Under Vibration".
Journal of Sound and Vibration (1979), 65(1), pp.107-123.

35. T. DAHLBERG
"Optimization Criteria for Vehicles Travelling on a Randomly Profiled Road - A Survey".
Vehicle System Dynamics 8, (1979), pp.239-252.

36. T. DAHLBERG
"Parametric Optimization of 1-DOF Vehicle Travelling on a Randomly Profiled Road".
Journal of Sound and Vibration (1977), 55(2), pp.245-253.

37. T. DAHLBERG
"Ride Comfort and Road Holding of a 2-DOF Vehicle Travelling on a Randomly Profiled Road".
Journal of Sound and Vibration (1978), 58(2), pp.179-187

38. E. ESMAILZADEH
"Design Synthesis of a Vehicle Suspension System Using Multi-Parameter Optimisation".
Vehicle System Dynamics 7(1978), pp.83-96.

39. E.M. MITSCHKE
"Influence of Road and Vehicle Dimensions on the Amplitude of Body Motions and Dynamic Wheel Loads (Theoretical and Experimental Evaluation Investigation)".
Trans. S.A.E., 1962, 70, pp.434-496.

40. B.E. QUINN, S.E. HILDEBRAND
"Effect of Road Roughness on Vehicle Steering"
Highway Research Record 471, 1973, pp.62-75.

41. ^EB.K. BENDER
"Optimisation of Random Vibration Characteristics of Vehicle Suspensions".
D.Sc. Thesis, M.I.T., 1967.

42. D. RYBA
"Improvements in Dynamic Characteristics of Automobile Suspension Systems".
Part 1. Two-Mass Systems.
Vehicle System Dynamics 3 (1974), pp.17-46.

43. W.W. METCALF.
"The Ride Behaviour of a Multi-Element Vehicle Traversing Cross-Country Terrain".
Cornell Aeronautical Laboratory,
Cornell University, Buffalo, New York, 1961.

44. H.B. SUTTON
"The Potential for Active Suspension Systems".
Automotive Engineer, April/May, 1979, pp.21-24.

45. B. PORTER
Synthesis of Dynamical Systems (Book)
NELSON (1969)

46. J.D. ROBSON, C.J. DODDS, C.J. MACLEAN, V.R. PALING
Random Vibrations (Book)
SPRINGER (1972)

47. R. MEISINGER
"Simulation of Maglev Vehicles Riding over Single and Double Span
Guideways".
Mathematics and Computers in Simulation
XX1 (1979) pp.197-206.

48. Ride and Vibration Data Manual,
Society of Automotive Engineers,
SAE J 6 a, 1965.

49. L.F. STIKELEATHER, G.O. HALL, A.O. RADKE
"A Study of Vehicle Vibration Spectra as Related to Seating Dynamics".
S.A.E. Transactions, Vol. 81, paper 72001, 1973.

50. A.G. THOMPSON
"Quadratic Performance Indices and Optimum Suspension Design".
Proc. Instn. Mech. Engineers, 1973, Vol. 187 9/73, pp.129-139.

51. A.G. THOMPSON
"An Active Suspension with Optimum Linear State Feedback".
Vehicle System Dynamics 5 (1976) pp.187-203.

52. A.G. THOMPSON
"Optimum Damping in a Randomly Excited Non-Linear Suspension".
Proc. Instn. Mech. Engineers, Vol. 184, Part 2A, No. 8, 1969-70
pp.169-178.

53. D. BASTOW
"Suspension and Steering"
Automobile Engineer, 10th May, 1968.

54. K.M. CAPTAIN, A.B. BOGHANI, D.N. WORMLEY
"Analytical Tyre Models of Dynamic Vehicle Simulation".
Vehicle System Dynamics 8 (1979) pp.1-32.

55. J. PAGE
"Dynamic Behaviour of Single Axle Vehicle Suspension System:
A Theoretical Study".
TRRL Report LR580, CROWTHORNE, 1973.

56. P.B. STILL, P.G. JORDAN
"Evaluation of the TRRL High-Speed Profilometer".
TRRL Report LR922, CROWTHORNE, 1980.

57. P.G. JORDAN, J.C. YOUNG
"Developments in the Calibration and Use of the Bump-Integrator
for Ride Assessment".
TRRL Report SR604, CROWTHORNE, 1980.

58. S.K. CLARK
"Mechanics of Pneumatic Tyres"
Monograph 122, National Bureau of Standards, 1971.

59. J.A. OVERTON, B. MILLS, C. ASHLEY
"The Vertical Response Characteristics of the Non-Rolling Tyre"
Proc. Inst. of Mech. Engineers, Vol. 184, Part 2A, No. 2, 1969-70.

60. V.E. GOUGH
"Tyres and Air Suspension, Advances in Automobile Engineering"
(Symposium on Vehicle Ride Problem),
PERGAMON PRESS, OXFORD, 1963.

61. A.G. THOMPSON
"A Simple Formula for Optimum Suspension Damping. Journal of Automotive Engineering".
April, 1972, page 20.

62. R.L. SWAIN, D.K. SCHMIDT, P.A. ROBERTS, A.J. HINSDALE
"An Analytical Method for Ride Quality of Flexible Airplanes".
A.I.A.A. Journal, Vol. 15, No. 1, Jan. 1977, pp.4-7.

63. J.K. HEDRICK, H. FIROUZTASH
"The Covariance Propagation Equation Including Time-Delayed Inputs"
I.E.E.E. Transactions on Automatic Control,
Oct. 1974, pp.578-589.

64. J.K. HEDRICK
"Some Optimal Control Techniques Applicable to Suspension System Design".
Trans. ASME, Paper No. 73-1.C.T.-55.

65. J.L. KUESTER, J. MIZE
Optimisation Techniques with FORTRAN
McGraw-Hill, 1973 (Book)

66. H. KWAKERNAAK, R. SIVAN
Linear Optimal Control Systems (Book)
WILEY-INTERSCIENCE, 1972.

67. K.J. ASTROM.
Introduction to Stochastic Control Theory (Book)
Academic Press, 1970.

68. A.E. BRYSON
Applied Optimal Control (Book)
BLAISDELL Publishing Co., 1967.

69. A.G. THOMPSON, C.E.M. PEARCE
"An Optimal Suspension for an Automobile on a Random Road"
S.A.E. Paper No. 790478, 1979.

70. J. MOUNT, A.G. THOMPSON
"Pseudo-Random Binary Sequences in Automobile Ride Simulation"
Automation and Control (N.Z.), July 1974, pp.26-37.

71. J.E. SNYDER, D.N. WORMLEY
"Dynamic Interactions Between Vehicles and Elevated, Flexible,
Randomly Irregular Guideways".
Journal of Dynamic Systems, Measurement and Control., March 1977,
pp.23-33.

72. R.W. MAYNE, S.M. METWALLI, K.A. AFIMIWALA
"Optimum of Design Vehicle Suspensions"
Trans. ASME, Paper No. 73-ICT-58.

73. D.C. KARNOPP
"Vehicle Response to Stochastic Roadways"
Vehicle System Dynamics 7 (1978), pp.97-109.

74. C.R. GUNTHER
"Application of Stochastic Optimal Control Theory to High-Speed
Vehicle Suspension Synthesis".
Ph.D. Thesis, University of California, Los Angeles.

75. M. BALAKNISHNA, D. HULLENDER
"Power Spectral Density for Constrained Long Wavelength Guideway Irregularities".
Journal of Dynamic Systems, Measurement and Control, March 1978, Vol. 100, pp.18-23.
76. P.C. MULLER, K. POPP, W.O. SCHIELEN
"Covariance Analysis of Non-Linear Guideway Vehicle Systems".
Vehicle System Dynamics, Vol. 6, Sept. 1977, pp.171-177.
77. C. GUENTHER
"A new Approach to High-Speed Tracked Vehicle Suspension Synthesis"
Mathematics and Computers in Simulation. XX1 (1979), pp.71-133.
78. A. SATTARIPOUR
"The Effect of Road Roughness on Vehicle Behaviour".
Vehicle System Dynamics, Vol. 6, No. 23, Sept. 1977, pp.157-161.
79. C.F. CHEN, L.S. SHIEH
"A Note on Expanding $PA + A^T P = -Q$ "
I.E.E. Transactions on Automatic Control,
February 1968, pp.122-123.
80. S.P. BINGULAC
"An Alternate Approach to Expanding $PA + A^T P = -Q$ "
I.E.E. Transactions on Automatic Control.
February 1970, pp.135-137.
81. C.F. CHEN, I.J. HAAS
Elements of Control Systems Analysis (Book)
Prentice-Hall, 1968.

82. J. DAVISON, F.T. MAN
"The Numerical Solution of $A'Q + QA = -C$ "
I.E.E. Transactions on Automatic Control
August, 1968, pp.448-449.
83. P.G. SMITH
"Numerical Solution of the Matrix Equation $AX + XA^T + B = 0$ "
I.E.E. Transactions on Automatic Control, June 1971, pp.278-279.
84. N.J. YOUNG
"Formulae for the Solution of LYAPUNOV Matrix Equations".
INT. JOURNAL CONTROL, 1980, Vol. 31, No. 1, 159-179.
85. E. FIALA, B. RICHTER
"Zur Optimierung von Fahrzeugfederungen" (German)
(Optimisation of Vehicle Suspensions)
Automobiltechnische Zeitschrift, No. 1, 1970, pp.1-3.
86. C.C. SMITH, Y.K. KWAK
"Identification of the Dynamic Characteristics of a Bench-Type
Automotive Seat for the Evaluation of Ride Quality".
Journal of Dynamic Systems, Measurement and Control, Vol. 100,
March 1978, pp.42-49.
87. T. DAHLBERG
"An Optimised Speed-Controlled Suspension of a 2-DOF Vehicle
Travelling on a Randomly Profiled Road".
Journal of Sound and Vibration (1979), 62(4), pp.541-546.
88. A.G. THOMPSON
"The Optimization of Automobile Spring and Damper Rates".
Paper Submitted to S.A.E. on 24-2-1981.